

Distribution Agreement

In presenting this thesis or dissertation as a partial fulfillment of the requirements for an advanced degree from Emory University, I hereby grant to Emory University and its agents the non-exclusive license to archive, make accessible, and display my thesis or dissertation in whole or in part in all forms of media, now or hereafter known, including display on the world wide web. I understand that I may select some access restrictions as part of the online submission of this thesis or dissertation. I retain all ownership rights to the copyright of the thesis or dissertation. I also retain the right to use in future works (such as articles or books) all or part of this thesis or dissertation.

Signature:

Eric Andreansky

Date

Synthetic Studies Toward Methanoquinolizidine-Containing
Akuammiline Alkaloids

By

Eric Andreansky
Doctor of Philosophy

Chemistry

Simon B. Blakey, Ph. D.
Advisor

Lanny S. Liebeskind, Ph. D.
Committee Member

Frank E. McDonald, Ph. D.
Committee Member

Accepted:

Lisa A. Tedesco, Ph.D.
Dean of the James T. Laney School of Graduate Studies

Date

Synthetic Studies Toward Methanoquinolizidine-Containing
Akuammiline Alkaloids

By

Eric Andreansky
B. A., New College of Florida, 2011

Advisor: Simon B. Blakey, Ph. D.

An abstract of
A dissertation submitted to the Faculty of the
James T. Laney School of Graduate Studies of Emory University
in partial fulfillment of the requirements for the degree of
Doctor of Philosophy
in Chemistry
2017

Abstract

Synthetic Studies Toward Methanoquinolizidine-Containing
Akuammiline Alkaloids

By Eric Andreansky

The akuammiline alkaloids are a family of indole monoterpenoids that are characterized by their congested, polycyclic cores. A subset of these alkaloids containing a methanoquinolizidine core has been the subject of much synthetic interest, but only recently have been the subject of successful total syntheses. A cascade annulation toward a tetracyclic akuammiline alkaloid core has been developed beginning from an accessible *N*-Cbz hemiaminal ether substrate containing pendant indole and allylsilane moieties. Unlike related cascades toward the Malagasy alkaloids, these cascade substrates were only tolerant of (*Z*)-allylsilane geometries, with the other isomers only providing an undesired diene product. Studies were performed on making this and related cascade enantioselective with both a chiral auxiliary and enantioselective catalysis. This tetracyclic intermediate was converted into a pentacyclic methanoquinolizidine core for the natural product strictamine. Additionally, this core could be converted into a pentacyclic furoindoline core that maps onto the currently unsynthesized natural product pseudoakuammigine. While successfully leading us to these structures, the currently developed routes require a significant number of steps. Studies are currently underway to develop a more succinct route to these natural products.

Synthetic Studies Toward Methanoquinolizidine-Containing
Akuammiline Alkaloids

By

Eric Andreansky
B. A., New College of Florida, 2011

Advisor: Simon B. Blakey, Ph. D.

A dissertation submitted to the Faculty of the
James T. Laney School of Graduate Studies of Emory University
in partial fulfillment of the requirements for the degree of
Doctor of Philosophy
in Chemistry
2017

Acknowledgements

The process of getting a doctoral degree is not an easy journey, requiring significant mental as well as emotional sacrifices. I would not have been able to make it to this point if it was not for the help of many people. First, I would like to thank my advisor Dr. Simon Blakey. You both encouraged me to pursue organic synthesis and provided me with the freedom to explore my own ideas about my project, both things that allowed me to grow significantly since I started graduate school. You always had an open door and were constantly willing to hear whatever ideas I had about this project or others. You are an exceptionally supportive advisor and hold your students to a high standard that I believe will benefit them throughout their careers. Additionally, I would like to thank my committee members, Dr. Frank McDonald and Dr. Lanny Liebeskind. Both of you have provided me advice and insights at various points of my degree that had allowed me to get out of holes in my project. I would also like to thank all of the members of the Blakey lab, both past and present, who provided a supporting atmosphere during my time of my PhD. In particular, I would like to thank Aidi Kong, who initially trained me when I started in the Blakey lab and whose careful research style rubbed off on me and benefited me in my graduate career. I would also like to thank Ricardo Delgado, Nadege Boudet, and Danny Mancheno, whose preliminary work provided the foundation for all the research contained in this thesis. I would also like to thank Jessica Hurtak for being a friend both willing to listen and understanding of the emotional frustrations that come with doing research. I would also want to thank my parents, Rebecca and Al, for always supporting me in whatever it was that I decided to pursue and for understanding the commitment required for me to pursue this degree. Lastly, I would like to thank Adam, for being my emotional rock for most of my time in graduate school.

Table of Contents

1. The Akuammiline Alkaloids: Structure, Biology, and Synthesis

1.1. Introduction.....	1
1.2. Biological Activity.....	6
1.3. Akuammiline Alkaloids: Prior Synthetic Studies.....	7
1.3.1. Total Syntheses of Vincorine.....	8
1.3.2. Total Syntheses of Aspidophylline A.....	11
1.3.3. Total Syntheses of Scholarisine A.....	15
1.3.4. Total Syntheses of Other Akuammiline Alkaloids.....	17
1.4. Methanoquinolizidine Alkaloids: Prior Synthetic Studies and Total Syntheses of Strictamine.....	21
1.5. Conclusion.....	33
1.6. References.....	33
2. Development of a Cascade Annulation Toward an Akuammiline Alkaloid Core	
2.1. Previous Studies: Iminium Ion Cascades Toward the Malagasy Alkaloids.....	37
2.2. Unexpected Regiodivergent Cascade Products During Malagasy Alkaloid Studies.....	41
2.3. Synthesis and Reactivity of <i>N,N'</i> -Bistosyltryptamine Hemiaminal Ether Substrates 2.31 and 2.32	44

2.4. Development of (<i>N</i> -Ts- <i>N</i> '-Cbz)Tryptamine-Based Substrates for Akuammiline Alkaloid Cascade Reactions.....	50
2.5. Optimization of Cascade with Z-Allylsilane Containing Substrate 2.62.....	59
2.6. Studies Toward the Development of Asymmetric Iminium Ion Cascades.....	60
2.6.1. Examination of Diastereoselective Additions to Hemiaminal Ethers Substituted with Ellman's Auxiliary.....	61
2.6.2. Studies Toward the Development of an Asymmetric Cascade Reaction with Ion-Pairing Catalysis.....	67
2.7. Conclusion.....	79
2.8. Experimental Procedures.....	80
2.9. Spectral Data for Key Intermediates.....	128
2.10. References.....	148
3. Synthetic Studies Toward Methanoquinolizidine-Containing Akuammiline Alkaloids	
3.1. Initial Strategy: Homologation of Exocyclic Olefin and Lactamization.....	150
3.2. Ketone Addition/Deoxygenation Strategy for Synthesis of the E Ring.....	155
3.3. Intramolecular Conjugate Addition Strategy for Synthesis of the E Ring.....	161
3.4. Lactamization Revisited: Cross-Coupling/Hydrogenation Strategy for the Synthesis of the E Ring.....	168
3.5. Synthesis of Pseudoakuammigine Furoindoline Core Model.....	177

3.6. New Directions: Development of an Alternative Akuammiline Alkaloid Cascade Annulation.....	181
3.7. Conclusion and Future Directions.....	188
3.8. Experimental Procedures.....	189
3.9. Spectral Data for Key Intermediates.....	216
3.10. References.....	253

Table of Figures

Figure 1-1. Representative akuammiline alkaloid structure and comparison of the topology of their methanoquinolizidine core with that of adamantane.....	1
Figure 1-2. Classification of akuammiline alkaloids based upon structural features.....	3
Figure 1-3. Representative biological activity of several akuammiline alkaloids.	6
Figure 2-1. X-ray crystal structure of obtained akuammiline alkaloid core tetracycle 2.63.....	54
Figure 2-2. Rationale for the observed product outcomes for the <i>Z</i> - and <i>E</i> -allylsilane isomers based upon the possible transition states for the allylsilane addition step.....	59
Figure 2-3. Proposed mechanism for disulfoninamide-catalyzed Mukaiyama aldol reaction invoking an <i>N</i> -trimethylsilyldisulfonimide intermediate.....	72
Figure 2-4. Proposed mechanism for reaction of <i>N</i> -trimethylsilyldisulfonimide catalysts with hemiaminal ether substrates.....	73

Table of Schemes

Scheme 1-1. Proposed biosynthesis of geissoschizine and conversion into marvacurine, akuammiline, and strychnos alkaloids.....	2
Scheme 1-2. Proposed biosynthetic pathway for representative akuammiline alkaloids from the biosynthetic precursor rhazimal (1.6).....	4
Scheme 1-3. Total synthesis of vincorine (1.16) by Yong Qin and coworkers using a key indole cyclopropanation/ring-opening/cyclization cascade.....	8
Scheme 1-4. Total synthesis of vincorine (1.16) by Dawei Ma and coworkers using a oxidative coupling cascade as the key step.....	9
Scheme 1-5. Total synthesis of vincorine (1.16) by David MacMillan and coworkers using an enantioselective Diels-Alder/cyclization cascade and intramolecular radical cyclization as key steps.....	10
Scheme 1-6. Total synthesis of aspidophylline A (1.12) by Neil Garg and coworkers using key Heck cyclization and interrupted Fischer Indolization steps.....	12
Scheme 1-7. Total synthesis of aspidophylline A (1.12) by Dawei Ma and coworkers using a key oxidative coupling/cyclization cascade.....	13
Scheme 1-8. Total synthesis of aspidophylline A (1.12) by Jieping Zhu and coworkers via key oxacyclization and intramolecular conjugate addition steps.....	14
Scheme 1-9. Total synthesis of aspidophylline A (1.12) by Yu-Rong Yang and coworkers using a key enantioselective iridium-catalyzed cyclization cascade.....	15
Scheme 1-10. Total synthesis of scholarisine A (1.17) by Amos Smith and coworkers featuring key aminocyclization and indole alkylation steps.....	16

- Scheme 1-11.** Total synthesis of scholarisine A (**1.17**) by Scott Snyder and coworkers using key radical cascade and C-H functionalization steps.....**17**
- Scheme 1-12.** The total synthesis of picrinine (**1.11**) by Neil Garg and coworkers using key Fischer indolization and diol cleavage/oxacyclization steps.....**18**
- Scheme 1-13.** Total synthesis of aspidodasycarpine (**1.13**) and lonicerine (**1.14**) by Ang Li and coworkers using key gold-catalyzed cyclization and indole alkylation steps.....**19**
- Scheme 1-14.** Total synthesis of calophyline A (**1.15**) by Liansuo Zu and coworkers, centering around an aza-Pinacol/Elimination/Conjugate Addition cascade.....**21**
- Scheme 1-15.** Studies by Dolby and coworkers toward an akuammiline alkaloid methanoquinolizidine core.....**23**
- Scheme 1-16.** Studies by Bosch and coworkers toward the akuammiline alkaloids.....**24**
- Scheme 1-17.** Synthetic attempts to form an akuammiline alkaloid core by Cook and coworkers.....**25**
- Scheme 1-18.** Successful synthesis of a tetracyclic akuammiline alkaloid core by Matsuo and coworkers.....**26**
- Scheme 1-19.** Synthetic studies of a ring-closing-metathesis/Ireland-Claisen approach toward strictamine by Hidetoshi Tokuyama and coworkers.....**27**
- Scheme 1-20.** Attempted synthesis of an akuammiline alkaloid tetracyclic core by Jieping Zhu and coworkers.....**28**
- Scheme 1-21.** Total synthesis of strictamine (**1.18**) and cathafoline (**1.141**) by Neil Garg and coworkers using a Fischer indolization/reduction and late state D ring cyclization.....**29**

- Scheme 1-22.** Total synthesis of (\pm)-strictamine (**1.18**) by Jieping Zhu and coworkers employing an intramolecular reductive Heck cyclization to forge the E ring.....**30**
- Scheme 1-23.** Formal synthesis of (\pm)-strictamine (**1.18**) by Fujii, Ohno, and coworkers employing a gold(I)-catalyzed cyclization to forge the C ring.....**31**
- Scheme 1-24.** Formal synthesis of (\pm)-strictamine (**1.18**) by Tanja Gaich and coworkers employing a [2,3]-Stevens rearrangement to forge the D ring.....**31**
- Scheme 1-25.** Formal synthesis of (+)-strictamine (**1.18**) by Snyder and coworkers using an enantioselective propargylation and gold(I)-catalyzed cyclization to forge the C ring...**33**
- Scheme 2-1.** Initially proposed iminium ion cascade annulation toward a core structure **2.3** of the Malagasy alkaloids.....**37**
- Scheme 2-2.** Initial attempts toward a direct imine condensation reaction for the synthesis of a Malagasy alkaloid core.....**38**
- Scheme 2-3.** Synthesis of hemiaminal ethers via reduction of amides and subsequent decomposition with Lewis acids to iminium ions, as reported by Suh and coworkers.....**39**
- Scheme 2-4.** Successful cyclization of *N*-tosyl hemiaminal ether **2.12** to form a Malagasy alkaloid core **2.13**.....**39**
- Scheme 2-5.** Cascade annulation reaction of hemiaminal ether substrates **2.14** and **2.16** toward C16 substituted cores **2.15** and **2.17**.....**40**
- Scheme 2-6.** Regiodivergent cascade reactions, relevant to the akuammiline alkaloids, discovered during studies toward the Malagasy alkaloids.....**41**

Scheme 2-7. Divergent pathways for iminium ion cyclizations due to differing nitrogen substituents.....	42
Scheme 2-8. Proposed retrosynthetic analysis for the development of more synthetically useful cascade reaction for the synthesis of an akuammiline alkaloid core.....	43
Scheme 2-9. Retrosynthetic analysis for synthesis of hemiaminal ether substrates 2.31 and 2.32	44
Scheme 2-10. Synthesis of <i>N,N'</i> -bistosyl-6-methoxytryptamine 2.33 via a key Japp-Klingeman/Fischer indolization reaction sequence.....	45
Scheme 2-11. Synthesis of <i>N,N'</i> -bistosyltryptamine 2.34	46
Scheme 2-12. Synthesis of allylsilane 2.33	47
Scheme 2-13. Coupling of tryptamines 2.33/2.34 and carboxylic acid 2.35 and concomitant reduction to the hemiaminal ether substrates 2.31/2.32	48
Scheme 2-14. Reaction of hemiaminal ether substrates 2.31 and 2.32 with $\text{BF}_3 \cdot \text{OEt}_2$ to provide Pictet-Spengler products 2.51 and 2.52	49
Scheme 2-15. Reexamination of (<i>N</i> -Ts- <i>N'</i> -Cbz)tryptamine substrate 2.20 shows that it would potentially provide a more synthetically useful akuammiline alkaloid core.....	50
Scheme 2-16. Synthesis of <i>N</i> -tosyltryptamine hydrochloride salt 2.53	51
Scheme 2-17. Synthesis of <i>Z</i> -allylsilane carboxylic acid intermediate 2.59	52
Scheme 2-18. Synthesis of hemiaminal ether substrate 2.62	53
Scheme 2-19. Cyclization of hemiaminal ether 2.62 to tetracycle 2.63 with Lewis acid...	54
Scheme 2-20. Synthesis of <i>E</i> -allylsilane carboxylic acid 2.67	55

Scheme 2-21. Synthesis of hemiaminal ether substrate 2.70	56
Scheme 2-22. Cyclization of hemiaminal ether substrate 2.70 to diene product 2.70 obtained by a Pictet-Spengler cyclization.....	56
Scheme 2-23. Synthesis of benzyl protected hemiaminal ether substrate 2.74	57
Scheme 2-24. Cyclization of hemiaminal ether substrate 2.74 to provide previously obtained diene 2.71	58
Scheme 2-25. Development of optimized reaction conditions for cyclization of <i>Z</i> -allylsilane isomer 2.62 to tetracyclic akuammiline core 2.63	60
Scheme 2-26. Utilization of Ellman's auxiliary 2.64 in diastereoselective additions to amines, and the proposed iminium ion cascade annulation using Ellman's auxiliary as a chiral activating group.....	62
Scheme 2-27. Synthesis of <i>N</i> -acyl- <i>N</i> -benzylsulfonamides 2.72 and 2.73	62
Scheme 2-28. Attempted reaction of hemiaminal ether 2.74 with allyltrimethylsilane.....	65
Scheme 2-29. Attempted synthesis of indole containing intramolecular substrate 2.77	66
Scheme 2-30. Synthesis of anisyl-substituted substrate 2.83 and attempted cyclization under acidic conditions.....	67
Scheme 2-31. Examples of ion-pairing catalysis as applied to reactions containing iminium ion intermediates.....	68
Scheme 2-32. Asymmetric catalysis of malagashanine cascade with chiral phosphoramidate 2.90	68

Scheme 2-33. Examples of early attempts by Ricardo Delgado to mediate our cascade annulation with Bronsted acids.....	70
Scheme 2-34. Examples of the use of chiral disulfonimide catalysts by Benjamin List and coworkers in asymmetric additions of silylated nucleophiles to aldehydes.....	71
Scheme 2-35. Proposed method for in situ generation of <i>N</i> -trimethylsilyldisulfonimide catalyst 2.103 without protodesilylation of substrate.....	73
Scheme 2-36. Synthesis of disulfonimide catalyst 2.109 from BINOL.....	75
Scheme 2-37. Initial test reactions with stoichiometric quantities of disulfonimide 2.109	76
Scheme 2-38. Reactions with catalytic quantities of disulfonimide 2.109	77
Scheme 2-39. Control reaction of hemiaminal ether 2.16 with chlorotrimethylsilane and silver carbonate.....	78
Scheme 2-40. Attempted reaction of hemiaminal ether using disulfonimide catalyst 2.109 in the presence of silyl ketene acetal 2.95 as an activating reagent.....	79
Scheme 3-1. Initial retrosynthetic analysis for the synthesis of the methanoquinolizidine core of strictamine via a hydrocarboxylation strategy.....	151
Scheme 3-2. Formal hydroacylation used in the total synthesis of malagashanine, and the proposed formal hydrocarboxylation strategy on akuammiline core 3.6	152
Scheme 3-3. Reaction of organoboranes to form aldehydes and carboxylic acids.....	153
Scheme 3-4. Unsuccessful attempts at hydroboration of akuammiline core 3.6 with 9-BBN-H and less sterically hindered $\text{BH}_3\cdot\text{SMe}_2$	153

- Scheme 3-5.** Removal of TBDPS protecting group from akuammiline core **3.6**, and subsequent attempts at hydroboration.....**154**
- Scheme 3-6.** Attempted hydrozirconation of alkene in akuammiline alkaloid substrate **3.6**.....**154**
- Scheme 3-7.** Successful Johnson-Lemieux oxidation of malagashanine core **3.7**, and attempted oxidative cleavage of tetracycle **3.6**.....**155**
- Scheme 3-8.** Stepwise dihydroxylation/cleavage process of a sterically congested exocyclic olefin in the total synthesis of aspidophytine by E. J. Corey and coworkers....**156**
- Scheme 3-9.** Application of dihydroxylation conditions containing DMAP to a TBDPS protected Malagasy alkaloid core **3.23**.....**157**
- Scheme 3-10.** Attempted dihydroxylation with OsO₄/DMAP of exocyclic olefin in akuammiline alkaloid core **3.6**.....**157**
- Scheme 3-11.** Successful development of Johnson-Lemieux conditions for cleavage of exocyclic olefin **3.6** under microwave irradiation conditions.....**158**
- Scheme 3-12.** Successful oxidative alkene cleavage of exocyclic olefin **3.6** via ozonolysis.....**159**
- Scheme 3-13.** Proposed closure of E ring via a ketone addition/deoxygenation sequence.....**159**
- Scheme 3-14.** Cbz protecting group removal and amine alkylation, along with significant beta-elimination seen under differing basic conditions.....**160**

Scheme 3-15. Deiodination observed during attempted intramolecular Nozaki-Hiyama-Kishi coupling reaction.....	161
Scheme 3-16. Proposed intramolecular conjugate addition approach to strictamine, with synthesis from a β -ketoester intermediate 3.33	161
Scheme 3-17. Attempted removal of TBDPS protecting group on ketone 3.19	162
Scheme 3-18. Ozonolysis with reductive quench of both TBDPS ether 3.7 and homoallylic alcohol 3.16	163
Scheme 3-19. Attempted dual oxidation to 1,3-dicarbonyl derivative 3.37	163
Scheme 3-20. Proposed selective primary alcohol oxidation/beta-elimination sequence and attempts of selective primary alcohol oxidation of diol 3.36	164
Scheme 3-21. Attempted Shapiro reaction strategy.....	165
Scheme 3-22. Attempted synthesis of thermodynamic vinyl triflate 3.43	166
Scheme 3-23. Successful synthesis of vinyl triflate 3.46 using Comin's reagent.....	167
Scheme 3-24. Attempted synthesis of Michael acceptor for intramolecular conjugate addition.....	168
Scheme 3-25. Proposed coupling of necessary two carbon E ring fragment via cross-coupling methodology.....	168
Scheme 3-26. Initial attempts at a Stille coupling of vinyl triflate 3.48 with vinyltributylstannane.....	169
Scheme 3-27. Successful Stille coupling protocol for the synthesis of diene 3.51	170

Scheme 3-28. Retrosynthetic analysis for conversion of diene 3.51 into a ring-closed lactam core 3.56	171
Scheme 3-29. Successful hydroboration of terminal olefin in diene 3.51 to homoallylic alcohol 3.58	171
Scheme 3-30. Analysis of faces of the internal olefin of the C ring of 3.58 in terms of potential for hydrogenation and proposed intermediate 3.59 for directed hydrogenation.....	172
Scheme 3-31. Exposure of axially-position alcohol 3.59 for directed hydrogenation.....	173
Scheme 3-32. Propensity of cationic iridium hydrogenation catalysts to undergo deactivating trimerization under typical hydrogenation conditions.....	174
Scheme 3-33. Successful hydrogenation of internal olefin 3.59 with successive dosing of Crabtree's catalyst.....	175
Scheme 3-34. Deprotection of terminal E ring alcohol and subsequent oxidation to carboxylic acid 3.63	176
Scheme 3-35. Successful synthesis of pentacycle 3.64 via Cbz deprotection and lactamization with Mukaiyama's reagent.....	177
Scheme 3-36. Proposed conversion of tetracycle 3.6 into pseudoakuammigine core 3.65	177
Scheme 3-37. Conditions explored for removal of the indoline tosyl substituent (3.6)...	178
Scheme 3-38. Oxidation of indoline 3.67 to indolenine 3.68	179
Scheme 3-39. Silyl deprotection and cyclization to furoindoline pentacycle 3.65	179

Scheme 3-40. Prior synthetic route to pentacycle 3.64 and proposed more succinct route to related pentacycle 3.70	181
Scheme 3-41. Synthesis of cyclic hemiaminal ether substrate 3.71	182
Scheme 3-42. Cyclization of hemiaminal ether substrate 3.71 to strychnos-like core 3.78	183
Scheme 3-43. Rationale for lack of observed akuammiline core with cyclic hemiaminal ether substrate 3.71	184
Scheme 3-44. Retrosynthetic analysis for proposed open-chain hemiaminal ether substrate 3.84	185
Scheme 3-45. Synthesis of open-chain hemiaminal ether substrate 3.84	186
Scheme 3-46. Cyclization of open-chain hemiaminal ether substrate 3.84 to tentative tetracycle 3.87	186
Scheme 3-47. Preliminary data on the synthesis of (<i>E</i>)-allylsilane 3.89	187
Scheme 3-48. Proposed Future Route of New Akuammiline Core Toward Strictamine (3.4) and Pseudoakuammigine (3.66).....	188

Table of Tables

Table 2-1. Optimization of the synthesis of <i>N</i> -sulfinyl hemiaminal ethers 2.74 and 2.75 from <i>N</i> -acylsulfonamides 2.72 and 2.73	63
Table 2-2. Reaction of hemiaminal ether 2.74 with <i>N</i> -benzylindole.....	65
Table 3-1. Attempted directed hydrogenations of internal olefin 3.59 under various pressures.....	173

Chapter 1. The Akuammiline Alkaloids: Structure, Biology, and Synthesis

1.1 Introduction

The akuammiline alkaloids, a family of indole monoterpeneoids, are a diverse group of natural products that have been known for well over a century. The name of this alkaloid comes from the traditional name of the shrub *Picralima nitida* in western Africa, ‘akuamma’, where some of the original alkaloids were isolated.¹ The defining structural feature of all members of this alkaloid family is the key C7-C16 bond, whose presence often leads to sterically congested, polycyclic architectures (**Figure 1-1**). This characteristic, along with their known biological activity, have made these natural products the subject of synthetic studies for decades. However, the inherent challenges present in their topologies have prevented successful total syntheses from being completed until 2009.

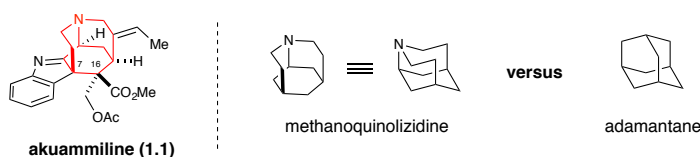
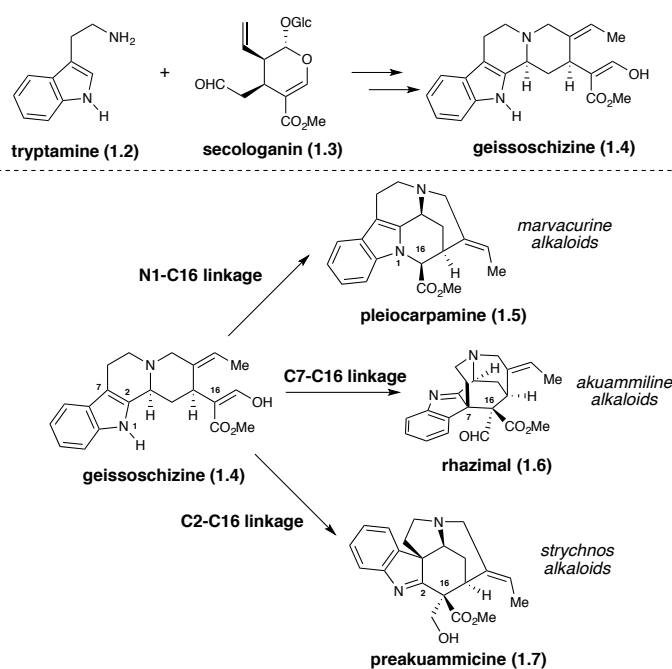


Figure 1-1. Representative akuammiline alkaloid structure and comparison of the topology of their methanoquinolizidine core with that of adamantane.

The complex polycyclic architecture of these indole alkaloids have inspired chemists for decades. The namesake alkaloid akuammiline (**1.1**), for example, contains a central cage-like methanoquinolizidine core composed of three six-membered rings and one eight-membered ring (**Figure 1-1**).² Initial visual inspection of this motif evokes comparison to the structure of adamantane, but also highlights some more inherent challenges into the synthesis of its structure. While sterically congested, the structure of

adamantane is inherently strain-free due to all four six-membered rings contained in its polycyclic structure sitting in a preferred chair conformation. With the methanoquinolizidine core, the medium-sized eight-membered ring introduces enough torsional strain that it enforces the two bridging six-membered rings to permanently sit in a boat conformation. This congested structure is the direct result of the defining C7-C16 linkage, a bond that essentially causes the molecule to be folded upon itself. These unusual features have both intimidated and intrigued synthetic chemists who have had interest in accessing these alkaloids for many years.

Scheme 1-1. Proposed biosynthesis of geissoschizine and conversion into marvacurine, akuammiline, and strychnos alkaloids.



The key C7-C16 linkage that leads to this complex structure appears to be born out from its possible biosynthesis (**Scheme 1-1**).³ Initial examination of the structural features of the akuammiline alkaloids show some similarities to other known alkaloid families, such as the strychnos and marvacurine alkaloids, revealing a potential shared biosynthetic origin

for these natural products.⁴ Geissoschizine (**1.4**), formed from the condensation of tryptamine **1.2** and the terpenoid secologanin (**1.3**), is proposed to be the biosynthetic precursor to for many indole monoterpene alkaloid families. This tetracyclic alkaloid can undergo various couplings or rearrangements to give a diverse array of natural products. Oxidative linkage of C16 and C7 in geissoschizine (**1.4**) provides the akuammiline alkaloid rhazimal (**1.6**), which is hypothesized to be the biosynthetic precursor for many alkaloids in this family. In comparison, a C2-C16 linkage with concomitant rearrangements provides the strychnos alkaloid preakuammicine (**1.7**), while a N1-C16 linkage leads to the formation of the marvacurine alkaloid pleiocarpamine (**1.5**). This shared biosynthetic pathway between these families of alkaloids foretells of the potential for shared synthetic strategies to access these natural products in the laboratory.

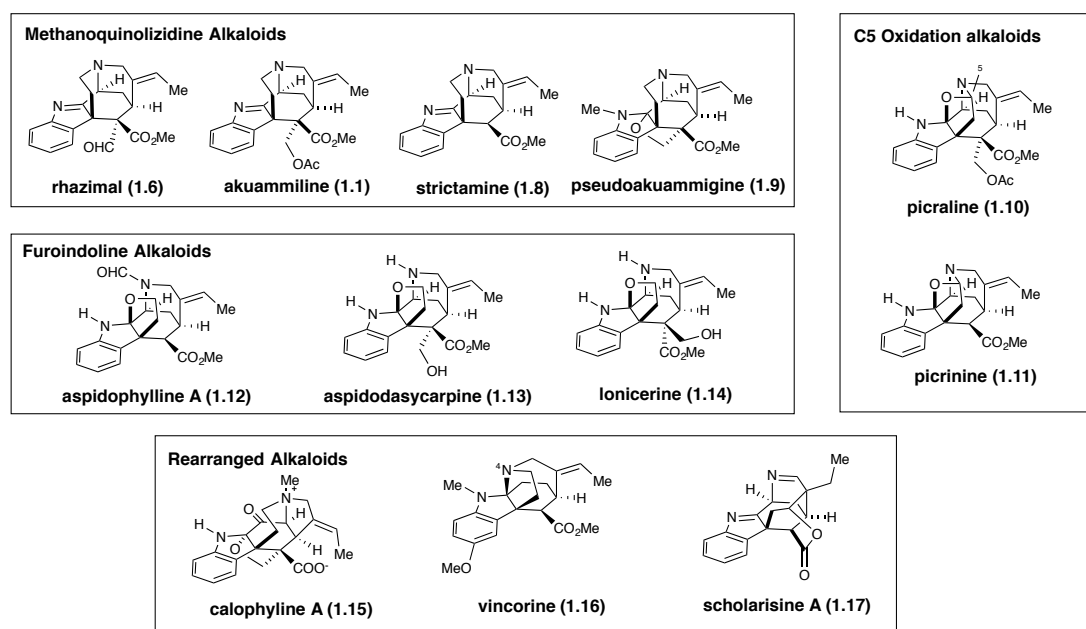
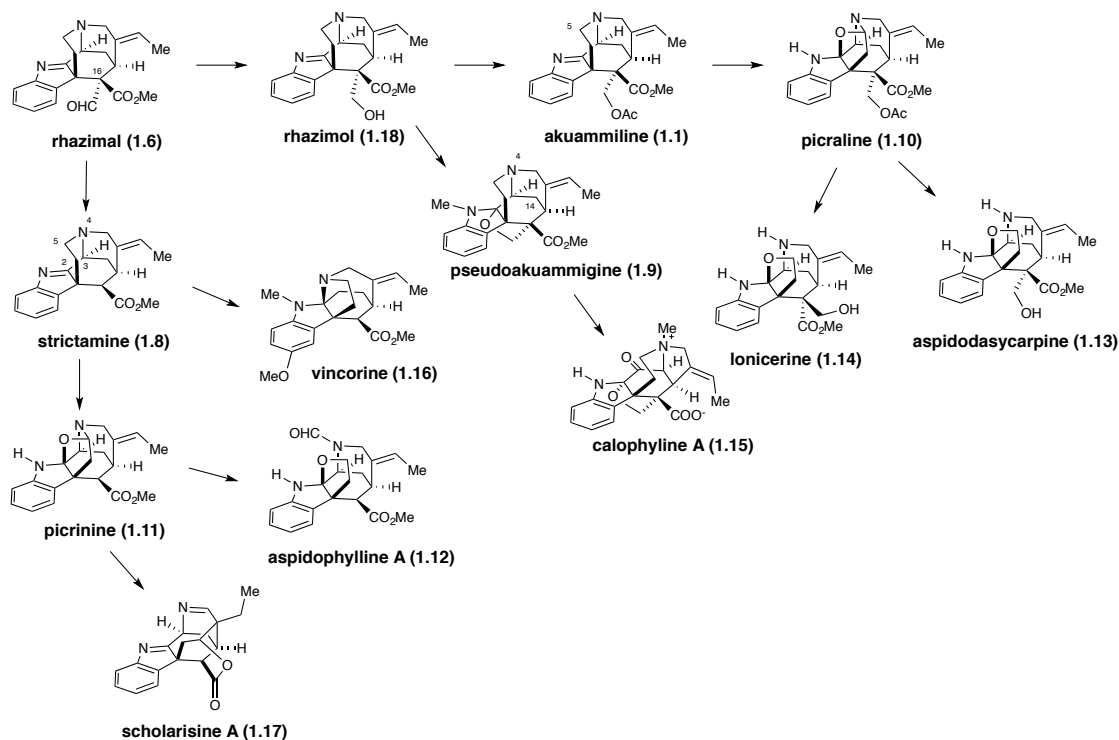


Figure 1-2. Classification of akuammiline alkaloids based upon structural features.

Scheme 1-2. Proposed biosynthetic pathway for representative akuammiline alkaloids from the biosynthetic precursor rhazimal (**1.6**).



The structural diversity of the akuammiline alkaloid family goes beyond the methanoquinolizidine alkaloids, such as rhazimal (**1.6**).⁵ This family of over 100 different alkaloids also contains many structurally diverse species that are the result of oxidations and rearrangements of the core structure (**Figure 1-2**). Examination of the structural features of these alkaloids leads to their categorization into several subgroups centering around modifications of the central methanoquinolizidine core. The parent alkaloid rhazimal (**1.6**) contains an unadulterated methanoquinolizidine core, and related members, such as akuammiline (**1.1**), strictamine (**1.8**), and pseudoakuammigine (**1.9**), can be grouped together based on this structural feature. C5 oxidation is the next differentiating feature that provides access to alkaloids such as picraline (**1.10**) and picrinine (**1.11**), which can be further modified via subsequent reductive cleavage toward another subgroup, the furoidoline derivatives such as aspidophylline A (**1.12**), aspidodasycarpine (**1.13**), and lonicerine (**1.14**). The last major grouping includes the rearranged alkaloids, which include

natural products such as scholarisine A (**1.17**), hypothesized to form from parent furoindoline alkaloids, and the alkaloids that are a product of N4 migration, such as calophylline A (**1.15**) and vincorine (**1.16**).

This structural diversity is again hypothesized to be the result of biosynthesis, all beginning with modifications of the alkaloid precursor rhazimal (**1.6**) via changes in oxidation state, acylations, alkylation, or subsequent rearrangements of the original skeletal framework (**Scheme 1-2**).⁴ Some major modifications stand out that provide access to unique structures within this family. First, reduction of the aldehyde in rhazimal (**1.6**) to rhazimol (**1.18**) provides access to numerous structures, such as the acetylated namesake alkaloid akuammiline (**1.1**) and the cyclized intermediate pseudoakuammigine (**1.9**). Alternatively, rhazimal may deformylate at C16, forming the natural product strictamine (**1.8**). From here, any of these intermediates may undergo a series of redox steps to provide eventual access to the furoindoline intermediates. C5 oxidation can provide access to a series of hemiaminal containing alkaloids, such as picraline (**1.10**) from akuammiline (**1.1**) and picrinine (**1.11**) from strictamine (**1.8**). Reduction of this hemiaminal intermediate provides the furoindoline alkaloids, such as aspidophylline A (**1.12**), lonicerine (**1.14**), and aspidodasycarpine (**1.13**). More structural diversity is obtained from skeletal rearrangements of these alkaloids. Migration of N4 from C3 to C2 in strictamine (**1.8**) leads to the alkaloid vincorine (**1.16**), while migration of N4 to C14 in pseudoakuammigine (**1.9**) with subsequent C3 oxidation would lead to calophylline A (**1.15**).

1.2 Biological Activity

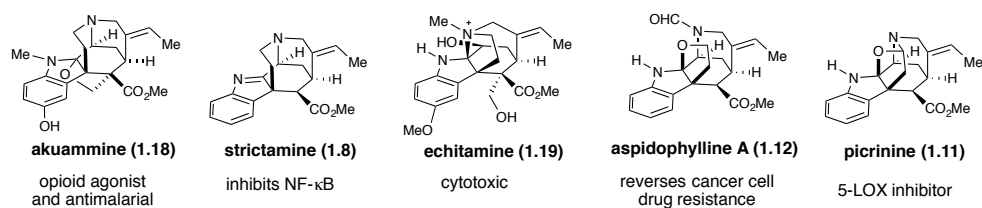


Figure 1-3. Representative biological activity of several akuammiline alkaloids.

Beyond just their interesting structural features, the akuammiline alkaloids also have promising biological activities, demonstrated by the significant use of plants containing these alkaloids in traditional medicine (**Figure 1-3**). Indeed, *Picralima nitida*, the tree from which akuammiline (**1.1**), akuammine (**1.18**), and pseudoakuammigine (**1.8**) are isolated, is used commonly to treat pain and malaria in Ghana, so much so that a Ghanaian pharmaceutical laboratory makes standardized capsules of the pulverized seeds.⁶ This ethnobotanical use of this shrub has been confirmed in laboratory studies, where the isolated alkaloid akuammine (**1.18**) has been confirmed both in vitro⁷ and in vivo⁸ to possess opioid receptor activity as well as antimalarial activity.⁹ The bark of the shrub *Rhazya stricta* is used in the Arabian Peninsula to treat helminthiasis.¹⁰ The natural product strictamine (**1.8**) isolated from this shrub has been demonstrated to inhibit the transcription factor NF-κB which is involved in the genetic regulation of inflammatory and immune responses.¹¹ Echitamine (**1.19**), an alkaloid related to vincorine (**1.16**) and isolate from *Winchia callophylla*, has demonstrated cytotoxicity both in vitro and in vivo.¹² Aspidophylline A (**1.12**), isolated from the Malaysian tree *Kopsia singaporensis*, was able to reverse drug resistance in resistant cancer cell lines.¹³ Picraline (**1.10**), also isolated from *P. nitida*, has been demonstrated to be an inhibitor of the SGLT2, a renal cortex protein involved in glucose reabsorption,¹⁴ while the related picrinine (**1.11**) has demonstrate anti-inflammatory activity by 5-LOX inhibition.⁸ These listed biological activities are just

representative, with more extensive examination of their pharmacological activity detailed in several reviews.^{4-5,15}

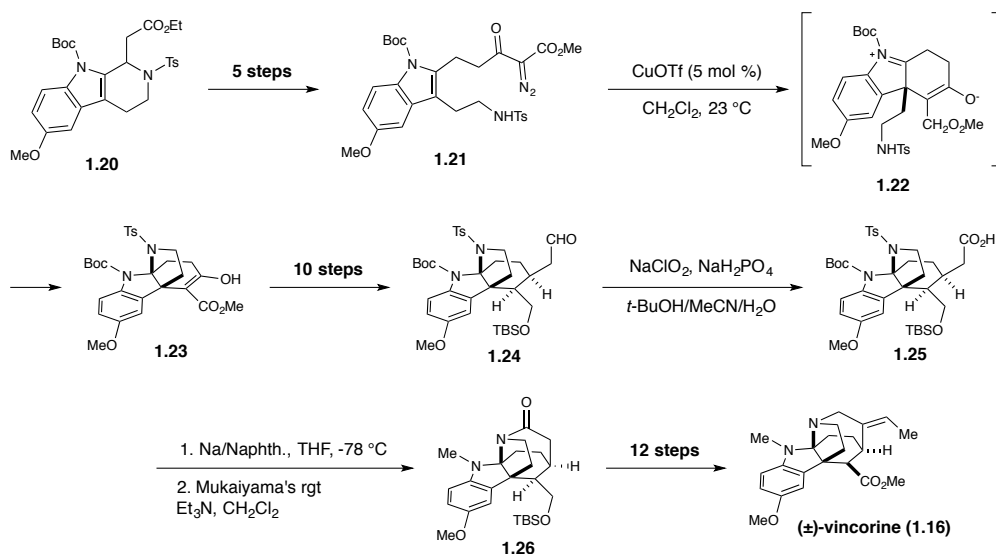
1.3 Akuammiline Alkaloids: Prior Synthetic Studies

Both these intriguing structural features and biological activity outlined above have caught the attention of synthetic chemists for some time, but it was only within the past decade that successful forays into this natural product family have occurred. The rest of this chapter will be composed of the analysis of prior total syntheses of this family of alkaloids; in particular, we will focus our attention on vincorine (**1.16**), aspidophylline A (**1.12**), and scholarisine A (**1.17**), some of the most heavily studied original alkaloids in this family, along with some related natural products that may have had single total syntheses completed. Lastly, our focus will center on the methanoquinolizidine-containing akuammiline alkaloids, natural products that have only very recently succumbed to successful total synthesis but that had been the topic of study since these alkaloids first caught the attention of the synthetic community. Indeed, no successful synthesis had been completed at the time the studies in this thesis had begun. We will delve more deeply into these early synthetic studies, both successful and unsuccessful, as well as the recently completed syntheses, as they are informative of the challenges present in the syntheses of these alkaloids.

1.3.1 Total Syntheses of Vincorine

Vincorine (**1.14**) was the first akuammiline alkaloid to successfully succumb to total synthesis. This alkaloid is characterized by its cyclotryptamine motif, formed as the result of the migration of N4 from C3 to C2 in the parent alkaloid strictamine. This particular motif subsequently became the focus of all groups who completed syntheses of this natural product, often using cascade processes to that end.

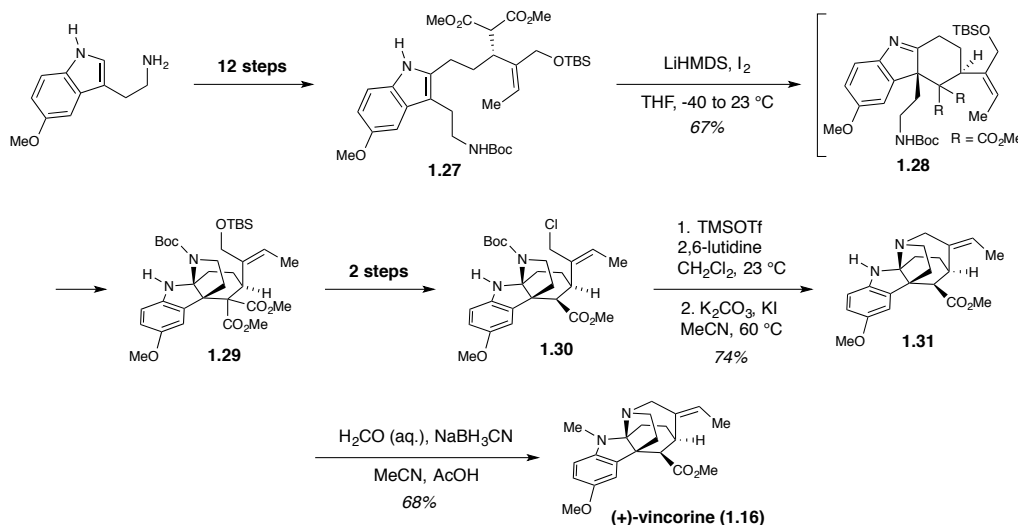
Scheme 1-3. Total synthesis of vincorine (1.16) by Yong Qin and coworkers using a key indole cyclopropanation/ring-opening/cyclization cascade.¹⁶



The first synthesis of vincorine (**1.14**) was completed by Yong Qin and coworkers in 2009 (Scheme 1-3).¹⁶ Their strategy centered around the use of a cyclopropanation/ring-opening/cyclization cascade to forge the key cyclotryptamine motif present in the natural product. The precursor diazo **1.21** for this cascade transformation was available in five steps from known tetrahydro- β -carboline **1.20**. Subsequent cyclopropanation of the indole ring provides an aminocyclopropane intermediate which readily ring opens to provide an indolenium ion **1.22** that is quickly trapped by the pendant ethylamine chain, forming cyclotryptamine **1.23**. While providing quick access to their desired core, the initial

intermediate proved challenging to move forward with their initially desired intramolecular Heck strategy, instead requiring significant manipulation to provide an intermediate that could close the final ring by intramolecular lactamization. Over 11 steps, cyclotryptamine **1.23** is oxidized to carboxylic acid **1.25**, which upon removal of the tosyl protecting group under reductive conditions and coupling with Mukaiyama's reagent provides lactam **1.26**. This intermediate was converted over 12 steps into vincorine (**1.16**), providing the natural product in a total of 30 steps. Despite the high step count, the Qin group was able to successfully gain access to the first natural product within this family, a significant accomplishment at the time.

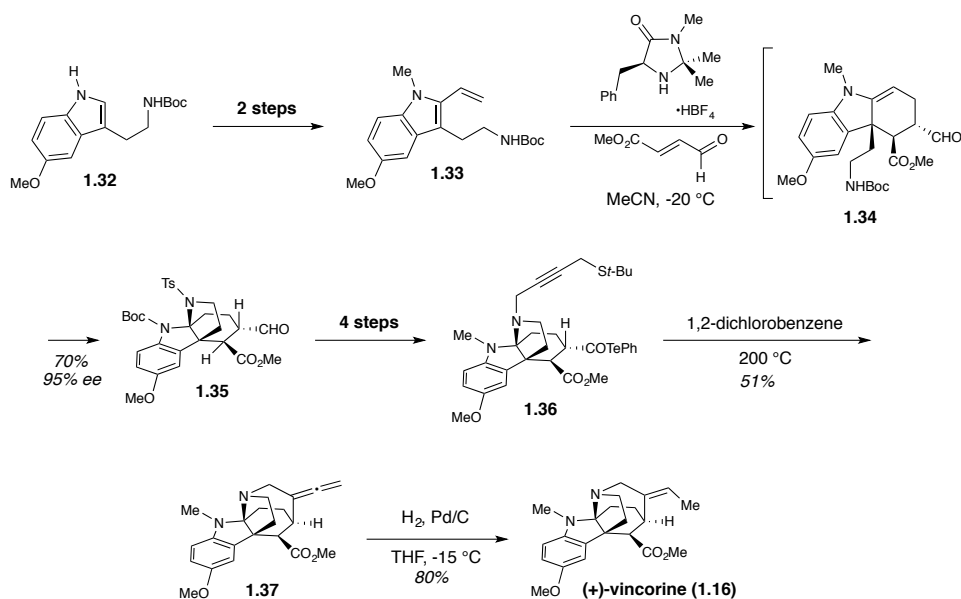
Scheme 1-4. Total synthesis of vincorine (1.16) by Dawei Ma and coworkers using a oxidative coupling cascade as the key step.¹⁷



In 2012, Dawei Ma and coworkers completed the first enantioselective synthesis of vincorine using an oxidative coupling cascade to forge the key cyclotryptamine core (**Scheme 1-4**).¹⁷ This approach used the same bond disconnections as the Qin cascade, but provided access to a more properly decorated product to complete the total synthesis,

effectively shortening the number of steps necessary to finish the natural product. The cyclization precursor **1.27** is available over twelve steps from 5-methoxytryptamine. Double deprotonation of indole N-H and malonate in intermediate **1.27**, followed by exposure to molecular iodine promotes an oxidative coupling between the central malonate carbon and the 3 position of the indole, forging an indolenine **1.28** that readily cyclizes with the pendant Boc-protected ethylamine chain, providing cyclotryptamine intermediate **1.29**. This intermediate contains the necessary functionality to synthesize the final ring of the natural product in short order. Conversion of the pendant allylic silyl ether into an allylic chloride **1.30**, followed by Boc deprotection of the D ring amine and reaction under basic alkylation conditions provided the pentacycle **1.31**, which could be converted to vincorine (**1.16**) over one step. Their route successfully provided vincorine in a total of 18 steps.

Scheme 1-5. Total synthesis of vincorine (1.16) by David MacMillan and coworkers using an enantioselective Diels-Alder/cyclization cascade and intramolecular radical cyclization as key steps.¹⁸



In 2013, David MacMillan and coworkers completed a very succinct enantioselective synthesis of vincorine (**1.16**) (**Scheme 1-5**).¹⁸ Their strategy centered around an organocatalytic Diels-Alder reaction between vinylindole **1.33**, available in two steps from protected 5-methoxyindole **1.32**, and an unsaturated aldehyde providing an intermediate **1.34** that would readily cyclize under the acidic reaction conditions to cyclotryptamine **1.35**. This approach mimics that used by Levy and coworkers in a model system toward this natural product. Cyclotryptamine **1.35** could be readily converted to intermediate **1.36** over four steps. The final ring in the natural product was constructed by cyclization of a secondary radical, formed by decomposition of an acyl telluride, onto the propargyl thioether chain, providing an exocyclic allene **1.37** that was selectively hydrogenated to vincorine (**1.16**). The MacMillan group was able to complete the shortest synthesis of vincorine (**1.16**) to date, providing the natural product in nine steps.

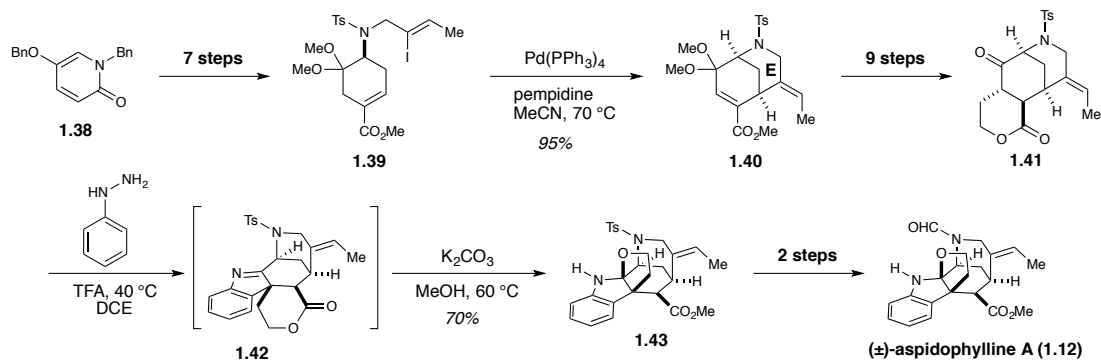
1.3.2 Total Syntheses of Aspidophylline A

Aspidophylline A (**1.12**) was one of the earliest targets, and subsequently turned into one of the most popular, within this alkaloid family, with four successful total syntheses having been completed to date. This natural product is a characteristic member of the furoindoline subgroup of akuammiline alkaloids. This characteristic motif has typically been the main focus of syntheses of this natural product, with many of the strategies focusing on ways to forge the key furoindoline moiety.

The seminal publication of the total synthesis of aspidophylline A (**1.12**) came from Neil Garg and coworkers in 2011.¹⁹ Their approach centered around two key steps: an intramolecular Heck reaction to form the E ring, and an interrupted Fischer indolization

reaction to forge the key furoindoline system in the natural product. Their Heck cyclization substrate **1.39**, readily prepared from 2-pyridinone **1.38** over seven steps, efficiently cyclized to form bicycle **1.40**, which was converted into lactone **1.41** over nine steps. Reaction of this substrate with phenylhydrazine in the presence of trifluoroacetic acid led to the synthesis of indolenine **1.42** via an interrupted Fischer indolization, whose lactone motif was subsequently opened in basic methanol to form the furoindoline intermediate **1.43**. This intermediate was readily converted to aspidophylline A (**1.12**), providing the natural product in a total sequence of 22 steps. Neil Garg and coworkers later published a shorter 17 step enantioselective synthesis of this natural product in 2016 that centered around a similar approach.²⁰

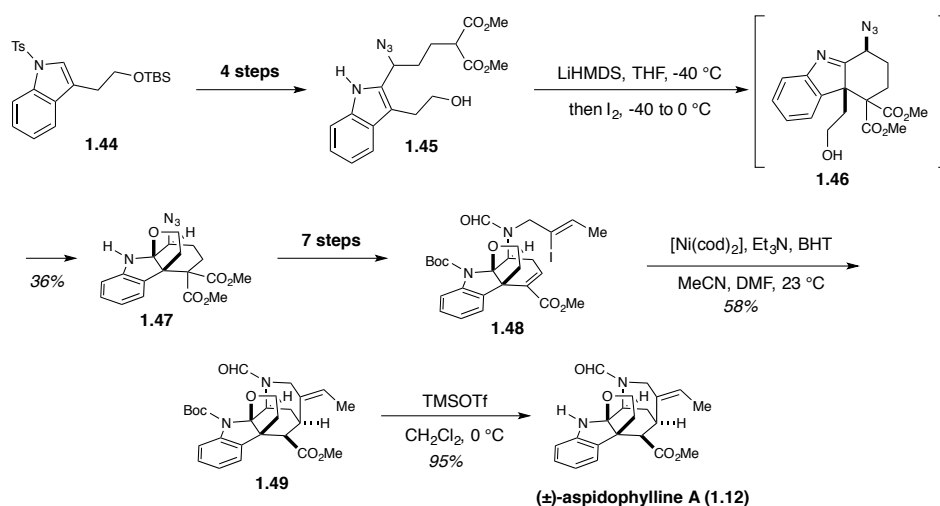
Scheme 1-6. Total synthesis of aspidophylline A (1.12**) by Neil Garg and coworkers using key Heck cyclization and interrupted Fischer Indolization steps.**¹⁹



Dawei Ma and coworkers completed a shorter synthesis of aspidophylline A (**1.12**) in 2014 centered around an oxidative indole/malonate coupling reaction, a strategy they have used in the synthesis of many different indole alkaloids (**Scheme 1-7**).²¹ Beginning from protected tryptophol derivative **1.44**, they were able to obtain the required substrate **1.45** for oxidative cyclization over four steps. Upon double deprotonation of this intermediate followed by reaction with iodine, this intermediate underwent efficient

oxidative coupling to indolenine **1.46** followed by cyclization to the furoindoline core **1.47**. Conversion of this intermediate over seven steps provided the intramolecular Heck reaction precursor **1.48**, which readily cyclized to the pentacycle **1.49**. This intermediate was readily converted into aspidophylline A (**1.12**) upon removal of Boc protection with trimethylsilyltriflate. Dawei Ma and coworkers were able to access this natural product over a total of 14 steps.

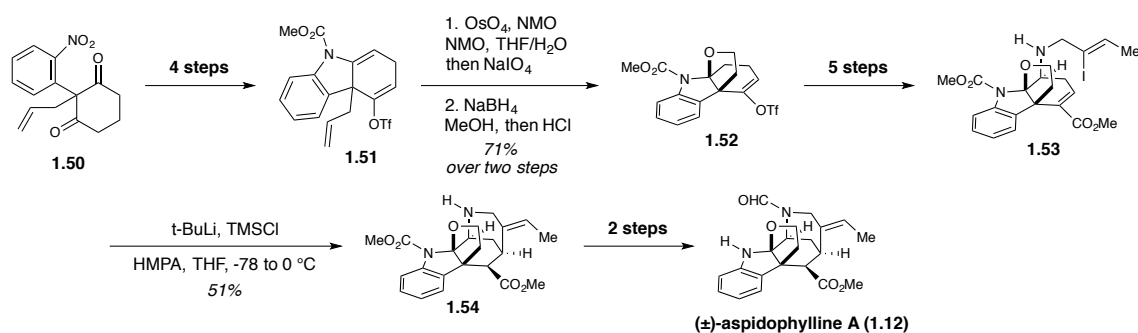
Scheme 1-7. Total synthesis of aspidophylline A (1.12) by Dawei Ma and coworkers using a key oxidative coupling/cyclization cascade.²¹



Concomitant with the previous Ma synthesis, Jieping Zhu and coworkers completed a short synthesis of aspidophylline A (**1.12**) that began from 1,3-diketone **1.50**, a known intermediate used in several syntheses of indole alkaloids (**Scheme 1-8**).²² This intermediate was readily converted into vinyl triflate **1.51**, whose pendant allyl chain was transformed into an aldehyde via sequential Upjohn dihydroxylation conditions followed by cleavage with sodium periodate. Reduction of this aldehyde to the alcohol with sodium borohydride followed by acid-mediated cyclization provided furoindoline core **1.52**. This tetracycle was then converted into vinyl iodide **1.53** over five steps, an intermediate that

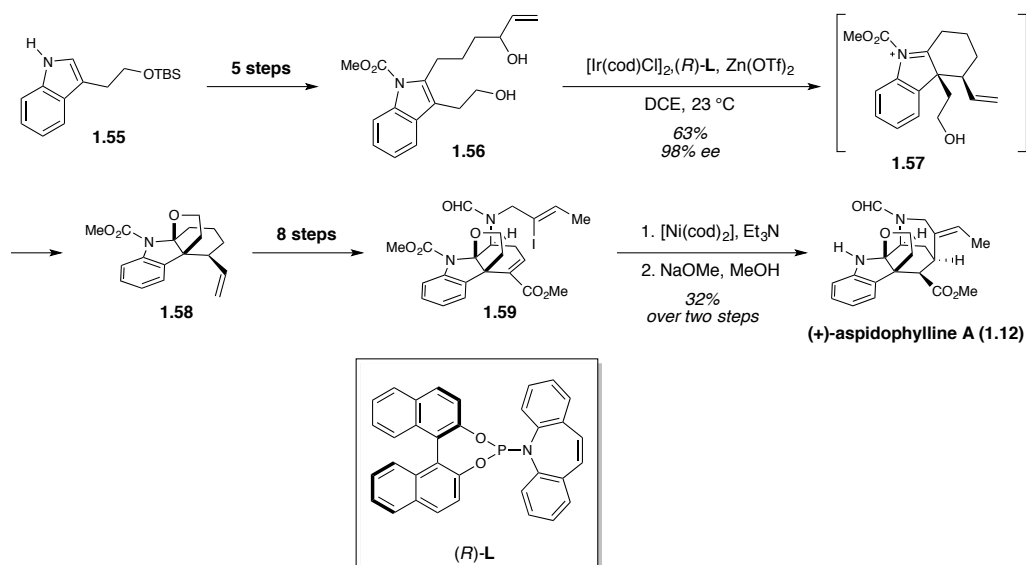
successfully underwent intramolecular conjugate addition via lithium-halogen exchange of the vinyl iodide, providing pentacycle **1.54**. This intermediate was readily converted to aspidophylline A (**1.12**) over two steps, providing a successful total synthesis over a total of 14 steps.

Scheme 1-8. Total synthesis of aspidophylline A (1.12) by Jieping Zhu and coworkers via key oxacyclization and intramolecular conjugate addition steps.²²



Yu-Rong Yang and coworkers successfully published the first enantioselective synthesis of aspidophylline A (**1.12**) in 2016 using a key iridium-catalyzed cyclization cascade (**Scheme 1-9**).²³ The cascade substrate **1.56** was readily accessed from protected tryptophol **1.55** over five steps. This key step involved reaction of a pendant indole with an allyliridium intermediate generated from allyl alcohol, followed by reaction of a pendant alcohol chain with the formed indolenium ion **1.57**, subsequently providing furoindoline core **1.58**. High enantioselectivity was able to be achieved by the use of the Carreira phosphoramidate ligand (*R*)-**L** in this process. This intermediate was readily converted into vinyl iodide **1.59** over eight steps, which was subjected to Nickel-mediated intramolecular conjugate addition followed by deprotection to provide aspidophylline A (**1.12**), completing the synthesis in a total of 16 steps.

Scheme 1-9. Total synthesis of aspidophylline A (1.12) by Yu-Rong Yang and coworkers using a key enantioselective iridium-catalyzed cyclization cascade.²³



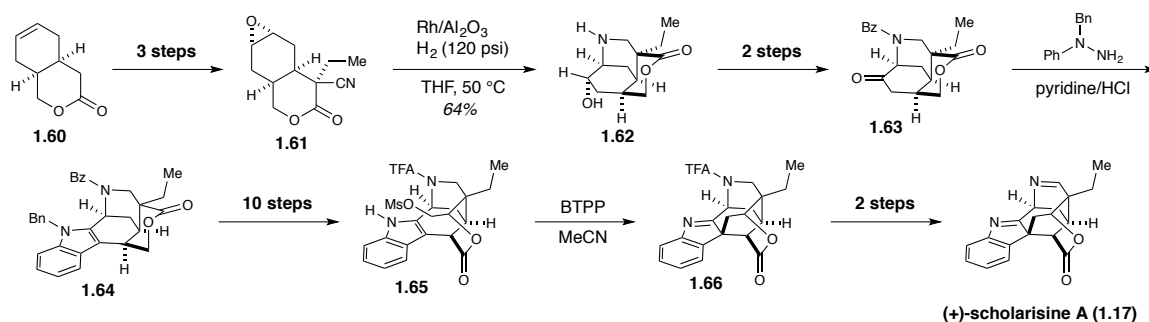
1.3.3 Total Syntheses of Scholarisine A

Scholarisine A (**1.17**) is one of the more structurally distinct of the akuammiline alkaloids due to its bridged bicyclic lactone structure, the result of a proposed rearrangement of a C5-oxidized alkaloid. This structural motif contains four of the five stereocenters present in the natural product, two of them being quaternary. Not surprisingly, this turned into one of the main challenges in this alkaloid's construction, becoming the focus of the two completed syntheses of this natural product.

The first successful synthesis of scholarisine A (**1.17**) by Amos Smith and coworkers was completed in 2012 (**Scheme 1-10**).²⁴⁻²⁵ Their synthetic sequence begins with bicyclic lactone **1.60**, a readily available Diels-Alder adduct, which was successfully manipulated to epoxide **1.61** in three steps. Hydrogenation over rhodium on alumina successfully reduced the nitrile present in this intermediate to the primary amine, which

readily cyclized onto the epoxide to form tricyclic intermediate **1.62**. Subsequent protection and oxidation provided ketone **1.63**, which underwent Fischer indole synthesis with 1-benzyl-1-phenylhydrazine to provide the indole **1.64**. To close the final ring in the structure, lactone **1.64** was converted into mesylate **1.65** over a non-trivial sequence of ten steps. Intramolecular cyclization of the mesylate with the indole under basic conditions provided indolenine **1.66**, which was converted over two steps into scholarisine A (**1.17**) and providing the natural product in a total of 20 steps.

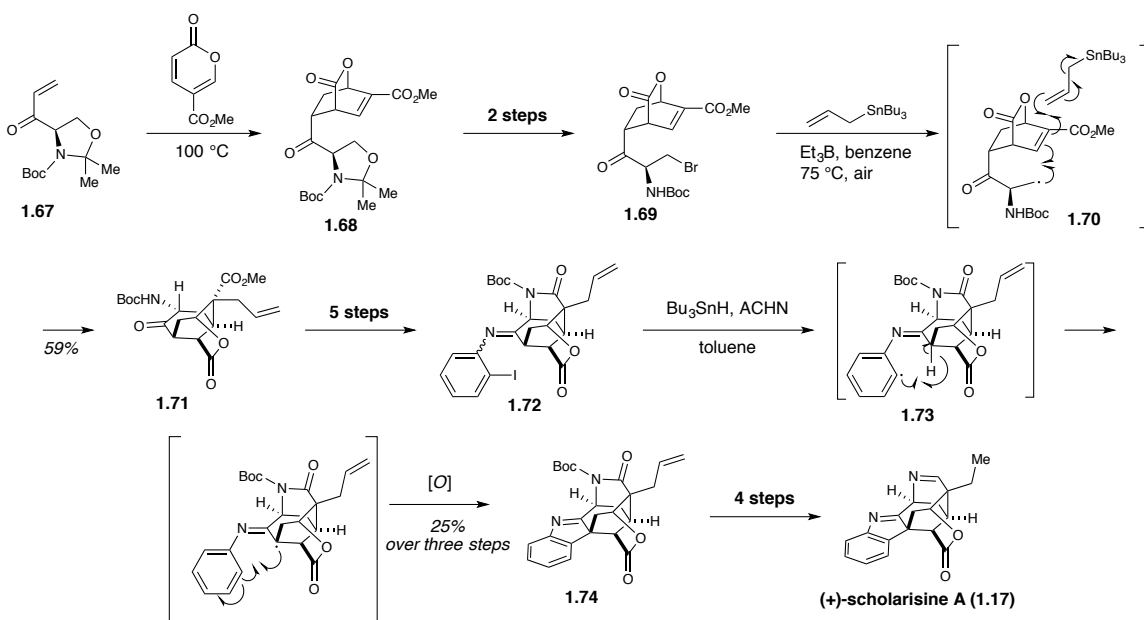
Scheme 1-10. Total synthesis of scholarisine A (1.17) by Amos Smith and coworkers featuring key aminocyclization and indole alkylation steps.²⁴



Scott Snyder and coworkers utilized a different approach to scholarisine A (**1.17**), instead forming the bridged bicyclic lactone system early in the synthesis and building the rest of the molecule around it (**Scheme 1-11**).²⁶ They intelligently noted that the bicyclic lactone in the natural product resembled ring structures obtained from a Diels-Alder reaction with 2-pyrone. The reaction of a substituted pyrone with α,β -unsaturated ketone **1.67** provided bicycle **1.68**, which was readily converted to bromide **1.69** over two steps. A cyclization cascade, consisting of decomposition of the alkyl bromide to primary radical **1.70**, conjugate addition onto the pendant α,β -unsaturated ester, and trapping of the resultant radical via Keck allylation, furnished the bridged tricyclic system **1.71**. The final

indolenine ring in the natural product was assembled via a radical-mediated C-H functionalization reaction, wherein (2-iodophenyl)imine **1.72**, prepared from tricycle **1.71** in five steps, underwent radical decomposition to the aryl radical **1.73**, which abstracted the adjacent proton from the tertiary C7 position. The newly formed tertiary radical cyclized onto the aromatic ring, providing indolenine **1.74** upon air oxidation. This intermediate was readily converted into scholarisine A (**1.17**) over four steps. Scott Snyder and coworkers completed a successful synthesis of this natural product over 14 steps.

Scheme 1-11. Total synthesis of scholarisine A (1.17**) by Scott Snyder and coworkers using key radical cascade and C-H functionalization steps.**²⁶

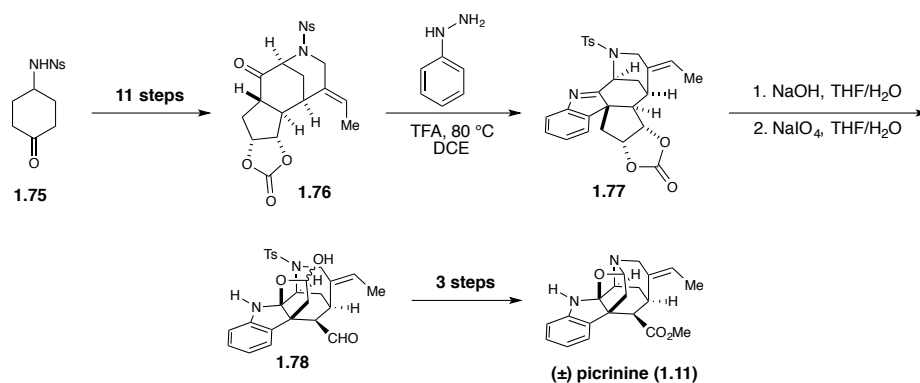


1.3.4 Total Syntheses of Other Akuammiline Alkaloids

Other alkaloids within this family have also been explored via synthesis, but often in single instances by individual groups. One of these alkaloids, the C5-oxidized alkaloid picrinine (**1.11**), had a total synthesis completed by Neil Garg and coworkers in 2014

(Scheme 1-12).²⁷⁻²⁸ Their approach paralleled the one they used in the synthesis of aspidophylline A (**1.12**) but was informed by the higher oxidation state present at the C5 stereocenter. The key ketone intermediate **1.76**, available over 11 steps from protected 4-aminocyclohexanone **1.75**, was cyclized under via Fischer indolization to provide indolenine **1.77**. Unlike the related aspidophylline A intermediate, which contained a lactone moiety, this intermediate contained a protected diol. Deprotection and oxidative cleavage of this diol would provide a dialdehyde wherein the more properly positioned of the two groups could cyclize onto the indolenine to form hydroxyfuroindoline intermediate **1.78**, which was readily converted into the natural product over three additional steps. Neil Garg and coworkers were able to successfully complete a total synthesis of picrinine (**1.11**) over a total of 17 steps.

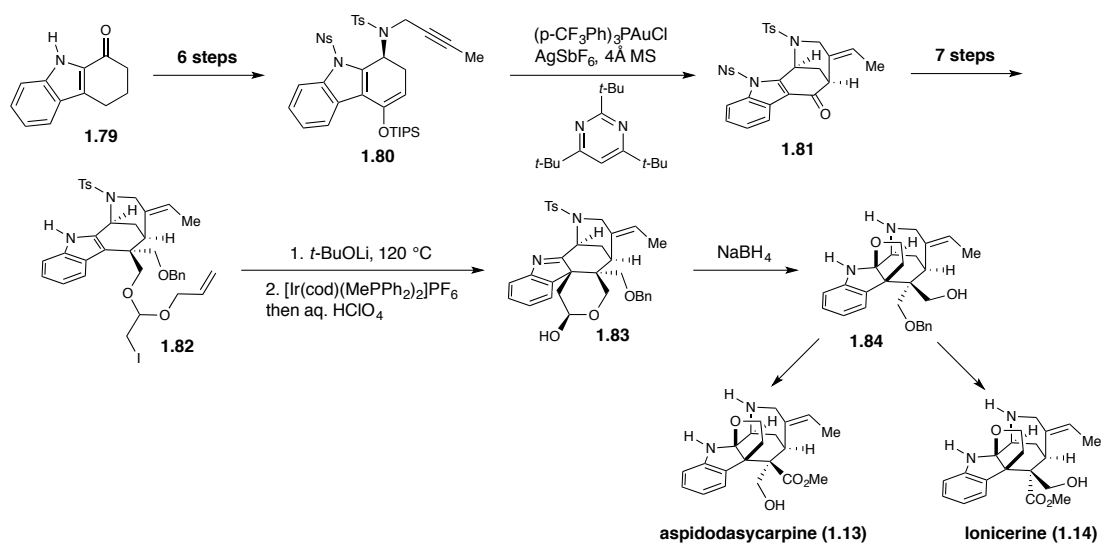
Scheme 1-12. The total synthesis of picrinine (1.11) by Neil Garg and coworkers using key Fischer indolization and diol cleavage/oxacyclization steps.²⁷



While most groups focused on the simpler furoindoline alkaloid aspidophylline A, Ang Li and coworkers instead sought out a successful synthesis of the more substituted natural products aspidodasycarpine (**1.13**) and lonicerine (**1.14**), completing total syntheses of these natural products in 2016 (Scheme 1-13).²⁹ These natural products would prove

significantly more challenging than some of the other previously explored alkaloids due to the presence of the vicinal C7 and C16 quaternary stereocenters in their central core. To address this issue, Ang Li had to use a somewhat different approach, using an intramolecular gold-catalyzed cyclization and an intramolecular alkylation to form key stereocenters. Beginning from indole intermediate **1.79**, they were successfully able to synthesize cyclization substrate **1.80** enantioselectively over six steps. Gold-mediated cyclization between the TIPS enol ether and the pendant alkyne furnished ketone intermediate **1.81**, which was readily converted into iodide **1.82** over seven steps. C-3 alkylation of the indole followed by allyl protecting group removal furnished lactol **1.83**, which readily cyclized to furoindoline **1.84** upon reduction with sodium borohydride. Subsequent protecting group manipulations and oxidations provided access to both aspidodasycarpine (**1.13**) and lonicerine (**1.14**).

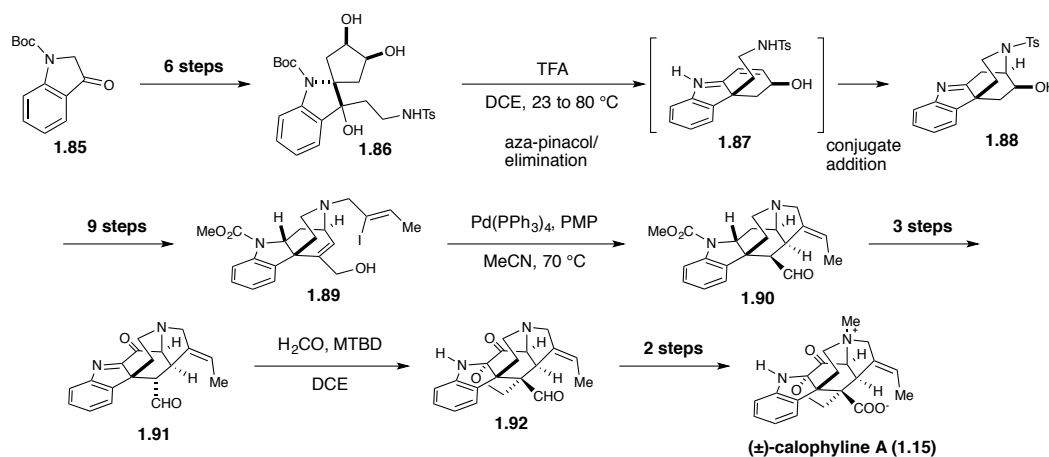
Scheme 1-13. Total synthesis of aspidodasycarpine (1.13) and lonicerine (1.14) by Ang Li and coworkers using key gold-catalyzed cyclization and indole alkylation steps.²⁹



In 2016, Liansuo Zu and coworkers published the first total synthesis of calophylline A (**1.15**), a rearranged akuammiline alkaloid characterized by migration of the N4 nitrogen from C3 to C14 (**Scheme 1-14**).³⁰ This is the only alkaloid in this family known to have this specific migration pattern. Additionally, it is one of the few alkaloids with a cyclized furoindoline motif derived from a C16 substituent, similar to that seen in akuammiline and pseudoakuammiline; no successful synthesis of an akuammiline alkaloid containing such a motif had been completed up to this point. Their approach centered around a cascade process beginning from spirocycle **1.86**, available from protected 3-indolenone **1.85** in six steps. Reaction of this intermediate in the presence of trifluoroacetic acid leads to formation of a tertiary carbocation that readily undergoes an aza-pinacol rearrangement, leading to a product that readily eliminates under the acidic conditions to unsaturated imine **1.87**. This intermediate is readily trapped with the pendant sulfonamide chain, forming tetracycle **1.88**. This intermediate is converted over nine steps to allylic alcohol **1.89** which undergoes an intramolecular Heck cyclization to provide aldehyde **1.90**. The last major goal for the synthesis of this natural product was the introduction of the final substituent on the C16 stereocenter which would subsequently cyclize to form the key furoindoline motif. In order for this to successfully work, they required both oxidation of the indoline up to the indolenine, as well as C3 oxidation, in order for successful aldol condensation on the C16 center to occur. Presumably these oxidations made the axial face of the formed enolate more accessible to reaction with formaldehyde. This could be readily accomplished in three steps, providing intermediate **1.91**. This substrate **1.91** successfully reacted under basic conditions with formaldehyde to provide furoindoline intermediate **1.92**, which was readily converted into calophylline A (**1.15**) over two steps. Ang Li and

coworkers were successfully able to complete a total synthesis of this natural product over 22 steps.

Scheme 1-14. Total synthesis of calophyline A (1.15) by Liansuo Zu and coworkers, centering around an aza-Pinacol/Elimination/Conjugate Addition cascade.³⁰



1.4 Methanoquinolizidine Alkaloids: Prior Synthetic Studies and Total Syntheses of Strictamine

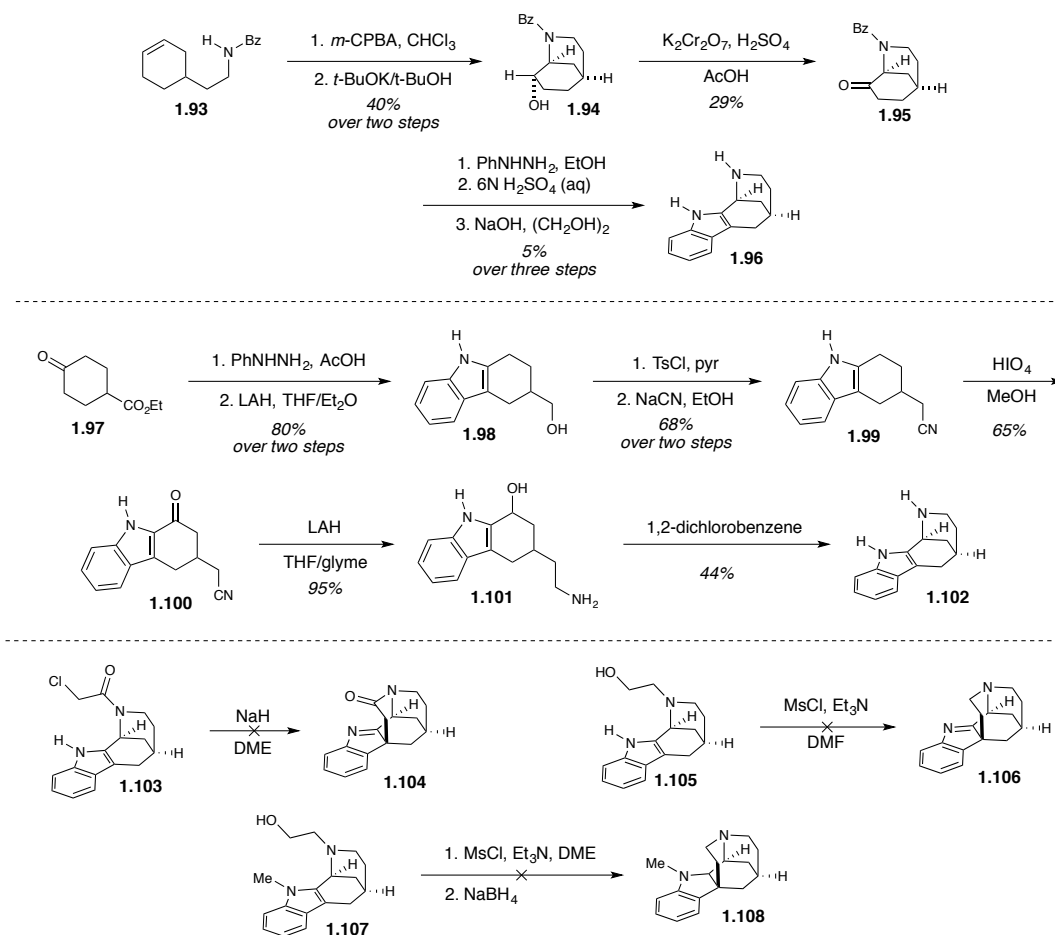
Despite the methanoquinolizidine subgroup of akuammiline alkaloids being some of the first isolated, success total syntheses of any members of this subgroup were not completed until 2016. However, many studies toward these alkaloids have been performed since the 1970s, all with varying levels of success. Despite this, the challenges faced when facing these motifs informed the strategy of those who were able to successfully complete syntheses of these natural products.

In the early 1970s, Lloyd Dolby and coworkers performed a series of model studies toward a methanoquinolizidine core of the akuammiline alkaloids (**Scheme 1-15**).³¹⁻³² Knowing that synthesizing the C7 quaternary center would be one of the more challenging

aspects of this synthesis, Dolby hypothesized that this center could potentially be formed by reaction of an indole and a pendant electrophilic chain, forging the C ring in a final step from an indole substituted bicyclic precursor. In order to test this hypothesis, they had to synthesize a prerequisite 1-aza-[3.3.1]bicyclononane substrate **1.96** containing a fused indole to react with the pendant electrophile. Initially they were able to access this structure from substituted cyclohexene **1.93** by epoxidation and base-mediated amide cyclization to provide alcohol **1.94**, which was subsequently oxidized to ketone **1.95**. Subsequent Fischer indole synthesis provided the desired structure **1.96**, albeit in low enough of yield to warrant an alternative approach. Beginning with 4-carbethoxycyclohexanone **1.97**, Fischer indolization and subsequent reduction with lithium aluminum hydride provided alcohol **1.98**, which was homologated with cyanide via a two-step protocol to intermediate **1.99**. Subsequent benzylic oxidation with periodic acid to ketone **1.100**, followed by reduction of both the ketone and nitrile moieties with lithium aluminum hydride provided the amino alcohol **1.101**, which cyclized to the desired core **1.102** upon heating in 1,2-dichlorobenzene. The free nitrogen of the bicycle could be coupled with various substituents for forming the C ring. Subsequent attempts to complete this final ring closure proved to be unsuccessful. Using either an α -chloroamide **1.103** or one pot mesylation/alkylation with alcohol **1.105** proved unsuccessful, as well as *N*-methylindole substrate **1.107**, presumably used to prevent possible N1 alkylation. While this strategy proved unsuccessful, it did provide insights for future groups looking to synthesize these natural products.

Scheme 1-15. Studies by Dolby and coworkers toward an akuammiline alkaloid methanoquinolizidine core.³¹⁻³²

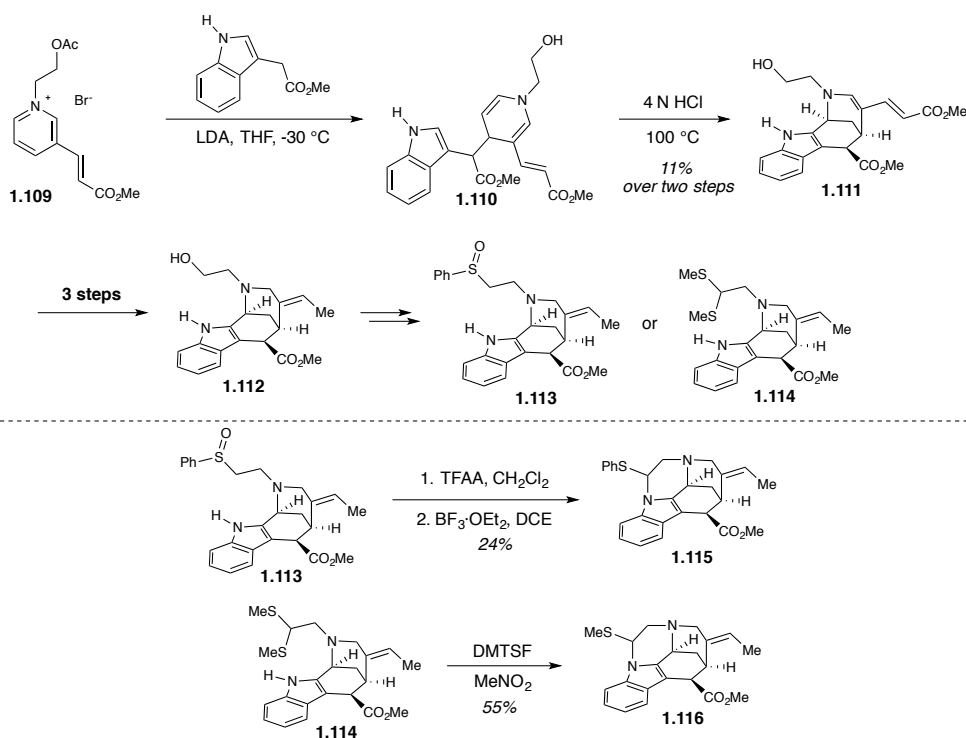
core.



Joan Bosch and coworkers further explored this strategy in the 1980s, providing a quick synthetic sequence to a 1-aza[3.3.1]bicyclononane core similar to that obtained by Dolby, but substituted with the functionality present in the natural product strictamine (**1.18**) (Scheme 1-16).³³⁻³⁴ Their synthesis of this core began by addition of the dianion of the methyl ester of indole-3-acetic acid to the pyridinium bromide **1.109**, providing dihydropyridine **1.110**. This material readily cyclized under acidic conditions to provide the 1-aza[3.3.1]bicyclononane core **1.111**. The extended carbamate in this intermediate could be readily converted over three steps to an intermediate **1.112** containing the

allylamine of the E ring as present in strictamine (**1.18**). The Bosch group explored the formation of this final bond via activation of the alcohol, but found no desired cyclization, similar to what was observed previously by Dolby. In addition, the Bosch group explored alternative strategies, such as the use of thionium ions either generated from a pummerer rearrangement of sulfoxide **1.113** or via a thioacetal intermediate **1.114**, to forge the final ring. However, these intermediates cyclized on the less sterically-hindered indole nitrogen instead of at the 3 position of the indole, providing pentacycles **1.115** and **1.116**, thus proving this strategy to be unsuccessful.

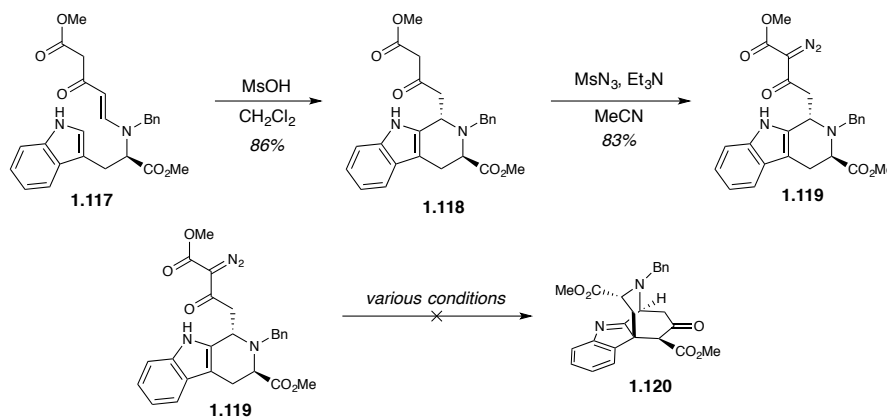
Scheme 1-16. Studies by Bosch and coworkers toward the akuammiline alkaloids.³³⁻³⁴



In 2012, James Cook and coworkers reported studies where they analyzed cyclization reactions of enaminones, producing the core structures of several types of indole alkaloids (**Scheme 1-17**).³⁵ Within these studies, they successfully cyclized

enaminone intermediate **1.117** to tetrahydro- β -carboline **1.118** whose motif could be mapped onto the akuammiline alkaloids. They envisioned cyclizing to a tetracyclic intermediate **1.120** via cyclopropanation of the indole ring, followed by ring opening to the indolenine. Conversion of the β -carboline intermediate **1.118** to diazo **1.119** was successful, but no cyclization was observed under a variety of conditions tested.

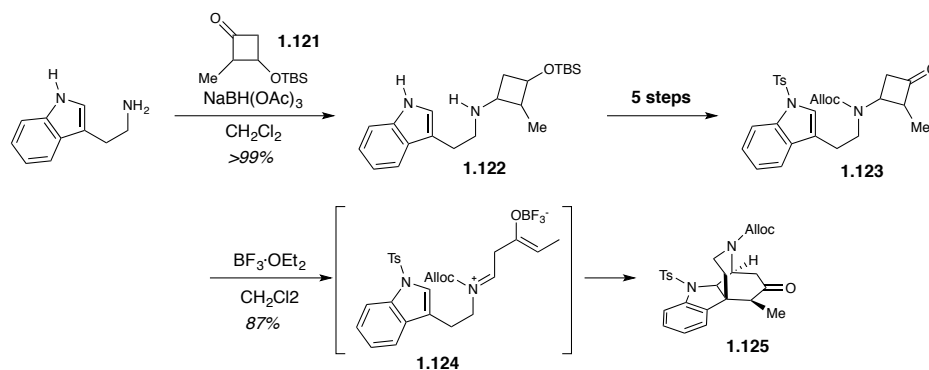
Scheme 1-17. Synthetic attempts to form an akuammiline alkaloid core by Cook and coworkers.³⁵



In 2013, Jun-ichi Matsuo and coworkers reported the development of a formal [4+2] cycloaddition between indoles and ring-opened 4-aminocyclobutanones, applying this methodology to the synthesis of various indole alkaloid motifs, including a successful total synthesis of aspidospermidine (**Scheme 1-18**).³⁶ Within this study, they successfully accessed a tetracyclic motif present within the methanoquinolizidine akuammiline alkaloids. The cyclobutanone substrate necessary for this study could be accessed over six steps beginning with the reductive amination of a precursor cyclobutanone intermediate **1.121** with tryptamine, followed by several protecting group manipulations and oxidation steps to provide 4-aminocyclobutanone **1.123**. Reaction of this substrate with Lewis acid opens the strained cyclobutanone ring, revealing a tethered iminium ion/enolate intermediate **1.124** that readily cyclized toward the desired tetracycle **1.125**. Intriguingly,

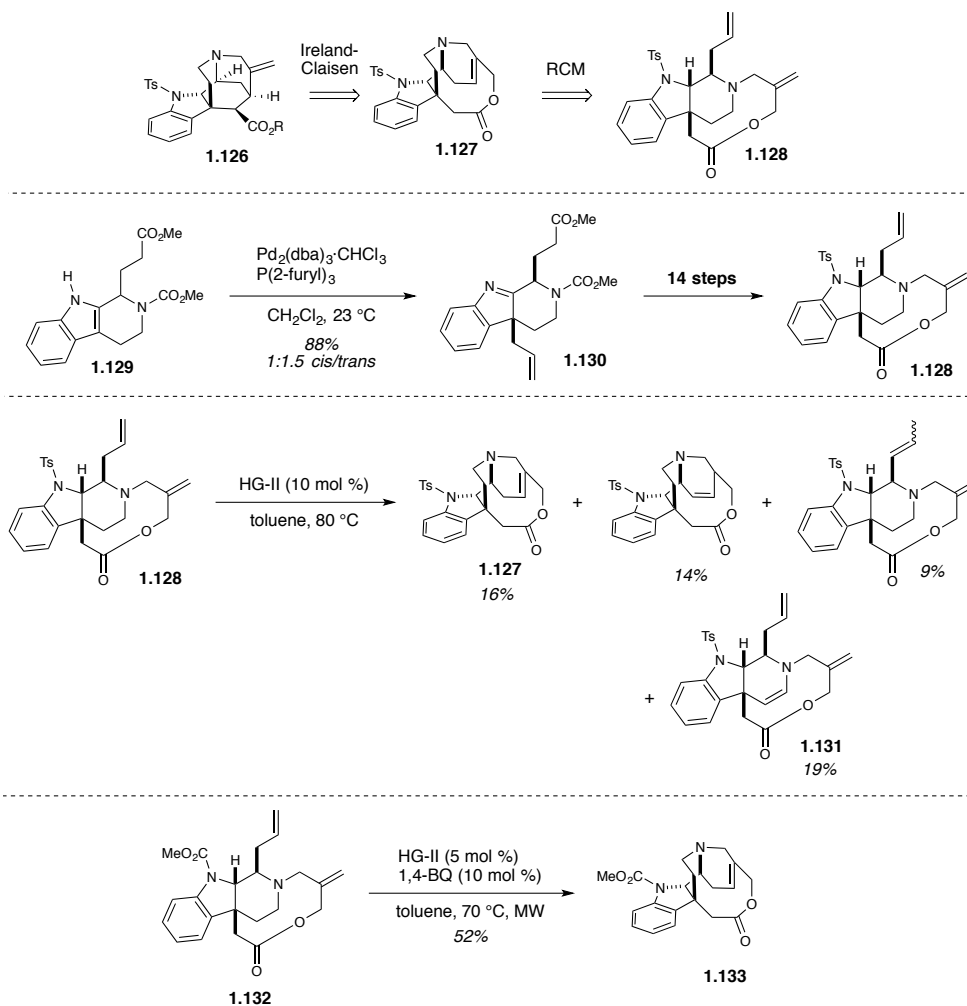
this intermediate successfully creates the hemisphere of the methanoquinolizidine subset of alkaloids that differs from the other members of the akuammiline alkaloid family and carries a similar nitrogen substitution pattern to an intermediate that worked successfully in our laboratory (**Chapter 2**).

Scheme 1-18. Successful synthesis of a tetracyclic akuammiline alkaloid core by Matsuo and coworkers.³⁶



Hidetoshi Tokuyama and coworkers completed a model study in 2013 toward the synthesis of a substrate **1.128** for an Ireland-Claisen rearrangement that would be used to synthesize methanoquinolizidine core **1.126** by closing the C ring (**Scheme 1-19**).³⁷ Their planned route to synthesize this substrate was via a ring-closing metathesis reaction of diene **1.128** that would synthesize the E ring. The required substrate was synthesized in 14 steps from indole allylation product **1.130**. When they attempted to synthesize affect the key RCM reaction, they got a low yield of their desired product **1.127** along with several byproducts (**1.129**, **1.130**, and **1.131**). Intriguingly, one of the byproducts (**1.131**) involved oxidation of the E ring under the catalytic conditions. They were able to get higher yields of product **1.133** with an alternative substrate **1.132** when run in the presence of 1,4-benzoquinone in the microwave, but do not disclose any further manipulations of this intermediate into an akuammiline core.

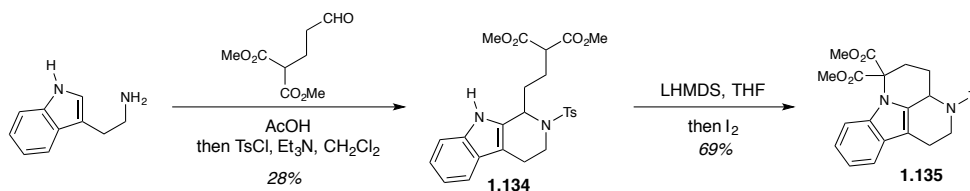
Scheme 1-19. Synthetic studies of a ring-closing-metathesis/Ireland-Claisen approach toward strictamine by Hidetoshi Tokuyama and coworkers.³⁷



Jieping Zhu and coworkers reported an attempted synthesis of an akuammiline alkaloid tetracyclic core using disconnections that parallel what was previously explored by Cook and coworkers (**Scheme 1-20**).³⁸ Instead, Zhu hoped to use an oxidative coupling reaction similar to that used by Dawei Ma and coworkers in other akuammiline alkaloid syntheses. The substrate for this cyclization was readily formed by Pictet-Spengler condensation on tryptamine, providing tetrahydro- β -carboline **1.134**. The conditions to perform the desired cyclization were similar to what we have seen previously, involving

double deprotonation of the indole and malonate substituent with LiHMDS, followed by reaction with molecular iodine. However, this substrate led exclusively to substitution on the indole nitrogen instead of the 3 position of the indole, forming tetracycle **1.135**.

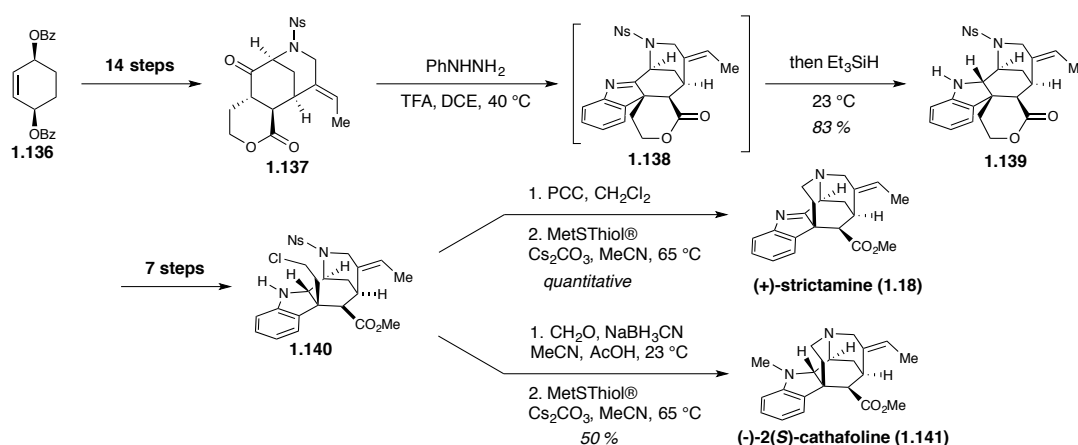
Scheme 1-20. Attempted synthesis of an akuammiline alkaloid tetracyclic core by Jieping Zhu and coworkers.³⁸



Neil Garg and coworkers published the first enantioselective total synthesis of strictamine (**1.18**) in 2016, along with a synthesis of the related natural product cathafole (**1.141**) (Scheme 1-21).²⁰ This work, published concurrently as the Jieping Zhu synthesis described below, represents the first successful synthesis of a member of the methanoquinolizidine-containing akuammiline alkaloids. Similar to their previous total synthesis of aspidophylline A (**1.12**), their strategy centered around a Fischer indolization protocol with ketone **1.137**, available enantioselectively over 14 steps from dibenzoate **1.136**, which furnished the indolenine core **1.138** and formed the key C7 quaternary stereocenter, followed by an in situ reduction with triethylsilane to provide a reduced indoline core **1.139**. Without being directly stated, this approach is apparently required to prevent cyclization upon the necessary formal alcoholysis of the parent lactone ring to a furoindoline core, a reaction used to their advantage in the synthesis of aspidophylline A. Additionally, a longer route is required to obtain the required chloride **1.140** for subsequent closure of the D ring due to problematic C16 epimerization when the indoline lactone underwent alcoholysis, leading to this intermediate being synthesized over seven steps.

Upon reoxidation to the indolenine with pyridinium chlorochromate, strictamine (**1.18**) was synthesized upon nosyl deprotection and spontaneous cyclization of the D ring. Cathafoline (**1.141**) was also obtained from the same precursor by reductive amination with formaldehyde to provide the *N*-methylindoline, followed by a similar deprotection and cyclization sequence. Both natural products were accessed enantioselectively in a total of 24 steps, and represent a significant achievement that was a long time coming in this area of alkaloid synthesis.

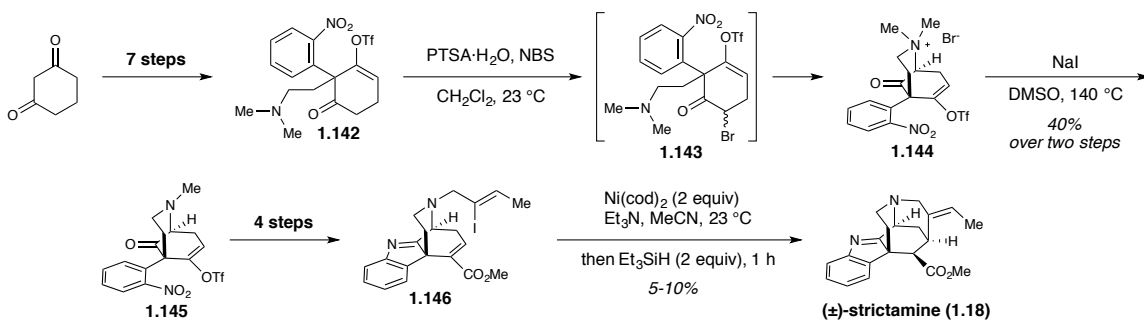
Scheme 1-21. Total synthesis of strictamine (1.18) and cathafoline (1.141) by Neil Garg and coworkers using a Fischer indolization/reduction and late state D ring cyclization.²⁰



Soon after, Jieping Zhu and coworkers published a shorter 14 step racemic synthesis of strictamine (**1.18**) (Scheme 1-22).³⁹ A key feature of their approach is that they introduce the difficult C7 quaternary center early in their synthetic route. Their strategy centered around the usage of an enol triflate intermediate **1.142**, available in seven steps from 1,3-cyclohexanedione and similar to an intermediate they used in their synthesis of aspidophylline A. The D ring was synthesized via sequential α -bromination to intermediate **1.143**, followed by immediate cyclization of the pendant dimethyl(ethyl)amine chain, providing dimethylammonium bromide salt **1.144** that was subsequently demethylated

with sodium iodide to bridged bicycle **1.145**. This intermediate was readily converted over four steps into indolenine intermediate **1.146** containing an α,β -unsaturated ester and a pendant vinyl iodide readily positioned for planned intramolecular reductive Heck cyclization to complete the synthesis. However, significant challenges were faced in getting this reaction to occur, and the only successful result was obtained with stoichiometric nickel in low yield (5-10%), providing strictamine (**1.18**) directly. The difficulty in this last cyclization may be due to the C ring needing to occupy a less favored boat conformation for the cyclization to occur. After the publication of the total synthesis of strictamine from the Zhu group, many groups published formal syntheses of strictamine (**1.18**) that end at the same unsaturated ester intermediate **1.146**. This implies several other groups might have looked into using a similar approach but were not able get the cyclization reaction to successfully occur on their own.

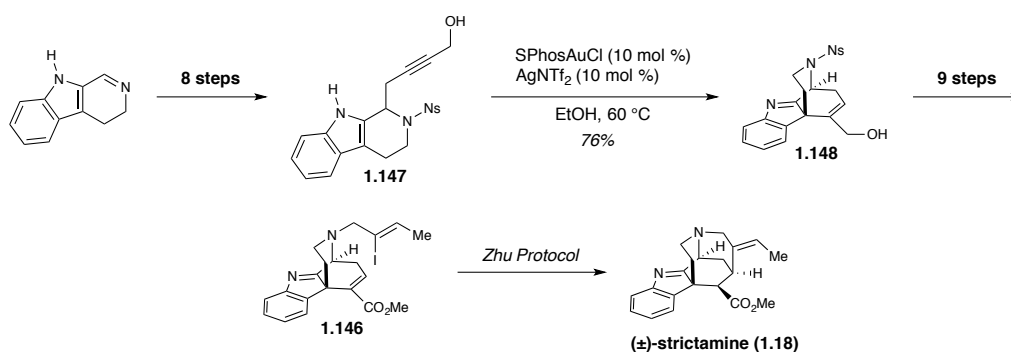
Scheme 1-22. Total synthesis of (\pm)-strictamine (1.18**) by Jieping Zhu and coworkers employing an intramolecular reductive Heck cyclization to forge the E ring.³⁹**



Nobutaka Fujii, Kiroaki Ohno, and coworkers completed a 14 step formal synthesis of strictamine (**1.18**) that centered around a gold-catalyzed cyclization to form the central D ring of the natural product (**scheme 1-23**).⁴⁰ Beginning with dihydro- β -carboline, propargyl alcohol **1.147** was successfully synthesized over a sequence of eight steps. This

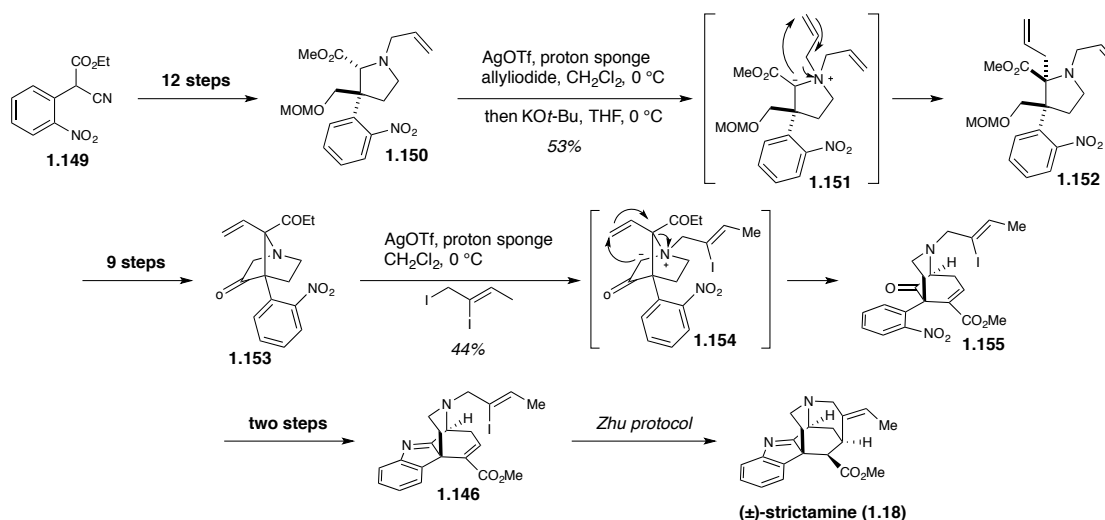
intermediate successfully underwent an intramolecular gold-catalyzed cyclization between the indole and the pendant alkyne to provide tetracycle **1.148**. This intermediate was converted in nine steps to intermediate **1.146** that the Zhu group successfully cyclized into strictamine (**1.18**).

Scheme 1-23. Formal synthesis of (±)-strictamine (1.18) by Fujii, Ohno, and coworkers employing a gold(I)-catalyzed cyclization to forge the C ring.⁴⁰



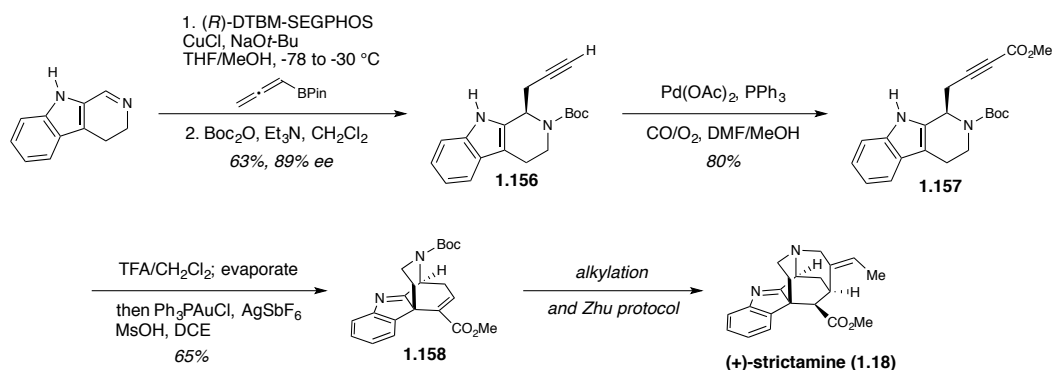
Tanja Gaich and coworkers has published a 26 step formal synthesis of strictamine (**1.18**) that centers around using several strategic [2,3]-Stevens rearrangements to synthesize the desired core (**Scheme 1-24**).⁴¹⁻⁴² Their goal was to access a zwitterionic intermediate **1.155** that would undergo a [2,3]-Stevens rearrangement to provide a C/D bicycle **1.156**. The route to this intermediate was lengthy, beginning with the synthesis of substituted pyrrolidine **1.151** from nitroarene **1.150** over twelve steps. Introduction of the allyl substituent that would later be necessary for the key rearrangement occurred by an earlier [2,3]-Stevens rearrangement with intermediate **1.152**, leading to intermediate **1.153**. This structure was converted into the key bicycle **1.154** over nine steps, with allylation and rearrangement of this intermediate leading to the desired C/D core **1.155**. This intermediate was converted over two steps to the previously reported Zhu intermediate **1.146**, leading to completion of the synthesis.

Scheme 1-24. Formal synthesis of (±)-strictamine (1.18) by Tanja Gaich and coworkers employing a [2,3]-Stevens rearrangement to forge the D ring.⁴¹



Scott Snyder and coworkers published a short enantioselective formal synthesis (1.18) of strictamine that has some parallels to the synthesis of Fujii and Ohno (Scheme 1-25).⁴³ An copper-catalyzed asymmetric propargylation of dihydro- β -carboline with allenyl pinacolborane was used to set the first stereocenter, providing alkyne intermediate 1.156. Palladium-catalyzed carbonylation of the terminal alkyne provided alkynyl ester 1.157. A key gold(I)-catalyzed cyclization provided the tetracyclic intermediate 1.158 in the correct oxidation state, which could provide the Zhu intermediate 1.146 after a simple alkylation. This route would provide strictamine over a total of seven steps, the shortest route to this natural product to date.

Scheme 1-25. Formal synthesis of (+)-strictamine (1.18) by Snyder and coworkers using an enantioselective propargylation and gold(I)-catalyzed cyclization to forge the C ring.⁴³



1.5 Conclusion

The akuammiline alkaloids have been a group of natural products that have attracted interest from the synthetic community for a long time, but the inherent challenges in their structure have limited their successful synthesis until recently. As can be seen, studies toward these alkaloids have been a proving ground for methodology in the synthesis of natural products containing complicated polycyclic architectures, leading to the development of many creative strategies to access these difficult motifs. Despite what has been accomplished, much more can still be done to come up with creative and succinct strategies to access these natural products.

1.6 References

1. Henry, T. A., 415. The Alkaloids of *Picralima Klaineana*, pierre. Part II. *Journal of the Chemical Society* **1932**, 2759-2768.
2. Eckermann, R.; Gaich, T., The Akuammiline Alkaloids; Origin and Synthesis. *Synthesis* **2013**, 2813-2823.
3. Joule, J. A., The Monoterpenoid Indole Alkaloids. Saxton, J. E., Ed. Wiley: Chemistry of Heterocyclic Compounds, Part Four, 1995; Vol. 25.

4. Smith, J. M.; Moreno, J.; Boal, B. W.; Garg, N. K., Cascade Reactions: A Driving Force in Akuammiline Alkaloid Total Synthesis. *Angewandte Chemie International Edition* **2015**, *54*, 400-412.
5. Adams, G. L.; Smith, A. B., The Chemistry of the Akuammiline Alkaloids. In *The Alkaloids*, Knolker, H.-J., Ed. 2016; Vol. 76, pp 171-257.
6. Oliver-Bever, B., Medicinal Plants in Tropical West Africa I. Plants Acting on the Cardiovascular System. *Journal of Ethnopharmacology* **1982**, *5*, 1-72.
7. Menzies, J. R.; Paterson, S. J.; Duwiejua, M.; Corbett, A. D., Opioid Activity of Alkaloids Extracted from *Picralima Nitida* (fam. Apocynaceae). *European Journal of Pharmacology* **1998**, *350*, 101-108.
8. Shang, J.-H.; Cai, X.-H.; Feng, T.; Zhao, Y.-L.; Wang, J.-K.; Zhang, L.-Y.; Yan, M.; Luo, X.-D., Pharmacological Evaluation of *Alstonia Scholaris*: Anti-inflammatory and Analgesic Effects. *Journal of Ethnopharmacology* **2010**, *129*, 174-181.
9. Kapadia, G. J.; Angerhofer, C. K.; Ansa-Asamoah, R., 16. Akuammiline: An Antimalarial Indolemonoterpene Alkaloid of *Picralima Nitida* Seeds. *Planta Medica* **1993**, *59*, 565-566.
10. Ali, B. H.; Al-Qarawi, A. A.; Bashir, A. K.; Tanira, M. O., Phytochemistry, Pharmacology and Toxicity of *Rhazya Stricta* Decne: A Review. *Phytotherapy Research* **2000**, *14*, 229-234.
11. Hou, Y.; Cao, X.; Wang, L.; Cheng, B.; Dong, L.; Luo, X.; Bai, G.; Gao, W., Microfractionation Bioactivity Based Ultra Performance Liquid Chromatography/Quadrupole Time-of-Flight Mass Spectrometry for the Identification of nuclear factor-kappaB Inhibitors and Beta2 Adrenergic Receptor Agonists in an Alkaloidal Extract of the Fold Herb *Alstonia Scholaris*. *Journal of Chromatography B: Analytical Technologies in Biomedical and Life Sciences* **2012**, *908*, 98-104.
12. Saraswathi, V.; Ramamoorthy, N.; Subramaniam, S.; Mathuram, V.; Gunasekaran, P.; Govindasamy, S., Inhibition of Glycolysis and Respiration of Sarcoma-180 Cells by Echitamine Chloride. *Chemotherapy* **1998**, *44*, 198-205.
13. Subramaniam, G.; Hiraku, O.; Hayashi, M.; Koyano, T.; Komiyama, K.; Kam, T.-S., Biologically Active Aspidofractinine, Rhazinilam, Akuammiline, and Vincorine Alkaloids from *Kopsia*. *Journal of Natural Products* **2007**, *70*, 1783-1789.
14. Arai, H.; Hirasawa, Y.; Rahman, A.; Kusumawati, I.; Zaini, N. C.; Sato, S.; Aoyama, C.; Takeo, J.; Morita, H., Alstiphyllanines E-H, Picraline, and Ajmaline-Type Alkaloids from *Alstonia Macrophylla* Inhibiting Sodium Glucose Cotransporter. *Bioorganic and Medicinal Chemistry* **2010**, *18*, 2152-2158.
15. Ramirez, A.; Garcia-Rubio, S., Current Progress in the Chemistry and Pharmacology of Akuammiline Alkaloids. *Current Medicinal Chemistry* **2003**, 1891-1915.
16. Zhang, M.; Huang, X.; Shen, L.; Qin, Y., Total Synthesis of the Akuammiline Alkaloid (\pm)-Vincorine. *Journal of the American Chemical Society* **2009**, *131*, 6013-6020.
17. Zi, W.; Xie, W.; Ma, D., Total Synthesis of Akuammiline Alkaloid (-)-Vincorine via Intramolecular Oxidative Coupling. *Journal of the American Chemical Society* **2012**, *134*, 9126-9129.
18. Horning, B. D.; MacMillan, D. W. C., Nine-Step Enantioselective Total Synthesis of (-)-Vincorine. *Journal of the American Chemical Society* **2013**, *135*, 6442-6445.
19. Zu, L.; Boal, B. W.; Garg, N. K., Total Synthesis of (\pm)-Aspidophylline A. *Journal of the American Chemical Society* **2011**, *133*, 8877-8879.
20. Moreno, J.; Picazo, E.; Morrill, L. A.; Smith, J. M.; Garg, N. K., Enantioselective Total Syntheses of Akuammiline Alkaloids (+)-Strictamine, (-)-2(S)-Cathafoline, and (-)-Aspidophylline A. *Journal of the American Chemical Society* **2016**, *138*, 1162-1165.
21. Teng, M.; Zi, W.; Ma, D., Total Synthesis of the Monoterpenoid Indole Alkaloid (\pm)-Aspidophylline A. *Angewandte Chemie International Edition* **2014**, *53*, 1814-1817.
22. Ren, W.; Wang, Q.; Zhu, J., Total Synthesis of (\pm)-Aspidophylline A. *Angewandte Chemie International Edition* **2014**, *53*, 1818-1821.

23. Jiang, S.-Z.; Zeng, X.-Y.; Liang, X.; Lei, T.; Wei, K.; Yang, Y.-R., Iridium-Catalyzed Enantioselective Indole Cyclization: Application to the Total Synthesis and Absolute Stereochemical Assignment of (-)-Aspidophylline A. *Angewandte Chemie International Edition* **2016**, *55*, 4044-4048.
24. Adams, G. L.; Carroll, P. J.; Smith, A. B., Total Synthesis of (+)-Scholarisine A. *Journal of the American Chemical Society* **2012**, *134*, 4037-4040.
25. Adams, G. L.; Carroll, P. J.; Smith, A. B., Access to the Akuammiline Family of Alkaloids: Total Synthesis of (+)-Scholarisine A. *Journal of the American Chemical Society* **2013**, *135*, 519-528.
26. Smith, M. W.; Snyder, S. A., A Concise Total Synthesis of (+)-Scholarisine A Empowered by a Unique C-H Arylation. *Journal of the American Chemical Society* **2013**, *135*, 12964-12967.
27. Smith, J. M.; Moreno, J.; Boal, B. W.; Garg, N. K., Total Synthesis of the Akuammiline Alkaloid Picrinine. *Journal of the American Chemical Society* **2014**, *136*, 4504-4507.
28. Smith, J. M.; Moreno, J.; Boal, B. W.; Garg, N. K., Fischer Indolizations as a Strategic Platform for the Total Synthesis of Picrinine. *The Journal of Organic Chemistry* **2015**, *80*, 8954-8967.
29. Li, Y.; Zhu, S.; Li, J.; Li, A., Asymmetric Total Syntheses of Aspidodasycarpine, Lonicerine, and the Proposed Structure of Lanciferine. *Journal of the American Chemical Society* **2016**, *138*, 3982-3985.
30. Li, G.; Xie, X.; Zu, L., Total Synthesis of Calophylline A. *Angewandte Chemie International Edition* **2016**, *55*, 10483-10486.
31. Dolby, L. J.; Esfandiari, Z., Model Studies of the Synthesis of Echitamine and Related Indole Alkaloids. *The Journal of Organic Chemistry* **1972**, *37*, 43-46.
32. Dolby, L. J.; Nelson, S. J., Model Studies of the Synthesis of Echitamine and Related Indole Alkaloids. II. *Journal of the American Chemical Society* **1973**, *38*, 2882-2887.
33. Bannasar, M.-L.; Zulaica, E.; Lopez, M.; Bosch, J., Studies on the Synthesis of Akuammiline-Type Alkaloids. Construction of the Hexahydro-1,5-Methanoazocino[3,4-b]indole Fragment. *Tetrahedron Letters* **1988**, *29*, 2361-2364.
34. Bannasar, M.-L.; Zulaica, E.; Ramirez, A.; Bosch, J., Synthetic Efforts Toward Akuammiline Alkaloids from Tetracyclic 6,7-seco Derivatives. *The Journal of Organic Chemistry* **1996**, *61*, 1239-1251.
35. Edwankar, R. V.; Edwankar, C. R.; Namjoshi, O. A.; Deschamps, J. R.; Cook, J. M., Bronsted Acid Mediated Cyclization of Enaminones. Rapid and Efficient Access to the Tetracyclic Framework of the Strychnos Alkaloids. *Journal of Natural Products* **2012**, *75*, 181-188.
36. Kawano, M.; Kiuchi, T.; Negishi, S.; Tanaka, H.; Hoshikawa, T.; Matsuo, J.-i.; Ishibashi, H., Regioselective Inter- and Intramolecular Formal [4+2] Cycloaddition of Cyclobutanone with Indoles and Total Synthesis of (±)-Aspidospermidine. *Angewandte Chemie International Edition* **2013**, *52*, 906-910.
37. Komatsu, Y.; Yoshida, K.; Ueda, H.; Tokuyama, H., Synthetic Studies on Strictamine: Unexpected Oxidation of Tertiary Amine in Ru-Catalyzed Ring-Closing Olefin Metathesis. *Tetrahedron Letters* **2013**, *54*, 377-380.
38. Ren, W.; Tappin, N.; Wang, Q.; Zhu, J., Synthetic Studies Toward Strictamine: The Oxidative Coupling Approach. *Synlett* **2013**, *24*, 1941-1944.
39. Ren, W.; Wang, Q.; Zhu, J., Total Synthesis of (±)-Strictamine. *Angewandte Chemie International Edition* **2016**, *55*, 3500-3503.
40. Nishiyama, D.; Ohara, A.; Chiba, H.; Kumagi, H.; Oishi, S.; Fujii, N.; Ohno, H., Formal Total Synthesis of (±)-Strictamine Based on a Gold-Catalyzed Cyclization. *Organic Letters* **2016**, *18*, 1670-1673.
41. Eckermann, R.; Breunig, M.; Gaich, T., Formal Total Synthesis of (±)-Strictamine - the [2,3]-Stevens Rearrangement for Construction of Octahydro-2H-2,8-methanoquinolizidines. *Chemical Communications* **2016**, *52*, 11363-11365.

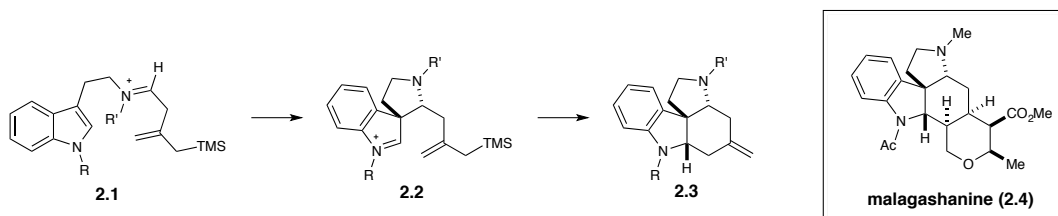
42. Eckermann, R.; Breunig, M.; Gaich, T., Formal Total Synthesis of (\pm)-Strictamine by [2,3]-Sigmatropic Stevens Rearrangements. *Chemistry: A European Journal* **2017**, *23*, 3938-3949.
43. Smith, M. W.; Zhou, Z.; Gao, A. X.; Shimbayashi, T.; Snyder, S. A., A 7-Step Formal Asymmetric Total Synthesis of Strictamine via an Asymmetric Propargylation and Metal-Mediated Cyclization. *Organic Letters* **2017**, *19*, 1004-1007.

Chapter 2. Development of a Cascade Annulation Toward an Akuammiline Alkaloid Core

2.1 Previous Studies: Iminium Ion Cascades Toward the Malagasy Alkaloids

The Blakey group has a long standing interest in the synthesis of nitrogen-containing natural products. Our laboratory had previously examined the development of an iminium ion cascade annulation that would lead to the core structure of a previously unsynthesized family of natural products, the Malagasy alkaloids, that have promising antimalarial activity (**Scheme 2-1**).¹ Toward this end, we envisioned tetracyclic core **2.3** as being a useful synthetic intermediate toward these natural products and that it could potentially be accessed by a cascade reaction, wherein reaction of an activated iminium ion **2.1** with the 3 position of a pendant indole would form an indolenium ion **2.2** that is then positioned to react with a pendant nucleophilic allylsilane, forming a tetracyclic core **2.3** of malagashanine (**2.4**), as shown.

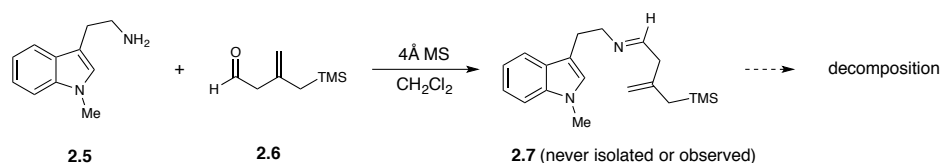
Scheme 2-1. Initially proposed iminium ion cascade annulation toward a core structure 2.3 of the Malagasy alkaloids.



A prior student in our laboratory, Ricardo Delgado, performed significant initial investigations into developing this cascade.² He initially proposed being able to access a desired imine precursor **2.7**, which he hypothesized would be directly activated into an iminium ion using an appropriate acyl chloride, by direct condensation of β,γ -unsaturated aldehyde **2.6** and 1-methyltryptamine **2.5** under both acidic and neutral conditions (**Scheme**

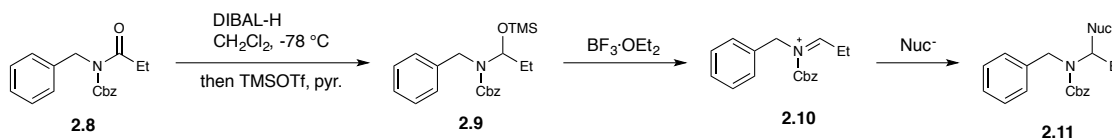
2-2). However, this intermediate was never isolated or observed, instead producing a complex mixture of possible decomposition products, believed to potentially be due to isomerization of the olefin into conjugation with the carbonyl. Therefore, a new method was required for formation of the iminium ion not by condensation, but under conditions that would prevent potential olefin isomerization.

Scheme 2-2. Initial attempts toward a direct imine condensation reaction for the synthesis of a Malagasy alkaloid core.²



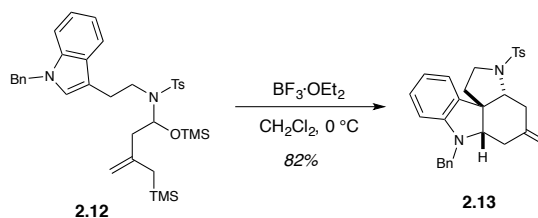
A solution to the problem was achieved using an alternative strategy, where instead coupling the two fragments together in a higher oxidation state, as a carboxylic acid derivative instead of an aldehyde, and then performing a strategic reduction would provide access to an intermediate that would be able to provide the desired iminium ion, preferably under aprotic conditions. Precedent for this process was found in prior work by the Suh group, where they were able to selectively form *N*-acyliminium ions like **2.10** by Lewis-acid-mediated decomposition of *O*-TMS hemiaminal ethers **2.9**, an intermediate in the desired aldehyde oxidation state but already condensed with the desired amine (**Scheme 2-3**).³ Subsequently, these iminium ion intermediates could react readily with nucleophiles. These hemiaminal ether intermediates were formed by selective reduction of the previously formed amides **2.8** with diisobutylaluminum hydride at low temperature, followed by trapping with a silylating reagent.

Scheme 2-3. Synthesis of hemiaminal ethers via reduction of amides and subsequent decomposition with Lewis acids to iminium ions, as reported by Suh and coworkers.³



Dr. Delgado was able to successfully use this approach to develop a cascade annulation that provided access to a Malagasy alkaloid core (**Scheme 2-4**).⁴ After exploring a variety of protecting group patterns for both the indole and hemiaminal ether nitrogens, he was able to obtain an effective cyclization protocol for the Malagasy core with substrate **2.12**. Decomposition of this *N*-Benzyl *N'*-Tosyl substrate with Lewis acid provided tetracycle **2.13** in 82% yield. Sulfonyl substitution on the hemiaminal ether nitrogen was found to be critical for obtaining the observed regioselectivity for reaction with the indole. Otherwise, Pictet-Spengler cyclizations would be found as the dominant product of the reaction.

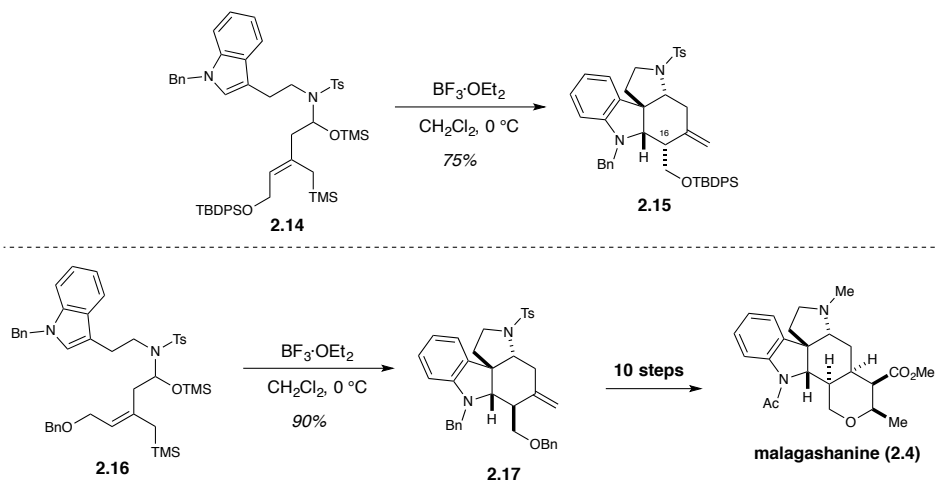
Scheme 2-4. Successful cyclization of *N*-tosyl hemiaminal ether **2.12 to form a Malagasy alkaloid core **2.13**.⁴**



In order to use this cascade reaction in a synthesis, a way to introduce substitution at the C16 position would be necessary (**Scheme 2-5**). This was deemed to be too synthetically challenging using tetracycle **2.13** formed above from a 1,1-disubstituted allylsilane, but could potentially be introduced by using a trisubstituted allylsilane in the

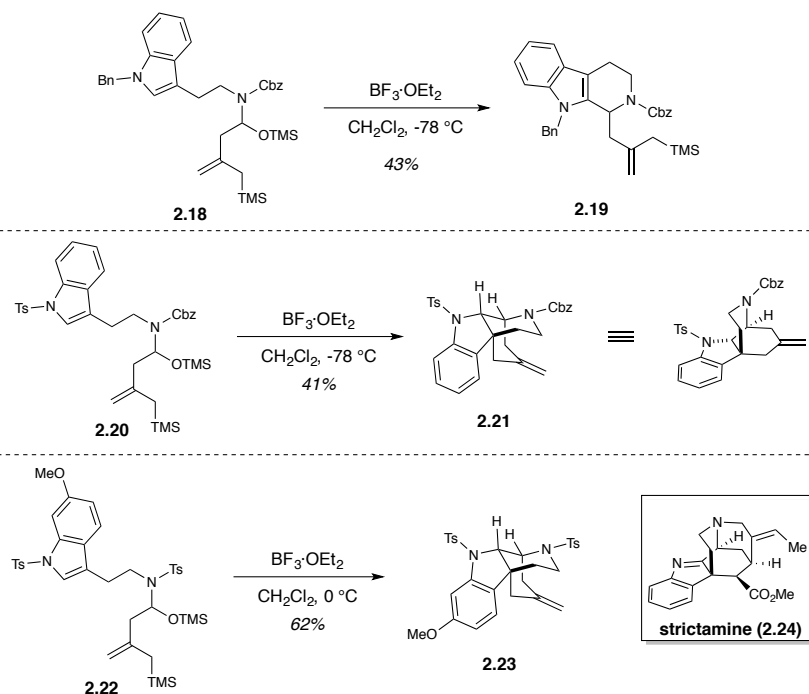
cascade. However, it was unknown if the cascade would tolerate the increased steric hindrance of an additional substituent on the olefin, or whether the cascade would be subsequently diastereoselective in the formation of the C16 stereocenter. To test this, two isomeric variants of a trisubstituted derivative, **2.14** and **2.16**, were synthesized and tested in the cascade reaction. Both isomers were found to successfully cyclize to Malagasy cores (**2.15** and **2.17**), and excitingly the geometry of the allylsilane directly translated into the stereochemistry of the C16 stereocenter. The stereochemistry formed from the benzyl protected *E*-allylsilane product **2.17** directly mapped onto that observed in the natural product malagashanine (**2.4**), so this intermediate was moved forward in a successful synthesis of the natural product.⁵

Scheme 2-5. Cascade annulation reaction of hemiaminal ether substrates 2.14 and 2.16 toward C16 substituted cores 2.15 and 2.17.⁵



2.2 Unexpected Regiodivergent Cascade Products During Malagasy Alkaloid Studies

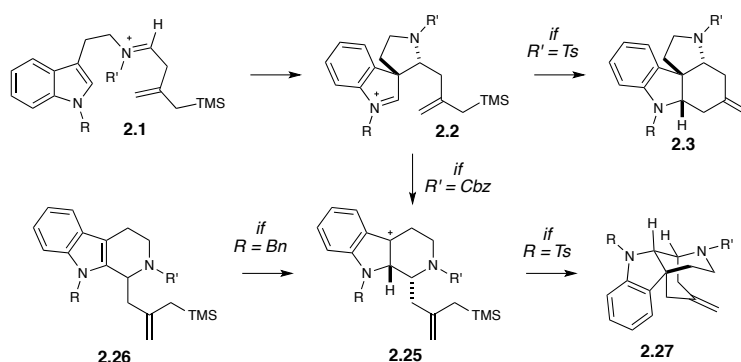
Scheme 2-6. Regiodivergent cascade reactions, relevant to the akuammiline alkaloids, discovered during studies toward the Malagasy alkaloids.²



During initial investigations toward a Malagasy alkaloid cascade, some trends were noted regarding the type of cyclization products formed when varying nitrogen substituents were used (**Scheme 2-6**). When an amide or carbamate protecting group was used on the hemiaminal ether nitrogen along with an alkyl protecting group on the indole nitrogen (**2.18**), Pictet-Spengler products (**2.19**) were typically formed as the major constituents of the reaction mixture. An electron-withdrawing substituent on the indole nitrogen (**2.20**) was hypothesized to suppress the formation of this product; instead, this pattern facilitated a second cyclization reaction, producing bridged product **2.21**.² Additionally, this product could also be formed when using a 6-methoxyindole substrate **2.22** that has both nitrogens protected with tosyl groups, possibly due to the increased nucleophilicity of the 2 position

with this substitution pattern. Intriguingly, these obtained bridged polycycles map well onto the methanoquinolizidine akuammiline alkaloids, such as strictamine (**2.24**), for which no successful syntheses had been completed at the time of this discovery.

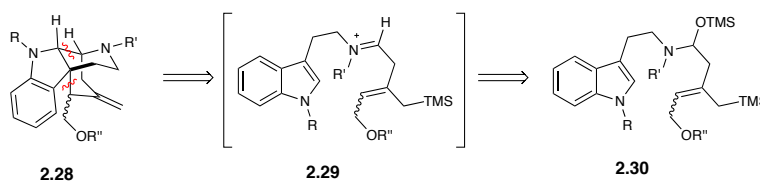
Scheme 2-7. Divergent pathways for iminium ion cyclizations due to differing nitrogen substituents.



The various products obtained in all of these cascades can be rationalized by examining the potential mechanistic intermediates for a Pictet-Spengler reaction with our substrate (**Scheme 2-7**). Initial reaction of the formed iminium ion **2.1** with the indole ring would most likely occur at the more nucleophilic 3 position of the indole, forming a subsequent indolenium ion intermediate **2.2**. If this intermediate is directly trapped by the pendant allylsilane, the observed Malagasy core **2.3** is formed, the typical result when a tosyl substituent is present on the hemiaminal ether nitrogen. If instead a benzyl carbamate substituent is used, the newly formed C-C bond in the indolenium ion intermediate will potentially undergo a migration from the 3 position to the 2 position, instead forming the benzylic cation intermediate **2.25**. This intermediate is also obtained when a 6-methoxy substituent is present on the indole, but most likely due to direct attack on the indole 2 position due to this substituent increasing this position's nucleophilicity. This benzylic cation can either undergo deprotonation/rearomatization to form Pictet-Spengler product **2.26**, as typically occurs with alkyl substituents on the indole nitrogen, or may undergo a

second cyclization with the allylsilane to form an akuammiline alkaloid core **2.27**, as occurs alternatively with a tosyl substituent on the indole. Therefore, it seems that the substituents on both the indole and hemiaminal ether nitrogens played a larger role than just protection, steering the mechanism down differing pathways that could lead to topologically contrasting products.

Scheme 2-8. Proposed retrosynthetic analysis for the development of more synthetically useful cascade reaction for the synthesis of an akuammiline alkaloid core.

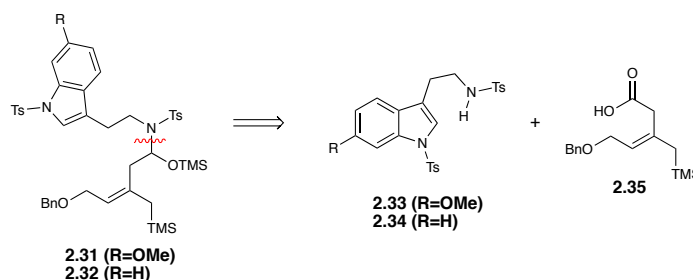


While these regiodivergent tetracyclic intermediates were promising in terms of their potential application to the synthesis of a subset of unsynthesized akuammiline alkaloids, their lack of substitution at C16 diminished their potential utility in this process. We envisioned that we could access the substitution at this stereocenter by using a trisubstituted allylsilane in this regiodivergent cascade process. Based on our ability to use related substrates in our Malagasy alkaloid cascades, we hypothesized that such a substrate with differing nitrogen substitution would allow us access to a more synthetically useful akuammiline alkaloid core. However, differences in the mechanism for these divergent cascades made us question the initial viability of this process. While trisubstituted allylsilanes were successfully able to add to a secondary indolenium ion in the Malagasy cascade, such an allylsilane would need to add to a more sterically congested tertiary benzylic cation in the akuammiline cascade; therefore, it wasn't clear whether the allylsilane would successfully add at all. Additionally, we were uncertain how drastic of

an effect potential additional transannular strain for the allylsilane addition step would have on the success of making an akuammiline alkaloid core. Herein, we describe our studies toward the development of a cascade reaction that would allow for the synthesis of a more synthetically useful akuammiline alkaloid core.

2.3 Synthesis and Reactivity of *N,N'*-Bistosyltryptamine Hemiaminal Ether substrates

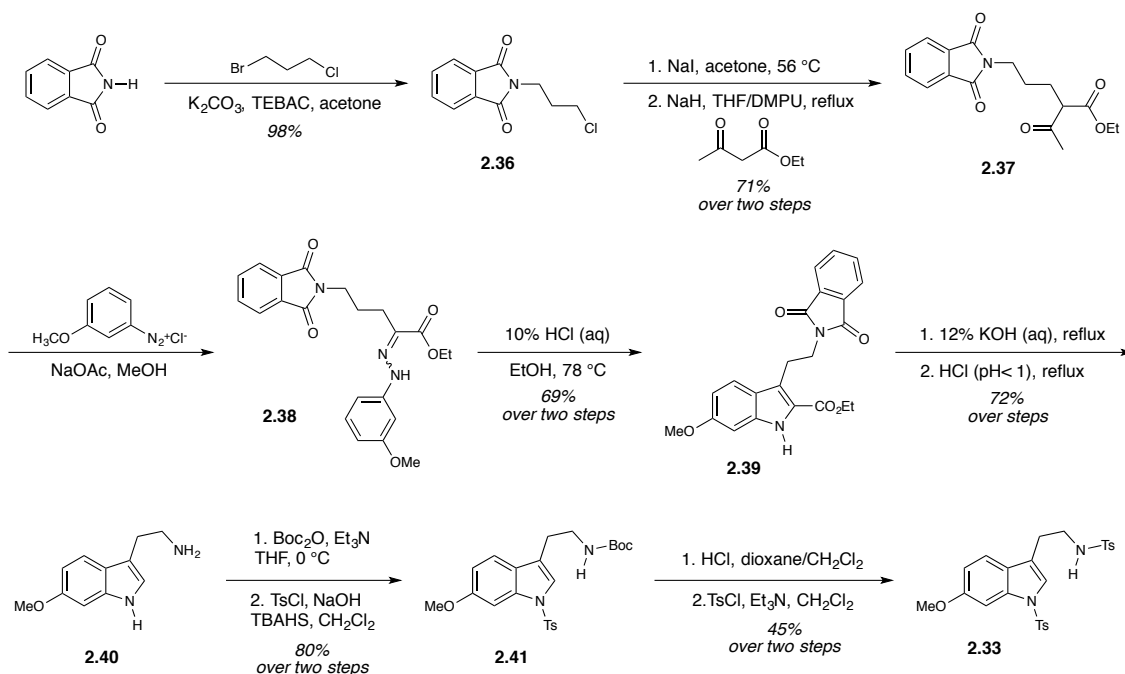
Scheme 2-9. Retrosynthetic analysis for synthesis of hemiaminal ether substrates 2.31 and 2.32.



Our studies into the development of a more synthetically useful akuammiline alkaloid cascade began with the examination of the *N,N'*-bistosyltryptamine substrates **2.31** and **2.32** (Scheme 2-9). This specific protecting group and indole substitution pattern was chosen for initial examination due to the 1,1-disubstituted allylsilane variant of this substrate providing the highest yield of our desired akuammiline alkaloid core out of all of the previous cascade annulations. Additionally, we wished to examine whether the bistosyl substitution on the substrate was potentially sufficient for the cascade or if the methoxy substitution was absolutely necessary. As would be the case with all our substrates, the hemiaminal ether moiety would be readily synthesized via reduction of the precursor

amide, so our initial forays into these systems involved developing a synthetic route to *N,N'*-bistosyltryptamines **2.33** and **2.35** and carboxylic acid **2.35**.

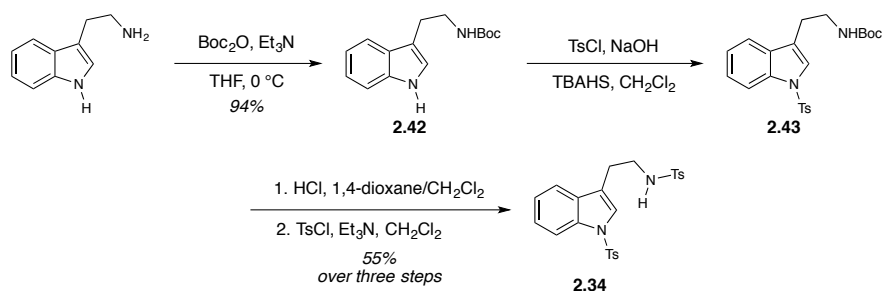
Scheme 2-10. Synthesis of *N,N'*-bistosyl-6-methoxytryptamine **2.33 via a key Japp-Klingeman/Fischer indolization reaction sequence.**



Our investigations began by developing a synthesis of *N,N'*-bistosyl-6-methoxytryptamine **2.33**. While unprotected 6-methoxytryptamine is commercially available and would seem to be a suitable precursor, the price for this compound is prohibitively expensive (\$66/100 mg from Sigma Aldrich) to be purchased directly as a starting material in a long synthetic sequence. Several different routes to this material were explored. A modification of a route developed by Fener Chen and coworkers was chosen to provide access to this key component (**Scheme 2-10**).⁶ Phthalimide was reacted with 1-bromo-3-chloropropane under basic conditions to provide 1-chloro-3-phthalimidopropane **2.36** in 98% yield. A Finkelstein reaction with sodium iodide, followed by reaction with

deprotonated ethyl acetoacetate provided the alkylated acetoacetate derivative **2.37** in 71% yield over two steps. The indole moiety was furnished over a sequence of two steps. First, a Japp-Klingeman reaction was performed on the 1,3-dicarbonyl to provide hydrazone **2.38**, which was directly subjected to acid to induce a Fischer indolization to provide the 6-methoxyindole **2.39** in 69% yield over two steps. To provide 6-methoxytryptamine **2.40**, the phthalimide protecting group and the ethyl carboxylate in the 2 position of the indole would need to be removed. Refluxing with aqueous potassium hydroxide removed the phthalimide group and saponified the ester, while subsequently refluxing with hydrochloric acid promoted the necessary decarboxylation, providing 6-methoxytryptamine **2.40** in 72% yield over two steps. Tosyl protection of both nitrogens occurred via a four step sequence. Temporary protection of the aliphatic nitrogen as the *tert*-butylcarbamate followed by tosyl protection of the indole nitrogen provided intermediate **2.41** in 80% yield over two steps. Subsequent removal of the carbamate under acidic conditions followed by tosyl protection of the aliphatic nitrogen provided *N,N'*-bistosyl-6-methoxytryptamine **2.33** in 45% yield over two steps.²

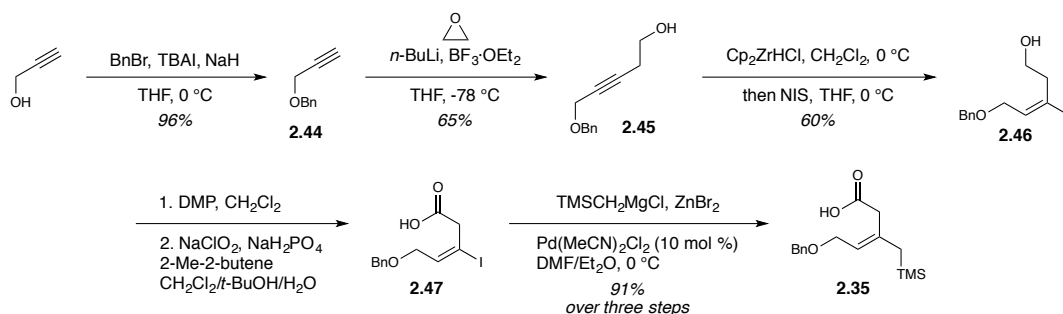
Scheme 2-11. Synthesis of *N,N'*-bistosyltryptamine 2.34.



To test a substrate without a methoxy substituent, we synthesized *N,N'*-bistosyltryptamine **2.34** over a sequence of four steps (**Scheme 2-11**). The aliphatic amine in tryptamine was protected as the *tert*-butylcarbamate **2.42** in 94% yield, and subsequently

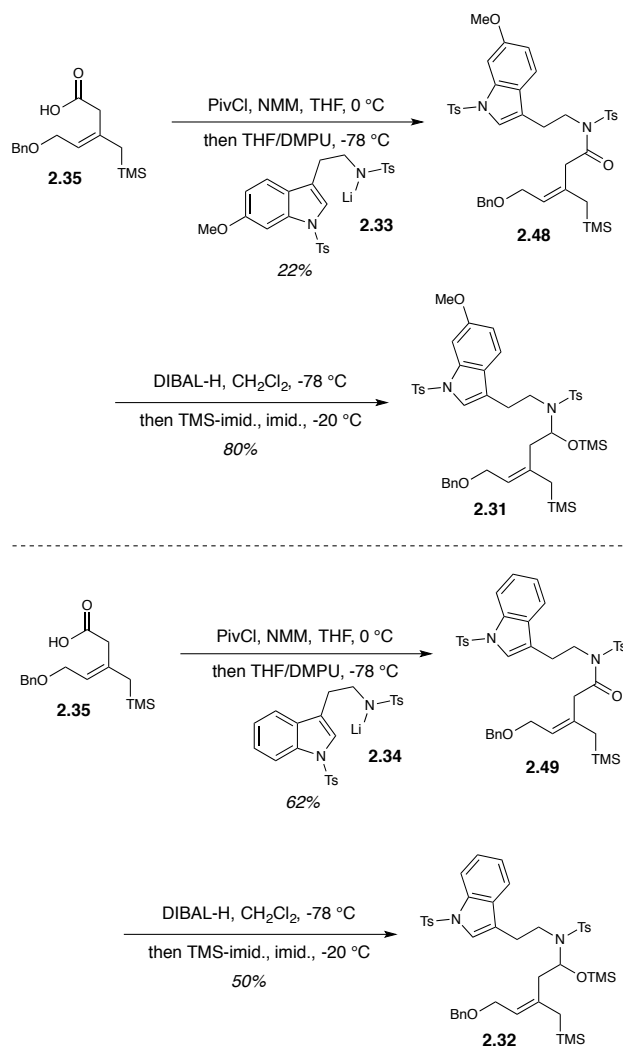
the indole nitrogen was protected as the sulfonamide **2.43**. This material was taken on crude to the next step due to the presence of residual tosyl chloride being inconsequential in later steps. Subsequent removal of the Boc protecting group under acidic conditions followed by tosyl protection of the aliphatic nitrogen provided *N,N'*-bistosyltryptamine **2.34** in 55% yield over three steps.

Scheme 2-12. Synthesis of allylsilane 2.33.



With our desired tryptamine fragments in hand, we next focused our attention on the synthesis of carboxylic acid **2.35**, a compound we had previously reported within our laboratory (**Scheme 2-12**).⁵ The synthesis of this compound began by benzyl protection of propargyl alcohol to provide propargyl ether **2.44** in 96% yield, followed by addition of the lithium acetylide of the terminal alkyne to oxirane to form the homopropargylic alcohol **2.45** in 65% yield. Alcohol-directed hydrozirconation of the alkyne, using methodology developed by Joseph Ready,⁷ followed by trapping with *N*-iodosuccinimide provided the desired vinyl iodide **2.46** in 60% yield. Sequential Dess-Martin and Pinnick oxidation to provide carboxylic acid **2.47**, followed by Negishi coupling⁸ with an organozinc species formed from trimethylsilylmethylmagnesium chloride provided the desired allylsilane **2.35** in 91% yield over three steps.

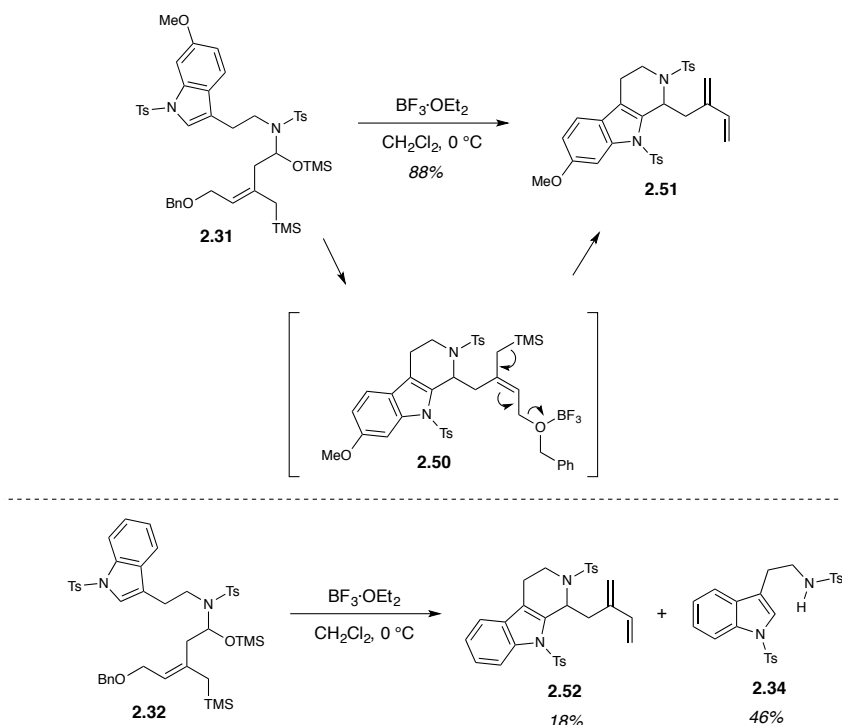
Scheme 2-13. Coupling of tryptamines 2.33/2.34 and carboxylic acid 2.35 and concomitant reduction to the hemiaminal ether substrates 2.31/2.32.



The syntheses of the desired hemiaminal ether substrates **2.31** and **2.32** were accomplished via a two reaction sequence (**Scheme 2-13**). The previously formed carboxylic acid **2.35** was converted into the pivaloyl mixed anhydride, of which the crude solution was transferred to a solution of the deprotonated 6-methoxytryptamine **2.33** or tryptamine **2.34**, providing the *N*-Ts amides **2.48** and **2.49** in 22% and 62% yield, respectively. Both *N*-Ts amides were reduced by diisobutylaluminum hydride at low

temperature followed by trapping with trimethylsilylimidazole in the presence of imidazole, providing hemiaminal ether substrate **2.31** in 80% yield and **2.32** in 50% yield.

Scheme 2-14. Reaction of hemiaminal ether substrates 2.31 and 2.32 with $\text{BF}_3 \cdot \text{OEt}_2$ to provide Pictet-Spengler products 2.51 and 2.52.

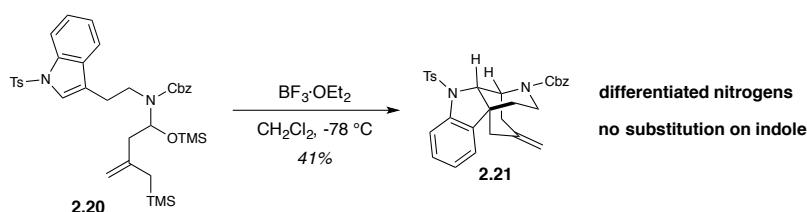


Upon decomposition of the hemiaminal ether substrates **2.31** and **2.32** with $\text{BF}_3 \cdot \text{OEt}_2$, diene products (**2.51** and **2.52**) were obtained in each case (Scheme 2-13). These products are the result of a classic Pictet-Spengler cyclization of the substrate, such as intermediate **2.50**, followed by decomposition of the allylsilane mediated by binding of the Lewis acid to the benzyloxy substituent. The reaction with the substrate lacking a 6-methoxy substituent produced less cyclized product **2.52** than the other cyclization, suggesting a possible necessity of the substituent in this case, albeit inconclusively. While disheartening, we decided to pursue studies using a different substrate for the cascade. These specific substrates do have some limitations in terms of its synthetic utility when

applied to an actual total synthesis of an akuammiline alkaloid. First, none of the desired targets contain a methoxy substituent in the 6 position of the indole, meaning that a difficult removal of this functionality would be necessary at a later stage in any synthetic sequence. Additionally, the use of tosyl protection on both nitrogens would prove difficult when later differentiation of both nitrogens would be necessary. Finally, the use of 6-methoxytryptamine as a starting material was both expensive, and the step count would increase significantly if it needed to be synthesized, requiring seven steps to successfully access. Therefore, our efforts focused on the development of cascade substrate that would provide a product with more synthetic utility.

2.4 Development of (*N*-Ts-*N'*-Cbz)tryptamine-based Substrates for Akuammiline Alkaloid Cascade Reactions

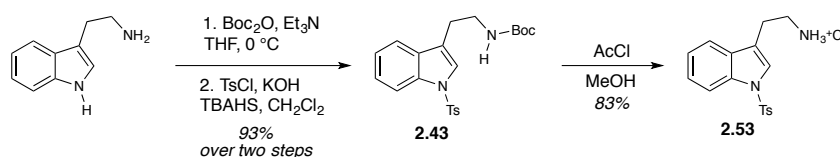
Scheme 2-15. Reexamination of (*N*-Ts-*N'*-Cbz)tryptamine substrate 2.20 shows that it would potentially provide a more synthetically useful akuammiline alkaloid core.



Upon reexamination of the prior cyclization results that provided akuammiline alkaloid cores with 1,1-disubstituted allylsilanes, we noted how a desired structure was able to be obtained with a hemiaminal ether substrate containing a tosyl substituent on the indole nitrogen and a Cbz substituent on the hemiaminal ether nitrogen, with no electron donating 6-methoxy substituent necessary on the indole ring to enforce the observed

regioselectivity (**Scheme 2-15**). While the yield obtained was low, we believed we could further optimize the reaction conditions if a substrate with a trisubstituted allylsilane would provide us our desired cascade product. Therefore, we set out to synthesize both allylsilane isomers of the (*N*-Ts-*N'*-Cbz)tryptamine hemiaminal ether substrates.

Scheme 2-16. Synthesis of *N*-tosyltryptamine hydrochloride salt **2.53.**

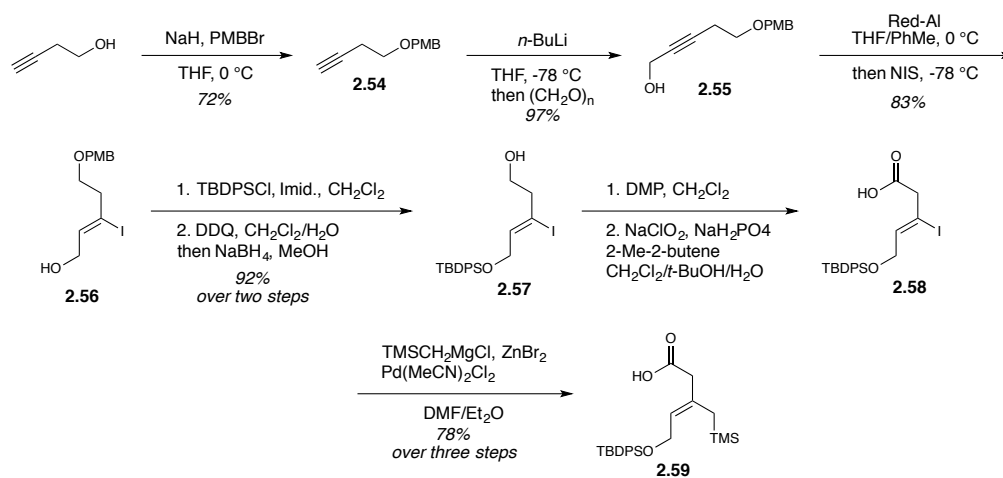


Our efforts toward these substrates began with the straightforward synthesis of the tryptamine hydrochloride salt of *N*-tosyltryptamine **2.53** (**Scheme 2-16**). This tryptamine intermediate was used in the later amide coupling step due to the ability to introduce the required Cbz substituent on an N-H amide intermediate, allowing for a logistically simpler amide coupling procedure. Protection of the aliphatic nitrogen of tryptamine as the *tert*-butylcarbamate followed by tosylation of the indole nitrogen provided known (*N*-Ts-*N'*-Boc)tryptamine **2.43** in 93% yield over two steps.⁹ Subsequent Boc deprotection in freshly prepared methanolic HCl (from acetyl chloride in methanol) provided the tryptamine hydrochloride salt **2.53** in 83% yield after a simple trituration from diethyl ether.

Initially, we set our sights on the synthesis of a *Z*-allylsilane hemiaminal ether isomer to examine in this cascade, requiring access to the *Z*-allylsilane-containing carboxylic acid precursor **2.59** (**Scheme 2-17**). We initially chose this substrate, with the pendant alkoxymethylene group protected as a silyl ether, to provide more useful differentiation of the protecting groups in later synthetic steps. Additionally, this specific allylsilane isomer was believed to provide our desired C16 stereochemistry if the

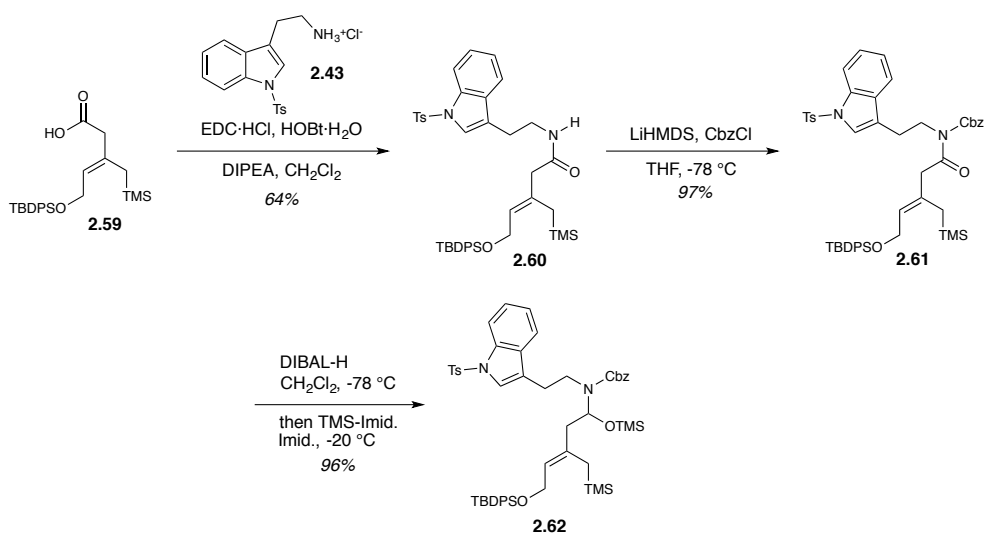
allylsilane addition occurred through a chair-like transition state. Synthesis of this precursor began with protection of 3-butyn-1-ol as the PMB ether **2.54** in 72% yield, followed by deprotonation of the terminal alkyne and subsequent addition to paraformaldehyde to provide the propargyl alcohol **2.55** in 97% yield. This alcohol was used to direct reduction of the alkyne with Red-Al[®], with subsequent trapping of the formed organoaluminate with *N*-iodosuccinimide to provide *Z*-vinyl iodide **2.56** in 83% yield.¹⁰ Protection of the allylic alcohol as the TBDPS ether followed by removal of the PMB group with DDQ provided homoallylic alcohol **2.57**. The desired product proved difficult to separate from the *p*-anisaldehyde byproduct formed from this oxidative cleavage step, so a subsequent reduction of the byproduct with sodium borohydride was required to facilitate purification, providing the desired homoallylic alcohol **2.57** in 92% yield over two steps. Sequential Dess-Martin and Pinnick oxidations provided the carboxylic acid **2.58**, which was subsequently subjected to our previously used Negishi coupling conditions to provide the desired allylsilane **2.59** in 78% yield over three steps.⁸

Scheme 2-17. Synthesis of *Z*-allylsilane carboxylic acid intermediate **2.59.**



Synthesis of our desired hemiaminal ether intermediate **2.62** was accomplished via a three step synthetic sequence (**Scheme 2-18**). Carboxylic acid **2.59** was coupled to tryptamine hydrochloride **2.53** using EDC and HOBT, providing N-H amide **2.60** in 64% yield. Subsequent deprotonation of the amide followed by trapping with CbzCl provided the N-Cbz amide **2.61** in 97% yield. Reduction of the N-Cbz amide with DIBAL-H followed by trapping with trimethylsilylimidazole provided hemiaminal ether **2.62** in 96% yield.

Scheme 2-18. Synthesis of hemiaminal ether substrate 2.62.



Reaction of the hemiaminal ether substrate **2.62** with BF₃·OEt₂ at 0 °C provided a cyclization product **2.63** in 53% yield with a mass that matched what was desired (**Scheme 2-19**). This obtained product proved initially difficult to assign structurally by ¹H NMR due to the presence of rotameric peaks from the Cbz substituent that only partially resolved in *d*₆-DMSO at 80 °C. ¹H NMR, COSY, and 1D NOE studies hinted at the formation of a product matching our desired regiochemistry, but the structural assignment only proved to be conclusive upon examination by X-ray crystallography (**Figure 2-1**). The product

obtained was an akuammiline alkaloid core with the desired C16 substituent sitting in the axial position. This relative stereochemistry does not match that of the methyl ester substituent in akuammiline alkaloid natural products. Due to our knowledge that both allylsilane isomers are tolerated and are able to provide differing C16 epimers selectively in our Malagasy alkaloid cascade, we next decided to examine *E*-allylsilane isomers of our substrate in the akuammiline cascade.

Scheme 2-19. Cyclization of hemiaminal ether 2.62 to tetracycle 2.63 with Lewis acid.

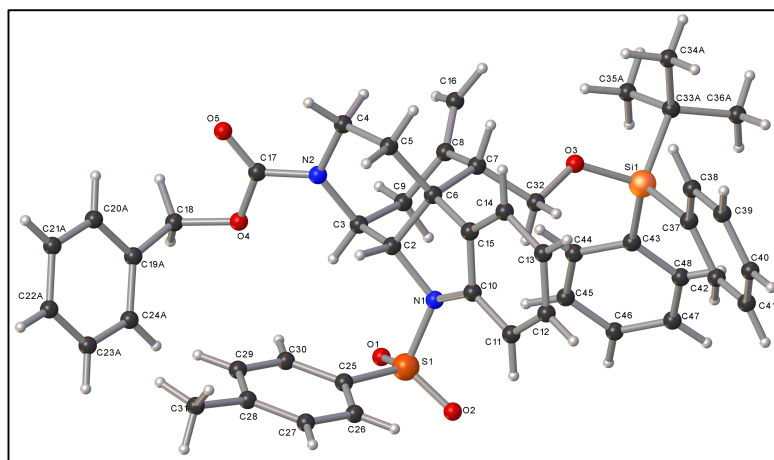
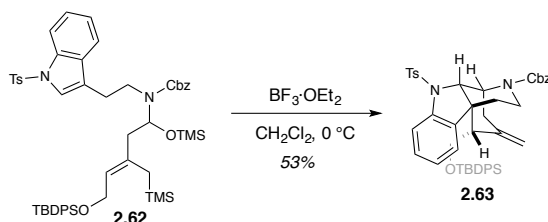
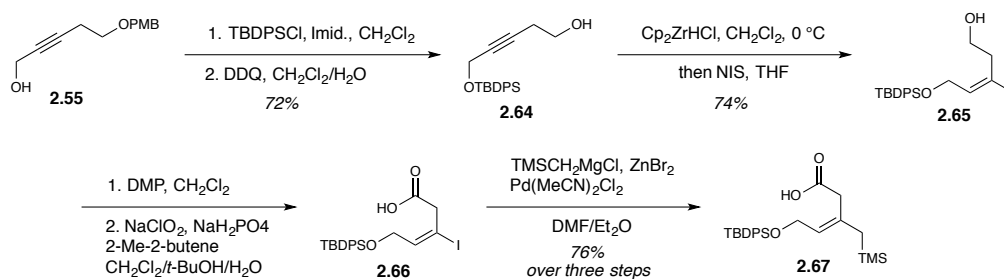


Figure 2-1. X-ray crystal structure of obtained akuammiline alkaloid core tetracycle 2.63.

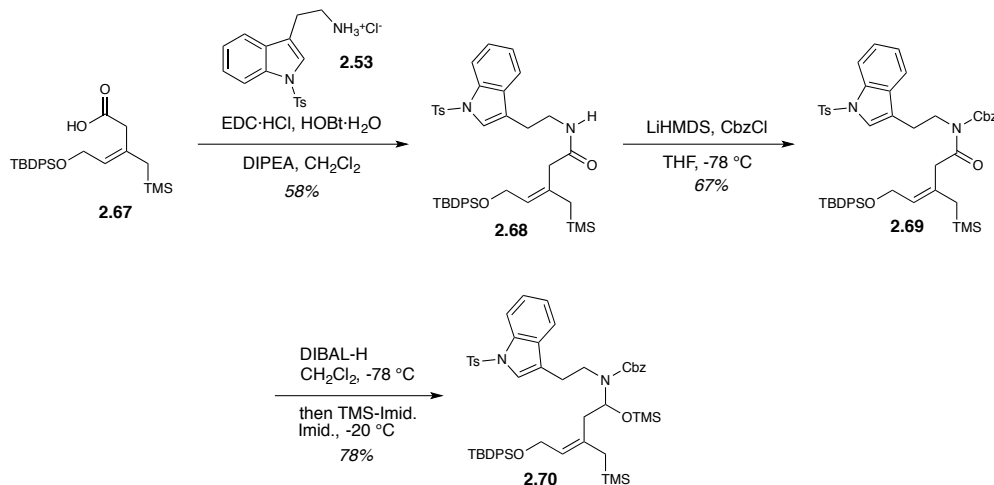
Access to an *E*-allylsilane hemiaminal ether intermediate required the synthesis of the TBDPS-ether-containing carboxylic acid **2.67** (Scheme 2-20). The synthesis of this intermediate closely paralleled that for the previously disclosed benzyl ether derivative **2.35** of this acid. Beginning with previously disclosed propargylic alcohol intermediate

2.55, TBDPS protection followed by removal of the PMB ether with DDQ provided homopropargylic alcohol **2.64** in 72% yield over two steps. Hydrozirconation of the homopropargylic alcohol followed by trapping with *N*-Iodosuccinimide provided the *E*-vinyl iodide **2.65** in 74% yield.⁷ Sequential Dess-Martin and Pinnick oxidation provided carboxylic acid **2.66**, which was subjected to a Negishi coupling to provide *E*-allylsilane **2.67** in 76% yield over three steps.⁸

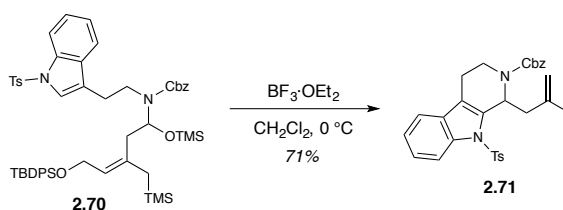
Scheme 2-20. Synthesis of *E*-allylsilane carboxylic acid **2.67.**



The desired hemiaminal ether substrate was synthesized in a similar fashion to the previously formed substrate (**Scheme 2-21**). Carboxylic acid **2.67** was coupled to tryptamine hydrochloride **2.53** using EDC and HOBT, providing *N*-H amide **2.68** in 58% yield. Subsequent deprotonation of the amide followed by trapping with CbzCl provided the *N*-Cbz amide **2.69** in 67% yield, and subsequent reduction with DIBAL-H followed by trapping with trimethylsilylimidazole provided hemiaminal ether **2.70** in 78% yield.

Scheme 2-21. Synthesis of hemiaminal ether substrate 2.70.

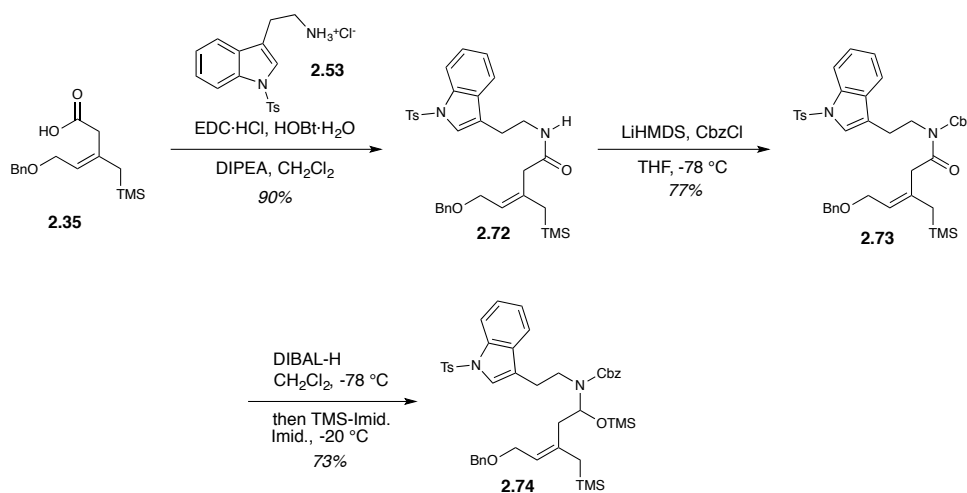
The *E*-allylsilane isomer of the hemiaminal ether substrate **2.70** did not cyclize to form the desired akuammiline alkaloid core like the prior substrate, instead providing a diene product **2.71** in 71% yield (**Scheme 2-22**). This is similar to the result observed with prior hemiaminal ether substrate containing a 6-methoxytryptamine moiety. We initially hypothesized that this cyclization might not have been successful due to steric hindrance caused by the large TBDPS ether, believing that switching to a less sterically congested benzyl ether might allow allylsilane addition step to occur.

Scheme 2-22. Cyclization of hemiaminal ether substrate 2.70 to diene product 2.70 obtained by a Pictet-Spengler cyclization.

We therefore set out to examine this by synthesizing the benzyl protected hemiaminal ether variant **2.74** (**Scheme 2-23**). Benzyl ether substrate was synthesized by

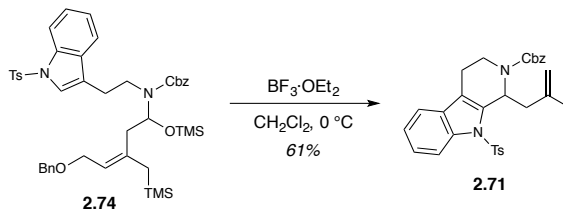
coupling the previously discussed carboxylic acid **2.35** with tryptamine hydrochloride **2.53** with EDC and HOBt, providing the *N*-H amide **2.72** in 90% yield. Reaction of the deprotonated amide with CbzCl provided the *N*-Cbz amide **2.73** in 77% yield. Reduction with DIBAL-H and trapping with trimethylsilylimidazole provided the desired hemiaminal ether **2.74** in 73% yield.

Scheme 2-23. Synthesis of benzyl protected hemiaminal ether substrate 2.74.



Disappointingly, reaction of the benzyl ether protected hemiaminal ether substrate **2.74** with Lewis acid provided diene product **2.71**, the same as was obtained with the TBDPS protected variant, in 61% yield (**Scheme 2-24**). Therefore, we can conclude from this that the *E*-allylsilane variants are just too sterically encumbered for the transition state of the allylsilane addition step to provide any of the desired tetracyclic product, requiring the use of the *Z*-allylsilane derivative for any future synthetic studies. While the stereochemistry of C16 carbon is incorrect in our obtained tetracycle, the pendant C16 axial substituent would be subsequently oxidized to a methyl ester in any potential synthetic pathway to the akuammiline alkaloids, providing a possible opportunity for this stereocenter to be epimerized to the desired equatorial positioning of the carbonyl.

Scheme 2-24. Cyclization of hemiaminal ether substrate 2.74 to provide previously obtained diene 2.71.



This difference in product selectivity between the two differing allylsilane isomers was rationalized by examination of the possible transition states for the allylsilane addition step (**Figure 2-2**). Examination of the chair-like transition states for the allylsilane addition step of both isomers reveals significant transannular strain between the trimethylsilylmethylene substituent of the allylsilane and the already formed piperidine D ring. This strain is relieved in a boat-like transition for *Z*-allylsilane intermediate. Additionally, the product formed from the *Z*-allylsilane isomer is that expected from a boat-like transition state for this step. Intriguingly, the products observed from the previously developed Malagasy alkaloid cascade are also those expected from a boat-like transition state for the allylsilane addition. In contrast, invoking a similar transition state for the *E*-allylsilane isomer introduces instead significant eclipsing interactions between the protected silyloxymethylene substituent of the allylsilane and the already formed D ring. Therefore, the *E*-allylsilane isomer experiences significant steric hindrance in either possible transition state for the allylsilane addition step, allowing rearomatization of the indole ring to outcompete. This is in direct contrast to what is observed with our previously developed Malagasy alkaloid cascades, where both allylsilane geometries are able to successfully cyclize to tetracyclic alkaloid cores. This demonstrates the increased steric demands for the bridged akuammiline alkaloid system in comparison to Malagasy alkaloid cores.

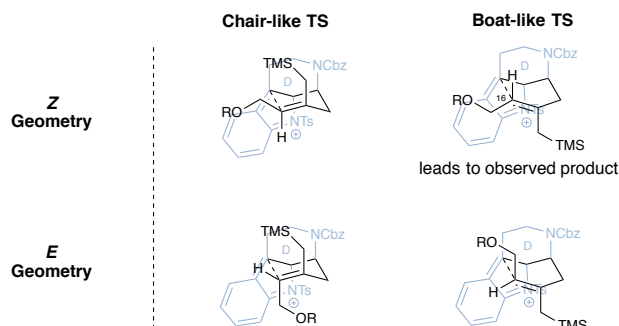
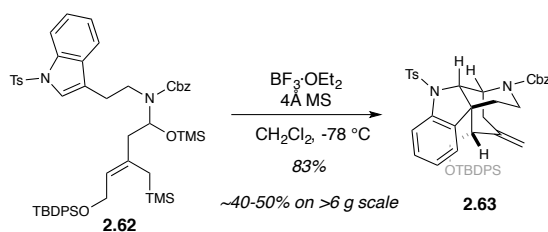


Figure 2-2. Rationale for the observed product outcomes for the *Z*- and *E*-allylsilane isomers based upon the possible transition states for the allylsilane addition step.

2.5 Optimization of the *Z*-Allylsilane Containing Hemiaminal Ether Cascade

Having successfully developed a cascade reaction with a trisubstituted allylsilane that would provide a properly substituted akuammiline alkaloid core, we sought out to optimize the reaction conditions to provide a more significant yield of our desired core (**Scheme 2-25**). The main byproduct observed from the reaction was (*N*-Ts-*N'*-Cbz)tryptamine, the result of hydrolysis of the formed iminium ion in the cascade. We found that the combination of running the reaction at lower temperature for longer times (-78 °C for 24 hours) with the addition of freshly dried 4Å molecular sieves provided a more useful yield of the desired core **2.63** (83%). Of note is that this cascade would begin to experience problems if attempted on a significantly larger scale (>6 grams of hemiaminal ether substrate), with the diene observed for the *E*-allylsilane isomers beginning to appear in this reaction. The desired core and the diene byproduct often proved difficult to separate by column chromatography, leading to lower isolated yields of the desired core **2.63** (~40-50%).

Scheme 2-25. Development of optimized reaction conditions for cyclization of *Z*-allylsilane isomer 2.62 to tetracyclic akuammiline core 2.63.



2.6 Studies Toward the Development of an Asymmetric Iminium Ion Cascade

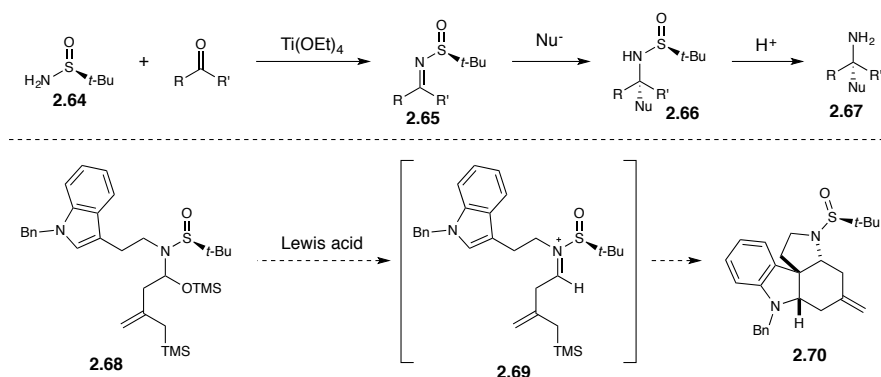
The cascade reactions we have developed toward both the Malagasy and akuammiline alkaloids have proven to be powerful methods, but both regiodivergent variants would be the first stereodetermining step in any synthetic sequence toward these alkaloids. Due to the formation of a stereoablated iminium ion intermediate, both cascades inherently lead to racemic products. Our laboratory has had a longstanding interest in developing an asymmetric variant of our cascade reactions, especially if induced by the use of an asymmetric catalyst. However, there are inherent challenges to the development of asymmetric methods for additions to C-N double bonds, an area much less developed than additions to carbonyls. Due to the decreased electronegativity of nitrogen compared to oxygen, an imine is inherently less electrophilic than a carbonyl. This decreased electronegativity also makes nitrogen more Lewis basic, sometimes leading to strong binding of the addition products to any typically used Lewis acidic catalyst, diminishing turnover. Asymmetric additions to iminium ions are even more difficult due to the absence of strong Lewis basic sites necessary for catalyst binding. Therefore, enantioselective total syntheses typically do not use iminium ion reactions as their stereodetermining step. We

will describe herein studies performed to examine both a chiral auxiliary approach and an asymmetric catalytic approach to our cascade reactions.

2.6.1 Examination of Diastereoselective Additions to Hemiaminal Ethers Substituted with Ellman's Auxiliary

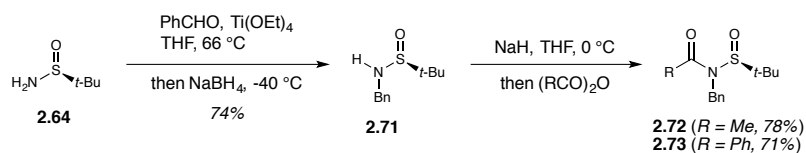
Since their introduction in 1997 by Jonathan Ellman and coworkers, chiral sulfinamides (**2.64**) have found extensive use as chiral ammonia equivalents for the asymmetric synthesis of amines (**Scheme 2-26**).¹¹ These chiral auxiliaries are commercially available and can be condensed with aldehydes and ketones to form sulfinimines **2.65** in high yields. Diastereoselective reduction or nucleophilic attack of these sulfinimines to sulfinamides **2.66**, followed by removal of the chiral auxiliary under mildly acidic conditions, leads to chiral amines **2.67** with high enantioselectivities. In our Malagasy alkaloid cascade, a tosyl group on the hemiaminal ether nitrogen is necessary for both iminium ion activation as well as to provide the desired regioselective outcome of the reaction. Observing the similarity between a sulfonamide and Ellman's sulfinamide auxiliaries, we hypothesized that we could develop an enantioselective variant of our cascade (**2.68-2.70**) using this auxiliary as a chiral directing group. However, this auxiliary had never been used in reactions of iminium ions, so the effectiveness of a sulfinyl substituent as an activating group, as well as its tolerance of the reaction conditions, were unclear. Therefore, we set out to explore several simple model systems to see if we could both synthesize sulfinyl-substituted hemiaminal ethers **2.68** as well as subject them to our cascade reaction conditions.

Scheme 2-26. Utilization of Ellman's auxiliary 2.64 in diastereoselective additions to amines,¹¹ and the proposed iminium ion cascade annulation using Ellman's auxiliary as a chiral activating group.



Two groups of model systems were explored to analyze the effect of a sulfinyl auxiliary on Lewis acid mediated decomposition of hemiaminal ethers and their subsequent reactions with nucleophiles. The first group involved simple substrates that could be synthesized in a small number of steps to explore the intermolecular addition of nucleophiles. We also synthesized a second group of substrates that would explore a potentially more favored intramolecular reaction.

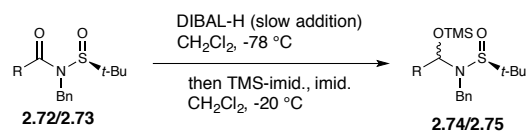
Scheme 2-27. Synthesis of *N*-acyl-*N*-benzylsulfinamides **2.72 and **2.73**.**



We chose substrates **2.72** and **2.73**, derived from acetic acid and benzoic acid respectively, as simple systems that could be readily prepared and tested for intermolecular reactions (**Scheme 2-27**). To explore these reactions, *N*-benzyl-*(S)*-tert-butylsulfinamide **2.71** was readily synthesized by reductive amination of *(S)*-tert-butylsulfinamide **2.64** with benzaldehyde.¹² Deprotonation with sodium hydride and subsequent reaction with the appropriate anhydride led to the acetyl- or benzoyl-substituted sulfinamides **2.72** and **2.73**.

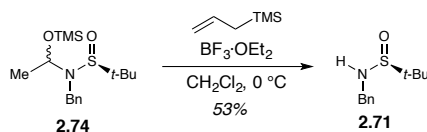
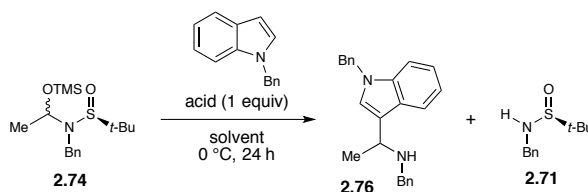
Selective reduction and silyl trapping of the acetylated sulfinamides **2.72** and **2.73** to form the desired hemiaminal ether substrates **2.74** and **2.75** proved to be initially difficult (Table 2-1). Yields for the reduction of acetamide **2.72** and benzamide **2.73** with DIBAL-H and trapping with trimethylsilylimidazole were initially low, but proceeded diastereoselectively, with a diastereomeric ratio of 3.3:1.0 and 4.3:1.0 obtained for the acetyl- and benzoyl-derived species **2.74** and **2.75**, respectively (entries 1-2). Alternative reductants (Red-Al[®] and L-Selectride[®]) led to significant decomposition of the starting material, presumably due to over-reduction. Of note was the presence of a thiol in these reaction mixtures, suggesting that the N-S bond was potentially being cleaved under these initially explored reaction conditions. Eventually, slow addition of DIBAL-H was found to be crucial in this reaction for both increased yields and diastereoselectivities. Addition of DIBAL-H over one hour increased the yield of **2.74** to 42% with a diastereomeric ratio of 7.0:1.0 (entry 3), while addition of the reductant over two hours increased the yield to 65% and led to the formation of a single diastereomer by ¹H NMR (entry 4). The absolute configuration of the major diastereomer could not be determined.

Table 2-1. Optimization of the synthesis of *N*-sulfinyl hemiaminal ethers **2.74 and **2.75** from *N*-acylsulfinamides **2.72** and **2.73**.**



entry	R	DIBAL-H addition time	yield (%)	dr
1	Me	15 min	27	3.3:1.0
2	Ph	15 min	18	4.3:1.0
3	Me	60 min	42	7.0:1.0
4	Me	120 min	65	>19.0:1.0

Reaction of hemiaminal ether **2.74** with $\text{BF}_3 \cdot \text{OEt}_2$ in the presence of trimethylallylsilane only led to the isolation of *N*-benzylsulfonamide **2.71** in 53% yield, the result of hydrolysis of the iminium ion intermediate (**Scheme 2-28**). We next examined reaction with more nucleophilic *N*-benzylindole, one that would closely model the actual nucleophile we would use in our reactions (**Table 2-2**). *N*-benzylindole did successfully couple with our generated iminium ion to benzylamine **2.76** in 13% yield, but the product isolated had the sulfinyl auxiliary cleaved under the reaction conditions (entry 1). A significant quantity of *N*-benzylsulfonamide **2.71** (61% yield) was also obtained from this reaction. No reactivity was observed when an alternative Lewis acid, chlorotrimethylsilane, was used (entry 4), and attempts to run the reaction in either diethyl ether or toluene did not provide any of the coupled product **2.76** (entry 2-3). Alternatively, using a Bronsted acid, *p*-toluenesulfonic acid, led to the addition product **2.76** being the major component in the reaction (52%), but again with the auxiliary being cleaved (entry 5). Adding 3 Å molecular sieves to the reaction shut down the hydrolysis side reaction, leading to 59% yield of the cleaved addition product **2.76** (entry 6). This product was disappointingly formed in 9% ee as determined by Mosher amide analysis. This implies that either the sulfonamide is insufficient at inducing chirality or that the auxiliary was being cleaved before the addition reaction had occurred. To diminish the amount of auxiliary cleavage observed, catalytic acid was used, but no reaction was observed (entry 7). Potassium hydrogen sulfate was also examined as a Bronsted acid its successful use in the synthesis of sulfinimines by condensation with no cleavage of the auxiliary being observed. KHSO_4 mediated the reaction, but still resulted in mainly the auxiliary cleavage product **2.76** (entry 8).

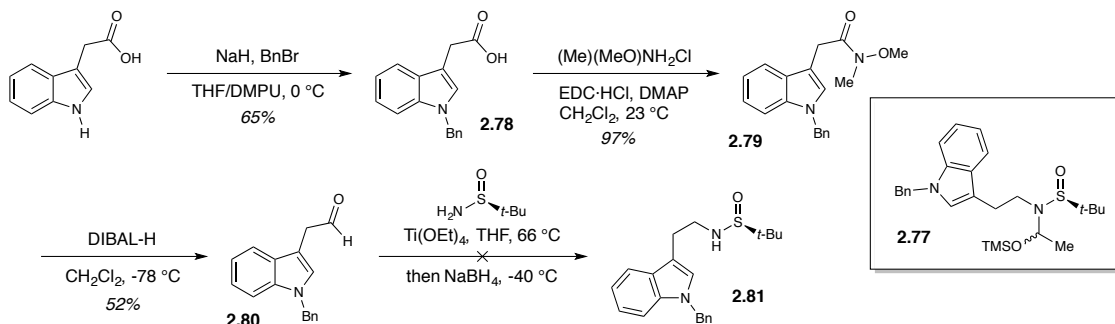
Scheme 2-28. Attempted reaction of hemiaminal ether **2.74** with allyltrimethylsilane.Table 2-2. Reaction of hemiaminal ether **2.74** with *N*-benzylindole.

entry	acid	solvent	2.76 (% yield)	2.71 (% yield)
1	$\text{BF}_3 \cdot \text{OEt}_2$	CH_2Cl_2	13	61
2	$\text{BF}_3 \cdot \text{OEt}_2$	Et_2O	-	74
3	$\text{BF}_3 \cdot \text{OEt}_2$	toluene	-	61
4	TMSCl	CH_2Cl_2	-	-
5	TsOH	CH_2Cl_2	52	21
6 ^a	TsOH	CH_2Cl_2	54	-
7 ^b	TsOH	CH_2Cl_2	-	-
8	KHSO_4	CH_2Cl_2	48	-

a. 3Å molecular sieves were added. b. 10% TsOH used.

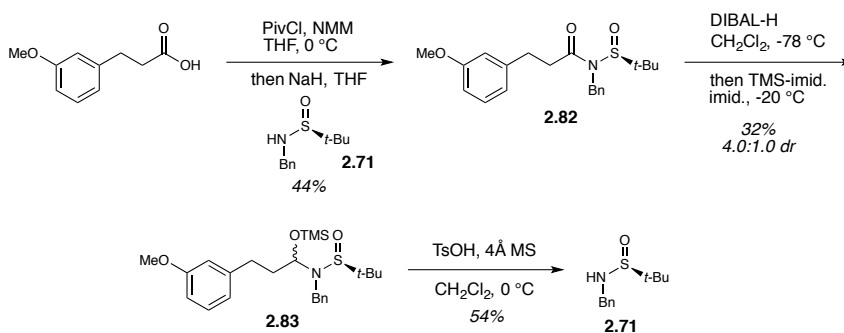
Given the difficulties apparent in the intermolecular addition reactions, as well as our desired reaction being an intramolecular cascade, we next sought to develop intramolecular test substrates containing tethered electron-rich aromatic rings. To this end, we first attempted the synthesis of indole-containing hemiaminal ether substrate **2.77** (Scheme 2-29). Beginning with indole-3-acetic acid, selective protection of the indole provided *N*-benzylindole-3-acetic acid **2.78** in 65% yield, which was subsequently converted into the Weinreb amide **2.79** and selectively reduced to *N*-benzylindole-3-acetaldehyde **2.80** in 50% yield over two steps. However, attempts to couple this material to sulfinamide **2.81** failed under the standard reductive amination conditions.

Scheme 2-29. Attempted synthesis of indole containing intramolecular substrate 2.77.



We also explored a substrate containing an electron rich anisole ring **2.83** (**Scheme 2-30**). Beginning with 3-(3-methoxyphenyl)propanoic acid, coupling with *N*-benzylsulfonamide **2.71** via the pivaloyl mixed anhydride provided the acetylated sulfonamide **2.82** in 44% yield. Reduction with DIBAL-H and trapping with trimethylsilylimidazole provided the hemiaminal ether substrate **2.83** in 32% yield in 4.0:1.0 dr. When this substrate was subjected to our best conditions found for the previous intermolecular reactions, only *N*-benzylsulfonamide **2.71** was obtained in 54% yield, most likely the result of iminium hydrolysis. Due to the combination of the observed significant auxiliary cleavage and the low enantioselectivity of coupled product that was obtained, the exploration of this approach as a method to form a chiral natural product core was abandoned.

Scheme 2-30. Synthesis of anisyl-substituted substrate 2.83 and attempted cyclization under acidic conditions.

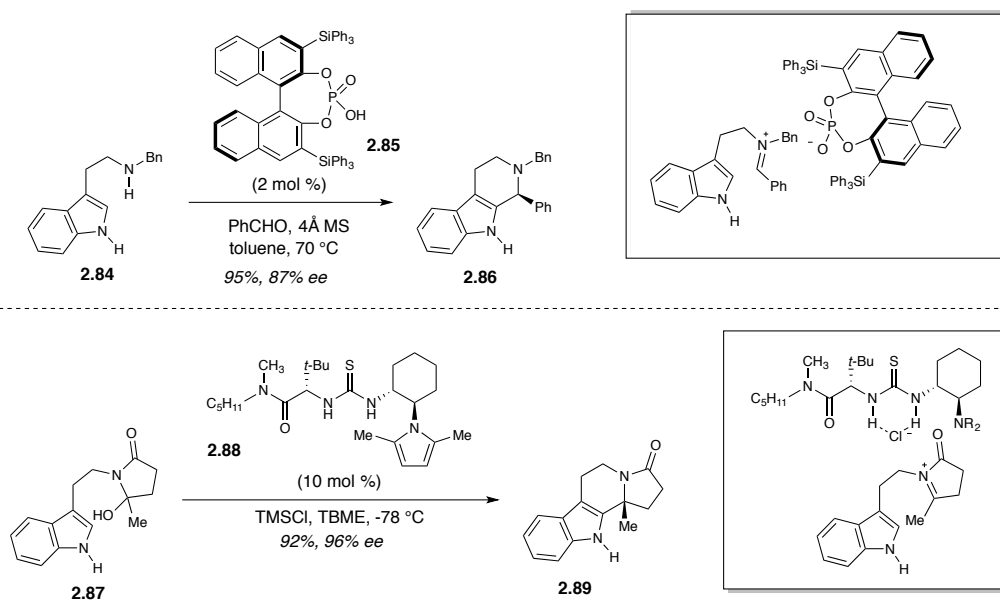


2.6.2 Studies Toward the Development of an Asymmetric Cascade Reaction with Ion-Pairing Catalysis

As stated above, asymmetric catalysis of iminium ion reactions is difficult due to the lack of Lewis basic functionality that traditional Lewis acid or metal-based catalysts can bind to. A recent advance in this area is the usage of ion-pairing catalysis, wherein a substrate and chiral catalyst are held in proximity via an ion-pairing interaction instead of the more typical covalent interactions used in traditional forms of catalysis (**Scheme 2-31**).¹³ One form of this catalysis involves a chiral Bronsted acid whose conjugate base can ion pair with a cationic intermediate formed either by acid-mediated decomposition or condensation within the substrate. For example, Rene de Gelder and coworkers have been able to demonstrate that BINOL-based chiral phosphoric acid **2.85** can catalyze asymmetric Pictet-Spengler reactions toward tetrahydro- β -carbolines **2.86**, wherein enantioselectivity is proposed to be induced by ion pairing between the conjugate base of the catalyst and the iminium formed by condensation of an aldehyde and tryptamine **2.84**.¹⁴ Alternatively, a strong hydrogen bonding catalyst can bind to an anion formed by

decomposition of a substrate, effectively holding the cationic intermediate formed in proximity of the catalyst by ion-pairing. This catalysis mode is invoked in Eric Jacobsen and coworkers' use of chiral thioureas in the catalysis of asymmetric Pictet-Spengler reactions on cyclic hemiaminals **2.87**, wherein the binding of the thiourea to a chloride anion effectively holds the chiral catalyst in close enough proximity of the *N*-acyliminium ion to induce enantioselectivity.¹⁵ Intrigued by these recent advances, we were curious if this form of catalysis would allow us to access an enantioselective variant of our cascade annulations we have developed.

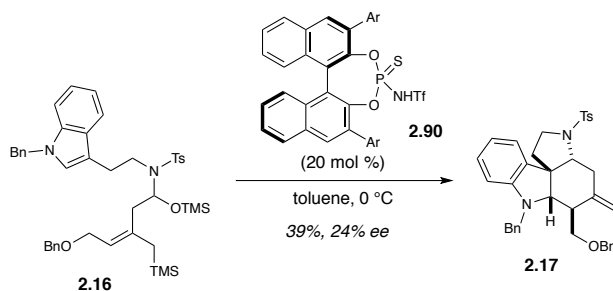
Scheme 2-31. Examples of ion-pairing catalysis as applied to reactions containing iminium ion intermediates.¹⁴⁻¹⁵



Our laboratory has been exploring the possibility of using ion pairing catalysis in our cascade with varying amounts of success for almost a decade. The best result in terms of enantioselectivity before the studies outlined below was achieved by former graduate student Aidi Kong (**Scheme 2-32**).¹⁶ Using chiral phosphoramidate catalyst **2.90**, she was

able to obtain the desired core of malagashanine **2.17** in 39% yield from hemiaminal ether **2.16**, but with only 24% ee. This was the best enantiomeric excess obtained after almost a year and a half of studies. Additionally, while this reaction was able to obtain a synthetically useable yield of product, typically these reactions were messy and led to multiple products.

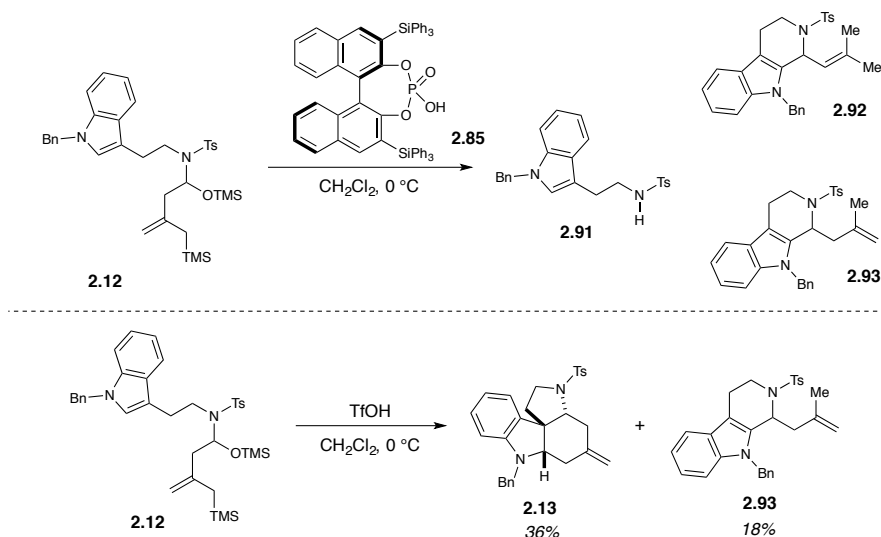
Scheme 2-32. Asymmetric catalysis of malagashanine cascade with chiral phosphoramidate 2.90.¹⁶



This problem of messy reactivity was noted by Ricardo Delgado during some of the earliest investigations into using this type of catalyst (**Scheme 2-33**).² Indeed, Ricardo noted that Bronsted acids typically led to issues with protodesilylation and alkene migration in the substrates, often leading to formation of several byproducts (**2.91-2.93**) with none of the desired tetracyclic core **2.13** being observed. While he was able to get a synthetically useful quantity of the desired Malagasy alkaloid core **2.13** with triflic acid, significant amounts of protodesilylated Pictet-Spengler product **2.93** was still obtained. In examining these results as a whole, it became apparent that we needed a catalytic system that would impart enantioselectivity by ion-pairing but that didn't use strong Bronsted acids to produce these conditions. While the chiral thiourea catalysts used by the Jacobsen group would possibly work, none have been able to successfully catalyze any reaction with our hemiaminal ether substrates. Therefore, we sought out a mode of

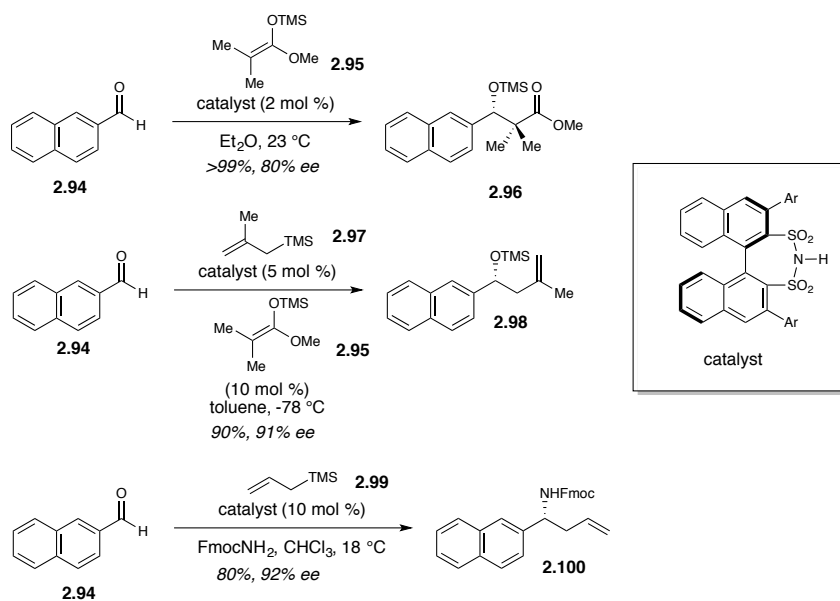
reactivity with these chiral BINOL-based catalysts that did not involve their use as Bronsted acids.

Scheme 2-33. Examples of early attempts by Ricardo Delgado to mediate our cascade annulation with Bronsted acids.²



Upon reexamination of the literature, we came across some published results from Benjamin List's group that we thought could potentially be applicable to our cascade annulation (**Scheme 2-34**).¹⁷ Using chiral disulfonimides based on the BINOL framework, List and coworkers were able to enantioselectively perform addition reactions with silylated nucleophiles such as silyl ketene acetals **2.95** and allylsilanes (**2.97** and **2.99**) to aldehydes (**2.94**). This was intriguing because these catalysts were typically used in reactions with silylated nucleophiles similar to those used in our cascade. Very few examples of these types of nucleophiles are used with the previously disclosed chiral phosphoric acid catalysts and their derivatives.¹⁸

Scheme 2-34. Examples of the use of chiral disulfonimide catalysts by Benjamin List and coworkers in asymmetric additions of silylated nucleophiles to aldehydes.¹⁷



Intriguingly, Benjamin List proposed that the active catalyst species within these reactions is the *N*-trimethylsilyl derivative formed by protodesilylation of a small portion of the nucleophile, as with the silylketene acetal shown (**Figure 2-3**).¹⁹ This species behaves like a silylium ion Lewis acid due to the weak coordination of the disulfonimide anion with the trimethylsilyl group, similar to the reactivity that has been evoked with the previously-disclosed achiral *N*-trimethylsilyltriflimide Lewis acid catalyst. Silylation of the terminal end of the carbonyl leads to formation of a silyloxycarbenium ion held in an ion pair with the disulfonamide anion. Addition of the nucleophile followed by nucleophilic attack of the disulfonimide anion on the then formed silylium ion would lead to reformation of the silylated catalyst. In a way, this catalyst involves similar ion-pairing binding modes as the chiral phosphoric acid catalysts, but instead involves transfers with a silylium ion instead of a proton, possibly eliminating any complications with Bronsted acid sensitive substrates.

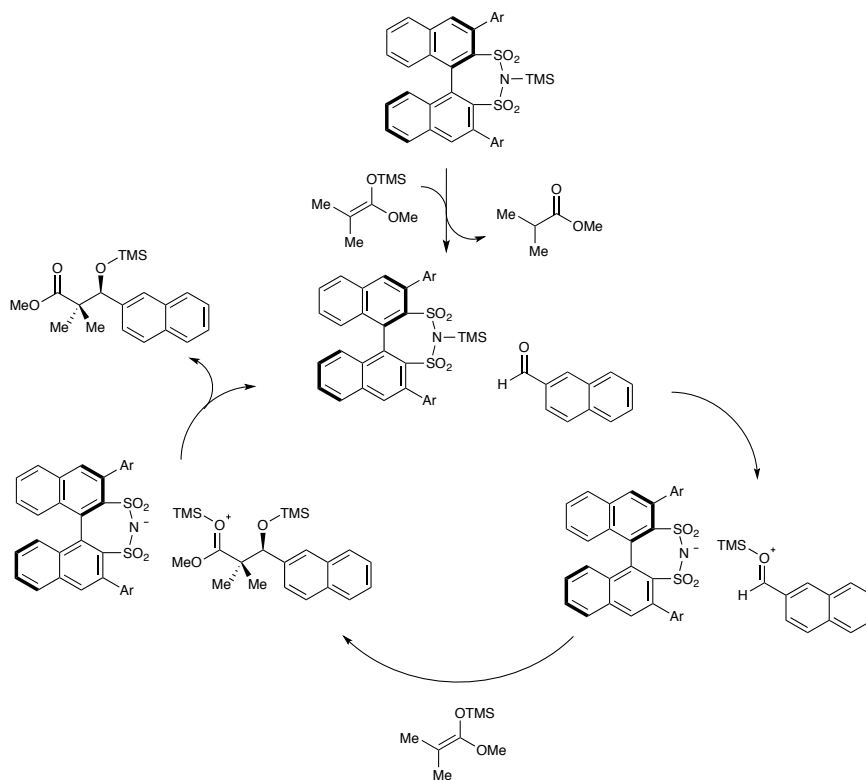


Figure 2-3. Proposed mechanism for disulfoninamide-catalyzed Mukaiyama aldol reaction invoking an *N*-trimethylsilyldisulfonamide intermediate.¹⁹

We envisioned a possible mechanism for our cascade involving an *N*-trimethylsilyldisulfonamide catalyst (**Figure 2-4**). This proposed mechanism in a way parallels what we believe is happening when decomposing our hemiaminal ether substrates with Lewis acids. The Lewis acidic silylated catalyst would promote decomposition of our hemiaminal ether, leading to generation of our iminium ion and disulfonamide anion with loss of bis(trimethylsilyl)ether. Upon reaction of the iminium ion with the indole, subsequent addition of the allylsilane to the indolenium ion would lead to formation of our desired product while regenerating the silylated catalyst conveniently with the trimethylsilyl group from the allylsilane moiety.

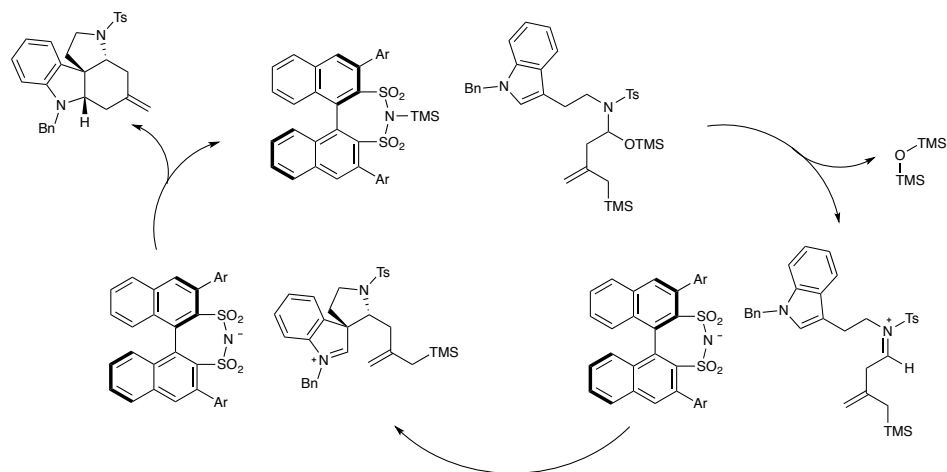
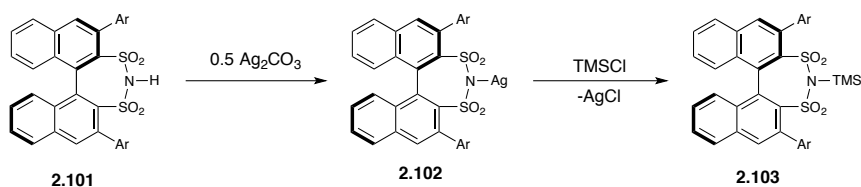


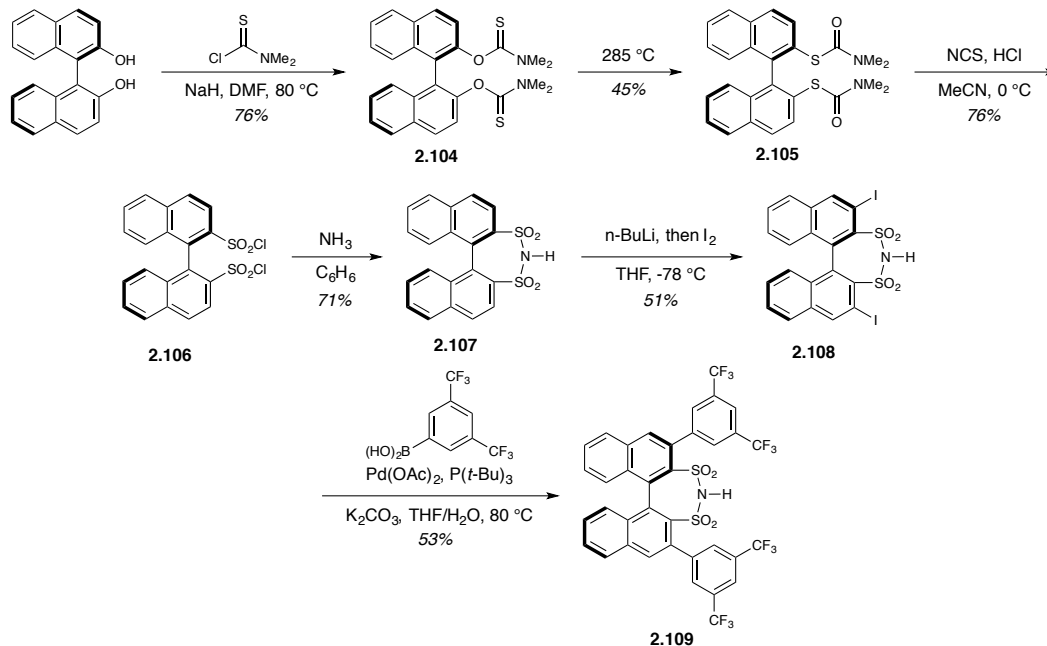
Figure 2-4. Proposed mechanism for reaction of *N*-trimethylsilyldisulfonimide catalysts with hemiaminal ether substrates.

Due to the sensitivity of our system to Bronsted acids, typically by protodesilylation, we wished to come up with a method for in situ generation of the silylated catalyst other than protodesilylation of a small quantity of the nucleophilic substrate (**Scheme 2-35**). In the previous phosphoric acid catalyst systems, silver salts had been invoked in some mechanisms,²⁰ and these species can sometimes be isolated and used in these reactions.²¹ We envisioned that if we could form the silver salt **2.102** of the disulfonimide **2.101**, reaction with trimethylsilylchloride would lead to formation of the silylated catalyst **2.103** with loss of insoluble silver chloride.

Scheme 2-35. Proposed method for in situ generation of *N*-trimethylsilyldisulfonimide catalyst **2.103 without protodesilylation of substrate.**

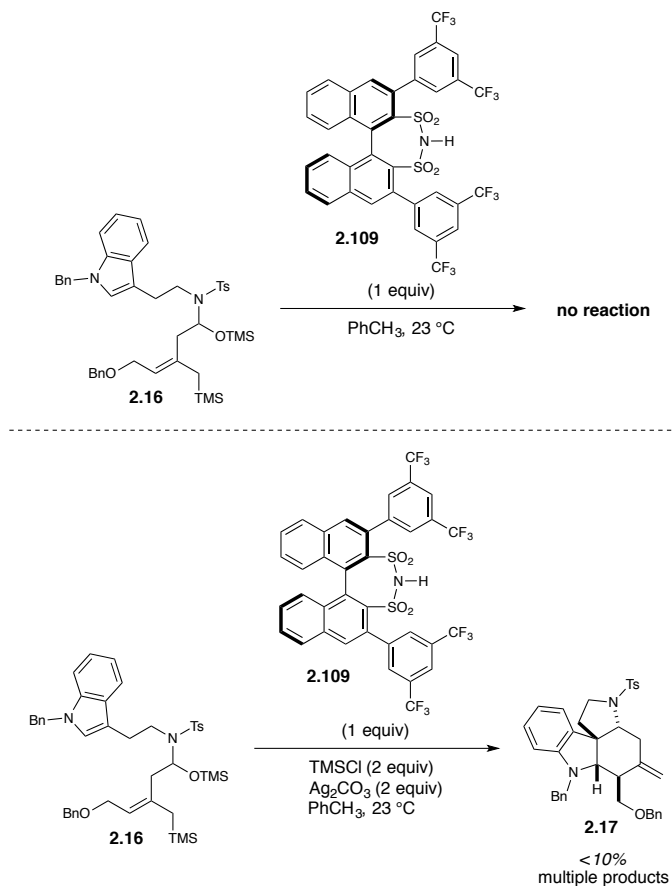


We therefore set out to examine if this aprotic catalyst system could provide us with both clean reactivity and useful enantioselectivity in our cascade. We first had to synthesize a test catalyst, a process that could be accomplished in six steps, using a modified route based on methods disclosed by List and coworkers (**Scheme 2-36**).¹⁹ BINOL was first converted into the *O*-thiocarbamate **2.104** by deprotonation and reaction with dimethylthiocarbamoyl chloride. This intermediate was converted into the *S*-thiocarbamate **2.105** via a Newman-Kwart rearrangement by heating this intermediate neat to 285 °C. This reaction proved to be capricious, never providing yields comparable to those reported by List and coworkers, with significant quantities of a thiophene byproduct typically being formed. The difficulties with Newman-Kwart rearrangements on BINOL-based substrates have been known, but none of the disclosed solutions gave satisfactory results in this reaction.²²⁻²⁴ The *S*-thiocarbamate derivative **2.105** was directly converted into the sulfonyl chloride **2.106** by acidic cleavage and subsequent reaction with in situ generated chloride gas, produced by the reaction of hydrochloric acid and *N*-chlorosuccinimide. The disulfonimide **2.107** was formed by stirring the sulfonyl chloride **2.106** in benzene under a balloon of ammonia. To introduce the 3,3'-substituents on the catalyst, the disulfonimide group was used as an ortho director for lithiation. Quenching this process with iodine provided the 3,3'-diiodide **2.108**.²⁵ Subsequent Suzuki coupling of the iodide **2.108** with our desired aryl boronic acid provided the desired disulfonimide catalyst **2.109**. Compared to methods to synthesize the related chiral phosphoric acid catalysts, this route was attractive because the 3,3'-substituents, often the key factor in determining selectivity with these types of catalysts, could be introduced in the last step, potentially allowing ready synthesis of a broad library of catalysts from a large batch of diiodide precursor **2.108**.

Scheme 2-36. Synthesis of disulfonimide catalyst **2.109** from BINOL.

To initially examine the feasibility of the disulfonimide to mediate our cascade, we began by testing reactions involving stoichiometric quantities of this reagent (**Scheme 2-38**). Within these studies, the hemiaminal ether substrate **2.16** that provides Malagasy core **2.17** was examined due to the presence of an already well developed chiral HPLC method. When hemiaminal ether **2.16** was exposed to an equivalent of chiral disulfonimide **2.109** at room temperature, no reaction was observed, even after 48 hours. However, when the chiral disulfonimide **2.109**, chlorotrimethylsilane, and silver carbonate were premixed and then added to a solution of hemiaminal ether **2.16**, complete consumption of the substrate occurred in less than 30 minutes. Multiple products were formed, as had been seen in previous attempts at asymmetric catalysis, but some the desired product **2.17** was isolated, albeit in less than 10% yield.

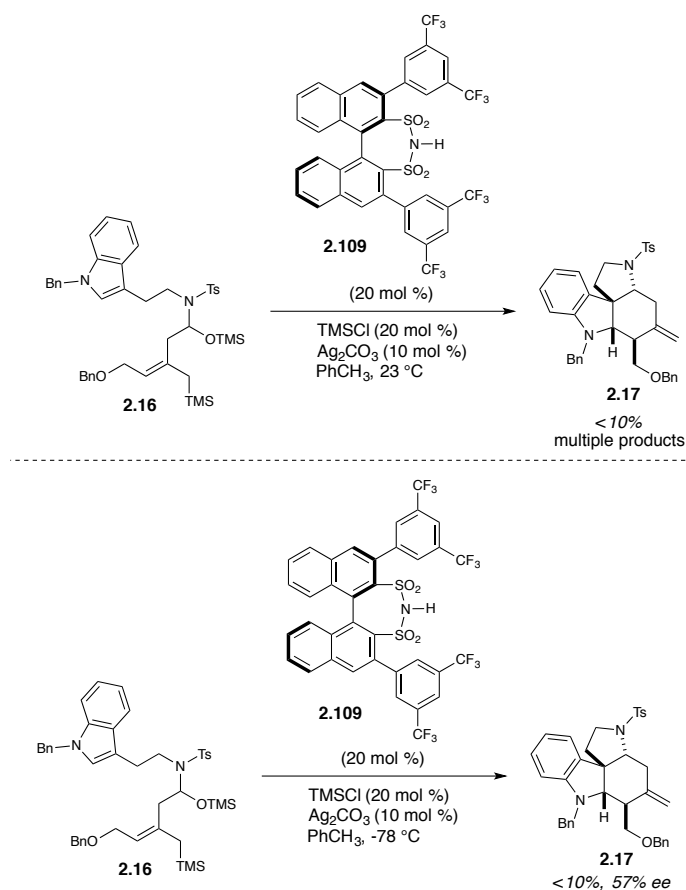
Scheme 2-37. Initial test reactions with stoichiometric quantities of disulfonimide **2.109.**



When the chiral disulfonimide **2.109** was used on a catalytic scale (20 mol %), hemiaminal ether starting material **2.16** was consumed, suggesting the possibility of catalysis (**Scheme 2-38**). To see if we could clean up the reactivity, we attempted the cyclization reaction at lower temperatures (-40 and $-78\text{ }^\circ\text{C}$). At both of these temperatures, it appeared the reaction would lead exclusively to the desired tetracyclic product **2.17**, with this product obtained gratifyingly in 57% ee at $-78\text{ }^\circ\text{C}$. This was the highest enantiomeric excess we had obtained with any catalyst up to this point. However, the product would be formed in small quantities in the first several minutes upon introduction of the

disulfonimide but would then stall, leading to significant amounts of starting material still being present in the reaction. This suggests that the active species mediating the desired cyclization could not turnover, only providing a small quantity of the desired core.

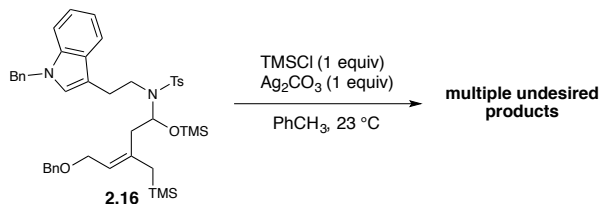
Scheme 2-38. Reactions with catalytic quantities of disulfonimide 2.109.



The next question we had was what other pathways were possibly occurring when we were running these reactions at room temperature. The answer came from a control that was run using only chlorotrimethylsilane and silver carbonate with our hemiaminal ether **2.16** (Scheme 2-39). When exposed to an equivalent of these reagents, the hemiaminal ether was successfully consumed into a mixture of unidentified byproducts, with none of the desired tetracyclic core **2.17** found in this reaction. Disappointingly, this

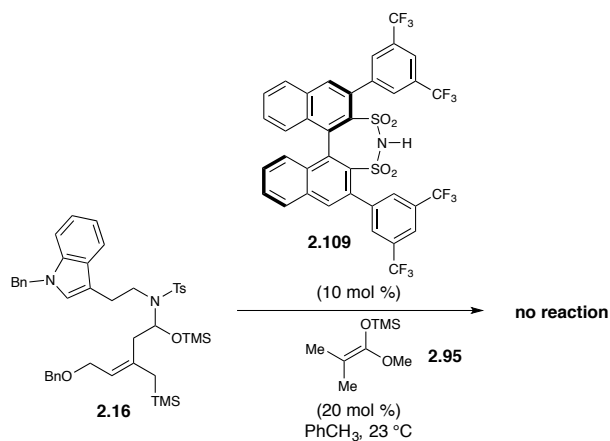
suggests that the combination of chlorotrimethylsilane and silver carbonate was facilitating detrimental background reactivity that was leading to many of the observed byproducts in our reaction.

Scheme 2-39. Control reaction of hemiaminal ether **2.16 with chlorotrimethylsilane and silver carbonate.**



To examine whether the silylated disulfonimide was truly competent to mediate our desired cascade, we examined an alternative method for forming this intermediate, instead using a substoichiometric quantity of silyl ketene acetal **2.95** as a silylating agent that was suggested to form the active catalyst in Benjamin List's prior studies (**Scheme 2-40**).¹⁹ Indeed, he found it necessary to add a small quantity of this silyl ketene acetal **2.95** in disulfonimide-catalyzed Sakurai allylations due to the allylsilane not forming a significant quantity of the active catalyst by protodesilylation. When these reaction conditions were tested at room temperature, no reaction was observed, even over 48 hours. This suggests that the silylated disulfonimide itself was not the active species that was mediating the desired above studied reactions and that this catalyst system would not be competent in mediating an enantioselective variant of our cascade.

Scheme 2-40. Attempted reaction of hemiaminal ether using disulfonimide catalyst 2.109 in the presence of silyl ketene acetal 2.95 as an activating reagent.



To this end, we still have an active interest in the development of a catalyst system that would be effective for our cascade. Currently, we are planning to explore the possible use of anion-binding catalysis as an alternative method for activation of trimethylsilyl halides as Lewis acids in our cascade. This is based off of some preliminary unpublished results from Eric Jacobsen's group, with whom we may collaborate to develop such a system. This would circumvent any problems involving excess Bronsted acidity as well the use of silver salts in the formation of active silylium catalysts.

2.7 Conclusion

We were able to successfully synthesize a trisubstituted allylsilane containing hemiaminal ether substrate and cyclize it to a bridged tetracyclic akuammiline alkaloid core. Demonstrating the increased steric demands of this catalytic system, only the *Z*-allylsilane geometry was able to successfully cyclize to this core, with two different variants of the *E*-allylsilane instead leading to Pictet-Spengler products. The *E*-allylsilane

faces steric clashing in both the boat- and chair-like transition states for the allylsilane addition step of the cascade, while the *Z*-allylsilane isomer is able to overcome this hindrance in its boat-like transition state.

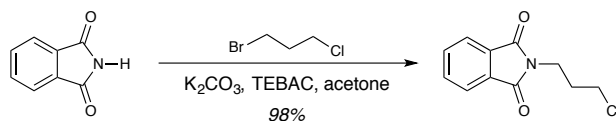
2.8 Experimental Procedures

General Experimental

Reactions were performed under a dry nitrogen atmosphere with anhydrous solvents using standard Schlenk techniques unless otherwise stated. Glassware was dried in an oven at 120 °C for a minimum of six hours prior to use. Anhydrous tetrahydrofuran (THF), diethyl ether (Et₂O), and dichloromethane (CH₂Cl₂) were obtained by passage through activated alumina using a *Glass Contours* solvent purification system. Anhydrous dimethyl sulfoxide (DMSO), *N,N*-dimethylformamide (DMF), acetonitrile (MeCN), and methanol (MeOH) were obtained from EMD Millipore and were stored over dry 4Å molecular sieves. *N,N*-diisopropylethylamine (DIPEA), pyridine (pyr), and triethylamine (Et₃N) were distilled from calcium hydride and stored over dry 4Å molecular sieves. Boron trifluoride diethyl etherate (BF₃·OEt₂) was distilled under vacuum from calcium hydride directly before use. 4Å powdered molecular sieves were activated by heating to 100 °C under reduced pressure (0.2 torr) for at least 12 hours. Lithium bis(trimethylsilyl)amide (LiHMDS), Schwartz reagent (Cp₂ZrHCl), copper(I) chloride (CuCl), lithium chloride (LiCl), and 9-borabicyclo(3.3.1)nonane dimer (9-BBN-H dimer) were stored and weighed in a nitrogen-filled glovebox. Pd(MeCN)₂Cl₂,²⁶ 2-iodoxybenzoic acid (IBX),²⁷ and Dess-Martin Periodinane (DMP)²⁸ were synthesized according to previously reported methods. All other reagents and solvents were obtained from commercial suppliers and used as

received. Ozone was supplied using a Pacific Ozone Supply L21 ozone generator. Reactions under pressurized hydrogen were performed in a Parr 4793 general purpose pressure vessel. Analytical thin layer chromatography (TLC) was performed on precoated glass backed Silicycle SiliaPure® 0.25 mm silica gel 60 plates. Visualization was accomplished with UV light, ethanolic *p*-anisaldehyde, ethanolic phosphomolybdic acid, or aqueous potassium permanganate. Flash column chromatography was performed using Silicycle SilaFlash® F60 silica gel (40-63 μm). Preparatory thin layer chromatography was performed on precoated glass backed Silicycle SiliaPure® 1.0 mm silica gel 60 plates. ^1H and ^{13}C nuclear magnetic resonance (NMR) spectra were recorded on a Varian Inova 600 spectrometer (600 MHz ^1H , 151 MHz ^{13}C), a Bruker 600 spectrometer (600 MHz ^1H , 151 MHz ^{13}C), a Varian Inova 500 spectrometer (500 MHz ^1H , 126 MHz ^{13}C), and a Varian Inova 400 spectrometer (400 MHz ^1H , 100 MHz ^{13}C) at room temperature in CDCl_3 (neutralized and dried over anhydrous K_2CO_3) with internal CHCl_3 as the reference (7.26 ppm for ^1H and 77.23 ppm for ^{13}C), unless otherwise stated. Chemical shifts were reported in parts per million (ppm) and coupling constants (J values) in Hz. Multiplicity was indicated using the following abbreviations: s = singlet, d = doublet, t = triplet, q = quartet, p = pentet, m = multiplet, b = broad. Infrared (IR) spectra were recorded using a Thermo Electron Corporation Nicolet 380 FT-IR spectrometer. High resolution mass spectra (HRMS) were obtained using a Thermo Electron Corporation Finigan LTQFTMS (at the Mass Spectrometry Facility, Emory University). We acknowledge the use of shared instrumentation provided by grants from the NIH and the NSF.

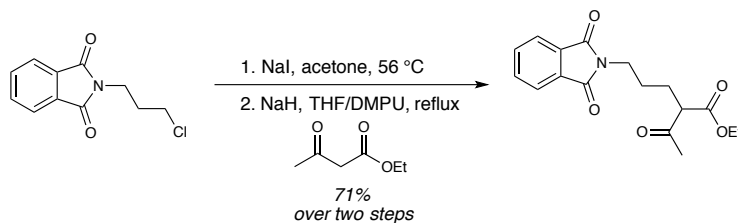
Alkyl Chloride 2.36:



Phthalimide (2.35 g, 16.0 mmol, 1.0 equiv), K_2CO_3 (6.63 g, 48.0 mmol, 3.0 equiv), and benzyltriethylammonium chloride (547.0 mg, 2.40 mmol, 20 mol %) was brought up in acetone (40.0 mL). 1-bromo-3-chloropropane (4.75 mL, 48.0 mmol, 3.0 equiv) was then added, and the resultant slurry was stirred for 24 hours at room temperature. The reaction mixture was concentrated under reduced pressure, and water (100.0 mL) and EtOAc (100.0 mL) were added. The layers were separated, and the aqueous phase was extracted with EtOAc (3 x 75.0 mL). The combined organic layer was washed with brine (100.0 mL), dried over anhydrous Na_2SO_4 , filtered, and concentrated under reduced pressure. Purification by flash column chromatography on silica gel (3:2 hexanes/EtOAc) provided alkyl chloride **2.36** (3.45 g, 96%) as a white solid. Spectral data matched that previously reported.⁶

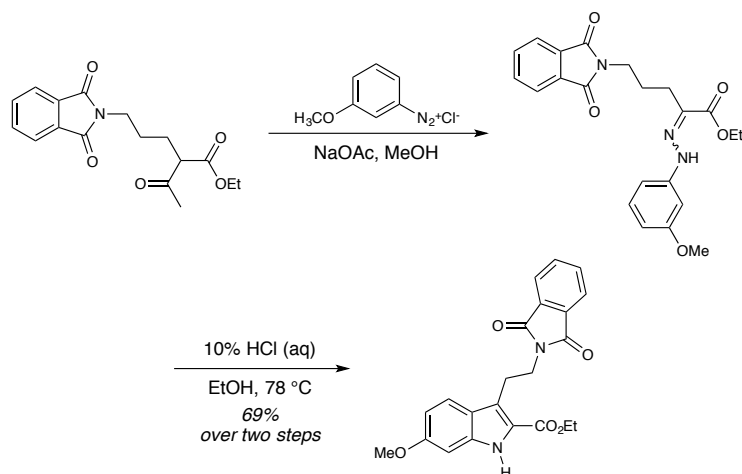
¹H NMR (400 MHz, CDCl_3) δ 7.84 (dd, $J = 4.8, 2.8$ Hz, 2H), 7.71 (dd, $J = 5.6, 3.2$ Hz, 2H), 3.84 (t, $J = 7.2$ Hz, 2H), 3.56 (t, $J = 6.8$ Hz, 2H), 2.16 (p, $J = 6.8$ Hz, 2H) ppm.

Ester 2.37:



Alkyl chloride **2.36** (1.00 g, 4.47 mmol, 1.0 equiv) and NaI (2.00 g, 13.41 mmol, 3.0 equiv) were dissolved in acetone (20.0 mL), and the reaction mixture was refluxed for ten hours. The mixture was cooled, and the precipitated salts were filtered over celite. The filter pad was washed with acetone (3 x 10.0 mL), and the filtrate was concentrated under reduced pressure to provide crude iodide, which was dissolved in THF (10.0 mL). To a suspension of NaH (214.0 mg, 60 wt % dispersion in mineral oil, 5.36 mmol, 1.2 equiv) in THF (10.0 mL) was added ethyl acetoacetate (0.63 mL, 4.92 mmol, 1.1 equiv) drop-wise. After gas evolution ceased, DMPU was added (2.0 mL). The alkyl iodide solution was then added via cannula, and the reaction mixture was refluxed for 12 hours. The reaction mixture was cooled to room temperature and quenched with saturated aqueous NH_4Cl (20.0 mL). The layers were separated, and the aqueous phase was extracted with Et_2O (3 x 20.0 mL). The combined organic layer was washed with water (3 x 20.0 mL) and brine (20.0 mL), dried over anhydrous Na_2SO_4 , filtered, and concentrated under reduced pressure. Purification by flash column chromatography on silica gel (3:2 hexanes/EtOAc) provided ester **2.37** (1.00 g, 71% over two steps) as a white solid. Spectral data matched that previously reported.⁶

$^1\text{H NMR}$ (400 MHz, CDCl_3) δ 7.82 (dd, $J = 5.6, 3.2$ Hz, 2H), 7.70 (dd, $J = 5.6, 2.8$ Hz, 2H), 4.16 (q, $J = 6.8$ Hz, 2H), 3.68 (t, $J = 7.2$ Hz, 2H), 3.48 (t, $J = 4.0$ Hz, 1H), 2.21 (s, 3H), 1.94-1.60 (m, 4H), 1.24 (t, $J = 6.8$ Hz, 3H) ppm.

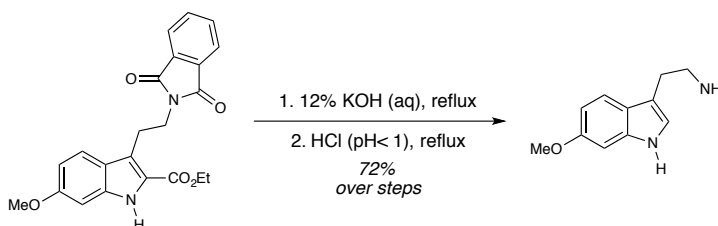
Tryptamine 2.39:

Meta-anisidine (0.71 mL, 6.30 mmol, 1.0 equiv) was dissolved in MeOH (4.8 mL) and water (19.7 mL), and the resultant solution was cooled to 0 °C. Hydrochloric acid (36%, 5.0 mL) was added drop-wise over 30 minutes. A solution of NaNO₂ (993.0 mg, 14.4 mmol, 2.3 equiv) in water (3.5 mL) was then added drop-wise over 30 minutes. The mixture was then stirred for 30 minutes at 0 °C to provide a solution of the desired diazonium salt. Ester **2.37** (2.80 g, 8.80 mmol, 1.4 equiv) and NaOAc (8.30 g, 101.0 mmol, 16.0 equiv) were dissolved in MeOH (40.0 mL) and stirred for one hour at room temperature. The diazonium salt solution was then added drop-wise to the ester solution over one hour, and the resultant reaction mixture was stirred for 16 hours. CH₂Cl₂ (60.0 mL) was added, and the layers were separated. The organic layer was washed with water (3 x 40.0 mL), dried over anhydrous Na₂SO₄, filtered, and concentrated under reduced pressure. The residue was brought up in EtOH (10.7 mL) and hydrochloric acid (36%, 10.7 mL) was added. The reaction mixture was refluxed for 24 hours and then cooled to room temperature. A precipitate formed, which was filtered and washed with water (3 x 20.0

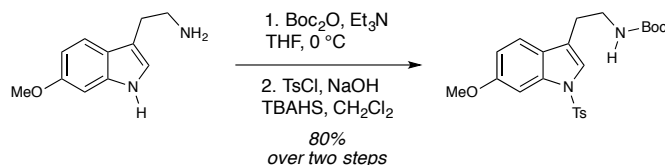
mL). The solid was dried under high vacuum to provide tryptamine **2.39** (1.60 g, 69% over two steps) as a pale tan solid. Spectral data matched that previously reported.⁶

¹H NMR (400 MHz, CDCl₃) δ 8.64 (bs, 1H), 7.80 (dd, $J = 5.6, 3.2$ Hz, 2H), 7.68 (dd, $J = 5.6, 3.2$ Hz, 2H), 7.60 (d, $J = 8.4$ Hz, 1H), 6.75 (m, 2H), 4.40 (q, $J = 7.2$ Hz, 2H), 3.99 (t, $J = 7.2$ Hz, 2H), 3.83 (s, 3H), 3.43 (t, $J = 8.0$ Hz, 2H), 1.44 (t, $J = 6.8$ Hz, 3H) ppm.

6-Methoxytryptamine **2.40**:



Tryptamine **2.39** (1.60 g, 4.35 mmol) was added to 15% aqueous KOH (10.0 mL), and the slurry was heated to reflux for 24 hours, the solution becoming homogenous upon progression of the reaction. The reaction was cooled to room temperature, and 1 M HCl was added drop-wise until pH < 1. The reaction mixture was then heated to reflux for 24 hours, and was again cooled to room temperature. The reaction was neutralized by slow addition of saturated aqueous NaHCO₃. The aqueous solution was extracted with EtOAc (3 x 50.0 mL). The combined organic layer was washed with brine (50.0 mL), dried over anhydrous Na₂SO₄, filtered, and concentrated under reduced pressure to provide 6-methoxytryptamine **2.40** (595.5 mg, 70% over two steps) as a white solid. Spectral data matched that previously reported.⁶

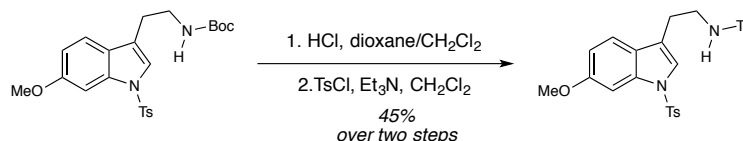
***N*-Ts-*N'*-Boc-6-methoxytryptamine 2.41:**

To a solution of 6-methoxytryptamine **2.40** (140.8 mg, 0.74 mmol, 1 equiv) in THF (4.0 mL) was added Et_3N (0.15 mL, 1.11 mmol, 1.5 equiv). The reaction mixture was cooled to $0\text{ }^\circ\text{C}$, and a solution of Boc_2O (161.5 mg, 0.74 mmol, 1.0 equiv) in THF (1.0 mL) was added. The reaction mixture was stirred for 14 hours, and then quenched with saturated aqueous NH_4Cl (5.0 mL). The layers were separated, and the aqueous phase was extracted with Et_2O (3 x 5.0 mL). The combined organic layer was washed with brine (10.0 mL), dried over anhydrous MgSO_4 , filtered, and concentrated under reduced pressure. The crude residue was brought up in CH_2Cl_2 (10.0 mL). Powdered NaOH (73.0 mg, 1.85 mmol, 2.5 equiv) and TBAHS (25.0 mg, 0.08 mmol, 10 mol %) were added, and the mixture was stirred for ten minutes. TsCl (212.0 mg, 1.11 mmol, 1.5 equiv) was added, and the suspension was stirred for 16 hours. Water (10.0 mL) was added, and the biphasic mixture was stirred for ten minutes. The layers were separated, and the aqueous phase was extracted with CH_2Cl_2 (3 x 25.0 mL). The combined organic layer was dried over anhydrous Na_2SO_4 , filtered, and concentrated under reduced pressure. Purification by flash column chromatography on silica gel (7:3 hexanes/ EtOAc) provided *N*-Ts-*N'*-Boc-6-methoxytryptamine **2.41** (266.0 mg, 80% over two steps) as a white solid. Spectral data matched that previously reported.²

$^1\text{H NMR}$ (400 MHz, CDCl_3) δ 7.73 (d, $J = 8.4$ Hz, 2H), 7.52 (d, $J = 2.0$ Hz, 1H), 7.35 (d, $J = 8.8$ Hz, 1H), 7.25 (d, 1H), 7.22 (d, $J = 8.4$ Hz, 2H), 6.86 (dd, $J = 8.8, 2.4$ Hz, 2H),

4.56 (bs, 1H), 3.88 (s, 3H), 3.39 (q, $J = 6.9$ Hz, 2H), 2.82 (t, $J = 6.9$ Hz, 2H), 2.18 (s, 3H), 1.45 (s, 9H) ppm.

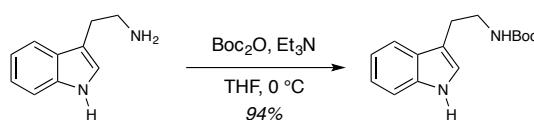
***N,N'*-bistosyl-6-methoxytryptamine 2.33:**



To a solution of carbamate **2.41** (266.0 mg, 0.59 mmol, 1.0 equiv) in CH_2Cl_2 (4.0 mL) was added a solution of HCl in 1,4-dioxane (4M, 4.0 mL), and the resultant mixture was stirred for one hour. The reaction was quenched by the slow addition of saturated aqueous NaHCO_3 until $\text{pH} > 7$, and the layers were separated. The aqueous phase was extracted with CH_2Cl_2 (3 x 10.0 mL), and the combined organic layer was wash with water (10.0 mL) and brine (10.0 mL). The combined organic layer was dried over anhydrous Na_2SO_4 , filtered, and concentrated under reduced pressure. The crude residue was brought up in CH_2Cl_2 (7.0 mL), and Et_3N (0.33 mL, 2.36 mmol, 4.0 equiv) and TsCl (124.0 mg, 0.65 mmol, 1.1 equiv) were added. The reaction mixture was stirred for 18 hours and was then quenched with water (10.0 mL). The layers were separated, and the aqueous layer was extracted with CH_2Cl_2 (3 x 20.0 mL). The combined organic layer was dried over anhydrous Na_2SO_4 , filtered, and concentrated under reduced pressure. Purification by flash column chromatography on silica gel (3:2 hexanes/ EtOAc) provided *N,N'*-bistosyl-6-methoxytryptamine **2.33** (133.0 mg, 45% over two steps) as a white solid. Spectral data matched that previously reported.²

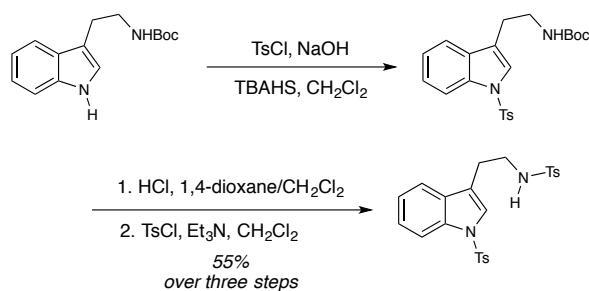
¹H NMR (400 MHz, CDCl₃) δ 7.73 (d, J = 8.4 Hz, 2H), 7.59 (d, J = 8.4 Hz, 2H), 7.50 (d, J = 2.0 Hz, 1H), 7.27 – 7.21 (m, 4H), 7.17 (d, J = 8.4 Hz, 2H), 6.81 (dd, J = 8.8, 2.4 Hz, 1H), 4.24 (t, J = 7.6 Hz, 1H), 3.88 (s, 3H), 3.23 (q, J = 5.6 Hz, 2H), 2.79 (t, J = 6.8 Hz, 2H), 2.41 (s, 3H), 2.35 (s, 3H) ppm.

Boc-tryptamine 2.42:



To a solution of Et₃N (15.7 mL, 112.3 mmol, 1.5 equiv) in THF (400.0 mL) at 0 °C was added tryptamine (12.0 g, 74.9 mmol, 1.0 equiv). A solution of Boc₂O (16.4 g, 74.9 mmol, 1.0 equiv) in THF (100.0 mL) was then added to the tryptamine solution by cannula. The reaction mixture was slowly warmed to room temperature and stirred for 16 hours. The reaction mixture was concentrated under reduced pressure. Purification by flash column chromatography on a short plug (2 inch) of silica gel (1:1 hexanes/EtOAc) provided Boc-tryptamine **2.42** (17.9 g, 94%) as a pale tan oil. Spectral data matched that previously reported.²⁹

¹H NMR (400 MHz, CDCl₃) δ 8.06 (s, 1H), 7.59 (d, J = 7.9 Hz, 1H), 7.32 (d, J = 7.9 Hz, 1H), 7.19 (t, J = 7.3 Hz, 1H), 7.10 (t, J = 7.0 Hz, 1H), 6.97 (bs, 1H), 4.61 (bs, 1H), 3.45 (q, J = 6.6 Hz, 2H), 2.95 (t, J = 6.7 Hz, 2H), 1.41 (s, 9H) ppm.

***N,N'*-bistosyltryptamine 2.34:**

To a solution of Boc-tryptamine **2.42** (17.9 g, 68.9 mmol, 1.0 equiv) in CH_2Cl_2 (250.0 mL) at 0 °C was consecutively added tosyl chloride (19.7 g, 103.4 mmol, 1.5 equiv), powdered NaOH (6.9 g, 172.3 mmol, 2.5 equiv) and TBAHS (2.3 g, 6.9 mmol, 10 mol %). The resultant slurry was warmed to room temperature and stirred for 24 hours. The reaction mixture was quenched with water (100.0 mL), and the layers were separated. The aqueous phase was extracted with CH_2Cl_2 (3 x 50.0 mL). The combined organic layer was dried over anhydrous Na_2SO_4 , filtered, and concentrated under reduced pressure. The residue was filtered over a plug of silica gel (2:1 hexanes/EtOAc) and concentrated under reduced pressure. The residue was dissolved in CH_2Cl_2 (200.0 mL) and cooled to 0 °C. 4 M HCl in 1,4-dioxane (60.0 mL) was added dropwise to the solution, and the mixture was stirred for one hour. The reaction mixture was concentrated under reduced pressure to provide the crude ammonium chloride salt. This residue was brought up in CH_2Cl_2 (250.0 mL) and cooled to 0 °C. Et_3N (39.0 mL, 275.6 mmol, 4.0 equiv) was added dropwise to the slurry. Tosyl chloride (14.5 g, 75.8 mmol, 1.1 equiv) was then added, and the resultant mixture was warmed up to room temperature and stirred for 14 hours. The reaction was quenched with water (100.0 mL), and the layers were separated. The aqueous phase was extracted with CH_2Cl_2 (3 x 100.0 mL). The combined organic layer was dried over anhydrous Na_2SO_4 , filtered, and concentrated under reduced pressure. The crude residue was triturated

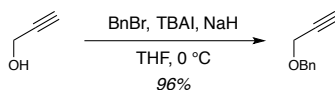
with methanol, sonicated, and filtered to provide *N,N'*-bistosyltryptamine **2.34** (16.9 g, 52% over three steps) as a white solid.

¹H NMR (300 MHz, CDCl₃) δ 7.95 (d, *J* = 8.1 Hz, 1H), 7.73 (d, *J* = 8.1 Hz, 2H), 7.60 (d, *J* = 8.4 Hz, 2H), 7.34 – 7.13 (m, 8H), 4.51 (t, *J* = 7.2 Hz, 1H), 3.23 (q, *J* = 6.9 Hz, 2H), 2.83 (t, *J* = 6.9 Hz, 2H), 2.40 (s, 3H), 2.33 (s, 3H) ppm.

¹³C NMR (126 MHz, CDCl₃) δ 145.0, 143.4, 136.7, 135.2, 135.1, 130.2, 129.9, 129.7, 126.9, 126.8, 124.9, 123.8, 123.2, 119.2, 118.7, 113.8, 42.3, 25.5, 21.6, 21.5 ppm.

HRMS (+APCI) calculated for C₂₅H₂₅O₄N₂S₂ [M+H]⁺ 469.1256, found 469.1255.

Benzyl Ether 2.44:

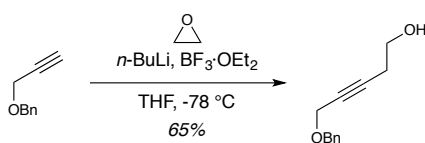


To a suspension of NaH (60 wt % dispersion in mineral oil, 3.60 g, 89.0 mmol, 1.0 equiv) in THF (250.0 mL) at 0 °C was added propargyl alcohol (5.20 mmol, 89.0 mmol, 1.0 equiv) drop-wise, and the reaction mixture was warmed to room temperature and stirred for one hour. TBAI (1.07 g, 2.90 mmol, 3 mol %) and benzyl bromide (11.7 mL, 97.9 mmol, 1.1 equiv) were added, and the resultant mixture was stirred at room temperature for 16 hours. The reaction was quenched with water (100.0 mL), and the organic solvent was removed under reduced pressure. The resultant aqueous phase was extracted with Et₂O (3 x 150.0 mL). The combined organic layer was washed with brine (150.0 mL), dried over anhydrous MgSO₄, filtered, and concentrated under reduced pressure. Purification by flash

column chromatography on silica gel (4:1 hexanes/EtOAc) provided benzyl ether **2.44** (9.88 g, 96%) as a colorless oil. Spectra data matched that previously reported.⁵

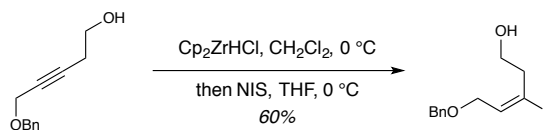
¹H NMR (300 MHz, CDCl₃) δ 7.41-7.22 (m, 5H), 4.61 (s, 2H), 4.19 (s, 2H), 2.42 (s, 1H) ppm.

Propargyl Alcohol **2.45**:



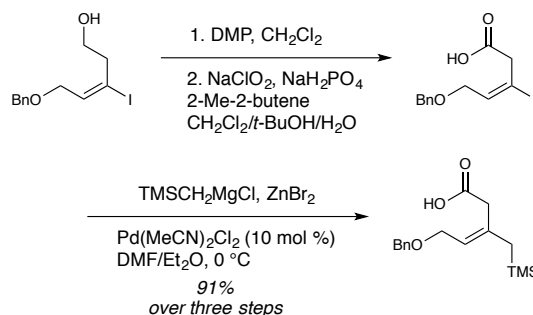
To a solution of benzyl ether **2.44** (3.52 g, 24.1 mmol, 1.0 equiv) in THF (125.0 mL) at -78 °C was added n-BuLi (2.5 M in hexanes, 12.5 mL, 31.3 mmol, 1.3 equiv) drop-wise over ten minutes, and the solution was stirred for one hour. BF₃·OEt₂ (3.86 mL, 31.3 mmol, 1.3 equiv) was then added drop-wise, and the solution was stirred for 15 minutes. A solution of oxirane (1.43 mL, 28.9 mmol, 1.2 equiv) in THF (3.0 mL) was quickly cannulated into the benzyl ether solution, and the resultant mixture was stirred for two hours. The reaction was quenched with saturated aqueous NH₄Cl (45.0 mL), and the layers were separated. The aqueous phase was extracted with Et₂O (3 x 100.0 mL). The combined organic layer was washed with brine (150.0 mL), dried over anhydrous Na₂SO₄, filtered, and concentrated under reduced pressure. Purification by flash column chromatography on silica gel (3:2 hexanes/EtOAc) provided propargyl alcohol **2.45** (2.99 g, 56%) as a yellow oil. Spectral data matched that previously reported.⁵

¹H NMR (400 MHz, CDCl₃) δ 7.38-7.30 (m, 5H), 4.60 (s, 2H), 4.18 (t, *J* = 2.1 Hz, 2H), 3.75 (q, *J* = 6.3 Hz, 2H), 2.54 (tt, *J* = 6.3, 2.2 Hz, 2H), 1.75 (bt, *J* = 5.4 Hz, 1H) ppm.

Vinyl Iodide 2.46:

To a slurry of Cp_2ZrHCl (12.2 g, 47.1 mmol, 3.0 equiv) in CH_2Cl_2 (75.0 mL) at 0 °C was added a solution of propargyl alcohol **2.45** (2.99 g, 15.7 mmol, 1.0 equiv) in CH_2Cl_2 (75.0 mL) via cannula, and the resultant mixture was stirred for three hours at 0 °C. A solution of *N*-iodosuccinimide (7.06 g, 31.4 mmol, 2.0 equiv) in THF (75.0 mL) was then added via cannula, and the reaction mixture was stirred for 30 minutes. The reaction was quenched with 1:1 saturated aqueous NaHCO_3 /saturated aqueous Na_2SO_3 (150.0 mL), and the mixture was stirred for 15 minutes. The biphasic mixture was filtered through celite, and the filter pad was washed with Et_2O (2 x 100.0 mL). The combined organic layers were washed with brine (150.0 mL), dried over anhydrous Na_2SO_4 , filtered, and concentrated under reduced pressure. Purification by flash column chromatography on silica gel (4:1 hexanes/ EtOAc) provided vinyl iodide **2.46** (2.98 g, 60%) as an orange oil. Spectral data matched that previously reported.⁵

$^1\text{H NMR}$ (400 MHz, CDCl_3) δ 7.38-7.30 (m, 5H), 6.62 (t, $J = 6.9$ Hz, 1H), 4.53 (s, 2H), 3.98 (d, $J = 6.9$ Hz, 2H), 3.74 (t, $J = 5.2$ Hz, 2H), 2.72 (t, $J = 5.7$ Hz, 2H), 1.99 (s, 1H) ppm.

Allylsilane 2.35:

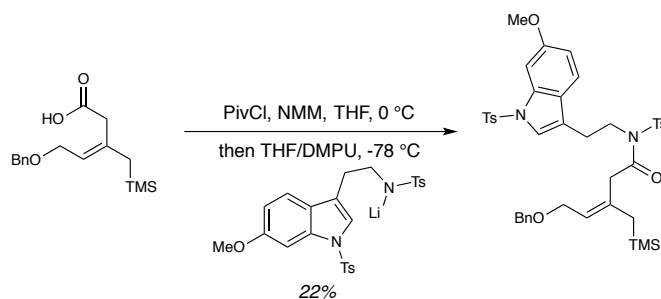
To a solution of vinyl iodide **2.46** (2.99 g, 9.40 mmol, 1.0 equiv) in CH₂Cl₂ (60.0 mL) was added DMP (5.98 g, 14.1 mmol, 1.5 equiv), and the reaction mixture was stirred for two hours. The reaction was quenched with 1:1 saturated aqueous NaHCO₃/saturated aqueous Na₂SO₃ (100.0 mL), and the biphasic mixture was stirred for 15 minutes. The layers were separated, and the aqueous phase was extracted with Et₂O (3 x 25.0 mL). The combined organic layer was dried over anhydrous Na₂SO₄, filtered, and concentrated under reduced pressure. The crude residue was brought up in CH₂Cl₂ (23.0 mL) and *t*-BuOH (86.0 mL), and 2-methyl-2-butene (46.0 mL) was added. A solution of NaClO₂ (9.0 g, 100.0 mmol, 10.6 equiv) and NaH₂PO₄ (10.9 g, 90.8 mmol, 9.6 equiv) in water (100 mL) was then added in one portion, and the biphasic reaction mixture was stirred for one hour. Brine (100.0 mL) was added, and the layers were separated. The aqueous phase was extracted with CH₂Cl₂ (3 x 50.0 mL). The combined organic layer was washed with brine (100.0 mL), dried over anhydrous Na₂SO₄, filtered, and concentrated under reduced pressure. The residue was azeotroped with toluene (3 x 50.0 mL) to remove residual *t*-BuOH, providing crude carboxylic acid **2.47** (2.90 g, 96%) as a yellow oil.

To anhydrous ZnBr₂ (3.96 g, 17.56 mmol, 3.1 equiv) was added TMSCH₂MgCl solution (1M in Et₂O, 18.1 mL, 18.10 mmol, 3.2 equiv), and the resultant slurry was stirred

at room temperature for 12 hours. DMF (12.0 mL) and Et₂O (4.0 mL) were added, and the reaction was cooled to 0 °C. A solution of carboxylic acid **2.43** (1.88 g, 5.66 mmol, 1.0 equiv) in DMF (10.0 mL) was cannulated into the reaction mixture. A solution of Pd(MeCN)₂Cl₂ (146.8 mg, 0.56 mmol, 10 mol %) in DMF (1.0 mL) was then added, and the reaction was stirred at 0 °C for two hours. The reaction was quenched by the slow addition of saturated aqueous NH₄Cl (20.0 mL), and the layers were separated. The aqueous layer was extracted with CH₂Cl₂ (3 x 50.0 mL). The combined organic layer was washed with saturated aqueous LiCl (3 x 50.0 mL), water (3 x 50.0 mL), and brine (50.0 mL). The organic layer was filtered through celite, and the filter pad was washed with CH₂Cl₂ (3 x 20.0 mL). The filtrate was dried over anhydrous Na₂SO₄, filtered, and concentrated under reduced pressure to provide allylsilane **2.35** (1.13 g, 95%) as a dark orange oil, which was used without further purification. Spectral data matched that previously reported.⁵

¹H NMR (400 MHz, CDCl₃) δ 8.25 (bs, 1H), 7.39-7.29 (m, 5H), 5.51 (t, *J* = 6.9 Hz, 1H), 4.56 (s, 2H), 4.03 (d, *J* = 6.9 Hz, 2H), 3.06 (s, 2H), 1.67 (s, 2H), 0.06 (s, 9H) ppm.

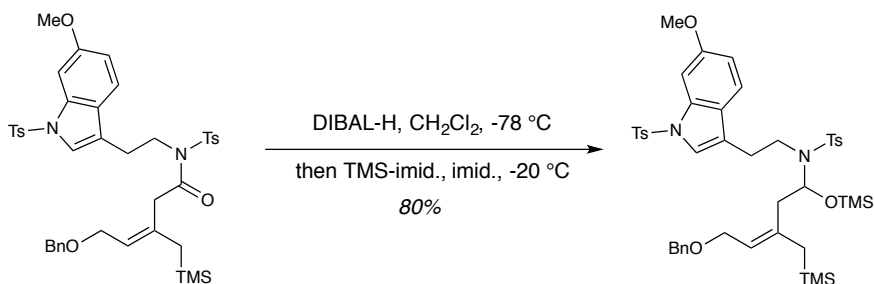
N-Ts Amide **2.48**:



To a solution of carboxylic acid **2.35** (87.0 mg, 0.30 mmol, 1.3 equiv) in THF (3.0 mL) was added pivaloyl chloride (37 μ L, 0.30 mmol, 1.3 equiv) and NMM (36 μ L, 0.32 mmol, 1.4 equiv), and the reaction was stirred for one hour at room temperature. To a solution of N,N'-bistosyl-6-methoxytryptamine **2.33** (115.0 mg, 0.23 mmol, 1.0 equiv) in THF (3.0 mL) and DMPU (0.3 mL) at -78 °C was added n-BuLi (0.13 mL, 2.2 M in hexanes, 0.28 mmol, 1.2 equiv), and the reaction was stirred for one hour. The precipitate was removed from the mixed anhydride solution via a syringe filter, and this was added to the lithiate solution. The anhydride flask was rinsed with THF (3.0 mL), and this solution was syringe filtered and added to the lithiate solution. The resultant reaction mixture was stirred for four hours at -78 °C, and the reaction was then quenched with saturated aqueous NH₄Cl (10.0 mL) and warmed to room temperature. The layers were separated, and the aqueous phase was extracted with Et₂O (3 x 15.0 mL). The combined organic layer was washed with saturated aqueous NaHCO₃ (15.0 mL) and brine (15.0 mL), dried over anhydrous MgSO₄, filtered, and concentrated under reduced pressure. Purification by flash column chromatography on silica gel (7:3 hexanes/EtOAc) provided N-Ts amide **2.48** (40.0 mg, 22%) as a colorless oil.

¹H NMR (400 MHz, CDCl₃) δ 7.83 (d, J = 8.0 Hz, 2H), 7.71 (m, 4H), 7.51 (m, 3H), 7.32-7.19 (m, 8H), 6.86 (dd, J = 8.4, 2.0 Hz, 1H), 5.41 (t, J = 6.8 Hz, 1H), 4.33 (s, 2H), 4.06-3.89 (m, 2H), 3.85 (s, 2H), 3.77 (d, J = 6.8 Hz, 2H), 3.35 (s, 2H), 2.40 (s, 3H), 2.32 (s, 3H), 1.48 (s, 2H), -0.05 (s, 9H) ppm.

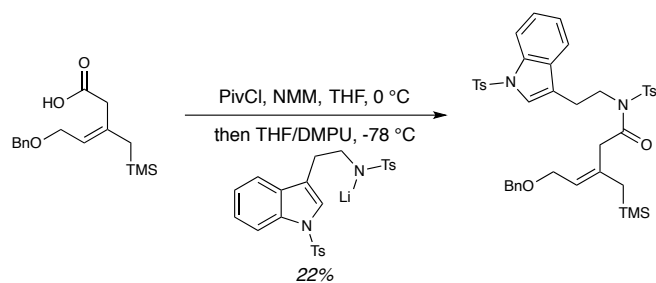
HRMS (+NSI) calculated for C₄₁H₄₈O₇N₂NaS₂Si [M+Na]⁺ 795.2570, found 795.2569.

Hemiaminal Ether 2.31:

To a solution of N-Ts amide **2.48** (40.0 mg, 0.05 mmol, 1.0 equiv) in CH_2Cl_2 (2.0 mL) at -78 °C was added DIBAL-H (1M in CH_2Cl_2 , 0.1 mL, 0.1 mmol, 2.0 equiv), and the reaction was stirred for one hour. Trimethylsilylimidazole (22 μL , 0.15 mmol, 3.0 equiv) and imidazole (4.0 mg, 0.05 mmol, 1.0 equiv) were added, and the reaction mixture was stirred at -20 °C for 24 hours. The reaction was quenched with saturated Rochelle's salt solution (2.0 mL), and the biphasic mixture was stirred till both layers were clear. The layers were separated, and the aqueous phase was extracted with CH_2Cl_2 (3 x 5.0 mL). The combined organic layer was dried over Na_2SO_4 , filtered, and concentrated under reduced pressure. Purification by flash column chromatography on silica gel (3:2 hexanes/EtOAc) provided hemiaminal ether **2.31** (37.0 mg, 84%) as a colorless oil.

^1H NMR (400 MHz, CDCl_3) δ 7.74 (d, $J = 8.0$ Hz, 2H), 7.67 (d, $J = 8.4$ Hz, 2H), 7.51 (d, $J = 1.6$ Hz, 1H), 7.45 (d, $J = 9.2$ Hz, 1H), 7.28-7.17 (m, 10H), 6.86 (dd, $J = 8.4, 2.4$ Hz, 1H), 5.46 (dd, $J = 9.2, 2.4$ Hz, 2H), 5.28 (t, $J = 5.6$ Hz, 1H), 4.41 (dd, $J = 20.1, 12.4$ Hz, 2H), 4.03 (m, 1H), 3.91 (m, 1H), 3.85 (s, 3H), 3.45 (m, 1H), 3.26 (m, 1H), 3.01 (m, 1H), 2.37 (s, 3H), 2.32 (s, 3H), 1.79 (dd, $J = 12.8, 2.8$ Hz, 1H), 1.57 (m, 1H), 1.31 (d, $J = 13.2$ Hz, 1H), 0.04 (s, 9H), -0.04 (s, 9H) ppm.

HRMS (+NSI) calculated for $\text{C}_{44}\text{H}_{58}\text{O}_7\text{N}_2\text{NaS}_2\text{Si}_2$ $[\text{M}+\text{Na}]^+$ 869.3122, found 869.3127.

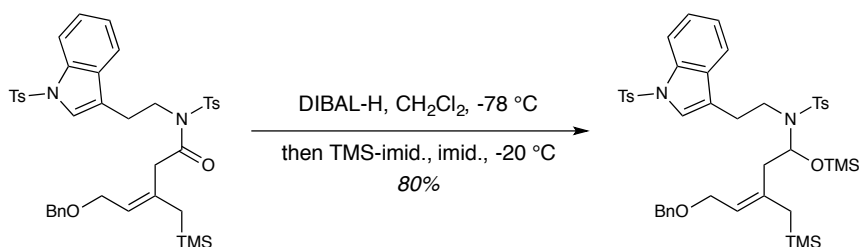
***N*-Ts amide **2.49**:**

To a solution of carboxylic acid **2.35** (82.0 mg, 0.28 mmol, 1.3 equiv) in THF (8.0 mL) was added NMM (33 μ L, 0.30 mmol, 1.4 equiv) and pivaloyl chloride (35 μ L, 0.28 mmol, 1.3 equiv), and the reaction was stirred for one hour. To a solution of *N,N'*-bistosyltryptamine **2.34** (100.0 mg, 0.22 mmol, 1.0 equiv) in THF (8.0 mL) and DMPU (0.8 mL) at -78 °C was added *n*-butyllithium (0.10 mL, 2.5 M in hexanes, 0.26 mmol, 1.2 equiv) drop-wise. The precipitate was removed from the anhydride solution via a syringe filter, and the anhydride solution was added drop-wise to the lithiate solution. The flask for the anhydride solution was rinsed with THF (8.0 mL), filtered through a syringe filter, and added drop-wise to the lithiate solution. The reaction mixture was stirred for four hours at -78 °C. Saturated aqueous NH_4Cl (20.0 mL) was then added, and the reaction was warmed up to room temperature. The layers were separated, and the aqueous phase was extracted with Et_2O (3 x 15.0 mL). The combined organic layer was washed with saturated aqueous NaHCO_3 (25.0 mL) and brine (25.0 mL), dried over anhydrous Na_2SO_4 , filtered, and concentrated under reduced pressure. Purification by flash column chromatography on silica gel (3:1 hexanes/ EtOAc) provided *N*-Ts amide **2.49** (101.3 mg, 62%) as a colorless oil.

¹H NMR (400 MHz, CDCl₃) δ 7.94 (d, *J* = 8.4 Hz, 1H), 7.73 (d, *J* = 7.6 Hz, 2H), 7.69 (d, *J* = 8.4 Hz, 2H), 7.66 (d, *J* = 8.0 Hz, 1H), 7.36 (s, 1H), 7.32-7.18 (m, 11H), 5.42 (t, *J* = 7.6 Hz, 1H), 4.33 (s, 2H), 3.92 (m, 2H), 3.77 (d, *J* = 6.8 Hz, 2H), 3.36 (s, 2H), 3.03 (m, 2H), 2.39 (s, 3H), 2.31 (s, 3H), 1.48 (s, 2H), -0.05 (s, 9H) ppm.

HRMS (+NSI) calculated for C₄₀H₄₆O₆N₂NaS₂Si [M+Na]⁺ 765.2464, found 765.2471.

Hemiaminal Ether **2.32**:

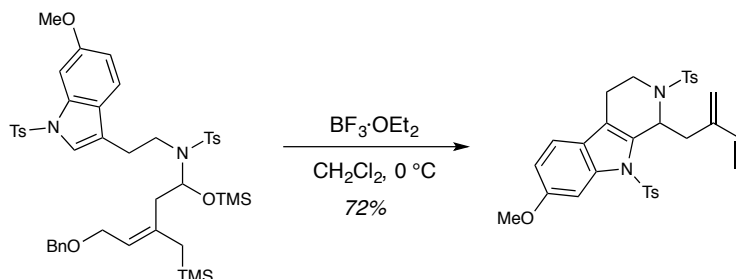


To a solution of *N*-Ts Amide **2.49** (101.9 mg, 0.13 mmol, 1.0 equiv) in CH₂Cl₂ (3.0 mL) at -78 °C was added DIBAL-H (0.27 mL, 1.0 M in CH₂Cl₂, 0.27 mmol, 2.0 equiv) drop-wise over 15 minutes. The reaction was stirred at -78 °C for two hours, and then trimethylsilylimidazole (60 μL, 0.41 mmol, 3.1 equiv) and imidazole (9.0 mg, 0.13 mmol, 1.0 equiv) were added. The reaction mixture was warmed up to -20 °C and stirred for 18 hours. The reaction was quenched with saturated Rochelle's salt solution (4.0 mL), and the biphasic mixture was stirred until both layers were clear. The layers were separated, and the aqueous phase was extracted with CH₂Cl₂ (3 x 5.0 mL). The combined organic layer was dried over anhydrous Na₂SO₄, filtered, and concentrated under reduced pressure. Purification by flash column chromatography on silica gel (4:1 hexanes/EtOAc) provided hemiaminal ether **2.32** (53.0 mg, 50%) as a colorless oil.

¹H NMR (400 MHz, CDCl₃) δ 7.96 (d, *J* = 8.0 Hz, 1H), 7.76 (d, *J* = 6.4 Hz, 2H), 7.68 (d, *J* = 8.4 Hz, 2H), 7.59 (d, *J* = 8.0 Hz, 1H), 7.34-7.19 (m, 12H), 5.35 (dd, *J* = 8.8, 2.8 Hz, 1H), 5.27 (t, *J* = 7.6 Hz, 1H), 4.41 (q, *J* = 11.6 Hz, 2H), 4.02 (dd, *J* = 12.8, 8.8 Hz, 1H), 3.91 (dd, *J* = 11.2, 4.8 Hz, 1H), 3.47 (m, 1H), 3.29 (m, 1H), 3.05 (m, 1H), 2.37 (s, 3H), 2.31 (s, 3H), 1.78 (dd, *J* = 13.6, 1.4 Hz, 1H), 1.53 (t, *J* = 16.0 Hz, 1H), 1.31 (d, *J* = 13.4 Hz, 1H), 0.04 (s, 9H), -0.05 (s, 9H) ppm.

HRMS (+NSI) calculated for C₄₃H₄₆O₆N₂NaS₂Si₂ [M+Na]⁺ 839.3016, found 839.3015.

Diene **2.51**:



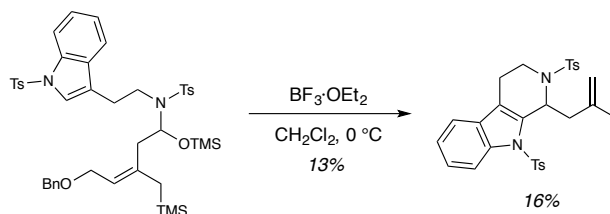
To a solution of hemiaminal ether **2.31** (37.0 mg, 0.04 mmol, 1.0 equiv) in CH₂Cl₂ (1.0 mL) at 0 °C was added BF₃·OEt₂ (25 μL, 0.20 mmol, 5.0 equiv), and the reaction was stirred for one hour. The mixture was quenched with saturated aqueous NaHCO₃ (2.0 mL), and the layers were separated. The aqueous phase was extracted with CH₂Cl₂ (3 x 2.0 mL). The combined organic layer was dried over anhydrous Na₂SO₄, filtered, and concentrated under reduced pressure. Purification by preparatory thin layer chromatography on silica gel (4:1 hexanes/EtOAc, silica washed with EtOAc) provided diene **2.51** (32.0 mg, 72%) as a white solid.

¹H NMR (600 MHz, CDCl₃) δ 7.82 (d, *J* = 7.8 Hz, 2H), 7.39 (d, *J* = 7.8 Hz, 2H), 7.37 (s, 1H), 7.36 (d, *J* = 1.8 Hz, 2H), 7.28 (d, *J* = 7.8 Hz, 2H), 7.03 (d, *J* = 7.8 Hz, 1H), 7.01 (d, *J* = 8.4 Hz, 2H), 6.94 (d, *J* = 8.4 Hz, 1H), 6.50 (dd, *J* = 7.8, 2.4 Hz, 1H), 5.59 (ddd, *J* = 16.8, 10.2, 6.6 Hz, 1H), 5.30 (d, *J* = 7.8 Hz, 1H), 5.14 (bs, 1H), 5.89 (d, *J* = 9.0 Hz, 1H), 3.77 (s, 3H), 2.95 (d, *J* = 3.0 Hz, 1H), 2.51 (s, 3H), 2.45-2.35 (m, 2H), 2.32 (s, 3H), 2.04 (m, 1H), 1.98 (m, 1H), 1.52 (dd, *J* = 13.8, 2.4 Hz, 1H), 1.29 (t, *J* = 13.2 Hz, 1H) ppm.

¹³C NMR (100 MHz, CDCl₃) δ 160.2, 145.1, 141.6, 137.4, 132.3, 131.1, 130.0, 129.5, 128.5, 128.2, 127.5, 127.3, 126.0, 122.1, 114.4, 109.7, 107.1, 103.2, 67.8, 66.0, 56.1, 54.1, 43.1, 42.5, 32.5, 32.0, 30.1, 22.0, 21.5 ppm.

HRMS (+APCI) calculated for C₃₁H₃₃O₅N₂S₂ [M+H]⁺ 577.1825, found 577.1832.

Diene 2.52:



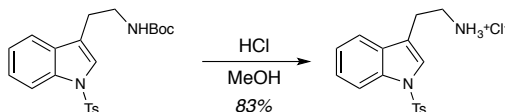
To a solution of hemiaminal ether 2.32 (58.0 mg, 0.07 mmol, 1.0 equiv) in CH₂Cl₂ (2.0 mL) at 0 °C was added BF₃·OEt₂ (41 μL, 0.33 mmol, 4.7 equiv) drop-wise over one minute. The reaction mixture was stirred for one hour and was then quenched with saturated aqueous NaHCO₃ (2.0 mL). The layers were separated, and the aqueous phase was extracted with CH₂Cl₂ (3 x 3.0 mL). The combined organic layer was dried over anhydrous Na₂SO₄, filtered, and concentrated under reduced pressure. Purification by

preparatory thin layer chromatography (4:1 hexanes/EtOAc, rinsed with EtOAc) provided diene **2.52** (5.0 mg, 18%) as a white solid.

¹H NMR (600 MHz, CDCl₃) δ 7.83 (d, J = 5.6 Hz, 2H), 7.64 (d, J = 5.6 Hz, 1H), 7.39 (d, J = 6.0 Hz, 2H), 7.27 (d, J = 5.6 Hz, 2H), 7.16 (m, 2H), 7.06 (d, J = 4.0 Hz, 2H), 7.00 (m, 2H), 5.60 (ddd, J = 11.6, 6.7, 4.4 Hz, 1H), 5.33 (d, J = 5.6 Hz, 1H), 5.16 (s, 1H), 4.90 (d, J = 7.2 Hz, 2H), 4.87 (s, 1H), 2.95 (d, J = 2.0 Hz, 1H), 2.51 (s, 3H), 2.47-2.37 (m, 2H), 2.32 (s, 3H), 2.06 (m, 1H), 2.03 (m, 1H), 1.53 (d, J = 2.0 Hz, 1H), 1.32 (t, J = 8.8 Hz, 1H) ppm.

HRMS (+APCI) calculated for C₃₀H₃₁O₄N₂S₂ [M+H]⁺ 547.1725, found 547.1831.

Tryptamine Hydrochloride **2.53**:



MeOH (215.0 mL) was cooled to 0 °C, and acetyl chloride (61.0 mL, 856.7 mmol, 20.0 equiv) was added drop-wise over ten minutes, providing an approximately 4 M methanolic HCl solution. Carbamate **2.47*** (17.7 g, 42.8 mmol, 1.0 equiv) was added in one portion, and the reaction was stirred at room temperature for 18 hours. The reaction mixture was concentrated under reduced pressure. The crude residue was triturated with Et₂O and filtered to provide tryptamine hydrochloride **2.53** (12.5 g, 83%) as a grey solid.

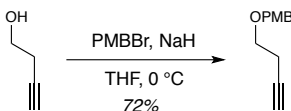
¹H NMR (500 MHz, *d*₆-DMSO) δ 8.21 (s, 3H), 7.90 (d, J = 8.2 Hz, 1H), 7.86 (d, J = 8.3 Hz, 2H), 7.74 (s, 1H), 7.65 (d, J = 7.8 Hz, 1H), 7.38 - 7.33 (m, 3H), 7.28 (t, J = 7.5, 1H), 3.10 (dq, J = 11.4, 5.7 Hz, 2H), 3.04 - 2.97 (m, 2H), 2.31 (s, 1H) ppm.

^{13}C NMR (126 MHz, d_6 -DMSO) δ 159.3, 145.4, 134.3, 134.2, 130.2, 126.8, 124.9, 124.3, 123.3, 119.7, 118.1, 113.2, 38.0, 22.5, 21.0 ppm.

IR (thin film, cm^{-1}) 2913, 1596, 1493, 1446, 1372, 1307, 1287, 1212, 1170, 1133, 1123, 1092, 1020, 976, 945, 807, 745, 701, 667, 630, 598, 577, 567, 536.

HRMS (+NSI) calculated for $\text{C}_{34}\text{H}_{38}\text{O}_4\text{N}_4\text{ClS}_2$ [2M-Cl] $^+$ 665.2018, found 665.2026.

PMB Ether 2.54:



4-methoxybenzyl alcohol (10.3 mL, 83.0 mmol, 1.0 equiv) was added drop-wise to 48% HBr (50.0 ml), and the mixture was stirred for one hour. Et_2O (100.0 mL) was then added, and the two layers were separated. The organic layer was washed with saturated aqueous NaHCO_3 (2 x 100.0 mL), dried over anhydrous CaCl_2 for thirty minutes, filtered, and concentrated under reduced pressure to provide crude 4-methoxybenzyl bromide, which was used immediately without further purification. A slurry of NaH (60 wt % dispersion in mineral oil, 5.27 g, 132 mmol, 1.6 equiv) in THF (50.0 mL) was cooled to 0 °C. 3-Butyn-1-ol (7.6 mL, 100.0 mmol, 1.2 equiv) was added drop-wise over 15 minutes, and the reaction was stirred for one hour. Crude 4-methoxybenzyl bromide was then added, and the reaction mixture was warmed up to room temperature and stirred for 14 hours. The reaction was quenched with saturated aqueous NH_4Cl (200.0 mL). The layers were separated, and the aqueous phase was extracted with Et_2O (3 x 100.0 mL). The combined organic layer was washed with brine (100.0 mL), dried over anhydrous MgSO_4 , filtered,

and concentrated under reduced pressure. Purification by flash column chromatography on silica gel (19:1 pentane/Et₂O) provided the PMB ether **2.54** (11.4 g, 72%) as a colorless oil.

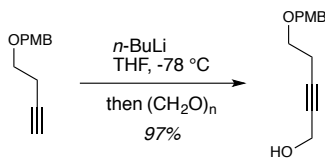
¹H NMR (500 MHz, CDCl₃) δ 7.29 (d, *J* = 8.3 Hz, 2H), 6.90 (d, *J* = 8.7 Hz, 2H), 4.51 (s, 2H), 3.83 (s, 3H) 3.59 (t, *J* = 7.0 Hz, 2H), 2.51 (td, *J* = 7.0, 2.7 Hz, 2H), 2.01 (t, *J* = 2.7 Hz, 1H) ppm.

¹³C NMR (126 MHz, CDCl₃) δ 159.4, 130.2, 129.5, 113.9, 81.5, 72.8, 69.4, 67.9, 55.4, 20.0 ppm.

IR (thin film, cm⁻¹) 3289, 2860, 1612, 1586, 1511, 1463, 1361, 1301, 1243, 1173, 1092, 1032, 819, 756, 636, 581.

HRMS (+APCI) calculated for C₁₂H₁₄O₂ [M]⁺ 190.0994, found 190.0991.

Propargyl Alcohol **2.55**:



A solution of PMB ether **2.54** (11.4 g, 59.9 mmol, 1.0 equiv) in THF (80.0 mL) was cooled to -78 °C. *n*-BuLi (2.5 M in hexanes, 26.4 mL, 65.9 mmol, 1.1 equiv) was added drop-wise over five minutes, and the resultant mixture was stirred for one hour. Paraformaldehyde (5.40 g, 179.4 mmol of monomer, 3.0 equiv) was added in one portion, and the reaction was warmed to room temperature and stirred for 12 hours. The mixture was quenched with saturated aqueous NH₄Cl (50.0 mL) and water (50.0 mL). Et₂O (100.0

mL) was added, and the layers were separated. The aqueous phase was extracted with Et₂O (3 x 100.0 mL). The combined organic layer was washed with brine (100.0 mL), dried over anhydrous MgSO₄, filtered, and concentrated under reduced pressure. Purification by flash column chromatography on silica gel (2:1 hexanes/EtOAc) provided propargyl alcohol **2.55** (12.8 g, 97%) as a colorless oil.

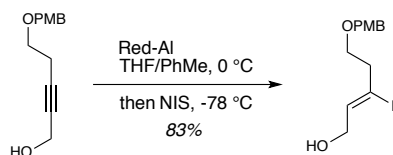
¹H NMR (500 MHz, CDCl₃) δ 7.29 (d, *J* = 8.7 Hz, 2H), 6.90 (d, *J* = 8.7 Hz, 2H), 4.50 (s, 2H), 4.25 (s, 2H), 3.82 (s, 3H), 3.57 (t, *J* = 6.9 Hz, 2H), 2.53 (tt, *J* = 6.9, 2.2 Hz, 2H) ppm.

¹³C NMR (126 MHz, CDCl₃) δ 159.4, 130.1, 129.5, 113.9, 83.2, 79.6, 72.7, 68.0, 55.4, 51.4, 20.3 ppm.

IR (thin film, cm⁻¹) 3405, 2910, 2863, 1612, 1586, 1512, 1462, 1361, 1302, 1244, 1174, 1135, 1089, 1026, 819, 755, 710, 637, 579.

HRMS (+NSI) calculated for C₁₃H₂₀O₃N [M+NH₄]⁺ 238.1438, found 238.1439.

Vinyl Iodide **2.56**:



Propargyl alcohol **2.55** (10.5 g, 47.7 mmol, 1.0 equiv) was dissolved in THF (50.0 mL) and cooled to 0 °C. Red-Al® (60 % wt/v solution in toluene, 27.3 mL, 81.0 mmol, 1.7 equiv) was added drop-wise over ten minutes. The resulting slurry was warmed to room temperature and stirred for three hours. The reaction mixture was cooled to -78 °C, and a solution of *N*-iodosuccinimide (19.3 g, 85.9 mmol, 1.8 equiv) in THF (50.0 mL) was added

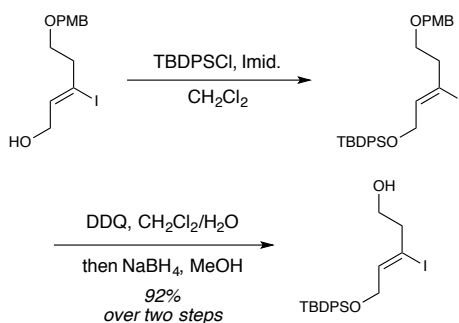
via cannula. The reaction mixture was stirred for 30 minutes. Upon warming to room temperature, the reaction mixture was quickly poured into a 1:1 mixture of saturated aqueous Na_2SO_3 /saturated Rochelle's salt solution (300.0 mL), and the biphasic mixture was stirred vigorously until both layers were clear and colorless. The layers were separated, and the aqueous phase was extracted with Et_2O (3 x 100.0 mL). The combined organic layer was washed with brine (100.0 mL), dried over anhydrous MgSO_4 , filtered, and concentrated under reduced pressure. Purification by flash column chromatography on silica gel (3:1 to 2:1 hexanes/ EtOAc) provided vinyl iodide **2.56** (13.7 g, 83%) as a pale yellow oil.

^1H NMR (500 MHz, CDCl_3) δ 7.27 (d, $J = 8.7$ Hz, 2H), 6.89 (d, $J = 8.7$ Hz, 2H), 5.91 (tt, $J = 5.7, 1.1$ Hz, 1H), 4.46 (s, 2H), 4.14 (d, $J = 5.6$ Hz, 2H), 3.80 (s, 3H), 3.60 (t, $J = 6.4$ Hz, 2H), 2.77 (td, $J = 6.4, 1.0$ Hz, 2H) ppm.

^{13}C NMR (126 MHz, CDCl_3) δ 159.2, 136.1, 130.0, 129.4, 113.8, 104.5, 72.7, 68.3, 67.2, 55.3, 45.1 ppm.

IR (thin film, cm^{-1}) 3370, 2859, 1611, 1511, 1460, 1360, 1301, 1244, 1173, 1081, 1030, 814, 755, 566.

HRMS (+NSI) calculated for $\text{C}_{13}\text{H}_{21}\text{O}_3\text{NI}$ [$\text{M}+\text{NH}_4$] $^+$ 366.0561, found 366.0563.

Alcohol 2.57:

Vinyl iodide **2.56** (8.57 g, 24.7 mmol, 1.0 equiv) and imidazole (3.36 g, 49.3 mmol, 2.0 equiv) were dissolved in CH₂Cl₂ (40.0 mL) and cooled to 0 °C. TBDPSCl (7.05 mL, 27.1 mmol, 1.1 equiv) was added drop-wise, and the reaction mixture was stirred at room temperature for three hours. The reaction was quenched with saturated aqueous NH₄Cl (60.0 mL), and the layers were separated. The aqueous phase was extracted with CH₂Cl₂ (3 x 50.0 mL). The combined organic layer was washed with water (100.0 mL) and brine (100.0 mL). The organic layer was dried over anhydrous Na₂SO₄, filtered, and concentrated under reduced pressure to provide the crude TBDPS ether, which was used directly in the next step without further purification.

The crude TBDPS ether was dissolved in CH₂Cl₂ (40.0 mL) and cooled to 0 °C. DDQ (6.15 g, 27.1 mmol, 1.1 equiv) and water (2.0 mL) were added, and the resultant black slurry was stirred for one hour. The reaction mixture was filtered over celite, and the filtrate quenched with of a 1:1 mixture of saturated aqueous Na₂SO₃/saturated aqueous NaHCO₃ (150.0 mL). The layers were separated, and the aqueous phase was extracted with DCM (3 x 100.0 mL). The combined organic layer was washed with brine (100.0 mL), dried over anhydrous Na₂SO₄, filtered, and concentrated under reduced pressure. The crude mixture was brought up in dry MeOH (40.0 mL) and cooled to 0 °C. NaBH₄ (2.80 g, 74.1

mmol, 3.0 equiv) was added in portions, and the mixture was stirred for four hours. The solution was concentrated under reduced pressure, and the residue was brought up in Et₂O (100.0 mL) and H₂O (100.0 ml). The layers were separated, and the aqueous phase was extracted with Et₂O (3 x 100.0 ml). The combined organic layer was washed with brine (100.0 mL), dried over anhydrous MgSO₄, filtered, and concentrated under reduced pressure. Purification by flash chromatography on silica gel (4:1 to 7:3 hexanes/EtOAc) provided alcohol **2.57** (10.52 g, 92% over three steps) as a colorless oil.

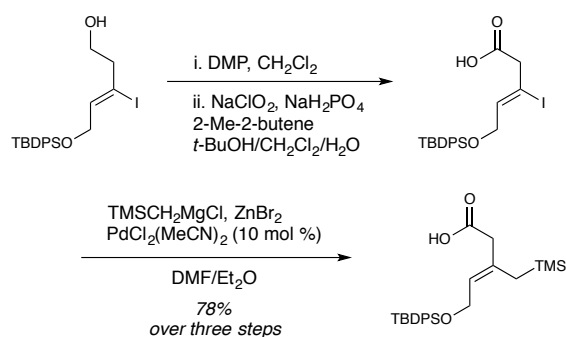
¹H NMR (500 MHz, CDCl₃) δ 7.72 – 7.64 (m, 4H), 7.48 – 7.37 (m, 6H), 6.01 (tt, *J* = 5.1, 1.1 Hz, 1H), 4.28 (dt, *J* = 5.0, 1.0 Hz, 2H), 3.71 (t, *J* = 5.8 Hz, 2H), 2.68 (tq, *J* = 6.0, 1.0 Hz, 2H), 1.07 (s, 9H) ppm.

¹³C NMR (126 MHz, CDCl₃) δ 138.0, 135.7, 133.5, 129.9, 127.9, 102.2, 69.1, 61.0, 47.9, 26.9, 19.3 ppm.

IR (thin film, cm⁻¹) 3392, 3071, 2931, 2858, 1472, 1427, 1264, 1110, 1051, 907, 823, 731, 701, 612.

HRMS (+NSI): calculated for C₂₁H₂₇O₂INaSi [M+Na]⁺ 489.0717, found 489.0718.

Allylsilane 2.59:



Alcohol **2.57** (10.52 g, 22.5 mmol, 1.0 equiv) was brought up in CH_2Cl_2 (50.0 mL). Dess-Martin Periodinane (11.48 g, 27.1 mmol, 1.2 equiv.) was then added, and the resultant slurry was stirred at room temperature for three hours. The reaction was diluted with EtOAc (100.0 mL) and quenched with a 1:1 mixture of saturated aqueous Na_2SO_3 /saturated aqueous NaHCO_3 (100.0 mL). The layers were separated, and the aqueous phase was extracted with EtOAc (3 x 50.0 mL). The combined organic layer was washed with brine (100.0 mL), dried over anhydrous Na_2SO_4 , filtered, and concentrated under reduced pressure. The crude residue was brought up in *t*-BuOH (100.0 mL) and CH_2Cl_2 (100.0 mL). 2-methyl-2-butene (50.0 mL) was then added, and the reaction was cooled to 0 °C. NaClO_2 (20.3 g, 225.0 mmol, 10.0 equiv.) and NaH_2PO_4 (21.6 g, 180 mmol, 8.0 equiv.) were dissolved in H_2O (100.0 mL), and the resultant solution was added in one portion to the reaction mixture. The biphasic mixture was stirred for one hour and then diluted with water (150.0 mL). CH_2Cl_2 (150.0 mL) was added, and the layers were separated. The organic layer was washed with water (100.0 mL) and brine (100.0 mL), dried over anhydrous Na_2SO_4 , filtered, and concentrated under reduced pressure. Residual *t*-BuOH was removed by azeotroping the residue with toluene (3 x 50.0 mL) to provide the crude carboxylic acid **2.58** as a yellow oil, which was used without further purification.

TMSCH_2Cl (9.4 mL, 67.5 mmol, 3.0 equiv.) was dissolved in dry Et_2O (68.0 mL). Mg turnings (1.68 g, 67.5 mmol, 3.0 equiv) and a crystal of iodine were added. An initial exotherm was observed, and the mixture was stirred for five hours at reflux until all magnesium was consumed. The freshly formed Grignard solution was cooled to room temperature and added via cannula to anhydrous ZnBr_2 (15.80 g, 69.8 mmol, 3.1 equiv), and the resultant slurry was stirred for 12 hours. DMF (68.0 mL) was then added. A

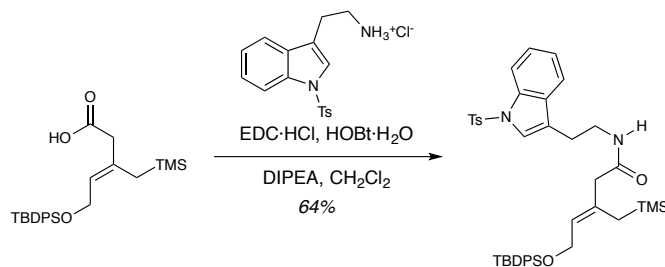
solution of crude carboxylic acid **2.53** in DMF (15.0 mL) was added, and the reaction mixture was cooled to 0 °C. A solution of Pd(MeCN)₂Cl₂ (583.7 mg, 2.25 mmol, 0.1 equiv) in DMF (10.0 mL) was then added, and the reaction was warmed to room temperature and stirred for three hours. The reaction was quenched with saturated aqueous NH₄Cl (50.0 mL) and Et₂O (100.0 mL), and the layers were separated. The aqueous phase was extracted with Et₂O (3 x 100.0 mL). The combined organic layer was washed with H₂O (2 X 150.0 mL), 5% aqueous LiCl (2 x 150.0 ml), and brine (100.0 mL). The organic layer was dried over anhydrous MgSO₄, filtered through celite, and concentrated under reduced pressure. Purification by flash column chromatography on silica gel (9:1 hexanes/EtOAc) provided allylsilane **2.59** (7.72 g, 78% over three steps) as a yellow oil.

¹H NMR (500 MHz, CDCl₃) δ 7.73 – 7.67 (m, 4H), 7.45 – 7.36 (m, 6H), 5.49 (t, *J* = 6.1 Hz, 1H), 4.17 (d, *J* = 6.1 Hz, 2H), 2.98 (s, 2H), 1.47 (s, 2H), 1.06 (s, 9H), -0.04 (s, 9H) ppm.

¹³C NMR (126 MHz, CDCl₃) δ 178.0, 135.7, 134.0, 131.5, 129.7, 126.6, 61.3, 44.6, 27.0, 22.1, 19.3, -0.9 ppm.

IR (thin film, cm⁻¹) 3071, 2954, 2856, 1708, 1427, 1249, 1111, 1079, 1046, 850, 824, 736, 701, 613.

HRMS (+NSI) calculated for C₂₅H₃₇O₃Si₂ [M+H]⁺ 441.2276, found 441.2273.

Amide 2.60:

A solution of tryptamine hydrochloride **2.43** (7.1 g, 28.4 mmol, 1.0 equiv) in CH₂Cl₂ (90.0 mL) was cooled to 0 °C, and DIPEA (29.7 mL, 170.4 mmol, 6.0 equiv) was added dropwise. A solution of carboxylic acid **2.59** (12.5 g, 28.4 mmol, 1.0 equiv) in CH₂Cl₂ (90.0 mL) was added via cannula. HOBt·H₂O (4.61 g, 34.1 mmol, 1.2 equiv) and EDCI·HCl (6.54 g, 34.1 mmol, 1.2 equiv) were added, and the reaction mixture was warmed to room temperature and stirred for 48 hours. The reaction was quenched with 0.5 N aqueous HCl (200.0 mL), and the layers were separated. The organic phase was washed with saturated aqueous NaHCO₃ (200.0 mL) and brine (200.0 mL), dried over anhydrous Na₂SO₄, filtered, and concentrated under reduced pressure. Purification by flash column chromatography on silica gel (9:1 to 4:1 hexanes/EtOAc) provided amide **2.60** (13.4 g, 64%) as a yellow oil.

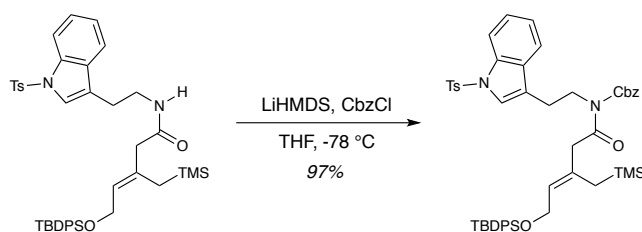
¹H NMR (600 MHz, CDCl₃) δ 7.98 (d, *J* = 8.4 Hz, 1H), 7.73 (d, *J* = 8.3 Hz, 2H), 7.68 – 7.65 (m, 4H), 7.49 (d, *J* = 7.7 Hz, 1H), 7.43 – 7.33 (m, 7H), 7.30 (t, *J* = 7.8 Hz, 1H), 7.24 – 7.19 (m, 3H), 5.87 (t, *J* = 6.0 Hz, 1H), 5.40 (t, *J* = 6.5 Hz, 1H), 4.13 (d, *J* = 6.4 Hz, 2H), 3.44 (q, *J* = 7.2 Hz, 2H), 2.85 – 2.77 (m, 4H), 2.33 (s, 3H), 1.28 (s, 2H), 1.03 (s, 9H), -0.09 (s, 9H) ppm.

^{13}C NMR (126 MHz, CDCl_3) δ 170.9, 144.9, 135.7, 135.4, 135.3, 134.9, 134.8, 133.8, 130.8, 130.0, 127.8, 126.9, 124.9, 123.4, 123.3, 119.8, 119.6, 113.8, 61.0, 47.7, 39.4, 29.8, 26.7, 25.2, 22.1, 21.7, 19.3, -0.8 ppm.

IR (thin film, cm^{-1}) 3304, 3069, 2926, 2855, 1646, 1533, 1448, 1428, 1368, 1249, 1172, 1112, 1086, 978, 909, 851, 823, 738, 669, 597, 574, 537.

HRMS (+NSI) calculated for $\text{C}_{42}\text{H}_{52}\text{O}_4\text{N}_2\text{NaSSi}_2$ $[\text{M}+\text{Na}]^+$ 759.3079, found 759.3077.

Cbz-Amide **2.61**:



A solution of amide **2.60** (1.93 g, 2.62 mmol, 1.1 equiv) in THF (17.0 mL) was cooled to $-78\text{ }^\circ\text{C}$. A solution of LiHMDS (1.0 M in THF, 2.48 mL, 2.48 mmol, 1.0 equiv) was added drop-wise over five minutes, and the solution was stirred for one hour. CbzCl (0.55 mL, 3.93 mmol, 1.6 equiv) was then added, and the solution was stirred at $-78\text{ }^\circ\text{C}$ for 24 hours. The reaction was quenched with saturated aqueous NH_4Cl (30.0 mL) and warmed to room temperature. The layers were separated, and the aqueous phase was extracted with Et_2O (3 x 30.0 mL). The combined organic phase was washed with brine (30.0 mL), dried over anhydrous MgSO_4 , filtered, and concentrated under reduced pressure. Purification by flash column chromatography on silica gel (9:1 to 4:1 hexanes/ EtOAc) provided Cbz-amide **2.61** (2.09 g, 97%) as a sticky foam.

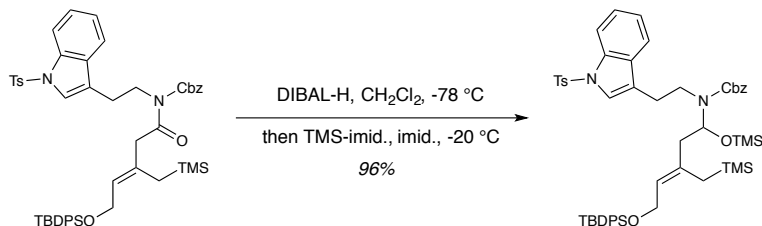
^1H NMR (600 MHz, CDCl_3) δ 7.95 (d, $J = 8.4$ Hz, 1H), 7.72 (d, $J = 8.4$ Hz, 2H), 7.71 – 7.65 (m, 4H), 7.43-7.25 (m, 14H), 7.19 (d, $J = 8.0$ Hz, 2H), 7.11 (t, $J = 7.4$ Hz, 1H), 5.33 (t, $J = 6.2$ Hz, 1H), 5.08 (s, 2H), 4.17 (d, $J = 6.2$ Hz, 2H), 4.00 – 3.89 (m, 2H), 3.57 (s, 2H), 2.93 – 2.81 (m, 2H), 2.32 (s, 3H), 1.46 (s, 2H), 1.02 (s, (H), -0.06 (s, 9H) ppm.

^{13}C NMR (151 MHz, CDCl_3) δ 173.7, 154.1, 144.9, 135.73, 135.65, 135.40, 135.25, 134.9, 134.1, 133.3, 130.8, 129.9, 129.6, 128.9, 128.7, 126.9, 126.8, 125.2, 125.1, 124.8, 123.2, 119.7, 113.8, 113.7, 77.4, 68.8, 61.3, 47.8, 44.4, 27.0, 24.5, 22.8, 21.7, 19.3, -0.8 ppm.

IR (thin film, cm^{-1}) 3068, 2953, 2856, 1735, 1695, 1597, 1447, 1427, 1357, 1265, 1248, 1169, 1112, 1043, 977, 908, 848, 823, 734, 700, 667, 601, 575, 537.

HRMS (+NSI) calculated for $\text{C}_{50}\text{H}_{62}\text{O}_6\text{N}_3\text{SSi}_2$ $[\text{M}+\text{NH}_4]^+$ 888.3892, found 888.3892.

Hemiaminal Ether **2.62**:



A solution of Cbz-amide **2.61** (3.17 g, 3.62 mmol, 1.0 equiv) in CH_2Cl_2 (25.0 mL) was cooled to $-78\text{ }^\circ\text{C}$. DIBAL-H (1.0 M in CH_2Cl_2 , 7.25 mL, 7.25 mmol, 2.0 equiv) was added drop-wise over ten minutes, and the reaction was stirred for one hour. TMS-imidazole (1.39

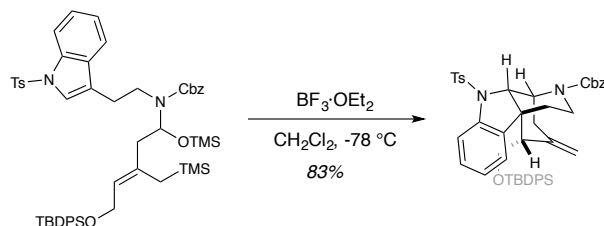
mL, 10.88 mmol, 3.0 equiv) and imidazole (246.4 mg, 3.62 mmol, 1.0 equiv) were then added, and the reaction was warmed up to -20 °C and stirred for 18 hours. The reaction was quenched with saturated Rochelle's salt solution (30.0 mL), and the biphasic mixture was stirred vigorously at room temperature until both layers were clear. The layers were separated, and the aqueous phase was extracted with CH₂Cl₂ (3 x 30.0 mL). The combined organic phase was dried over anhydrous Na₂SO₄, filtered, and concentrated under reduced pressure. Purification by flash column chromatography on silica gel (9:1 hexanes/EtOAc) provided hemiaminal ether **2.62** (3.21 g, 96%) as a sticky foam.

¹H NMR (600 MHz, CDCl₃) (1:0.6 mixture of rotamers) δ 7.98 – 7.94 (m, 1.6H), 7.77 – 7.71 (m, 3.8H), 7.66 – 7.65 (m, 6.4H), 7.42 – 7.23 (m, 22.4H), 7.21 – 7.19 (m, 3.2H), 7.06 (t, *J* = 7.6 Hz, 1H), 5.93 (t, *J* = 6.3 Hz, 1H), 5.75 (t, *J* = 6.3 Hz, .6H), 5.35 (t, *J* = 6.3 Hz, 1H), 5.29 (t, *J* = 6.3 Hz, .6H), 5.24 – 5.13 (m, 2.2H), 5.08 (d, *J* = 12.1 Hz, 1H), 4.09 – 4.04 (m, 3.2H), 3.56 – 3.25 (m, 3.2H), 3.04 – 2.82 (m, 3.2H), 2.35 – 2.11 (m, 8H), 1.50 (d, *J* = 13.7 Hz, 1H), 1.43 (d, *J* = 13.6 Hz, 1H), 1.36 (d, *J* = 13.8 Hz, .6H), 1.24 (d, *J* = 14.2 Hz, .6H), 1.00 (s, 14.4H), 0.12 (s, 9H), 0.05 (s, 5.4H), -0.06 (s, 9H), -0.13 (s, 5.4H) ppm.

¹³C NMR (126 MHz, CDCl₃) (1:0.6 mixture of rotamers) δ 164.6, 155.5, 154.7, 144.9, 136.6, 135.7, 135.5, 135.3, 134.5, 134.1, 131.1, 130.9, 130.0, 129.6, 128.7, 128.5, 128.4, 127.8, 126.9, 125.1, 125.0, 124.7, 123.3, 123.3, 120.7, 120.4, 120.1, 119.8, 113.8, 79.4, 79.2, 67.5, 61.2, 46.0, 45.7, 41.7, 41.4, 26.9, 26.5, 25.4, 22.2, 21.7, 19.3, 0.0, -0.7, -0.8 ppm.

IR (thin film, cm⁻¹) 2954, 2856, 1699, 1598, 1447, 1416, 1372, 1341, 1250, 1210, 1173, 1110, 1027, 976, 943, 909, 842, 740, 701, 669, 603, 576, 537.

HRMS (+NSI) calculated for C₅₃H₇₂O₆N₃SSi₃ [M+NH₄]⁺ 962.4444, found 962.4475.

Tetracycle 2.63:

A solution of hemiaminal ether **2.62** (900.0 mg, 0.96 mmol, 1.0 equiv) and 4 Å MS (900.0 mg) in CH_2Cl_2 (9.0 mL) was cooled to -78°C . Freshly distilled $\text{BF}_3 \cdot \text{OEt}_2$ (0.18 mL, 2.91 mmol, 3.0 equiv) was added drop-wise over five minutes, and the reaction was stirred at -78°C for 24 hours. The mixture was warmed up to room temperature and quenched via the slow addition of saturated aqueous NaHCO_3 (15.0 mL) and CH_2Cl_2 (5.0 mL). The biphasic mixture was stirred for 30 minutes. The layers were separated, and the aqueous phase was extracted with CH_2Cl_2 (3 x 10.0 mL). The combined organic layer was dried over anhydrous Na_2SO_4 , filtered, and concentrated under reduced pressure. Purification by flash column chromatography on silica gel (9:1 to 4:1 hexanes/EtOAc) provided tetracycle **2.63** (601.1 mg, 83%) as a crunchy foam.

Tetracycle **2.63** was present as a 1.0:1.0 mixture of rotamers in CDCl_3 at 23°C . The rotameric peaks could be partially resolved at 80°C in d^6 -DMSO.

Structural assignment was confirmed by X-ray crystallography analysis (*vide infra*). X-ray quality crystals were grown by slow evaporation of a solution of tetracycle **2.63** from 1:1 *n*-heptane/ CH_2Cl_2 at 4°C .

$^1\text{H NMR}$ (600 MHz, CDCl_3) (1.0:1.0 mixture of rotamers) δ 7.70 – 7.60 (m, 4H), 7.50 – 7.25 (m, 32 H), 7.15 (d, $J = 8.0$ Hz, 2H), 7.07 (t, $J = 7.8$ Hz, 2H), 6.93 (t, $J = 8.6$ Hz, 2H), 6.86 (t, $J = 7.4$ Hz, 2H), 6.76 (d, $J = 7.3$ Hz, 2H), 5.41 – 5.36 (m, 2H), 5.24 – 5.12 (m, 4H),

4.99 (s, 1H), 4.99 (s, 2H), 4.92 (d, $J = 7.3$ Hz, 2H), 4.03 – 3.91 (m, 4H), 3.54 (dt, $J = 33.1$, 10.1, 2H), 2.83 – 2.73 (m, 4H), 2.52 – 2.37 (m, 4H), 2.29 (d, $J = 26.6$ Hz, 6H), 2.11 (dd, $J = 27.4$, 12.4 Hz, 2H), 1.80 – 1.71 (m, 2H), 0.90 (s, 18H) ppm.

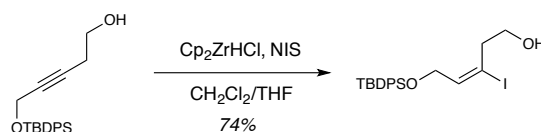
$^1\text{H NMR}$ (600 MHz, d^6 -DMSO, 80 °C) δ 7.86 (bs, 1H), 7.78 (d, $J = 8.2$ Hz, 1H), 7.71 – 7.65 (m, 7H), 7.68 – 7.58 (m, 9H), 7.52 (bs, 2H), 7.41 (t, $J = 8.5$ Hz, 1H), 7.33 (d, $J = 7.4$ Hz, 1H), 7.32 (t, $J = 7.3$ Hz, 1H), 5.61 (s, 1H), 5.48 – 5.42 (m, 2H), 5.29 (s, 1H), 5.21 (s, 1H), 4.21 – 4.07 (m, 2H), 3.76 (t, $J = 10.2$ Hz, 1H), 3.18 (s, 1H), 3.03 – 2.90 (m, 2H), 2.68 – 2.56 (m, 4H), 2.51 (bs, 1H), 2.08 – 1.99 (m, 1H), 1.15 (s, 9H) ppm.

$^{13}\text{C NMR}$ (126 MHz, CDCl_3) (1:1 mixture of rotamers) δ 164.6, 155.9, 155.7, 144.6, 144.4, 143.9, 143.1, 137.1, 136.0, 135.7, 135.6, 133.9, 133.7, 131.4, 131.2, 129.9, 129.5, 129.4, 128.8, 128.6, 128.5, 128.3, 128.2, 127.9, 127.6, 127.5, 124.7, 122.3, 122.2, 115.0, 114.8, 114.5, 69.3, 69.0, 67.4, 62.6, 60.5, 54.1, 54.0, 51.1, 51.0, 44.5, 40.0, 36.0, 35.7, 31.2, 30.6, 27.1, 27.0, 21.6, 21.2, 19.4, 14.3 ppm.

IR (thin film, cm^{-1}) 3069, 2931, 2857, 1691, 1470, 1455, 1170, 1084, 907, 729, 700, 577.

HRMS (+NSI) calculated for $\text{C}_{47}\text{H}_{51}\text{O}_5\text{N}_2\text{SSi}$ $[\text{M}+\text{H}]^+$ 783.3283, found 783.3275.

Vinyl iodide 2.65:



A round bottom flask was charged with Cp_2ZrHCl (7.66 g, 29.70 mmol, 3.0 equiv) in a glove box. The flask was removed from the glove box and placed under nitrogen pressure.

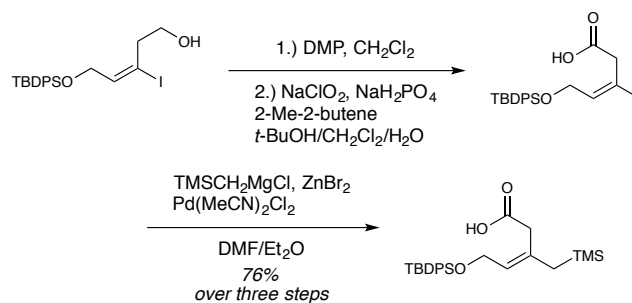
The solid was brought up in CH_2Cl_2 (80.0 mL) and cooled to 0 °C. A solution of the alcohol **2.64** (3.35 g, 9.90 mmol, 1.0 equiv) in CH_2Cl_2 (80.0 mL) was added via cannula, and the resultant mixture was stirred for three hours. The reaction mixture was subsequently cooled to -78 °C, and a solution of NIS (4.45 g, 19.80 mmol, 2.0 equiv) in dry THF (80.0 mL) was then added via cannula. The reaction was stirred for thirty minutes and was subsequently quenched via the addition of a 1:1 mixture of saturated aqueous Na_2SO_3 /saturated aqueous NaHCO_3 (200.0 mL) and warmed to room temperature. The biphasic mixture was filtered over celite and rinsed with Et_2O (3 x 50.0 mL). The layers were separated, and the aqueous phase was extracted with Et_2O (3 x 100.0 mL). The combined organic layer was washed with brine (100.0 mL), dried over anhydrous MgSO_4 , filtered, and concentrated under reduced pressure. Purification by flash chromatography on silica gel (9:1 hexanes/ EtOAc) afforded vinyl iodide **2.65** (3.45 g, 74%) as a pale yellow oil.

^1H NMR (400 MHz, CDCl_3) δ 7.71-7.65 (m, 4H), 7.47-7.39 (m, 6H), 6.56 (t, 1H, $J = 6.7$ Hz), 4.15 (d, 2H, $J = 6.7$ Hz), 3.65 (q, 2H, $J = 5.9$ Hz), 2.54 (t, 2H, $J = 5.8$ Hz), 1.62 (t, 1H, $J = 6.1$ Hz), 1.05 (s, 9H) ppm.

^{13}C NMR (100 MHz, CDCl_3) δ 143.0, 135.7, 133.2, 130.0, 127.9, 101.6, 61.6, 60.8, 42.5, 26.9, 19.3 ppm.

IR (thin film, cm^{-1}) 3500-2500, 3070, 2929, 2856, 1712, 1427, 1106, 699.8.

HRMS (+NSI) calculated for $\text{C}_{21}\text{H}_{25}\text{INaO}_3\text{Si}$ $[\text{M}+\text{Na}]^+$ 503.0515, found 503.0510.

Allylsilane 2.67:

Vinyl iodide **2.65** (3.44 g, 7.4 mmol, 1.0 equiv) was dissolved in CH₂Cl₂ (35.0 mL). DMP (3.75 g, 8.8 mmol, 1.2 equiv) was added, and the reaction was stirred for three hours. The reaction was quenched with a 1:1 mixture of saturated aqueous Na₂SO₃/saturated aqueous NaHCO₃ (50.0 mL), and the layers were separated. The aqueous phase was extracted with EtOAc (3 x 50.0 mL). The combined organic layers were washed with brine (50.0 mL), dried over anhydrous Na₂SO₄, filtered, and concentrated under reduced pressure. The residue was dissolved in *t*-BuOH (62.0 mL) and CH₂Cl₂ (14.0 mL). 2-methyl-2-butene (33.0 mL) was then added and the mixture was cooled to 0 °C. NaClO₂ (6.67 g, 73.7 mmol, 10.0 equiv) and NaH₂PO₄ (7.08 g, 59.0 mmol, 8.0 equiv) were dissolved in H₂O (68.0 mL). The resultant aqueous solution was added to the reaction mixture in one portion, and the biphasic mixture was stirred for one hour. The reaction was quenched with water (100.0 mL) and CH₂Cl₂ (100.0 mL). The layers were separated, and the aqueous phase was extracted with CH₂Cl₂ (3 x 100.0 mL). The combined organic phase was washed with brine (100.0 mL), dried over anhydrous Na₂SO₄, filtered, and concentrated under reduced pressure. Residual *t*-BuOH was removed by azeotroping the residue with toluene (3 x 50.0 mL) to provide the crude carboxylic acid **2.66** as a yellow oil, which was used without further purification.

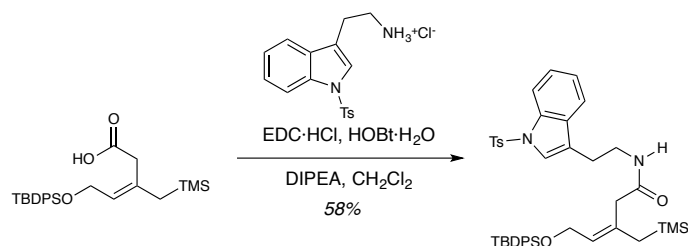
ZnBr₂ (5.31 g, 23.6 mmol, 3.2 equiv) and TMSCH₂MgCl (1.0 M in Et₂O, 22.1 mL, 22.1 mmol, 3.0 equiv) were combined and stirred for 12 hours at room temperature. The mixture was cooled to 0 °C, and DMF (30.0 mL) and Et₂O (10.0 mL) were slowly added. A solution of crude carboxylic acid **X** in DMF (20.0 mL) was added to the reaction mixture via cannula. A solution of Pd(MeCN)₂Cl₂ (191.2 mg, .737 mmol, 10 mol %) in DMF (5.0 mL) was added, and the resultant mixture was stirred for three hours. The reaction was quenched with saturated aqueous NH₄Cl (150.0 mL) and Et₂O (100.0 mL), and the layers were separated. The aqueous phase was extracted with Et₂O (3 x 75.0 mL). The combined organic layer was washed with water (2 x 100.0 mL), 5% aqueous LiCl (100.0 mL), and brine (100.0 mL). The organic layer was dried over anhydrous Na₂SO₄, filtered through celite, and concentrated under reduced pressure. Purification by column chromatography on silica gel (4:1 to 7:3 hexanes/EtOAc) provided allylsilane **2.67** (2.48 g, 76% over three steps) as a yellow oil.

¹H NMR (500 MHz, CDCl₃) δ 7.71 – 7.66 (m, 4H), 7.46 – 7.36 (m, 6H), 5.48 (t, *J* = 7.0 Hz, 1H), 4.17 (d, *J* = 6.9 Hz, 2H), 3.00 (s, 2H), 1.63 (s, 2H), 1.03 (s, 9H), 0.02 (s, 2H) ppm.

¹³C NMR (126 MHz, CDCl₃) δ 174.8, 135.7, 133.5, 129.9, 127.9, 125.3, 60.8, 39.0, 27.9, 26.9, 19.3, -1.2 ppm.

IR (thin film, cm⁻¹) 3200, 2857, 1706, 1248, 1110, 1045, 842, 823, 700, 612.

HRMS (-NSI) calculated for C₂₅H₃₅O₃Si₂ [M-H]⁻ 439.2125, found 439.2136.

Amide 2.68:

Tryptamine hydrochloride **2.53** (1.48 g, 5.9 mmol, 1.1 equiv) was brought up in CH₂Cl₂ (20.0 mL). The resultant slurry was cooled to 0 °C, and DIPEA (6.2 mL, 35.4 mmol 4.5 equiv) was added drop-wise. HOBT·H₂O (799.0 mg, 5.9 mmol, 1.1 equiv) was then added to the tryptamine solution. A solution of carboxylic acid **2.67** (2.48 g, 5.6 mmol, 1.0 equiv) in CH₂Cl₂ (20.0 mL) was added to the tryptamine solution. EDC·HCl (1.13 g, 5.9 mmol, 1.1 equiv) was then added, and the reaction was stirred for three hours. The reaction was quenched with aqueous 0.5 N HCl (100.0 mL) and stirred for 15 minutes. CH₂Cl₂ (100.0 mL) was added, and the layers were separated. The organic phase was washed with aqueous 2 N HCl (100.0 mL), saturated aqueous NaHCO₃ (2 x 100.0 mL), and brine (100.0 mL). The organic layer was dried over anhydrous Na₂SO₄, filtered, and concentrated under reduced pressure. Purification by flash chromatography on silica gel (4:1 to 3:1 hexanes/EtOAc) provided the amide **2.68** (2.40 g, 58%) as a sticky foam.

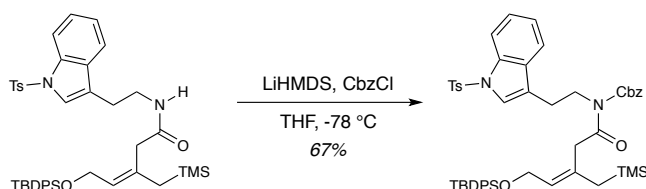
¹H NMR (400 MHz, CDCl₃) δ 7.95 (d, *J* = 8.5 Hz, 1H), 7.72 (d, *J* = 8.3 Hz, 2H), 7.65 (dd, *J* = 7.8, 1.6 Hz, 4H), 7.46 – 7.34 (m, 6H), 7.29 (d, *J* = 10.1 Hz, 2H), 7.19 (dd, *J* = 7.6, 6.1 Hz, 4H), 6.42 (t, *J* = 6.4 Hz, 1H), 5.43 (t, *J* = 7.2 Hz, 1H), 4.13 (d, *J* = 7.1 Hz, 2H), 3.35 (q, *J* = 6.6 Hz, 2H), 2.91 (s, 2H), 2.72 (t, *J* = 7.2 Hz, 2H), 2.32 (s, 3H), 1.47 (s, 2H), 1.01 (s, 9H), 0.00 (s, 9H) ppm.

^{13}C NMR (126 MHz, CDCl_3) δ 170.3, 144.9, 137.6, 135.7, 135.6, 133.6, 130.9, 130.0, 128.0, 126.9, 124.9, 124.6, 123.4, 123.2, 119.9, 119.6, 113.8, 60.5, 41.1, 39.4, 27.7, 27.0, 25.2, 19.3, -1.3 ppm.

IR (thin film, cm^{-1}) 3338, 3069, 2954, 2930, 2857, 1675, 1370, 1173, 1112, 851, 703.

HRMS (+NSI) calculated for $\text{C}_{42}\text{H}_{52}\text{O}_4\text{N}_2\text{NaSSi}_2$ $[\text{M}+\text{Na}]^+$ 759.3079, found 759.3112.

Cbz-Amide **2.69**:



A solution of amide **2.68** (2.40 g, 3.30 mmol, 1.1 equiv) in THF (16.0 mL) was cooled to -78 °C. A solution of LiHMDS (0.31 M in THF, 1.00 mL, 3.10 mmol, 1.0 equiv) was added drop-wise over five minutes, and the mixture was stirred for one hour. CbzCl (0.55 mL, 3.90 mmol, 1.3 equiv) was then added, and the reaction was stirred at -78 °C for 18 hours. The reaction was quenched with saturated aqueous NH_4Cl (25.0 mL), and the biphasic mixture was warmed to room temperature. The layers were separated, and the aqueous phase was extracted with Et_2O (3 x 25.0 mL). The combined organic layer was washed with brine (50.0 mL), dried over anhydrous MgSO_4 , filtered, and concentrated under reduced pressure. Purification by flash column chromatography on silica gel (9:1 to 4:1 hexanes/ EtOAc) provided Cbz-amide **2.69** (1.80 g, 67%) as a sticky foam.

^1H NMR (500 MHz, CDCl_3) δ 7.97 (s, 1H), 7.74 (d, $J = 8.4$ Hz, 2H), 7.70 (dd, $J = 7.6, 1.7$ Hz, 4H), 7.44 – 7.33 (m, 13H), 7.30 – 7.27 (m, 1H), 7.21 (d, $J = 8.1$ Hz, 2H), 7.12 (t, $J =$

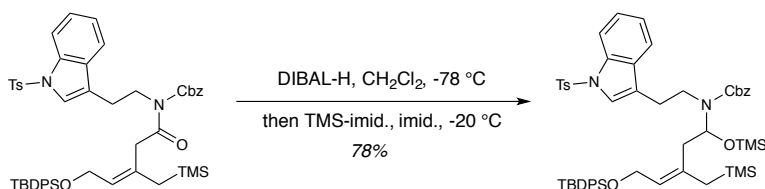
7.6 Hz, 1H), 5.50 (t, $J = 6.4$ Hz, 1H), 5.09 (s, 2H), 4.18 (d, $J = 6.4$ Hz, 2H), 3.93 – 3.83 (m, 2H), 3.58 (s, 2H), 2.85 – 2.75 (m, 2H), 2.34 (s, 3H), 1.57 (s, 2H), 1.06 (s, 9H), 0.06 (s, 9H) ppm.

^{13}C NMR (126 MHz, CDCl_3) δ 173.1, 154.0, 144.8, 135.6, 135.3, 135.1, 134.8, 134.0, 132.8, 130.6, 129.8, 129.5, 128.8, 128.6, 127.6, 126.8, 126.0, 124.7, 123.5, 123.1, 119.6, 119.3, 113.6, 68.7, 61.04, 44.4, 41.7, 29.7, 28.2, 26.8, 24.4, 21.6, 19.2, -1.2 ppm.

IR (thin film, cm^{-1}) 2954, 2856, 1734, 1697, 1170, 736, 701.

HRMS (+NSI) calculated for $\text{C}_{50}\text{H}_{58}\text{O}_6\text{N}_2\text{NaSSi}_2$ $[\text{M}+\text{Na}]^+$ 893.3446, found 893.3468.

Hemiaminal Ether 2.70:



A solution of Cbz-amide **2.69** (1.80 g, 2.10 mmol, 1.0 equiv) in CH_2Cl_2 (40.0 mL) was cooled to $-78\text{ }^\circ\text{C}$. A solution of DIBAL-H (1.0 M in CH_2Cl_2 , 4.13 mL, 4.13 mmol, 2.0 equiv) was added over five minutes, and the reaction was stirred for one hour. TMS-imidazole (0.91 mL, 6.20 mmol, 3.0 equiv) and imidazole (140.9 mg, 2.10 mmol, 1.0 equiv) were added, and the resultant mixture was warmed to $-20\text{ }^\circ\text{C}$ and stirred for 20 hours. The reaction was warmed to room temperature and quenched with saturated aqueous Rochelle's salt solution (50.0 mL). The biphasic mixture was stirred at room temperature until both layers were clear. The layers were separated, and the aqueous phase was extracted with CH_2Cl_2 (3 x 50.0 mL). The combined organic layer was dried over

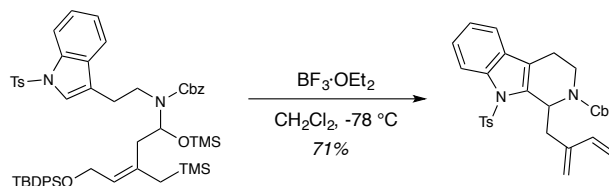
anhydrous Na_2SO_4 , filtered, and concentrated under reduced pressure. Purification by flash column chromatography on silica gel (9:1 hexanes/EtOAc) provided hemiaminal ether **2.70** (1.53 g, 78%) as a sticky foam.

^1H NMR (600 MHz, CDCl_3) (1.0:0.8 mixture of rotamers) δ 7.97 (d, $J = 8.3$ Hz, 0.8H), 7.94 (d, $J = 8.4$ Hz, 1H), 7.75 (d, $J = 8.1$ Hz, 1.6H), 7.72 (d, $J = 8.1$ Hz, 2H), 7.66-7.57 (m, 7.2H), 7.38 – 7.16 (m, 28.8H), 7.12 (t, $J = 7.4$ Hz, .8H), 6.93 (t, $J = 7.6$ Hz, 1H), 5.69 (dd, $J = 8.2, 4.2$ Hz, 1H), 5.48 (dd, $J = 8.2, 4.2$ Hz, .8H), 5.32 (dd, $J = 2.5, 1.8$ Hz, 1H), 5.29 (dd, $J = 2.5, 1.8$ Hz, .8H), 5.18 – 5.03 (m, 3.6H), 4.25 – 4.07 (m, 3.6H), 3.40 – 3.24 (m, 2H), 3.19 – 3.08 (m, 1.6H), 2.92 – 2.69 (m, 3.6H), 2.31 (s, 5.4H), 2.18 (dd, $J = 13.1, 8.3$ Hz, 1H), 2.11 (dd, $J = 13.3, 8.2$ Hz, .8H), 1.92 (dd, $J = 13.1, 4.3$ Hz, 1H), 1.86 (dd, $J = 13.3, 4.4$ Hz, .8H), 1.50 – 1.43 (m, 2H), 1.31 – 1.25 (m, 1.6H), 1.00 (s, 16.2H), 0.03 (s, 18H), -0.03 (s, 6.2H), -0.05 (s, 6.2H) ppm.

^{13}C NMR (151 MHz, CDCl_3) (1.0:0.8 mixture of rotamers) δ 155.0, 154.2, 144.7, 136.5, 136.3, 135.5, 135.2, 135.1, 134.8, 134.0, 130.9, 130.7, 129.8, 129.7, 129.5, 128.6, 128.5, 128.3, 128.1, 127.7, 117.6, 127.5, 126.8, 125.7, 125.6, 124.6, 123.1, 120.4, 120.1, 119.9, 119.6, 113.6, 79.2, 79.0, 67.2, 61.0, 60.8, 60.0, 41.5, 41.2, 39.7, 39.4, 31.9, 29.7, 29.4, 27.7, 27.5, 26.8, 26.6, 25.4, 22.7, 21.6, 19.2, 19.0, 14.1, -0.3, -1.3 ppm.

IR (thin film, cm^{-1}) 3070, 2956, 2929, 2857, 1702, 1427, 1306, 1174, 1112, 846, 703, 577.

HRMS (+NSI) calculated for $\text{C}_{53}\text{H}_{72}\text{O}_6\text{N}_3\text{SSi}_3$ $[\text{M}+\text{NH}_4]^+$ 962.4444, found 962.4469.

Diene 2.71:

A solution of hemiaminal ether **2.70** (100.0 mg, 0.11 mmol, 1.0 equiv) in CH_2Cl_2 (1.0 mL) was cooled to $-78\text{ }^\circ\text{C}$. $\text{BF}_3 \cdot \text{OEt}_2$ (0.04 mL, 0.32 mmol, 2.9 equiv) was added dropwise over five minutes, and the reaction was stirred at $-78\text{ }^\circ\text{C}$ for 24 hours. The reaction was quenched with saturated aqueous NaHCO_3 (3.0 mL) and CH_2Cl_2 (3.0 mL), warmed to room temperature, and stirred for one hour. The layers were separated, and the aqueous phase was extracted with CH_2Cl_2 (3 x 10.0 mL). The combined organic layer was dried over anhydrous Na_2SO_4 , filtered, and concentrated under reduced pressure. Purification by preparatory thin layer chromatography on silica gel (4:1 hexanes/EtOAc) provided diene **2.71** (41.0 mg, 71%) as a colorless oil.

$^1\text{H NMR}$ (400 MHz, CDCl_3) (1.0:0.8 mixture of rotamers) δ 8.18 (d, $J = 8.7$ Hz, 1H), 7.71 (d, $J = 8.1$ Hz, 2H), 7.47 – 7.06 (m, 18.8H), 6.73 (d, $J = 8.1$ Hz, 1.6H), 6.51 – 6.26 (m, 2.8 H), 6.09 (dd, $J = 11.6, 2.4$ Hz, 1H), 5.76 (d, $J = 17.6$ Hz, 1H), 5.67 (d, $J = 17.6$ Hz, .8H), 5.23 – 5.02 (m, 8.8H), 4.47 (dd, $J = 13.7, 6.4$ Hz, 1H), 4.30 (dd, $J = 13.7, 6.4$ Hz, 1H), 3.39 – 3.19 (m, 3.6H), 2.92 – 2.51 (m, 5.2H), 2.27 (s, 2.4H), 2.19 (s, 3H) ppm.

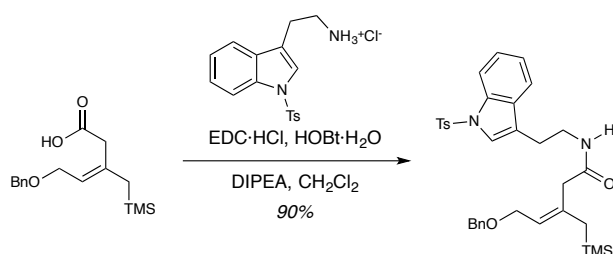
$^{13}\text{C NMR}$ (151 MHz, CDCl_3) (1.0:0.8 mixture of rotamers) δ 156.2, 155.9, 144.7, 144.6, 137.5, 137.4, 137.1, 137.0, 136.9, 136.8, 136.6, 136.5, 135.8, 135.7, 134.4, 134.1, 130.5, 129.7, 124.1, 124.0, 118.6, 118.5, 117.9, 116.6, 115.7, 115.6, 67.8, 67.4, 62.7, 62.2, 51.0,

50.8, 38.6, 38.0, 36.7, 36.4, 36.1, 35.8, 35.2, 32.4, 32.0, 31.2, 29.9, 29.2, 27.0, 22.9, 21.7, 21.4, 20.8, 19.3, 14.3 ppm.

IR (thin film, cm^{-1}) 3045, 2931, 2858, 1693, 1414, 1358, 1170, 1104, 1081, 910, 734, 702, 584.

HRMS (+NSI) calculated for $\text{C}_{31}\text{H}_{30}\text{O}_4\text{N}_2\text{NaS}$ $[\text{M}+\text{Na}]^+$ 549.1819, found 549.1819.

N-H Amide **2.72**:

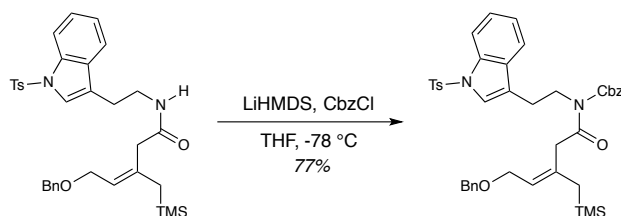


To a solution of carboxylic acid **2.35** (500.0 mg, 1.70 mmol, 1.0 equiv) in CH_2Cl_2 (15.0 mL) was added tryptamine hydrochloride **2.53** (631.5 mg, 1.80 mmol, 1.05 equiv), and the mixture was then subsequently cooled to 0 °C. $\text{HOBt}\cdot\text{H}_2\text{O}$ (270.2 mg, 2.0 mmol, 1.1 equiv) and $\text{EDC}\cdot\text{HCl}$ (383.4 mg, 2.0 mmol, 1.1 equiv) were then added, and the reaction was warmed to room temperature and stirred for 24 hours. The reaction was quenched by the addition of 10% aqueous citric acid (20.0 mL) and CH_2Cl_2 (10.0 mL), and the layers were separated. The organic layer was washed with 10% aqueous citric acid (20.0 mL), saturated aqueous NaHCO_3 (2 x 20.0 mL), and brine (20.0 mL). The organic layer was dried over anhydrous Na_2SO_4 , filtered, and concentrated under reduced pressure. Purification by flash column chromatography on silica gel (4:1 hexanes/ EtOAc) provided N-H amide **2.72** (902.5 mg, 90%) as a colorless oil.

¹H-NMR (400 MHz, CDCl₃) δ 7.95 (d, *J* = 8.3 Hz, 1H), 7.73 (d, *J* = 8.1 Hz, 2H), 7.40 (d, *J* = 7.8 Hz, 1H), 7.35 – 7.15 (m, 10H), 6.92 (t, *J* = 5.9 Hz, 1H), 5.51 (t, *J* = 7.2 Hz, 1H), 4.40 (s, 2H), 3.95 (d, *J* = 7.4 Hz, 2H), 3.23 (q, *J* = 6.8 Hz, 2H), 2.97 (s, 2H), 2.57 (t, *J* = 7.2 Hz, 2H), 2.33 (s, 3H), 1.55 (s, 2H), 0.02 (s, 9H) ppm.

HRMS (+NSI) calculated for C₃₃H₄₀O₄N₂NaSSi [M+Na]⁺ 611.2376, found 611.2372.

Cbz Amide **2.73**:



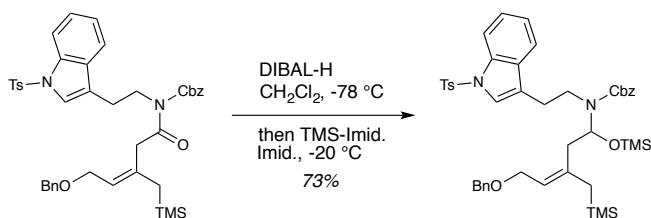
To a solution of N-H amide **2.72** (905.2 mg, 1.53 mmol, 1.05 equiv) in THF (7.5 mL) at -78 °C was added freshly prepared LiHMDS solution (0.31M in THF, 4.70 mL, 1.46 mmol, 1.0 equiv), and the reaction mixture was stirred for one hour. CbzCl (0.32 mL, 2.30 mmol, 1.6 equiv) was then added, and the reaction was stirred at -78 °C for 28 hours. The reaction mixture was quenched with saturated aqueous NH₄Cl (20.0 mL) and warmed to room temperature. The layers were separated, and the aqueous phase was extracted with Et₂O (3 x 20.0 mL). The combined organic layer was washed with brine (30.0 mL), dried over anhydrous MgSO₄, filtered, and concentrated under reduced pressure. Purification by flash column chromatography on silica gel (9:1 to 4:1 hexanes/EtOAc) provided N-Cbz Amide **2.73** (853.1 mg, 77%) as a colorless oil.

¹H-NMR (400 MHz, CDCl₃) δ 7.92 (d, *J* = 8.4 Hz, 1H), 7.70 (d, *J* = 7.6 Hz, 2H), 7.41 – 7.15 (m, 15H), 7.09 (t, *J* = 7.6 Hz, 1H), 5.46 (t, *J* = 7.0 Hz, 2H), 5.07 (s, 2H), 4.43 (s, 2H),

3.95 (d, $J = 6.7$ Hz, 2H), 3.93 – 3.83 (m, 2H), 3.64 (s, 2H), 2.83 – 2.76 (m, 2H), 2.30 (s, 3H), 1.60 (s, 2H), 0.02 (2, 9H) ppm.

HRMS (+NSI) calculated for $C_{41}H_{46}O_6N_2NaSSi$ $[M+Na]^+$ 745.2744, found 745.2746.

Hemiaminal Ether **2.74**:



To a solution of Cbz Amide **2.73** (853.1 mg, 1.18 mmol, 1.0 equiv) in CH_2Cl_2 (25.0 mL) at $-78\text{ }^\circ\text{C}$ was added DIBAL-H (1 M in CH_2Cl_2 , 2.36 mL, 2.36 mmol, 2.0 equiv), and the resultant mixture was stirred for one hour. TMS-imidazole (0.54 mL, 3.54 mmol, 3.0 equiv) and imidazole (80.3 mg, 1.18 mmol, 1.0 equiv) were then added, and the reaction was warmed up to $-20\text{ }^\circ\text{C}$ and stirred for 20 hours. The reaction was warmed to room temperature and quenched with saturated Rochelle's salt solution (50.0 mL), and the resultant biphasic mixture was stirred until both layers were clear. The layers were separated, and the aqueous phase was extracted with CH_2Cl_2 (3 x 50.0 mL). The combined organic layer was dried over anhydrous Na_2SO_4 , filtered, and concentrated under reduced pressure. Purification by flash column chromatography on silica gel (9:1 hexanes/EtOAc) provided hemiaminal ether **2.74** (686.3 mg, 73%) as a sticky foam.

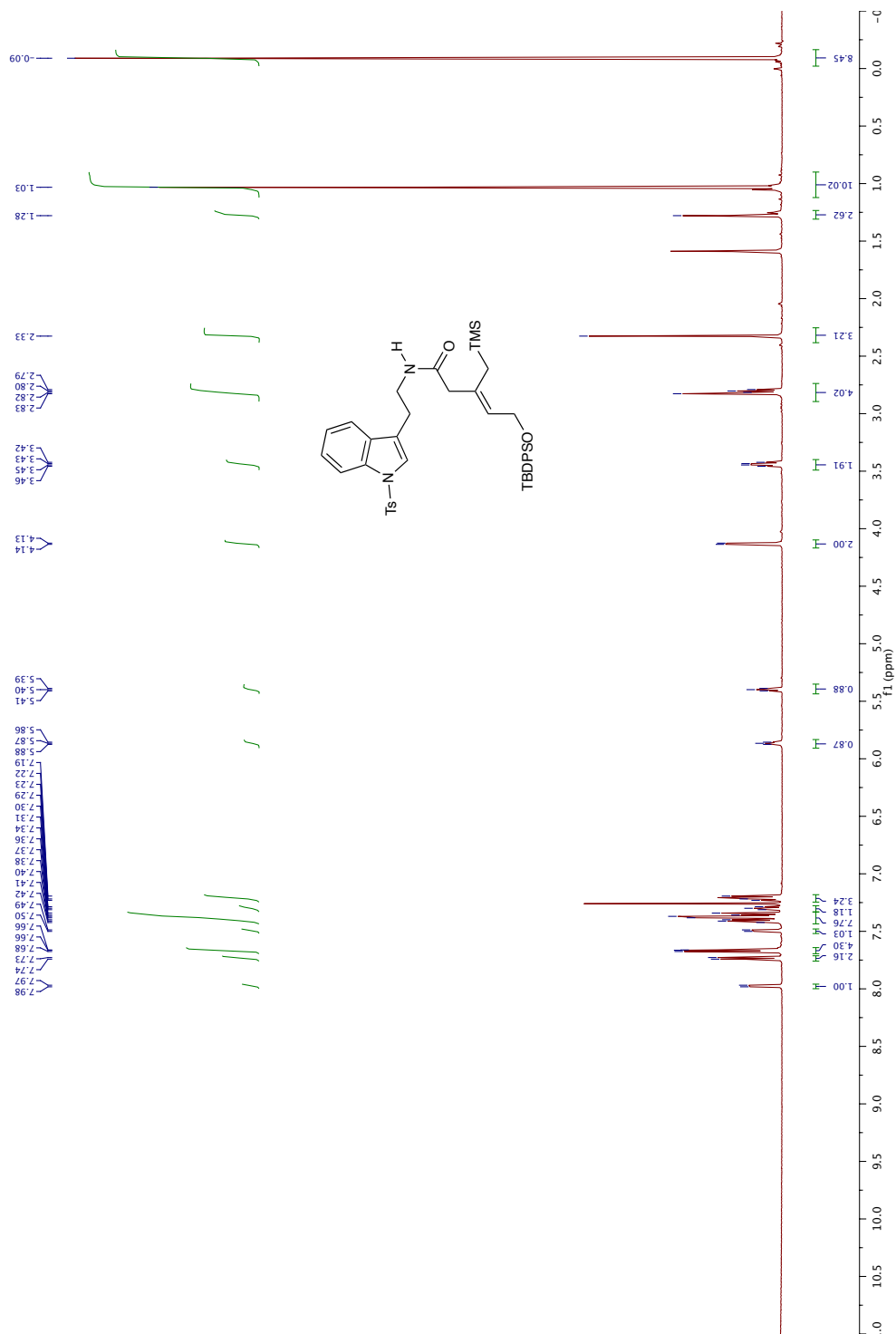
$^1\text{H-NMR}$ (400 MHz, CDCl_3) (1:0.7 mixture of rotamers) δ 7.98 – 7.93 (m, 1.7H), 7.77 – 7.64 (m, 4.1H), 7.41 – 7.13 (m, 25.5H), 7.04 (t, $J = 7.5$ Hz, 1H), 5.80 (dd, $J = 8.3, 4.3$ Hz, 1H), 5.61 (dd, $J = 8.3, 4.3$ Hz, .7H), 5.30 (t, $J = 6.9$ Hz, 1H), 5.27 – 5.07 (m, 4.1H), 4.48-

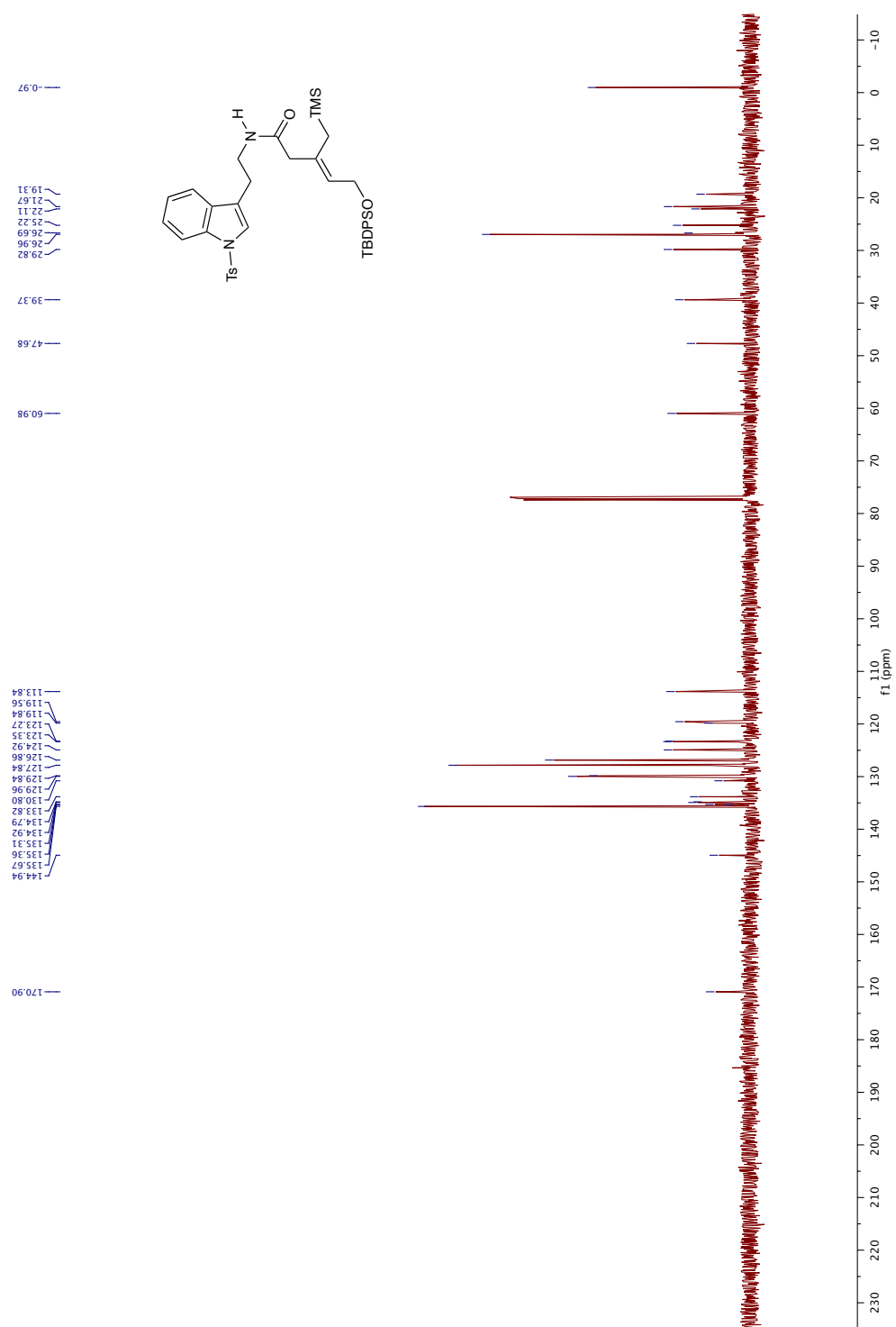
4.27 (m, 3.4H), 4.10 – 3.84 (m, 3.4H), 3.52 – 3.17 (3.4H), 3.02 – 2.75 (m, 3.4H), 2.39 – 2.25 (m, 6.5H), 2.19 – 2.00 (m, 2H), 1.64 (d, $J = 13.5$ Hz, 1H), 1.57 – 1.49 (m, 1.7H), 1.36 (d, $J = 13.5$ Hz, .7H), 0.08 (s, 9H), 0.03 (s, 15.3H), -0.04 (s, 6.3H) ppm.

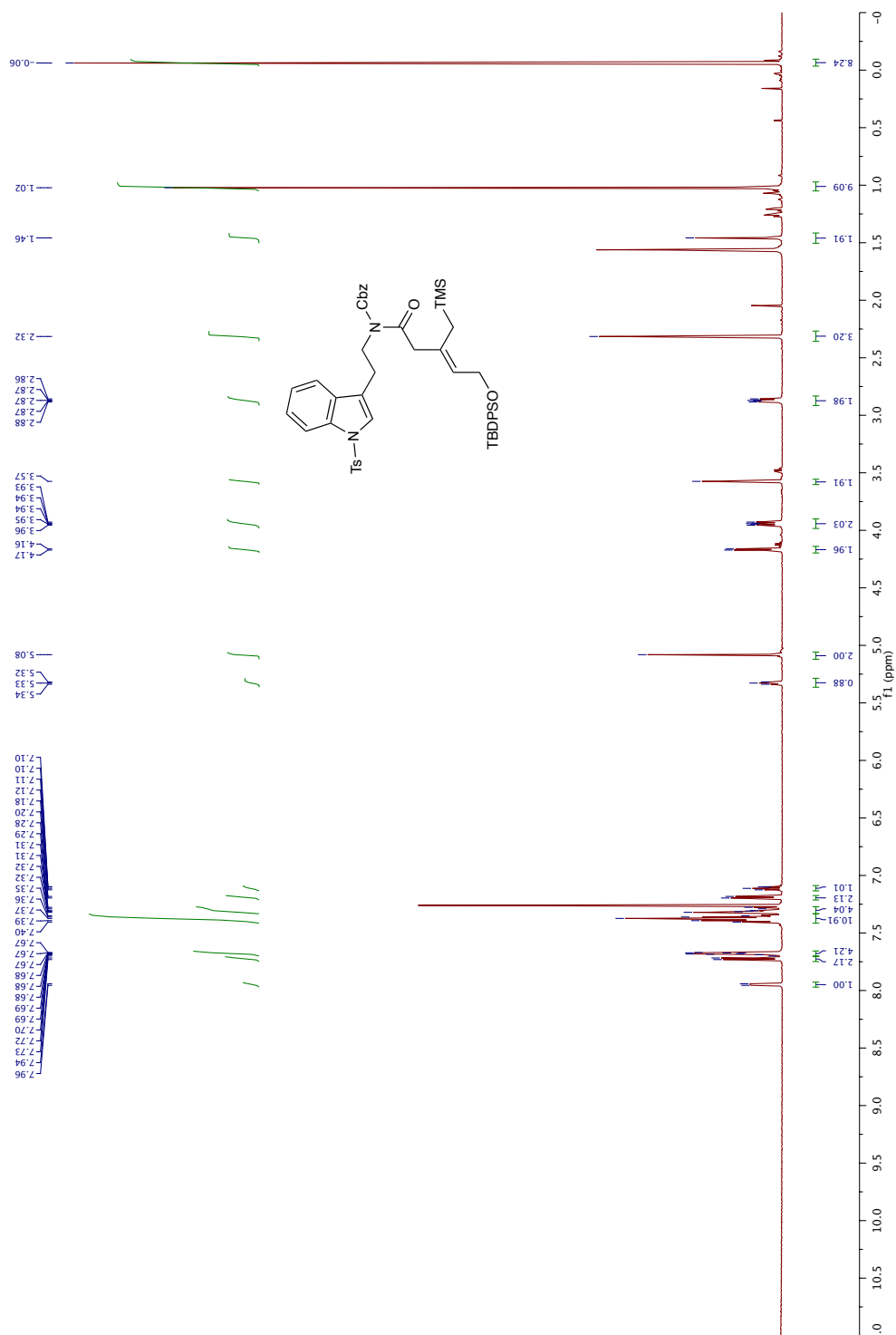
HRMS (+NSI) calculated for $C_{44}H_{60}O_3N_3SSi_2$ $[M+NH_4]^+$ 814.3741, found 814.3739.

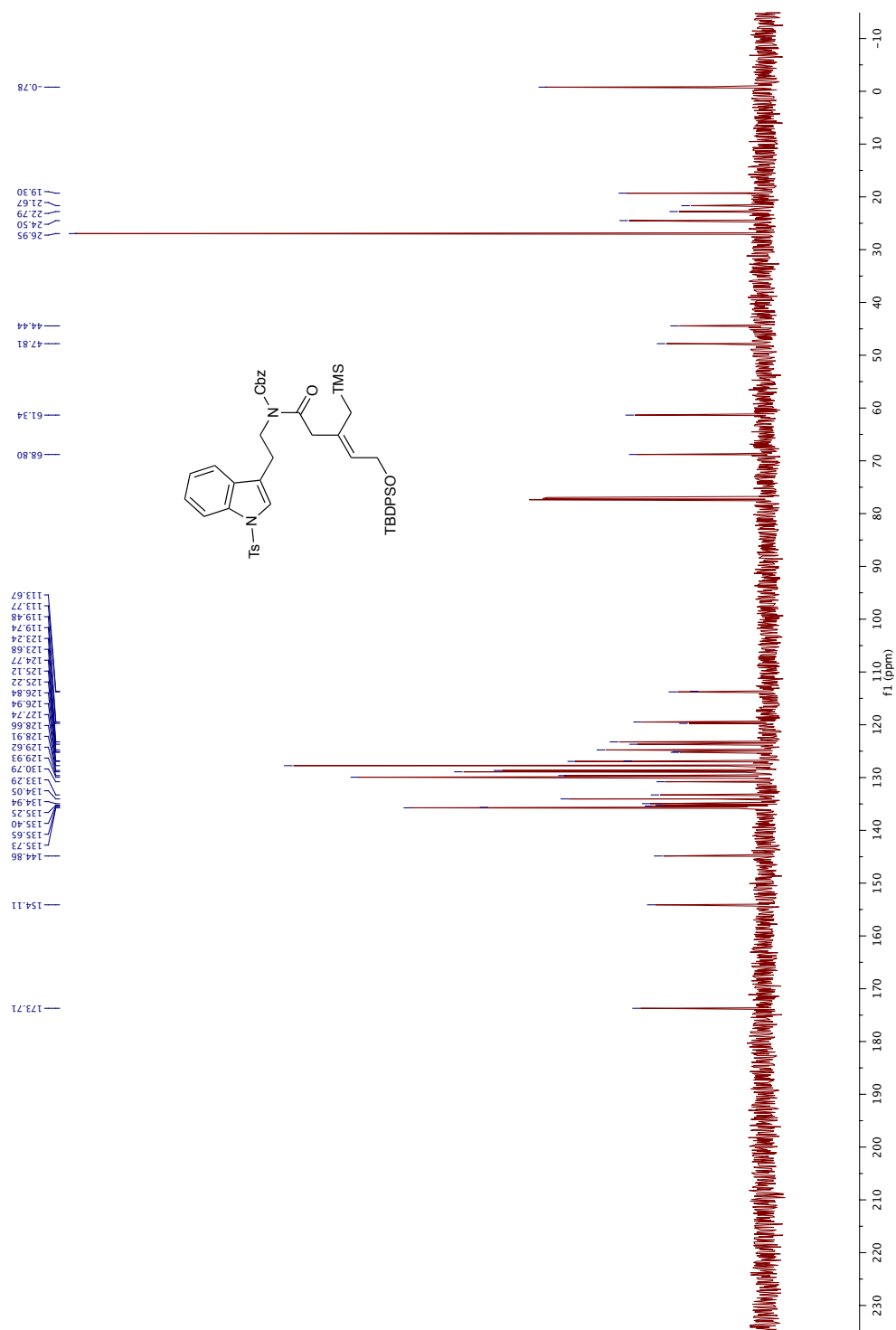
2.9 Spectral Data for Key Intermediates

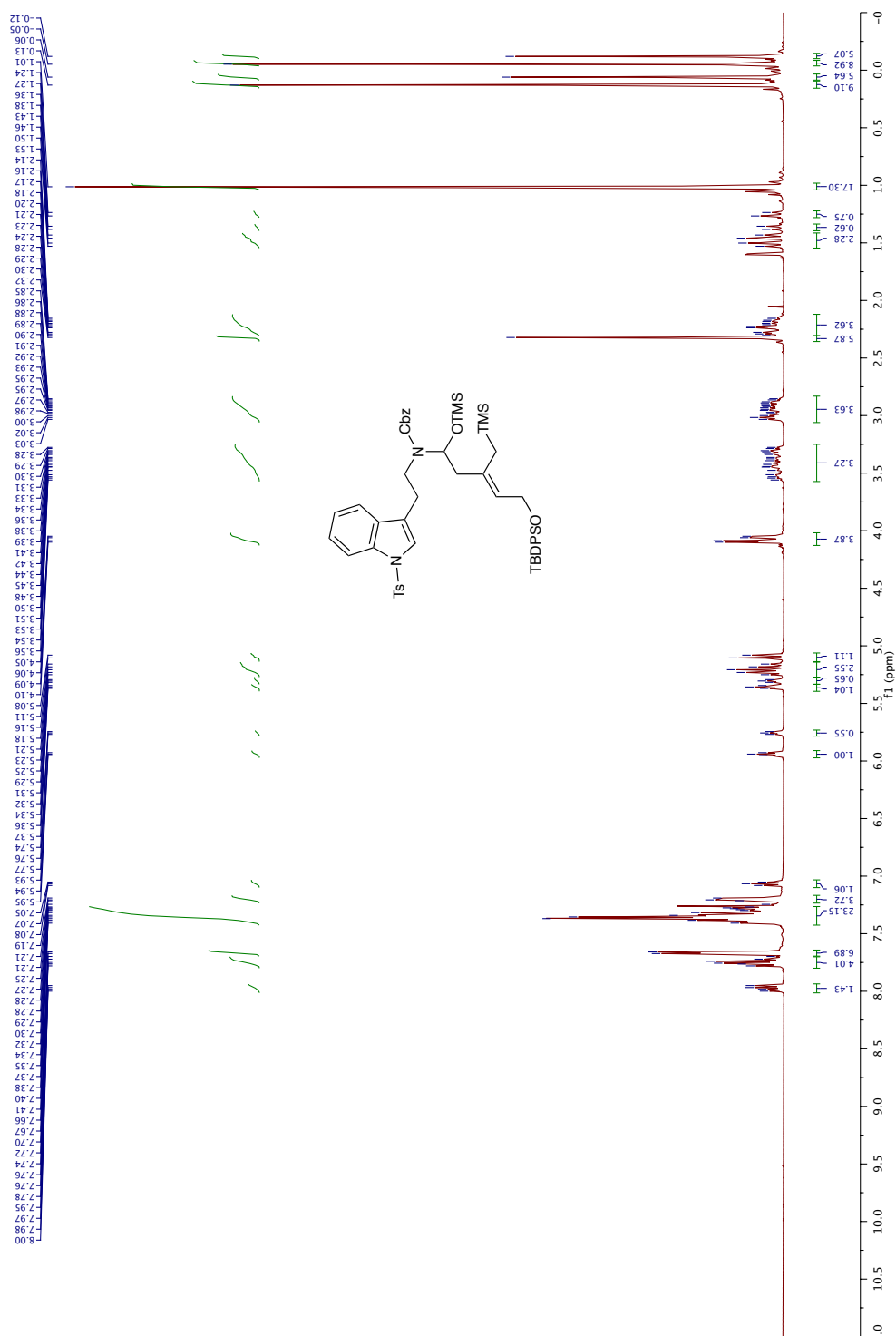
Amide 2.60: ^1H NMR (600 MHz, CDCl_3)

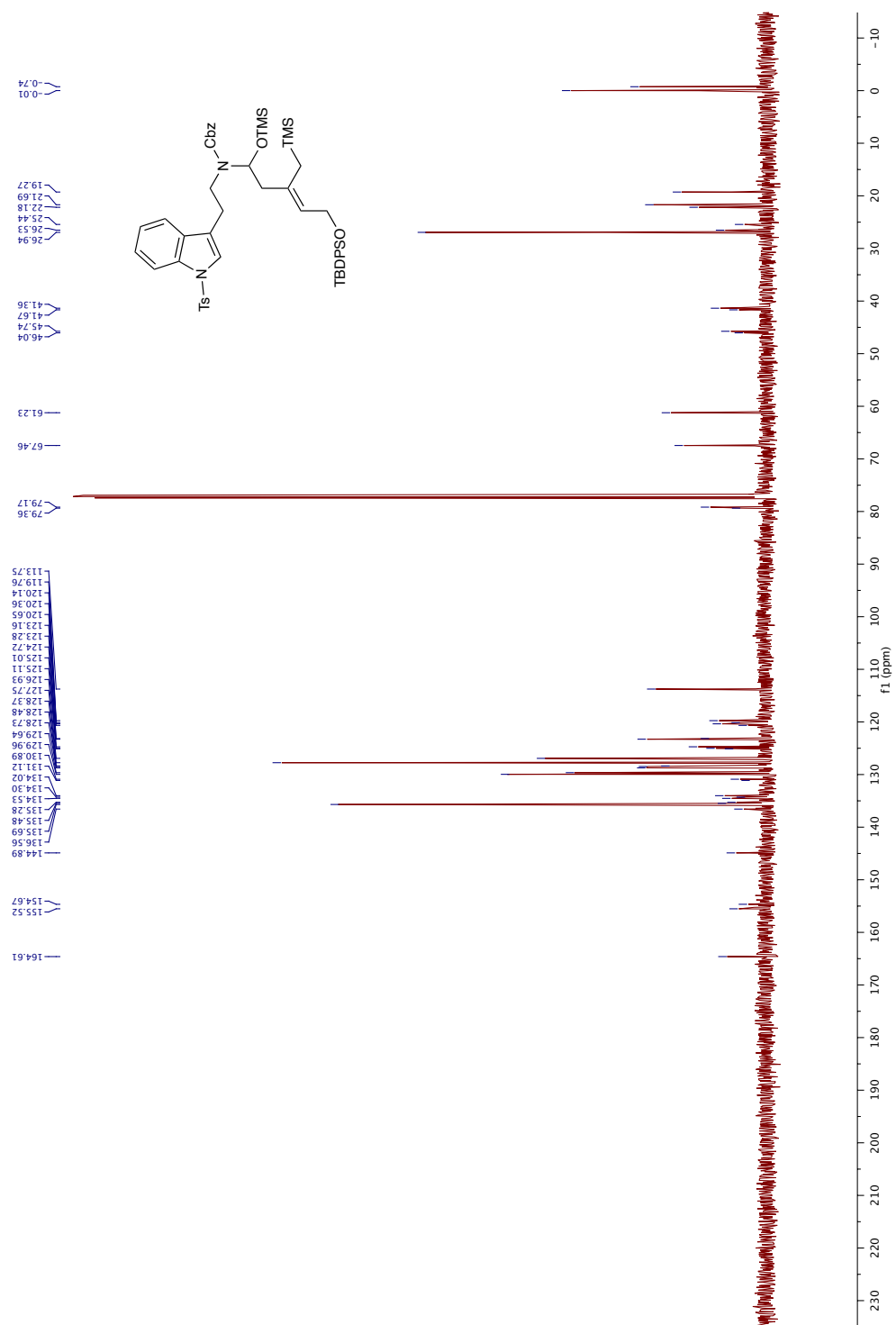


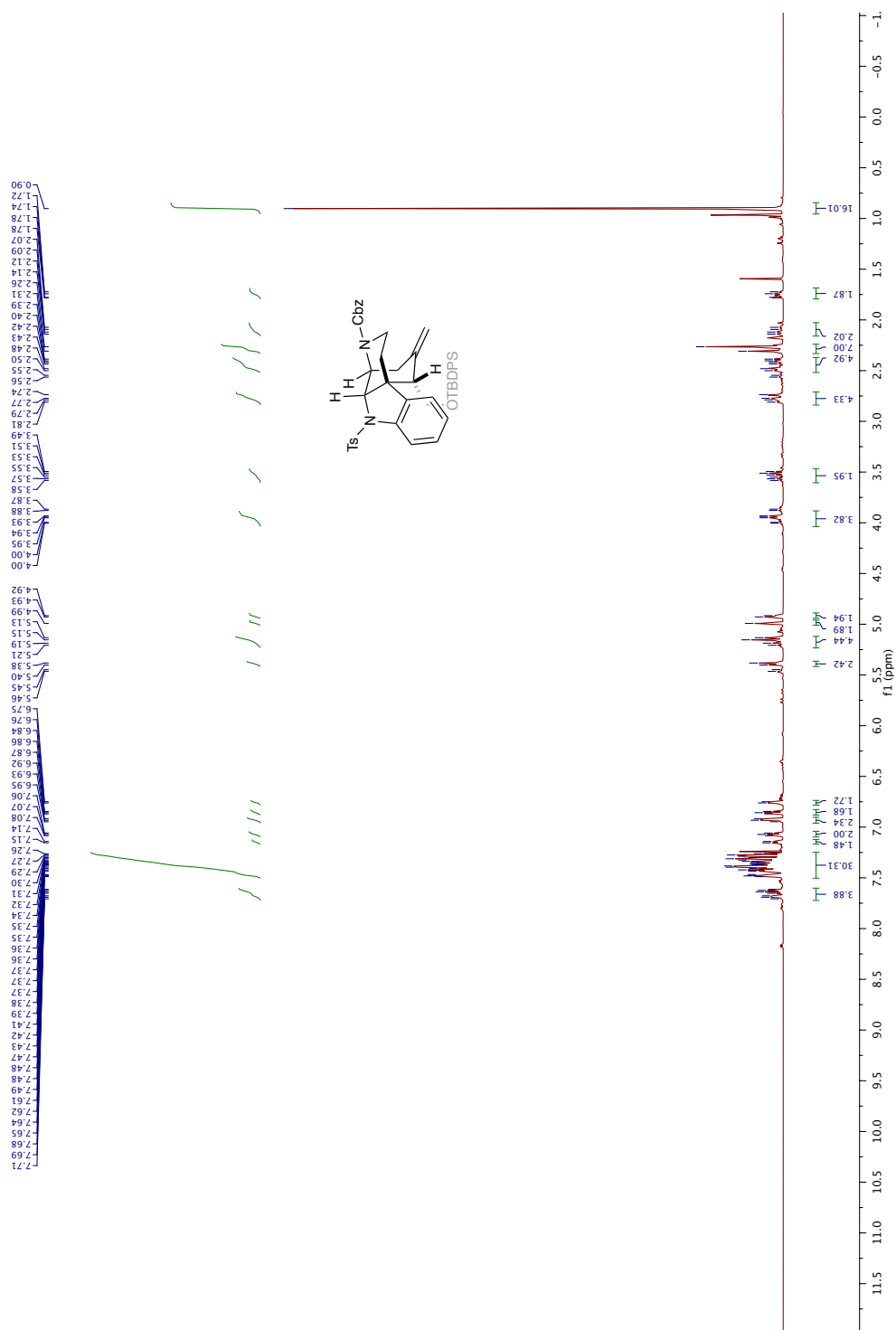
Amide 2.60: ^{13}C NMR (126 MHz, CDCl_3)

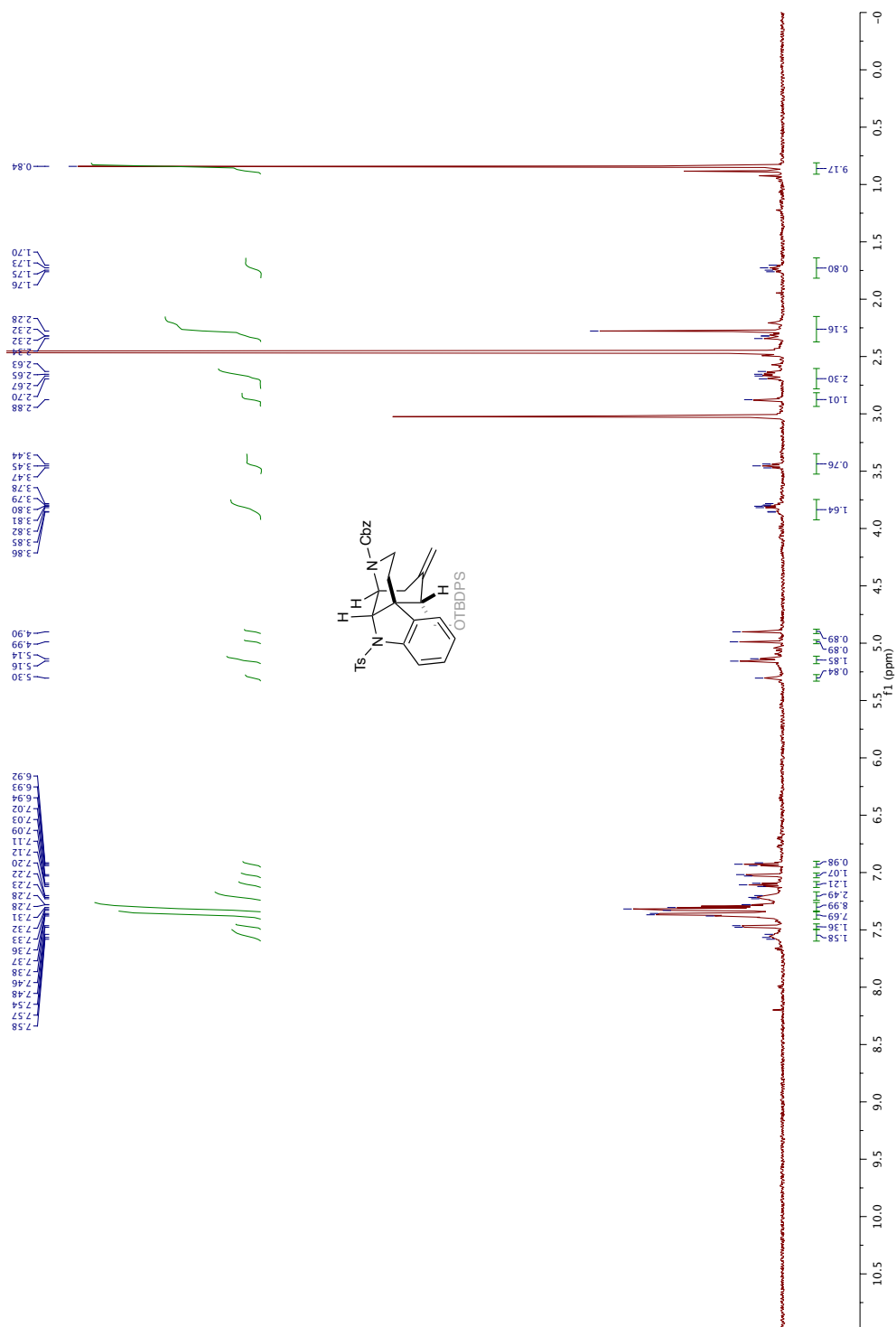
Cbz-Amide 2.61: ^1H NMR (600 MHz, CDCl_3)

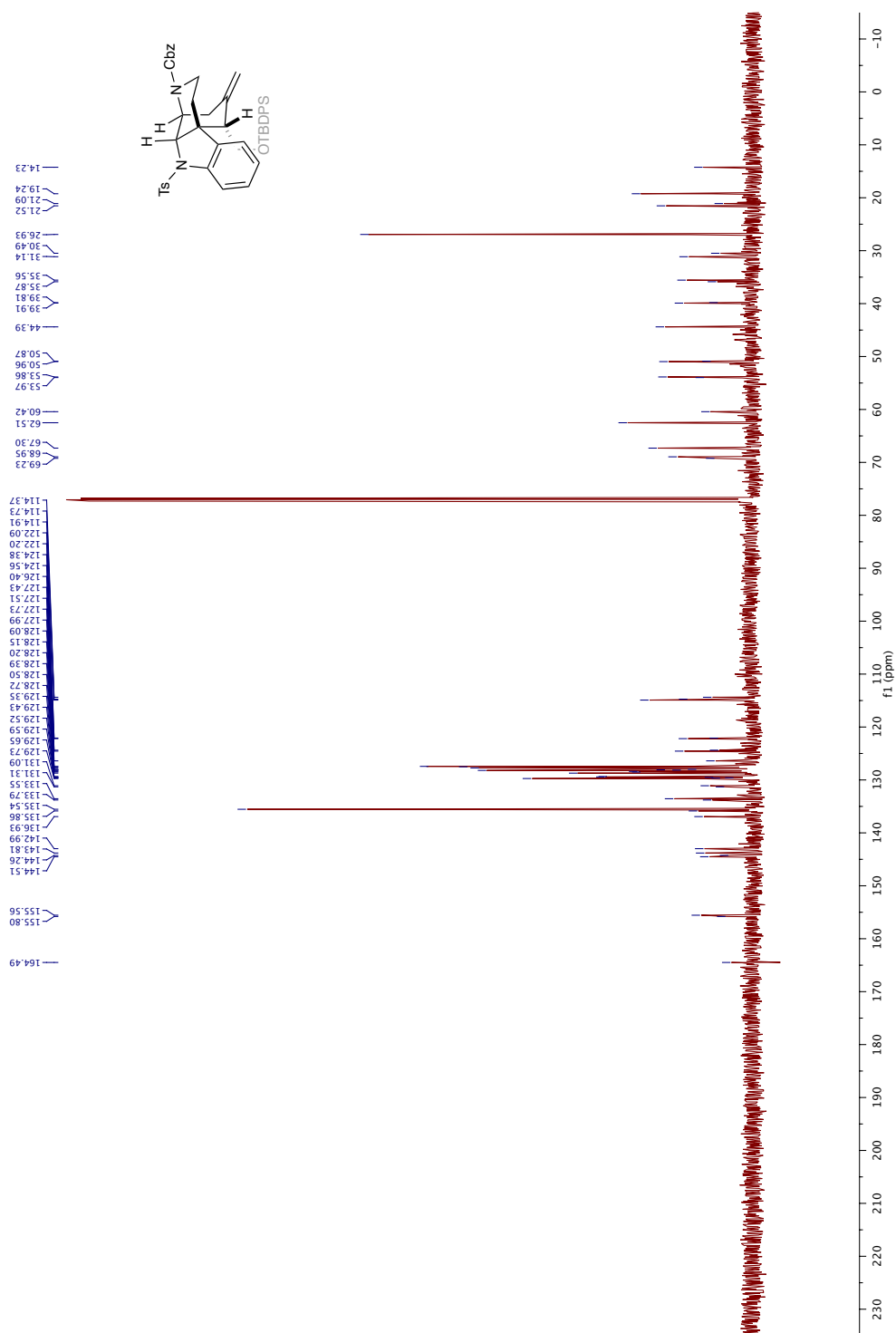
Cbz-Amide 2.61: ^{13}C NMR (151 MHz, CDCl_3)

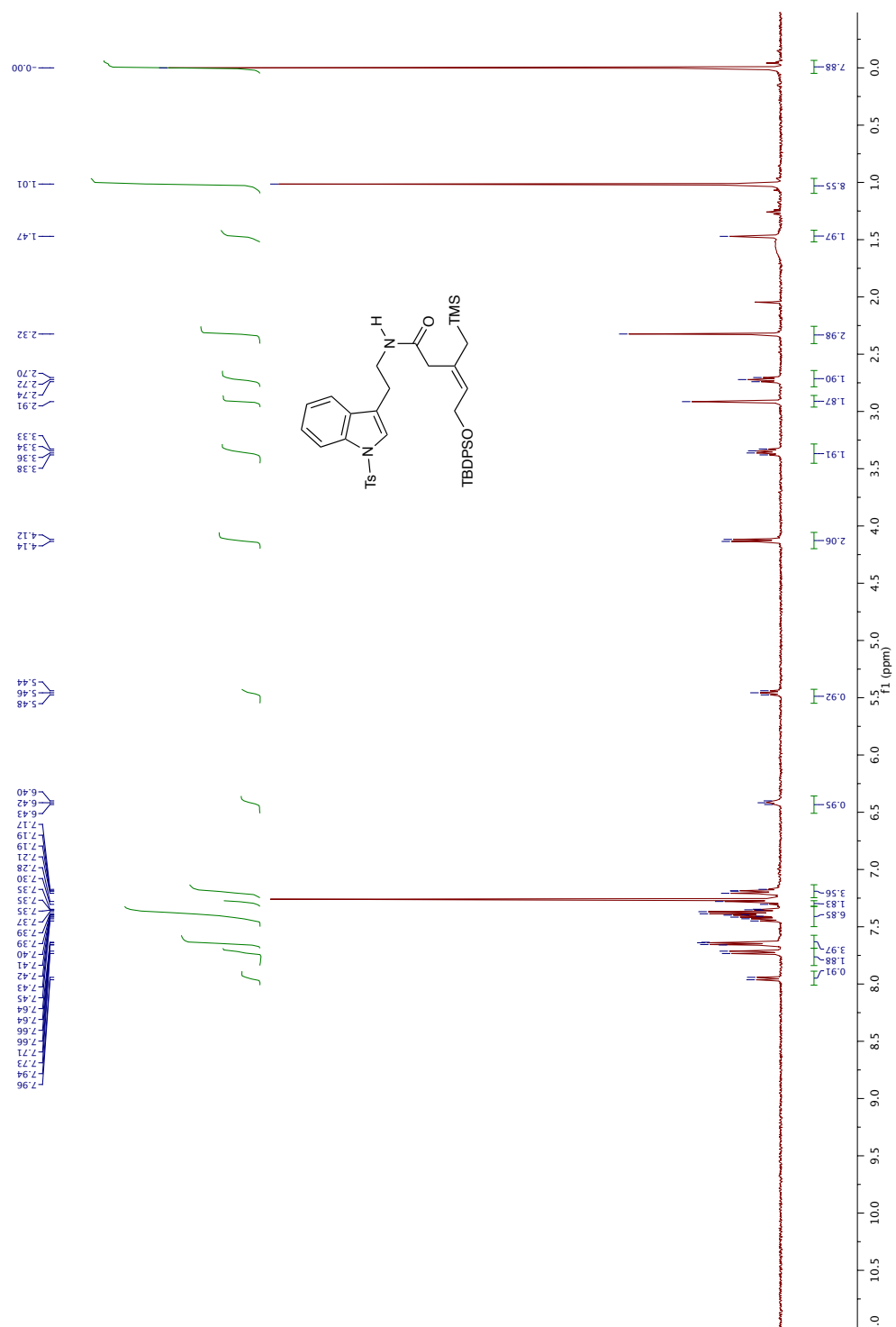
Hemiaminal Ether 2.62: ^1H NMR (600 MHz, CDCl_3)

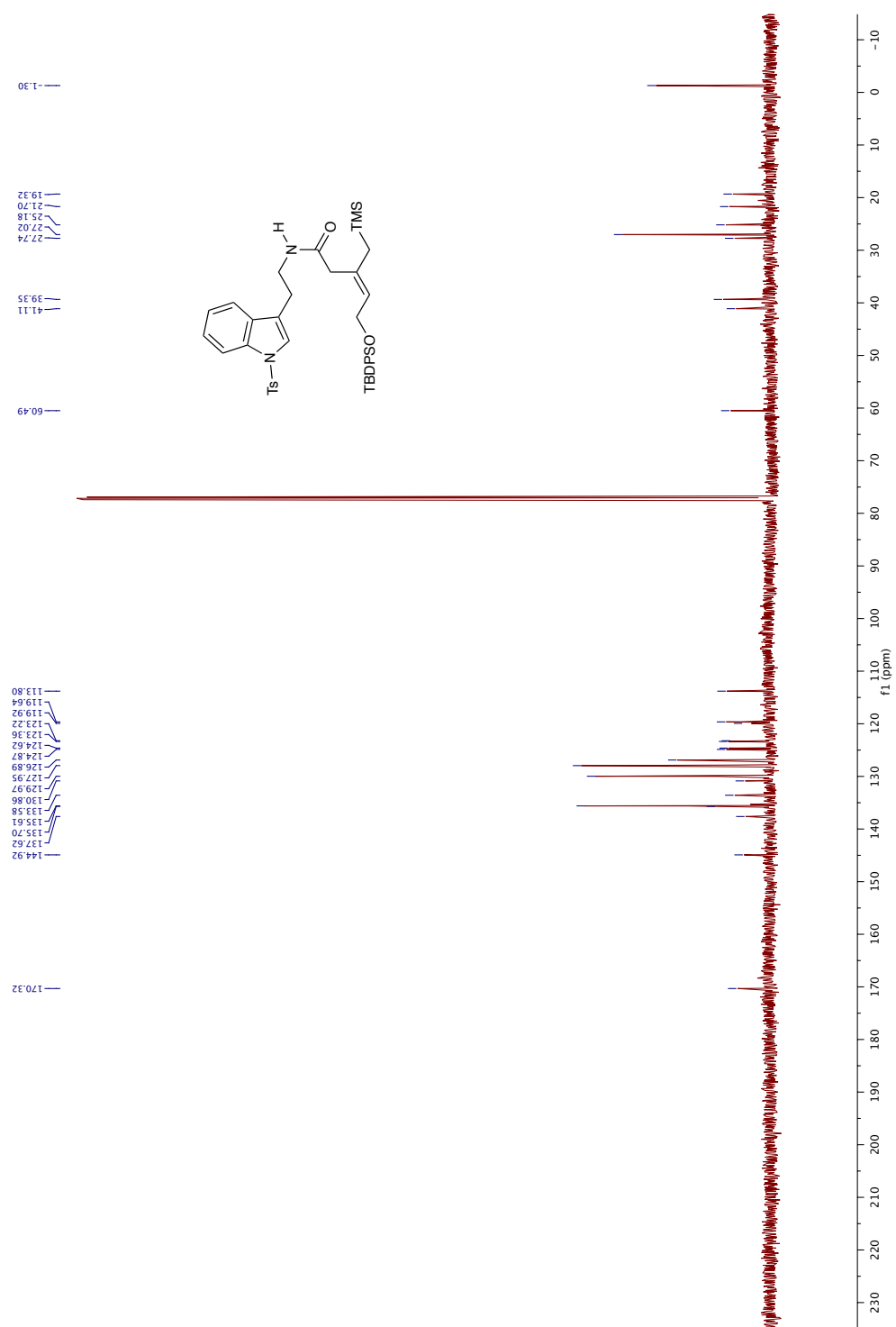
Hemiaminal Ether 2.62: ^{13}C NMR (126 MHz, CDCl_3)

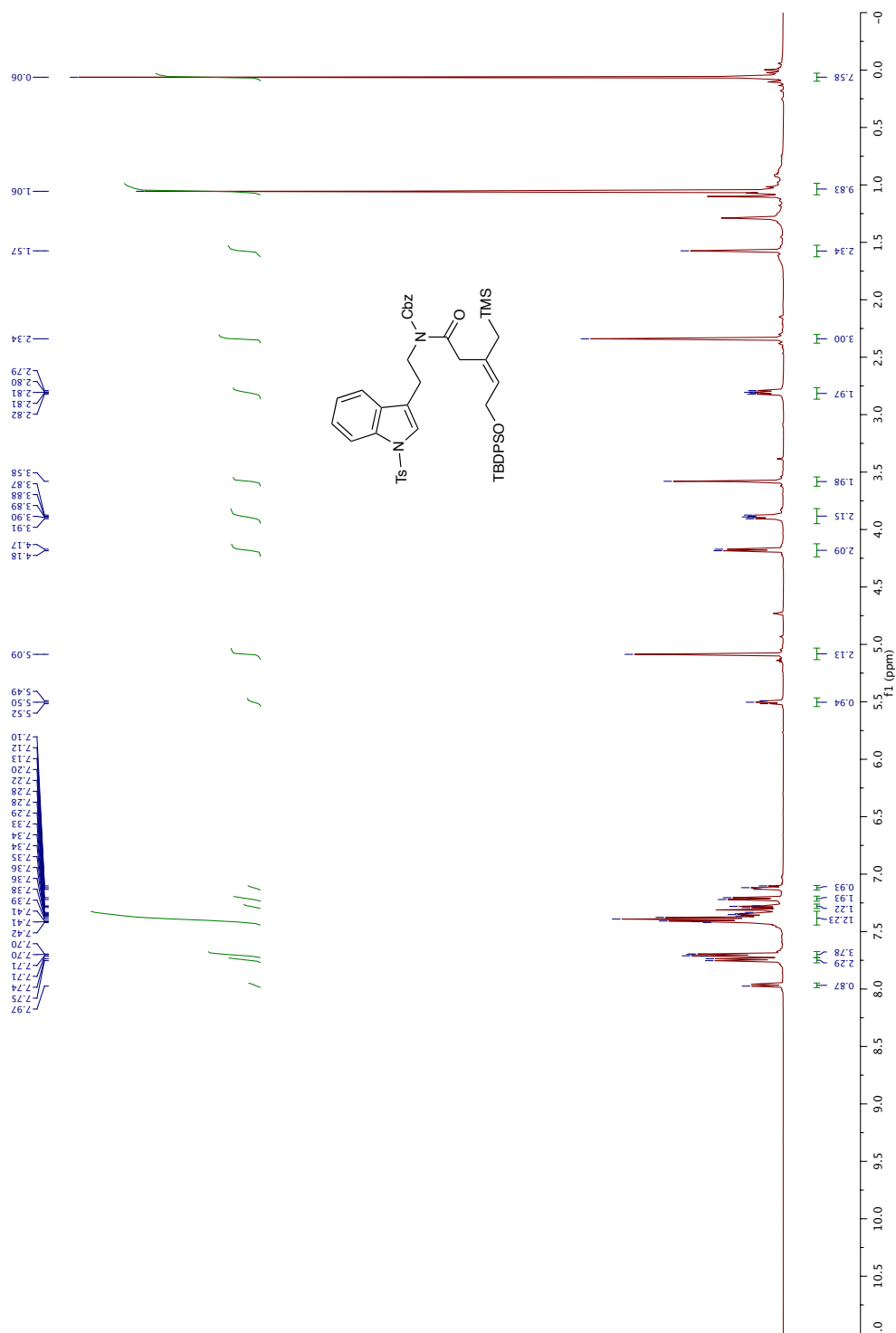
Tetracycle 2.63: ^1H NMR (600 MHz, CDCl_3 , 23 °C)

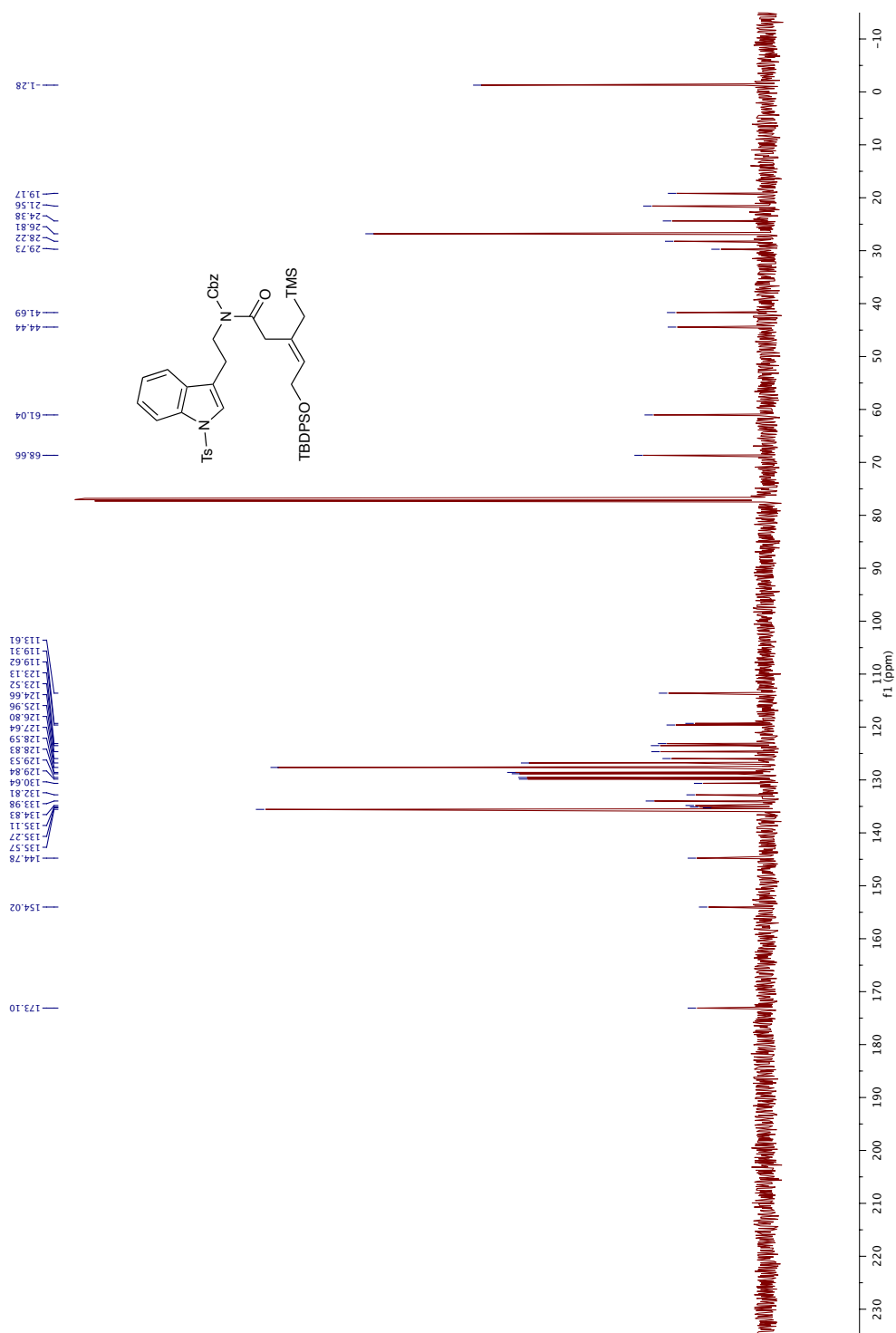
Tetracycle 2.63: ^1H NMR (600 MHz, d_6 -DMSO, 80 °C)

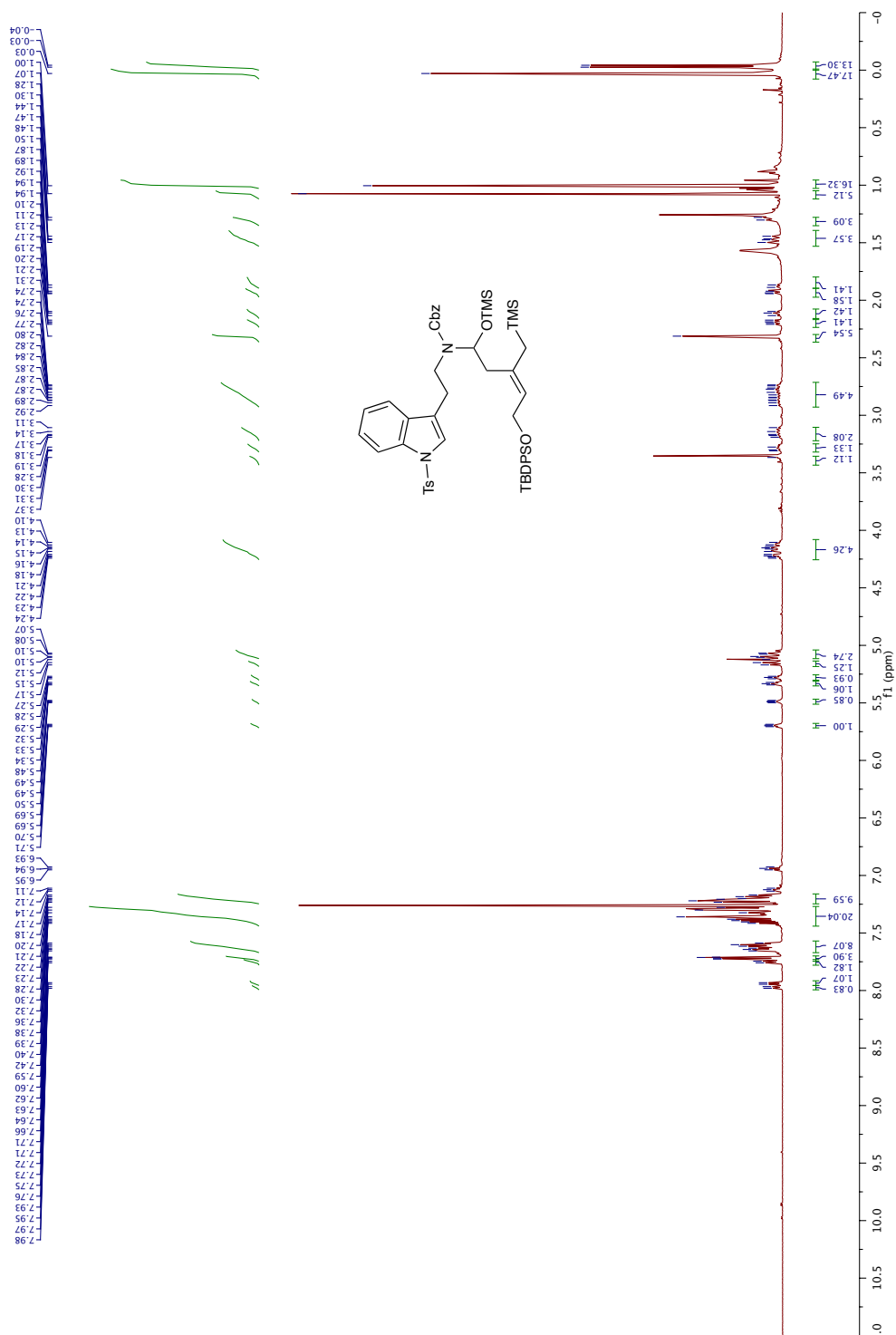
Tetracycle 2.63: ^{13}C NMR (126 MHz, CDCl_3)

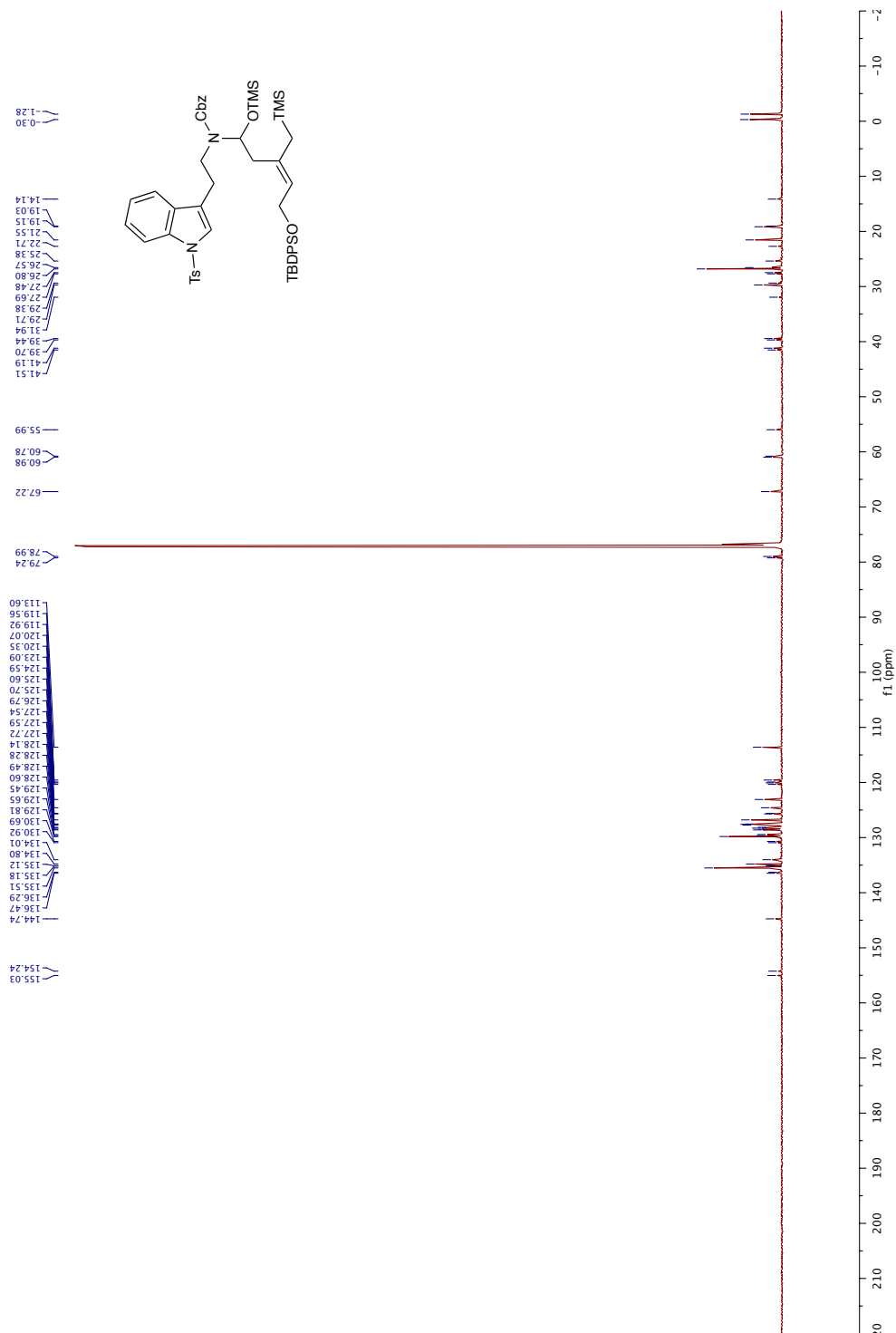
Amide 2.68: ^1H NMR (400 MHz, CDCl_3)

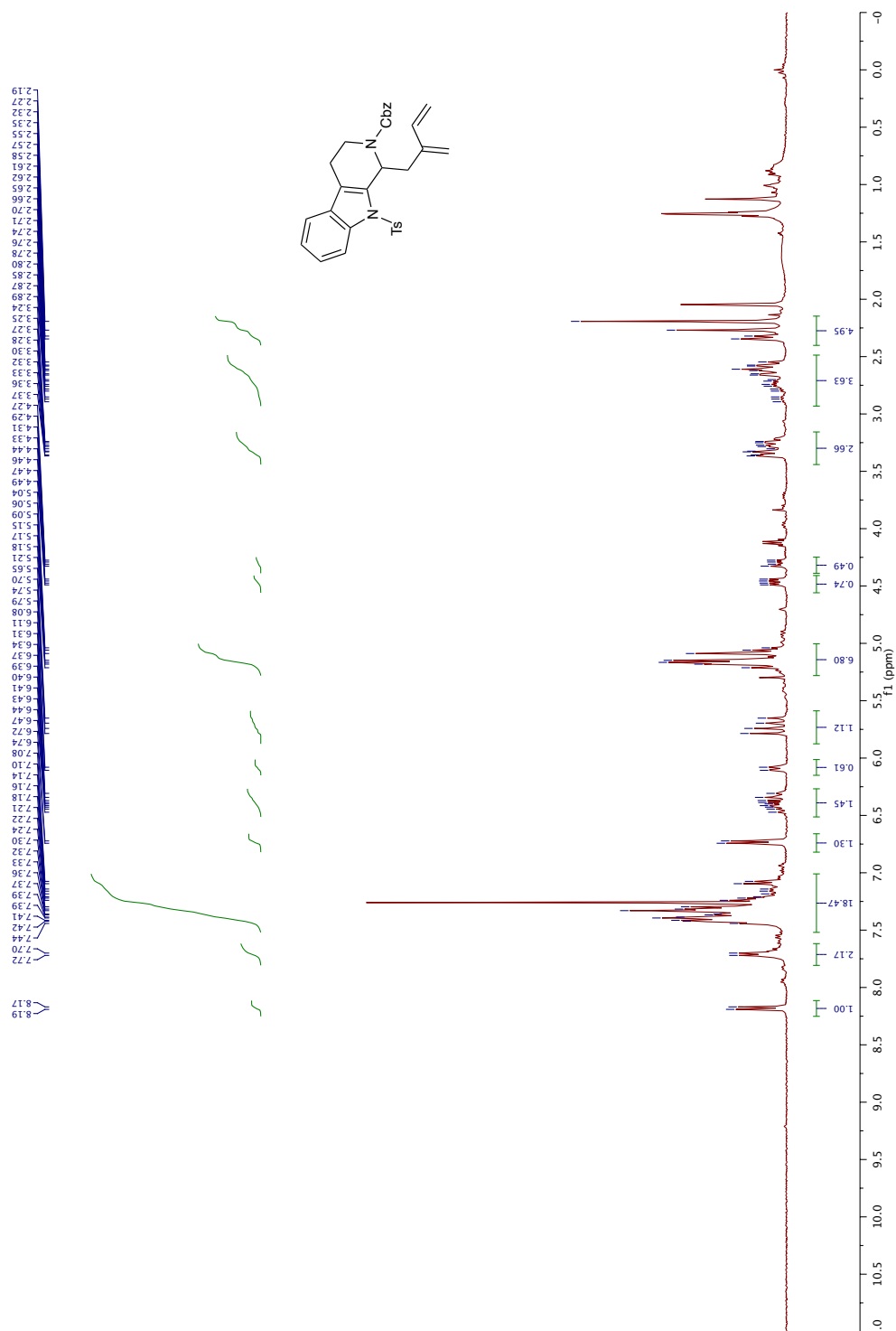
Amide 2.68: ^{13}C NMR (126 MHz, CDCl_3)

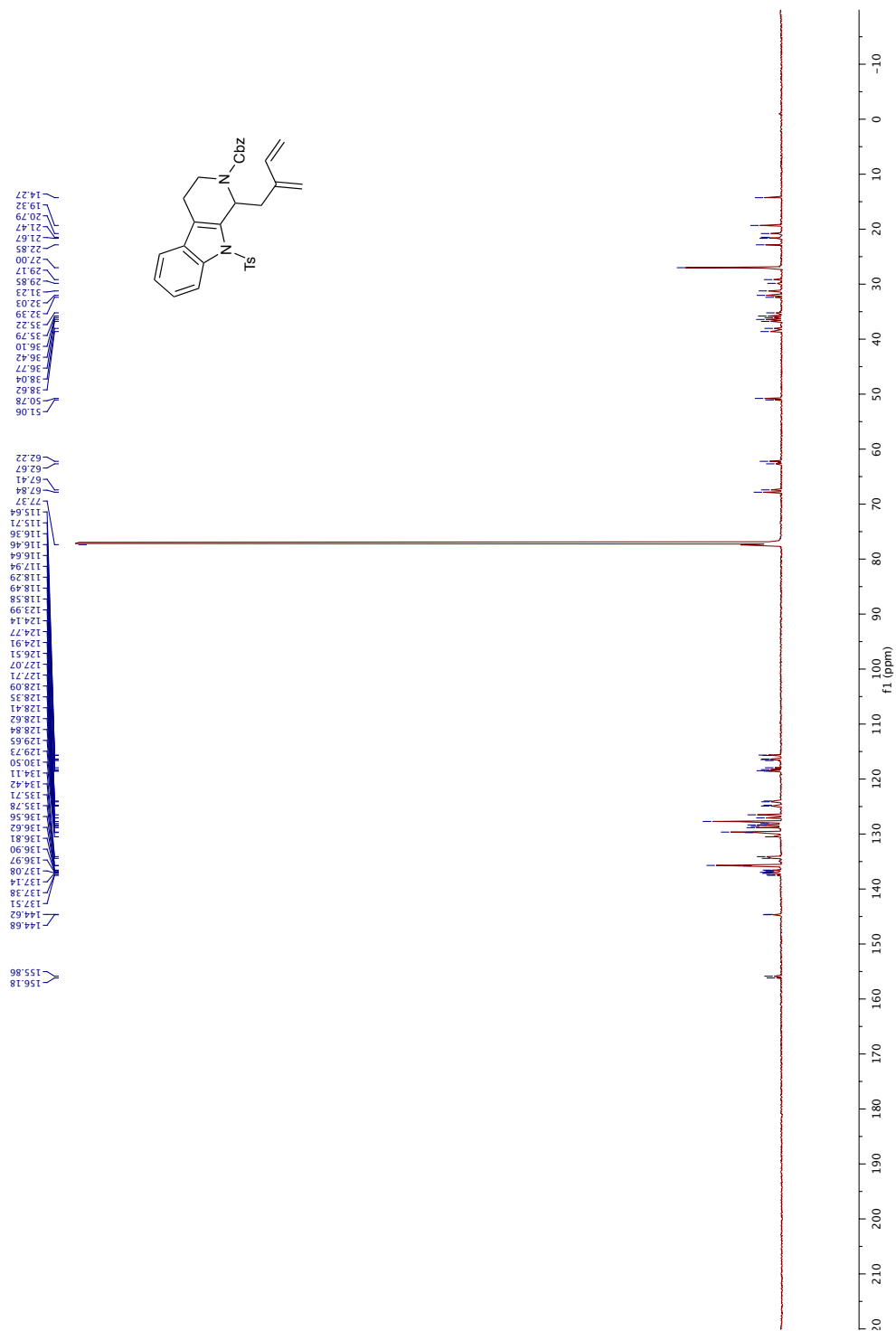
Cbz-Amide 2.69: ¹H NMR (500 MHz, CDCl₃)

Cbz-Amide 2.69: ^{13}C NMR (126 MHz, CDCl_3)

Hemiaminal Ether 2.70: ^1H NMR (600 MHz, CDCl_3)

Hemiaminal Ether 2.70: ^1H NMR (151 MHz, CDCl_3)

Diene 2.71: ^1H NMR (400 MHz, CDCl_3)

Diene 2.71: ^{13}C NMR (151 MHz, CDCl_3)

X-Ray Crystallography Data for Tetracycline 2.63:

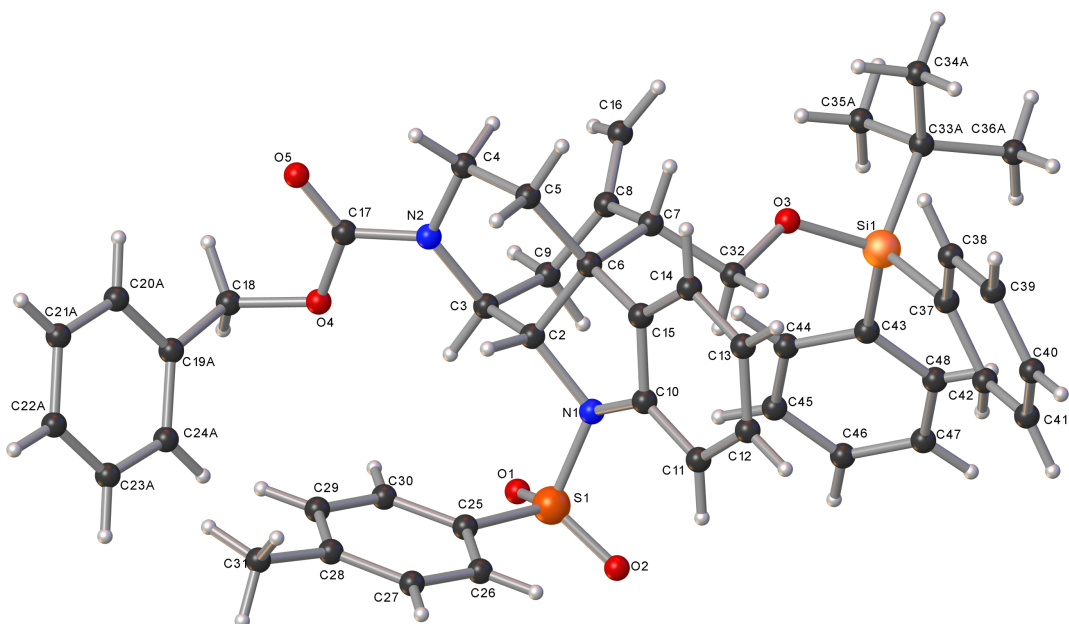


Table 1. Crystal data and structure refinement for ESA9613

Identification code	ESA9613
Empirical formula	C ₄₇ H ₅₀ N ₂ O ₅ SSi
Formula weight	783.04
Temperature/K	110(2)
Crystal system	monoclinic
Space group	C2/c
a/Å	16.0823(17)
b/Å	18.0956(19)
c/Å	28.619(3)
α/°	90
β/°	97.4057(16)
γ/°	90
Volume/Å ³	8259.2(15)
Z	8
ρ _{calc} /mg/mm ³	1.259
m/mm ⁻¹	0.156
F(000)	3328.0
Crystal size/mm ³	0.797 × 0.483 × 0.355
Radiation	MoKα (λ = 0.71073)
2θ range for data collection	3.404 to 54.206°
Index ranges	-20 ≤ h ≤ 20, -23 ≤ k ≤ 23, -36 ≤ l ≤ 36
Reflections collected	36451
Independent reflections	9120[R(int) = 0.0412]
Data/restraints/parameters	9120/318/601
Goodness-of-fit on F ²	1.155
Final R indexes [I ≥ 2σ(I)]	R ₁ = 0.0684, wR ₂ = 0.1326
Final R indexes [all data]	R ₁ = 0.0941, wR ₂ = 0.1526
Largest diff. peak/hole / e ⁻³	0.49/-0.38

Table 2. Fractional Atomic Coordinates ($\times 10^4$) and Equivalent Isotropic Displacement Parameters ($\text{\AA}^2 \times 10^3$) for ESA9613. U_{eq} is defined as 1/3 of the trace of the orthogonalised U_{ij} tensor.

Atom	x	y	z	U_{eq}
C18	6559(2)	6214.5(15)	4433.1(10)	38.4(7)
C19A	6893(7)	6381(8)	4939.3(19)	35.5(8)
C20A	6288(6)	6418(7)	5244(3)	43.0(12)
C21A	6519(7)	6598(7)	5713(3)	58.4(16)
C22A	7350(7)	6743(9)	5885(3)	55.7(17)
C23A	7942(7)	6706(11)	5587(4)	47.8(9)
C24A	7723(7)	6528(11)	5118(4)	37.5(13)
C19B	6840(4)	6308(4)	4952.6(13)	35.5(8)
C20B	6386(3)	6057(4)	5302.5(16)	43.0(12)
C21B	6691(3)	6172(4)	5771.9(17)	58.4(16)
C22B	7459(4)	6517(4)	5897.5(19)	55.7(17)
C23B	7912(4)	6746(5)	5556(2)	47.8(9)
C24B	7612(3)	6647(4)	5085.5(19)	37.5(13)
C37	8261(19)	914(8)	2721(6)	32.8(10)
C38	7869(5)	427(4)	2987(3)	51.3(16)
C39	8319(5)	-150(4)	3225(3)	69(2)
C40	9165(12)	-245(10)	3197(5)	58.4(19)
C41	9557(4)	265(4)	2921(2)	48.0(16)
C42	9104(4)	833(3)	2687(2)	37.2(13)
C37'	8227(18)	905(8)	2736(5)	32.8(10)
C38'	8021(4)	159(3)	2720(2)	43.0(13)
C39'	8528(5)	-384(4)	2948(3)	52.7(14)
C40'	9286(10)	-170(10)	3207(5)	55.4(19)
C41'	9505(4)	526(4)	3254(3)	51.4(15)
C42'	9001(4)	1068(4)	3014(2)	44.6(14)
C33A	6684(3)	1464(4)	1993.5(19)	39.4(9)
C34A	6028(5)	1023(5)	2212(3)	63.8(18)
C35A	6297(5)	2207(4)	1809(3)	44.7(15)
C36A	6968(6)	1028(5)	1581(3)	51.4(18)
C33B	6733(5)	1365(7)	1989(3)	39.4(9)
C34B	6267(9)	696(8)	2148(5)	63.8(18)
C35B	6089(8)	1993(7)	1865(6)	44.7(15)
C36B	7131(13)	1164(11)	1545(6)	51.4(18)
Si1	7593.5(5)	1695.0(4)	2454.3(3)	29.87(17)
C2	7632.0(14)	3527.0(13)	4206.7(8)	22.1(5)
C3	7214.3(15)	4187.3(13)	3944.6(8)	23.7(5)
C4	5860.5(16)	3658.4(15)	4198.6(10)	30.2(6)
C5	6322.2(15)	2942.2(14)	4352.3(9)	26.5(5)
C6	7100.0(14)	2832.2(13)	4102.7(8)	22.8(5)
C7	6839.4(15)	2682.5(14)	3565.0(9)	26.4(5)
C8	6530.5(16)	3370.4(15)	3292.8(9)	28.6(5)
C9	7044.9(16)	4057.3(14)	3414.3(9)	26.7(5)
C10	8533.9(15)	2524.8(14)	4287.1(8)	25.4(5)
C11	9225.4(16)	2066.0(15)	4385.5(9)	30.4(6)
C12	9084.0(17)	1334.8(15)	4509.9(10)	33.5(6)
C13	8285.8(17)	1072.2(15)	4536.3(10)	32.5(6)
C14	7596.6(16)	1536.9(14)	4431.0(9)	27.8(5)
C15	7724.5(15)	2260.1(13)	4303.8(8)	23.9(5)
C16	5875.4(19)	3364.7(17)	2965.1(11)	38.2(7)
C17	6189.3(16)	4948.5(15)	4316.8(9)	29.8(6)
C25	9288.5(15)	4149.1(14)	4817.8(9)	27.1(5)
C26	9761.7(16)	3747.1(15)	5173.1(10)	32.8(6)
C27	9732.9(17)	3949.9(16)	5637.5(10)	36.0(6)
C28	9236.3(18)	4526.8(16)	5756.2(10)	34.6(6)
C29	8782.4(18)	4929.3(15)	5394.6(10)	33.4(6)
C30	8805.4(16)	4742.8(14)	4925.4(9)	29.7(6)
C31	9164(2)	4716.2(19)	6262.3(10)	45.9(8)
C32	7512.9(16)	2312.3(16)	3313.7(9)	31.3(6)
C43	8307.6(18)	2377.6(16)	2220.6(10)	35.4(6)
C44	8249(2)	3128.5(17)	2318.5(10)	42.0(7)
C45	8786(2)	3636.5(18)	2153.7(12)	49.6(8)
C46	9392(2)	3407(2)	1888.7(13)	56.3(9)
C47	9447(3)	2675(2)	1774.1(16)	66.2(11)
C48	8920(2)	2171(2)	1940.0(15)	58.2(10)
N1	8483.8(12)	3279.2(11)	4117.8(7)	24.2(4)
N2	6433.8(13)	4287.1(12)	4162.0(8)	28.0(5)

O1	9029.9(11)	4497(1)	3934.8(6)	30.9(4)
O2	10016.4(11)	3478.0(11)	4178.3(7)	36.2(5)
O3	7117.2(12)	2092.2(11)	2859.8(6)	35.4(4)
O4	6769.0(12)	5484.3(10)	4274.3(7)	34.0(4)
O5	5540.8(12)	5058.0(11)	4477.5(7)	39.4(5)
S1	9266.9(4)	3873.8(4)	4228.1(2)	26.98(15)

Table 3. Bond Lengths for ESA9613.

Atom	Atom	Length/Å	Atom	Atom	Length/Å
C18	C19A	1.509(5)	C2	N1	1.494(3)
C18	C19B	1.507(4)	C3	C9	1.525(3)
C18	O4	1.451(3)	C3	N2	1.482(3)
C19A	C20A	1.390(6)	C4	C5	1.530(4)
C19A	C24A	1.393(6)	C4	N2	1.477(3)
C20A	C21A	1.385(6)	C5	C6	1.531(3)
C21A	C22A	1.388(7)	C6	C7	1.565(3)
C22A	C23A	1.358(7)	C6	C15	1.504(3)
C23A	C24A	1.381(6)	C7	C8	1.518(4)
C19B	C20B	1.389(5)	C7	C32	1.530(4)
C19B	C24B	1.393(5)	C8	C9	1.509(4)
C20B	C21B	1.385(5)	C8	C16	1.317(4)
C21B	C22B	1.388(6)	C10	C11	1.387(3)
C22B	C23B	1.358(6)	C10	C15	1.394(3)
C23B	C24B	1.381(5)	C10	N1	1.447(3)
C37	C38	1.37(3)	C11	C12	1.396(4)
C37	C42	1.38(3)	C12	C13	1.380(4)
C37	Si1	1.877(4)	C13	C14	1.393(4)
C38	C39	1.397(10)	C14	C15	1.381(3)
C39	C40	1.38(2)	C17	N2	1.352(3)
C40	C41	1.41(2)	C17	O4	1.361(3)
C41	C42	1.382(9)	C17	O5	1.209(3)
C37'	C38'	1.39(2)	C25	C26	1.394(4)
C37'	C42'	1.42(2)	C25	C30	1.383(4)
C37'	Si1	1.877(4)	C25	S1	1.756(3)
C38'	C39'	1.386(9)	C26	C27	1.385(4)
C39'	C40'	1.398(16)	C27	C28	1.383(4)
C40'	C41'	1.309(17)	C28	C29	1.393(4)
C41'	C42'	1.396(8)	C28	C31	1.508(4)
C33A	C34A	1.521(6)	C29	C30	1.390(4)
C33A	C35A	1.545(5)	C32	O3	1.428(3)
C33A	C36A	1.538(5)	C43	C44	1.393(4)
C33A	Si1	1.886(3)	C43	C48	1.399(4)
C33B	C34B	1.524(7)	C44	C45	1.385(5)
C33B	C35B	1.547(6)	C45	C46	1.374(5)
C33B	C36B	1.541(6)	C46	C47	1.370(5)
C33B	Si1	1.889(4)	C47	C48	1.372(5)
Si1	C43	1.868(3)	N1	S1	1.656(2)
Si1	O3	1.637(2)	O1	S1	1.4279(19)
C2	C3	1.520(3)	O2	S1	1.4249(19)
C2	C6	1.528(3)			

2.10 References

1. Ramanitrahassimbola, D.; Rasoanaivo, P.; Ratsimamanga, S.; Vial, H., Malagashanine Potentiates Chloroquine Antimalarial Activity In Drug Resistant Plasmodium Malaria by Modifying Both Its Efflux and Influx. *Molecular and Biochemical Parasitology* **2006**, *146*, 58-67.
2. Delgado, R. Development of a Novel Cascade Cyclization Reaction and its Application Towards the Synthesis of Malagashanine: A Chloroquine Efflux Inhibitor. Emory University, 2010.
3. Suh, Y.-G.; Shin, D.-Y.; Jung, J.-K.; Kim, S.-H., The Versatile Conversion of Acyclic Amides to Alpha-alkylated Amines. *Chemical Communications* **2002**, 1064-1065.
4. Delgado, R.; Blakey, S. B., Cascade Annulation Reactions To Access the Structural Cores of Stereochemically Unusual Strychnos Alkaloids. *European Journal of Organic Chemistry* **2009**, 1506-1510.
5. Kong, A.; Mancheno, D. E.; Boudet, N.; Delgado, R.; Andreansky, E. S.; Blakey, S. B., Total Synthesis of Malagashanine: A Chloroquine Potentiating Indole Alkaloid with Unusual Stereochemistry. *Chemical Science* **2017**, *8*, 697-700.
6. Kuang, Y.; Huang, J.; Chen, F., Practical and Phase Transfer-Catalyzed Synthesis of 6-Methoxytryptamine. *Synthetic Communications* **2006**, *36*, 1515-1519.
7. Liu, X.; Ready, J. M., Directed Hydrozirconation of Homopropargylic Alcohols. *Tetrahedron* **2008**, *64*, 6955-6960.
8. Duchene, A.; Abarbri, M.; Parrain, J.-L.; Kitamura, M.; Nyori, R., Synthesis of 3-Substituted But-3-enoic Acids via Palladium Catalyzed Cross-Coupling Reaction of 3-Iodobut-3-enoic Acid with Organometallic Reagents. *Synlett* **1994**, 524-526.
9. Kuwano, R.; Kashiwabara, M.; Sato, K.; Ito, T.; Kaneda, K.; Ito, Y., Catalytic Asymmetric Hydrogenation of Indoles Using a Rhodium Complex with a Chiral Bisphosphine Ligand PhTRAP. *Tetrahedron: Asymmetry* **2006**, *17*, 521-535.
10. Corey, E. J.; Katzenellenbogen, J. A.; Posner, G. H., New Stereospecific Synthesis of Trisubstituted Olefins. Stereospecific Synthesis of Farnesol. *Journal of the American Chemical Society* **1967**, *89*, 4245-4247.
11. Robak, M. T.; Herbage, M. A.; Ellman, J. A., Synthesis and Application of tert-Butanesulfinamide. *Chemical Reviews* **2010**, *110*, 3600-3740.
12. Brun, S.; Parera, M.; Pla-Quintana, A.; Roglans, A.; Leon, T.; Achard, T.; Sola, J.; Verdaguer, X.; Riera, A., Chiral N-Phosphino Sulfinamide Ligands in Rhodium(I)-Catalyzed [2+2+2] Cycloaddition Reactions. *Tetrahedron* **2010**, *66*, 9032-9040.
13. Brak, K.; Jacobsen, E. N., Asymmetric Ion-Pairing Catalysis. *Angewandte Chemie International Edition* **2013**, *52*, 534-561.
14. Sewgobind, N. V.; Wanner, M. J.; Ingemann, S.; Gelder, R. d.; Maarseveen, J. H. v.; Hiemstra, H., Enantioselective BINOL-Phosphoric Acid Catalyzed Pictet-Spengler Reactions of N-Benzyltryptamine. *The Journal of Organic Chemistry* **2008**, *73*, 6405-6408.
15. Raheem, I. T.; Thiara, P. S.; Peterson, E. A.; Jacobsen, E. N., Enantioselective Pictet-Spengler-Type Cyclizations of Hydroxylactams: H-Bond Donor Catalysis by Anion Binding. *Journal of the American Chemical Society* **2007**, *129*, 13404-13405.
16. Kong, A. Synthetic Studies for Heterocycle Synthesis. Part I: Intra/intermolecular Olefin Diamination for the Stereoselective Synthesis of 3-Aminopiperidines Part II: Total Synthesis of Malagashanine and Synthetic Studies Toward Related Alkaloids. Emory University, 2014.
17. James, T.; Gemmeren, M. v.; List, B., Development and Applications of Disulfonimides in Enantioselective Organocatalysis. *Chemical Reviews* **2015**, *115*, 9388-9409.
18. Nakashina, D.; Yamamoto, H., Design of Chiral N-Triflyl Phosphoramidate as a Strong Chiral Bronsted Acid and Its Application to Asymmetric Diels-Alder Reaction. *Journal of the American Chemical Society* **2006**, *128*, 9626-9627.

19. Garcia-Garcia, P.; Lay, F.; Garcia-Carcia, P.; Rabalakos, C.; List, B., A Powerful Chiral Counteranion Motif for Asymmetric Catalysis. *Angewandte Chemie International Edition* **2009**, *48*, 4363-4366.
20. Hamilton, G. L.; Kanai, T.; Tost, F. D., Chiral Anion-Mediated Asymmetric Ring Opening of Meso-Aziridinium and Episulfonium Ions. *Journal of the American Chemical Society* **2008**, *130*.
21. Hamilton, G. L.; Kang, E. J.; Mba, M.; Toste, F. D., A Powerful Chiral Counterion Strategy for Asymmetric Transition Metal Catalysis. *Science* **2007**, *317*, 496-499.
22. Bandarage, U. K.; Simpson, J.; Smith, R. A. J.; Weavers, R. T., Conformation Polymorphism and Thermorearrangement of 2,2'-bis-O-(N,N-dimethylthiocarbamate)-1,1'-Binaphthalene. A Facile Synthesis of 1,1'-Binaphthalene-2,2'-dithiol. *Tetrahedron* **1994**, *50*, 3463-3472.
23. Cossu, S.; Lucchi, O. D.; Fabbri, D.; Valle, G.; Painter, G. F.; Smith, R. A. J., Synthesis of Structurally Modified Atropisomeric Biaryl Dithiols. Observations on the Newman-Kwart Rearrangement. *Tetrahedron* **1997**, *53*, 6073-6084.
24. Knoppe, S.; Azoulay, R.; Dass, A.; Burgi, T., In Situ Reaction Monitoring Reveals a Diastereoselective Ligand Exchange Reactions Between the Intrinsically Chiral Au₃₈(SR)₂₄ and Chiral Thiols. *Journal of the American Chemical Society* **2012**, *134*, 20302-20305.
25. He, H.; Chen, L.-Y.; Wong, W.-Y.; Chan, W.-H.; Lee, A. W. M., Practical Synthetic Approach to Chiral Sulfonimides (CSIs) - Chiral Brønsted Acids for Organocatalysis. *European Journal of Organic Chemistry* **2010**, 4181-4184.
26. Mathews, C. J.; Smith, P. J.; Welton, T., Novel Palladium Imidazole Catalysts for Suzuki Cross-Coupling Reactions. *Journal of Molecular Catalysis A: Chemical* **2003**, *206*, 77-82.
27. Frigerio, M.; Santagostino, M.; Sputore, S., A User-Friendly Entry to 2-Iodoxybenzoic Acid. *The Journal of Organic Chemistry* **1999**, *64*, 4537-4538.
28. Ireland, R. E.; Liu, L., An Improved Procedure for the Preparation of the Dess-Martin Periodinane. *The Journal of Organic Chemistry* **1993**, *58*, 2899.
29. Roy, S.; Haque, S.; Gribble, G. W., Synthesis of Novel Oxazolyl-indoles. **2006**, *Synthesis*, 3948-3954.

Chapter 3. Synthetic Studies Toward Methanoquinolizidine-Containing Akuammiline Alkaloids

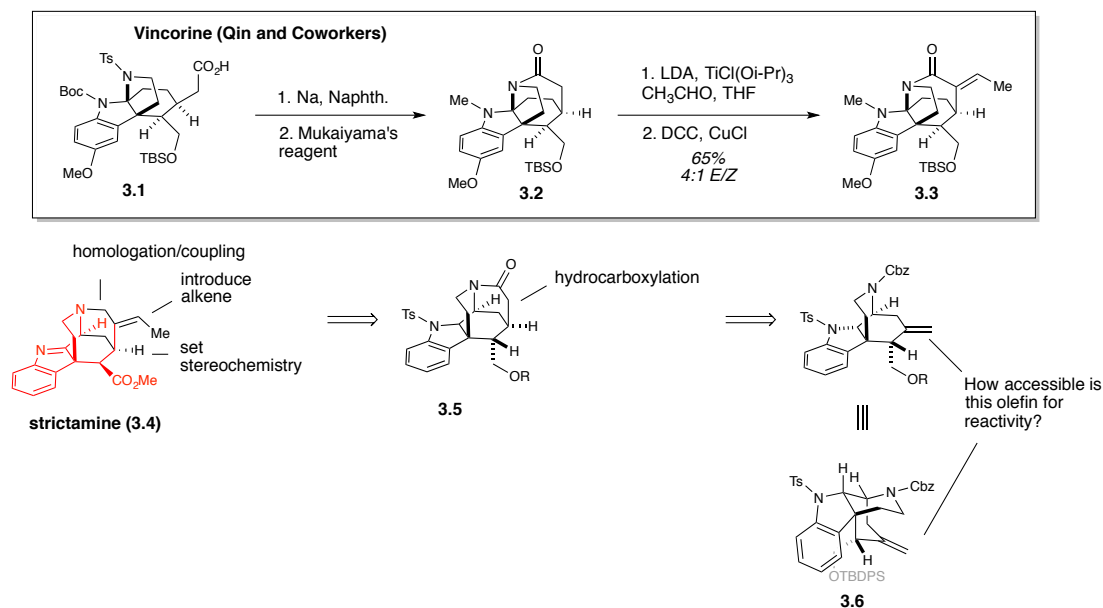
Upon access to a tetracyclic core for the akuammiline alkaloids, we set out to develop a synthetic route, starting from such an intermediate, to successfully access an unsynthesized member of this alkaloid family. We set our initial sights on strictamine, arguably the simplest of the methanoquinolizidine-containing akuammiline alkaloids that had not been synthesized at that time. Upon the examination of our tetracycle compared to that of the desired natural products, these structures lacked the E ring necessary to furnish the methanoquinolizidine core present in these natural products. Therefore, much of the discussion in this section will center on the exploration of possible methods to furnish this E-ring structure.

3.1 Initial Strategy: Homologation of Exocyclic Olefin and Lactamization

Examination of our tetracyclic core synthesized from our previously developed cascade reveals how our structure maps onto the structure of the natural product strictamine (**3.4**) (**Scheme 3-1**). Beyond the required functional group manipulations and oxidations required on the western half of the molecule, the main structural challenge was the synthesis of the E ring. Mapping the structure of our core onto strictamine reveals that tetracycle **3.6** contains at this point all of the carbons, except for one, of a methanoquinolizidine core. Therefore, a one carbon homologation on the terminal end of the olefin, preferably containing functionality to enable E ring closure, would be necessary, in addition to introduction of a C15 stereocenter via reduction. Both transformations could occur via a formal hydrocarboxylation across the alkene. The introduction of a carboxylic

acid functionality was desired both for its ability to provide ring closure via lactamization (**3.5**), as well as providing a functional handle for introduction of the alkene via an aldol condensation in subsequent steps. Indeed, this approach parallels that used in the synthesis of vincorine by Yong Qin and coworkers, where they closed the final ring in the natural product by lactamization (**3.2**), and then introduced the exocyclic olefin **3.3** by aldol condensation with acetaldehyde followed by *syn* elimination with DCC and CuCl.¹

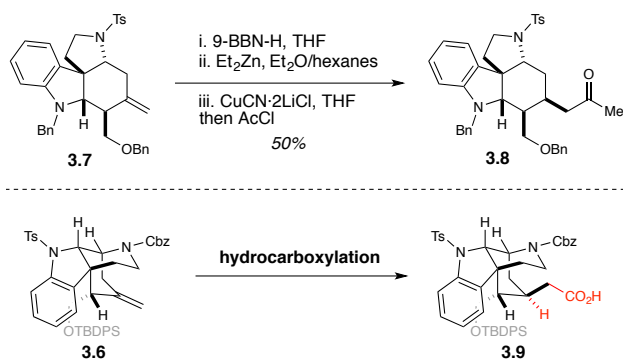
Scheme 3-1. Initial retrosynthetic analysis for the synthesis of the methanoquinolizidine core of strictamine via a hydrocarboxylation strategy.¹



A similar approach was used in our group's synthesis of malagashanine (**Scheme 3-2**),² where we performed a formal hydroacylation on the exocyclic olefin of the malagashanine core **3.7** using methodology developed by Paul Knochel and coworkers.³ Initial hydroboration of the exocyclic olefin with 9-BBN-H provided the terminal organoborane. Sequential transmetalation of this organoborane with zinc followed by copper provided an organocuprate intermediate that readily reacted with acetyl chloride to

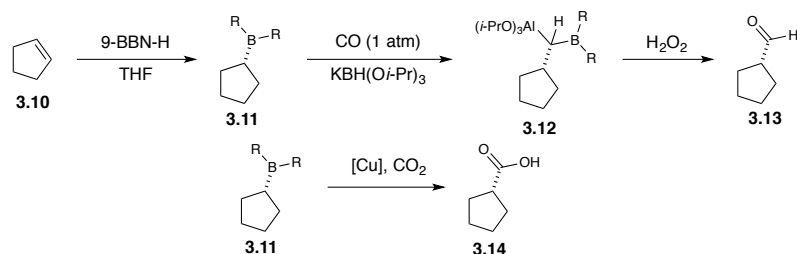
provide methyl ketone **3.8** as a 2:1 mixture of C15 diastereomers, with 50% yield of the desired isomer being obtained.

Scheme 3-2. Formal hydroacylation used in the total synthesis of malagashanine,² and the proposed formal hydrocarboxylation strategy on akuammiline core 3.6.



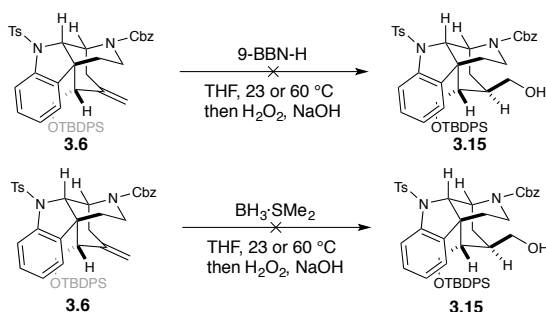
The desired product from our reaction sequence is a carboxylic acid **3.9**, not a ketone, and therefore a modified approach would be required for our desired reactivity. Danny Mancheno had attempted to adapt the above conditions for the formation of an ester intermediate by reacting the intermediate organocuprate with a chloroformate, but did not get successful reactivity.⁴ However, organoborane intermediates **3.11** are known to react with carbon monoxide, providing a proposed acylborane intermediate that can be trapped with a reductant (**3.12**) and subsequently quenched with oxidant to provide aldehydes **3.13** (Scheme 3-3).⁵ Additionally, organoboranes are known to react with carbon dioxide, providing carboxylic acids **3.14**, under transition metal catalysis.⁶ These approach appeared attractive because it provided us a product directly in useable oxidation states, as we as being operationally simpler than the multistep formal hydroacylation protocol previously used.

Scheme 3-3. Reaction of organoboranes to form aldehydes and carboxylic acids.⁴⁻⁵



Therefore, we were highly interested in the possibility of using such a route, as it would provide a very succinct and direct method for the synthesis of the E ring. Before advancing toward a more complicated homologation protocol, we wished to examine simple hydroboration/oxidation of our substrate **3.6** to alcohol **3.15** (Scheme 3-4). Initial attempts at hydroboration with excess 9-BBN-H proved unsuccessful, even at higher temperatures. Even though there would be possible complications with the carbonylation protocol due to most successful cases involving alkyl-9-BBN derivatives, we wished to see if less sterically hindered borane dimethylsulfide would be able to add to our substrate. However, even the addition of this simple borane was found not to occur.

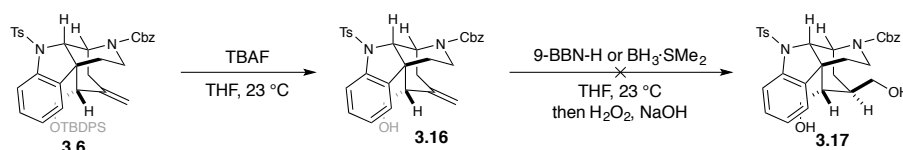
Scheme 3-4. Unsuccessful attempts at hydroboration of akuammiline core 3.6 with 9-BBN-H and less sterically hindered $\text{BH}_3\cdot\text{SMe}_2$.



We hypothesized that the steric hindrance of the system, in particular the large TBDPS protecting group, was preventing successful addition to the exocyclic olefin, and

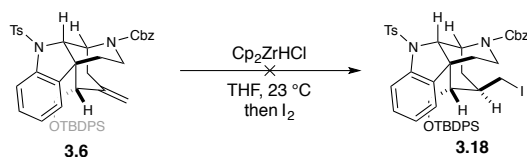
next examined the addition to deprotected homoallylic alcohol **3.17** (**Scheme 3-5**). Removal of the TBDPS protecting group on **3.6** proceeded readily with TBAF to provide homoallylic alcohol **3.17**. This species was next subjected to hydroboration with 9-BBN-H and borane dimethylsulfide, but neither of these boranes successfully added to the exocyclic olefin.

Scheme 3-5. Removal of TBDPS protecting group from akuammiline core 3.6, and subsequent attempts at hydroboration.



To see if another reagent that would provide anti-Markovnikov addition would react, we also attempted hydrozirconation with Schwartz reagent (**Scheme 3-6**). Organozirconocenes also known to undergo a similar carbonylation reaction with carbon monoxide, and the formed acylzirconocene can undergo oxidation to provide the desired carboxylic acid directly.⁷ However, when hydrozirconation followed by a quench with iodide was attempted on tetracycle **3.6**, no reaction was observed with our substrate. Due to the lack of success with our initial examination of an alkene addition approach, we examined other possible reactions with the exocyclic olefin, something which later informed our choices about synthetic strategy.

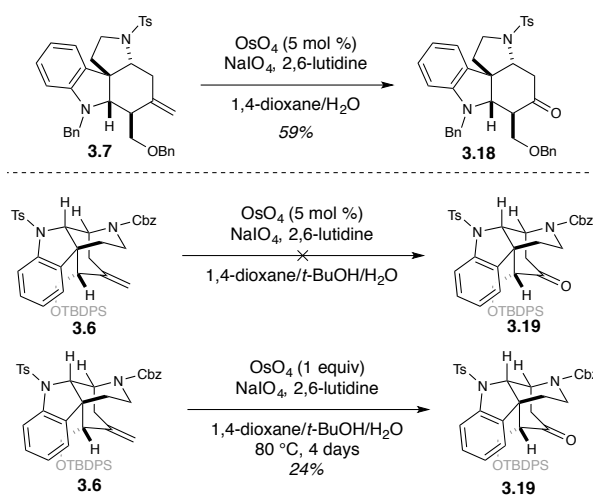
Scheme 3-6. Attempted hydrozirconation of alkene in akuammiline alkaloid substrate 3.6.



3.2 Ketone Addition/Deoxygenation Strategy for Synthesis of the E ring

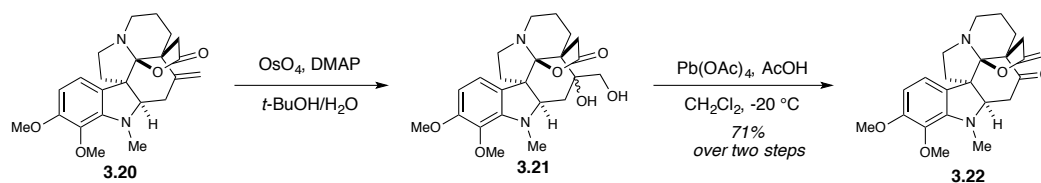
An alternative to alkene addition is oxidative cleavage, a reaction that would provide a ketone product with our substrate. While less desirable in respect to synthetic strategy, for we would be removing a carbon atom that would otherwise map onto a portion of the E ring of strictamine (**3.4**), the formed ketone **3.19** would still be present as a functional handle on C15, the important bridgehead junction between the E ring and the C ring. Oxidative cleavage was demonstrated in our previously developed malagashanine core **3.7**, where ketone **3.18** could be provided successfully under Johnson-Lemieux conditions (Scheme 3-7).⁸ Therefore, we initially set out to examine whether our akuammiline alkaloid core **3.6** could react under such conditions. Initial attempts at standard Johnson-Lemieux conditions with catalytic osmium tetroxide showed no reactivity. Using more forcing conditions with stoichiometric osmium showed some reactivity, but the desired ketone **3.19** was only observed in low yield at 80 °C over a period of four days.

Scheme 3-7. Successful Johnson-Lemieux oxidation of malagashanine core 3.7,⁸ and attempted oxidative cleavage of tetracycle 3.6.



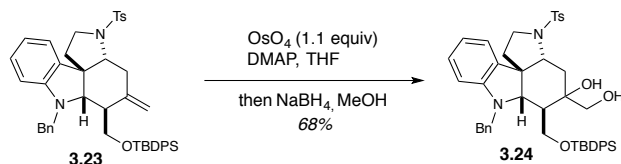
The lack of reactivity is not surprising, as sterically congested olefins can be difficult to successfully dihydroxylate, often allowing for selective olefin cleavage among several olefins in a complex substrate. A similar substrate caused problems in the synthesis of aspidophytine by E. J. Corey and coworkers, where standard Johnson-Lemieux or Upjohn reaction conditions were not found to successfully cleave or dihydroxylate the exocyclic olefin **3.20** (Scheme 3-8).⁹ They found in the course of these studies that adding electron-rich DMAP promoted osmium tetroxide addition to sterically hindered systems, and these reaction conditions, followed by cleavage of the formed diol **3.21** with $\text{Pb}(\text{OAc})_4$, provided their desired ketone **3.22**.

Scheme 3-8. Stepwise dihydroxylation/cleavage process of a sterically congested exocyclic olefin in the total synthesis of aspidophytine by E. J. Corey and coworkers.⁹



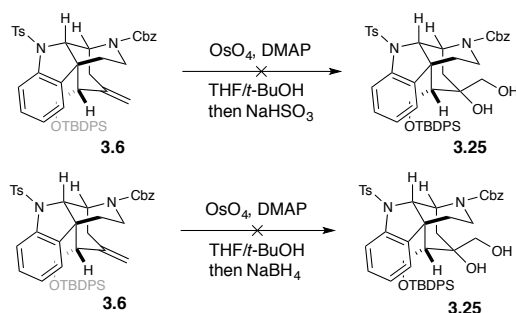
Similar problems with standard Johnson-Lemieux conditions occurred with the TBDPS protected variant of the malagashanine core **3.23** when attempting to synthesize ketone **3.24**, therefore requiring the use of the above disclosed conditions from Corey (Scheme 3-9).⁸ Interestingly, the steric congestion also made reductive cleavage of the osmate ester with sodium sulfite problematic, requiring instead the use of the stronger reductant sodium borohydride. Therefore, we wished to see if these differing conditions for dihydroxylation would work for our desired system.

Scheme 3-9. Application of dihydroxylation conditions containing DMAP to a TBDPS protected Malagasy alkaloid core **3.23**.⁸



Attempts to apply the conditions developed by Corey to our akuammiline alkaloid core **3.6** proved to be unsuccessful, providing mostly recovered starting material as well as a small quantity of what was believed to be the osmate ester that clung to the baseline in thin layer chromatography (**Scheme 3-10**). Additionally, using an alternative sodium borohydride quench also proved to be unsuccessful, providing similar results to what was seen before.

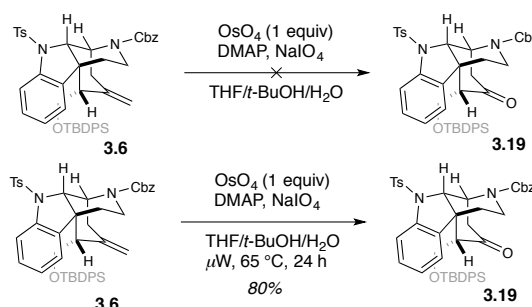
Scheme 3-10. Attempted dihydroxylation with OsO_4 /DMAP of exocyclic olefin in akuammiline alkaloid core **3.6**.



Osmate esters may either be cleaved reductively, as above, or oxidatively, as occurs in the Johnson-Lemieux reaction, allowing for the use of catalytic osmium tetroxide under typical reaction conditions. To examine if our osmate ester would more readily cleave under oxidative conditions, we reexamined the Johnson-Lemieux conditions, but this time using DMAP as the amine additive (**Scheme 3-11**). No reactivity was observed under

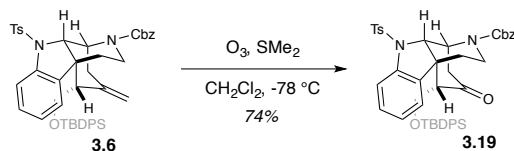
standard conditions at room temperature, as was seen in our prior examples, but surprisingly, synthetically useful yields of the ketone **3.19** could be obtained by running the reaction under microwave irradiation. While promising, stoichiometric quantities of toxic osmium tetroxide were still required to get useful quantities of material, so other approaches to olefin cleavage were also examined.

Scheme 3-11. Successful development of Johnson-Lemieux conditions for cleavage of exocyclic olefin **3.6 under microwave irradiation conditions.**



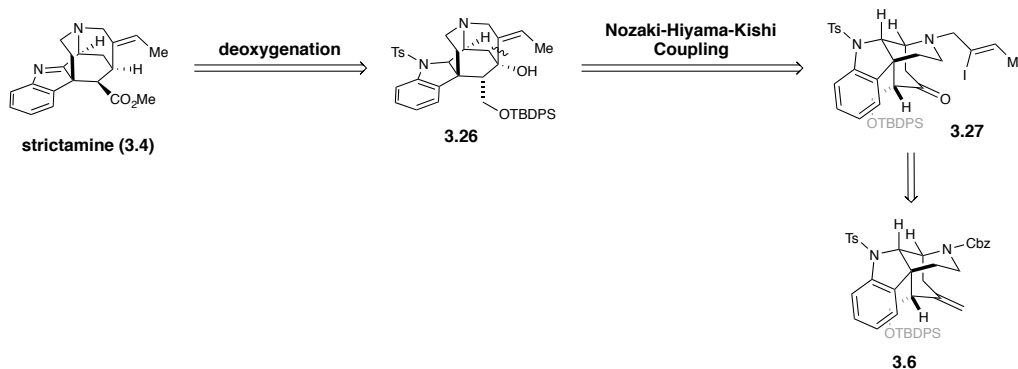
In prior studies on the malagashanine core, ozonolysis was not examined as an alkene cleavage method, presumably due to the presence of an electron rich *N*-benzylindoline in the core that would most likely undergo oxidation with these reaction conditions. However, the indoline nitrogen of our akuammiline is protected as the sulfonamide, significantly reducing the potential reactivity of this portion of the molecule under oxidative conditions. Therefore, ozonolysis seemed like an attractive alternative approach that avoided the use of stoichiometric quantities of toxic osmium (**Scheme 3-12**). To our delight, ozonolysis proceeded cleanly in five minutes with our akuammiline core **3.6**, providing our desired ketone **3.19** in 74% yield. Presumably, the smaller size of ozone provided it easier access to the sterically hindered exocyclic olefin compared to the larger reagents we were using previously.

Scheme 3-12. Successful oxidative alkene cleavage of exocyclic olefin **3.6 via ozonolysis.**



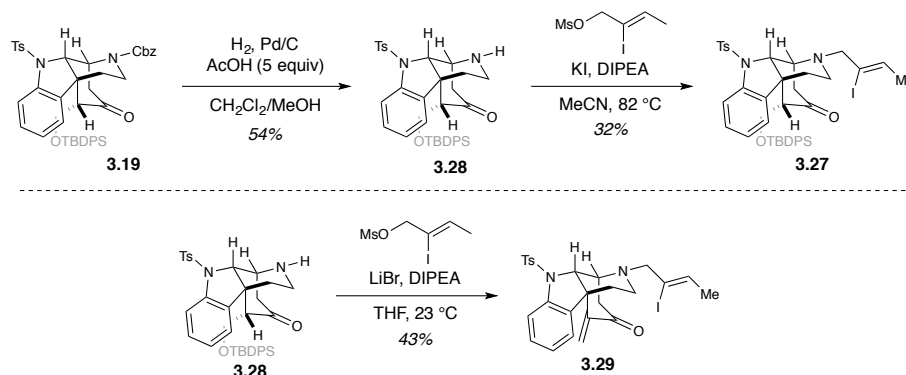
With now having easy access to ketone **3.19**, we reevaluated our synthetic approach to these natural products (**Scheme 3-13**). The C15 ketone provided an electrophilic center directly on the key bridgehead carbon required for building the E ring. Therefore, we imagined an approach where intramolecular addition of a vinyl nucleophile to the ketone could form the key C15-C20 bond (**3.26**) with the desired stereochemistry. This approach was attractive due to the ability to introduce the required alkene substituent in the C-C bond forming step instead of through later functional group manipulation. We desired a method that would not lead to isomerization of the precursor olefin, ruling out traditional metal-halogen exchange methods which have been shown to isomerize the olefin in related systems. Nozaki-Hiyama-Kishi couplings typically do not lead to scrambling of alkene geometry;¹⁰ therefore, we examined chromium-mediated methodology to explore the feasibility of such an addition step.

Scheme 3-13. Proposed closure of E ring via a ketone addition/deoxygenation sequence.



Examination of such an intramolecular addition reaction required synthesis of the vinyl iodide precursor **3.27**, which could be accessed from ketone **3.19** over two steps (Scheme 3-14). Removal of the Cbz protecting group proceeded under mild conditions via hydrogenation to provide secondary amine **3.28** with the addition of a large excess of acetic acid being necessary for successful removal. This intermediate was subsequently alkylated with an allyl mesylate available in three steps from crotonaldehyde.¹¹ While allylamine **3.27** was successfully obtained, this reaction was fairly capricious, most likely due to the sensitivity of the doubly β -substituted ketone to basic conditions. Just reacting this substrate under alternative conditions provided significant quantities of unsaturated ketone **3.29**, the result of ready β -elimination of the TBDPS ether under the reaction conditions.

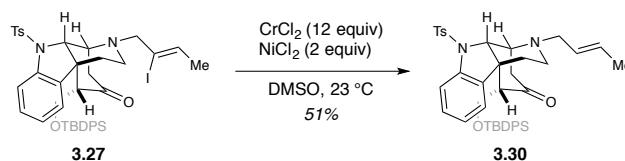
Scheme 3-14. Cbz protecting group removal and amine alkylation, along with significant beta-elimination seen under differing basic conditions.



When the vinyl iodide intermediate was subjected to standard Nozaki-Hiyama-Kishi coupling conditions, only deiodinated product **3.30** was ever observed across several attempts (Scheme 3-15). While disappointing, this result was later found to be not surprising. Additions of organometallic reagents to ketones are known to be more difficult due to increased steric demand, and Nozaki-Hiyama-Kishi couplings conditions are more

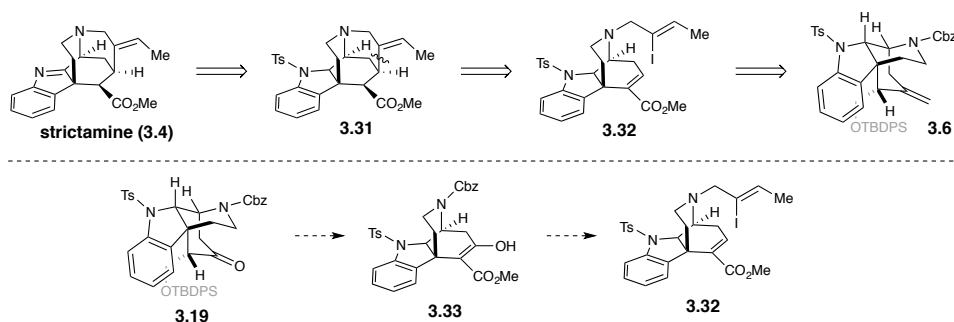
commonly applied to less sterically hindered aldehydes. While this approach was not explored further in order to examine alternative routes to a methanoquinolizidine structure, it might be worth examining this disconnection in the future to see if other methods specifically designed for ketone additions could be applied.

Scheme 3-15. Deiodination observed during attempted intramolecular Nozaki-Hiyama-Kishi coupling reaction.



3.3 Intramolecular Conjugate Addition Strategy for Synthesis of the E ring

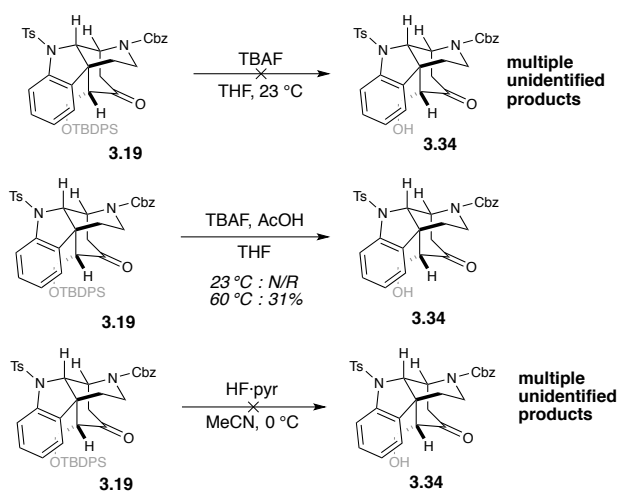
Scheme 3-16. Proposed intramolecular conjugate addition approach to strictamine, with synthesis from a β -ketoester intermediate 3.33.



Another approach we examined was the use of an intramolecular conjugate addition reaction to form the E ring (**Scheme 3-16**). A similar approach has been used in the synthesis of several strychnos and akuammiline alkaloids.¹²⁻¹³ We imagined testing this reaction on α,β -unsaturated ester substrate **3.32**, which we believed we could readily synthesize from our ketone precursor **3.19**. The question came to be what method would

work best, especially accounting for the apparent sensitivity of ketone **3.19**. Initially, we believed that silyl deprotection and oxidation of the pendant alcohol chain in ketone **3.19** would provide the most succinct method for ready access to a β -ketoester intermediate **3.33**, which we believed could be readily deoxygenated into our desired α,β -unsaturated ester **3.32**.

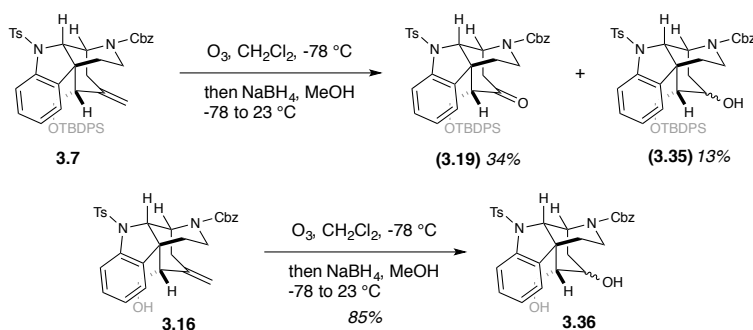
Scheme 3-17. Attempted removal of TBDPS protecting group on ketone 3.19.



Initial attempts at silyl deprotection of ketone **3.19** demonstrated the high sensitivity of this intermediate to overly acidic or basic conditions (**Scheme 3-17**). When initial deprotection of the silyl ether with TBAF was attempted, a messy slew of unidentified products was obtained. This suggested that the TBAF solution that was used was too basic, so the reaction was subsequently run buffered with acetic acid. However, the addition of acetic acid buffer now completely shut down reactivity at room temperature, and sluggish reactivity was only restored at 60 °C, providing 31% yield of the β -hydroxyketone **3.34**. To see if more acidic deprotection conditions would be favored, HF-pyridine was tested, but this reagent also led to a messy mixture of products. We believe that the ready susceptibility of this ketone intermediate to β -elimination on both sides,

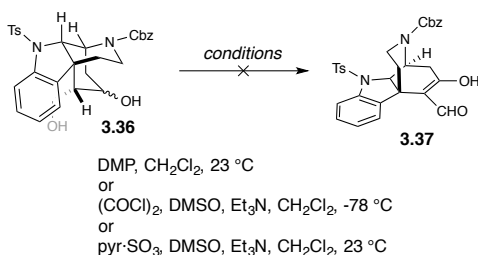
combined with the possibility of retro-aldol reactions of the β -hydroxyketone product, rendered using this approach with the ketone ineffective. To alleviate this, we hypothesized that reducing the ketone would remove this side reactivity and allow us to further explore this synthetic pathway.

Scheme 3-18. Ozonolysis with reductive quench of both TBDPS ether **3.7 and homoallylic alcohol **3.16**.**



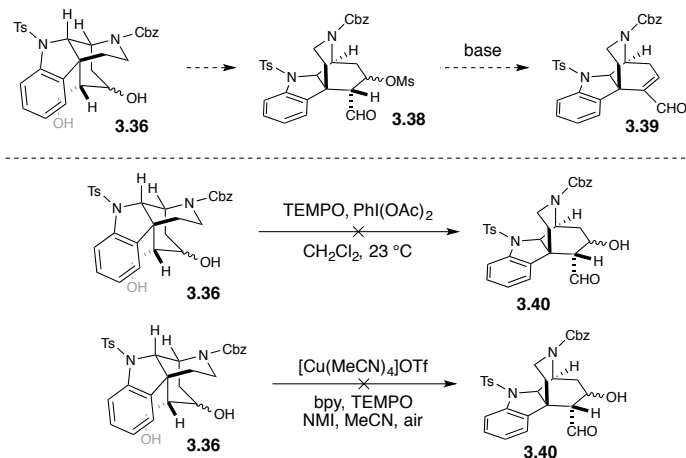
One way to obtain the desired alcohol would be during the prior ozonolysis step, where instead the quench occurs with sodium borohydride to provide a secondary alcohol (**Scheme 3-18**). Attempts at this with the silyl protected tetracycle **3.7** were only marginally successful, leading to only 13% yield of the desired alcohol **3.35** along with 34% yield of the previously obtained ketone **3.19**. Believing that the TBDPS ether could possibly block effective reduction during this step, we instead explored this reaction with homoallylic alcohol **3.16**. Gratifyingly, this reaction successfully provided diol **3.36** in high yield.

Scheme 3-19. Attempted dual oxidation to 1,3-dicarbonyl derivative **3.37.**



With diol in hand, we next examined whether it could be successfully oxidized to a 1,3-dicarbonyl intermediate (**Scheme 3-19**). However, no successful oxidation was ever observed over several different attempts with DMP, Swern, or Parikh-Doering oxidations. When we observed this structure, we wondered if we could get access to a shorter route to our intermediate if we could selectively oxidize the primary alcohol and subsequently form an unsaturated carbonyl by β -elimination of the secondary alcohol.

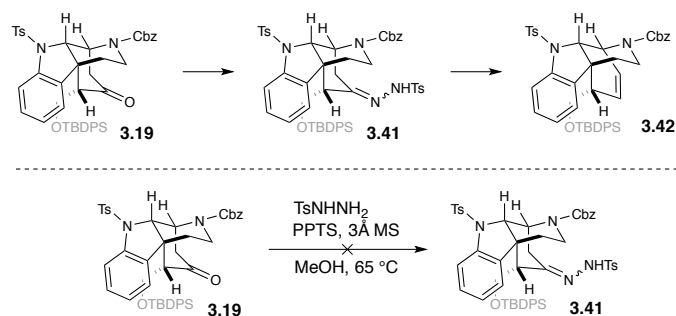
Scheme 3-20. Proposed selective primary alcohol oxidation/beta-elimination sequence and attempts of selective primary alcohol oxidation of diol 3.36.



To test this reaction, we first used TEMPO-catalyzed conditions that were known to provide selective oxidation of primary alcohols in the presence of secondary alcohols, but observed no reaction (**Scheme 3-20**).¹⁴ Knowing that particular catalytic oxidation conditions developed by Shannon Stahl and coworkers would also be potentially selective for primary alcohol oxidation, this reaction was attempted but led to no observable conversion of the starting material.¹⁵ Many of these reactions were believed to be unsuccessful due to the general insolubility of the diol starting material **3.36** in many

common organic solvents necessary for these reactions. We believed this general insolubility drastically inhibited its reactivity in the oxidations attempted.

Scheme 3-21. Attempted Shapiro reaction strategy.

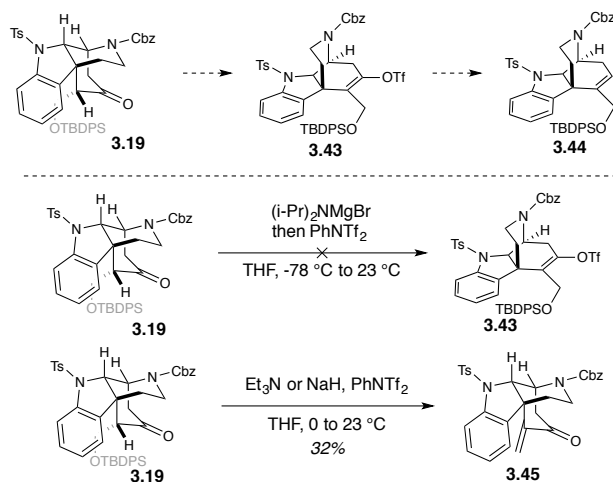


With this route proving problematic, we next wondered if altering the order of steps toward unsaturated ester **3.32** would provide us with a reasonable path forward. This would involve conversion of ketone **3.19** into an olefin before oxidation of the C16 pendant alcohol. We first examined the possibility of using a Shapiro reaction as a method to convert the ketone into an olefin (**Scheme 3-21**). Conversion of the ketone **3.19** into a tosylhydrazone **3.41**, followed by subsequent decomposition with base would provide the C4-C15 olefin **3.42**. While the formed olefin would not be in the desired position for our final intermediate, we believed it would readily migrate into position upon oxidation of the pendant alcohol to a carbonyl. However, attempted formation of the required tosylhydrazone **3.41** was not successful. Even attempts to condense the ketone **3.19** proved to be unfruitful. Therefore, we explored alternative methods for deoxygenation of our ketone **3.19**.

The same formal process can also be performed by converting a carbonyl into a vinyl triflate followed by subsequent reduction. This approach could allow for the olefin to be introduced along the desired C15/C16 portion of the C ring without requiring

subsequent migration in later steps via intermediacy of the formed thermodynamic vinyl triflate. Several methods for the formation of the thermodynamic vinyl triflate were trialed, but none successfully provided the desired intermediate (**Scheme 3-22**). Attempted thermodynamic deprotonation with *i*-PrNMgBr showed no reactivity, presumably due to the steric hindrance of the desired site of deprotonation.¹⁶ Going in with less sterically congested bases, such as sodium hydride and the weaker triethylamine, instead led to messy reactivity, with the beta-eliminated product **3.45** being observed. This result is not surprising, due to the equatorial C16 hydrogen being properly aligned with the ketone, preventing successful enolate formation in the chair conformation and instead favoring elimination. Therefore, we focused our next efforts on forming the kinetic triflate of the ketone.

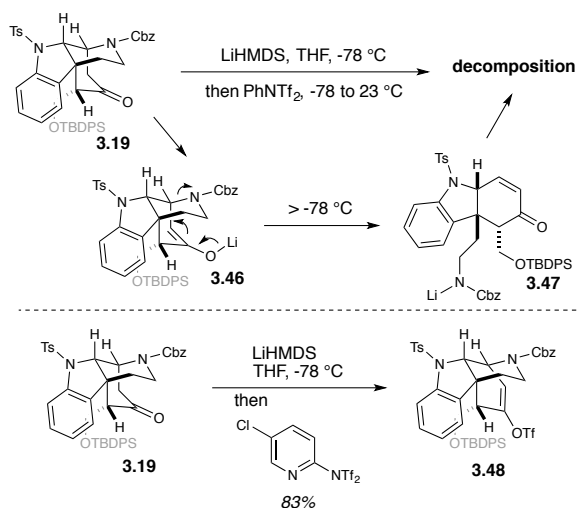
Scheme 3-22. Attempted synthesis of thermodynamic vinyl triflate 3.43.



Initial attempts to form the kinetic vinyl triflate proved unsuccessful (**Scheme 3-23**). Deprotonation with LiHMDS followed by trapping with phenyl triflimide led to the decomposition of the material at the warmer temperatures necessary for triflation with this reagent. Significant unidentifiable polymeric orange byproduct was formed that clung to

the baseline under silica gel chromatography. Presumably, this material resulted from β -elimination of the Cbz substituent at warmer temperatures, revealing an α,β -unsaturated ketone **3.47** that could potentially polymerize under the reaction conditions. In order to overcome this problem, a triflating reagent was necessary that could trap the kinetic enolate formed at low temperature. Phenyl triflimide could not successfully react at these temperatures, but using the more reactive Comins' reagent led to the successful formation of vinyl triflate **3.48** in good yields.¹⁷

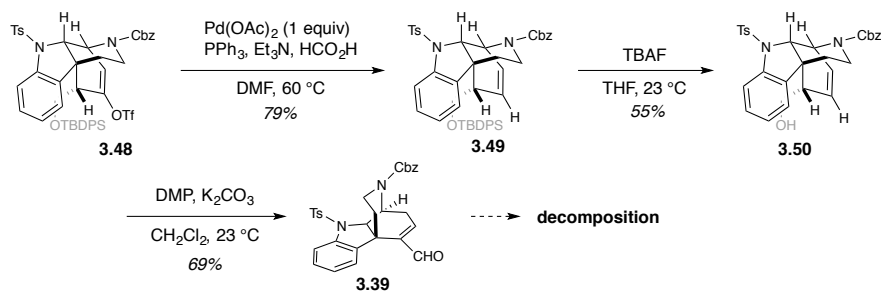
Scheme 3-23. Successful synthesis of vinyl triflate 3.46 using Comins' reagent.



With vinyl triflate in hand, we next examined the synthesis of the α,β -unsaturated ester moiety necessary for a successful conjugate addition reaction (**Scheme 3-24**). We were able to successfully remove the vinyl triflate using formic acid as a hydride surrogate, but stoichiometric quantities of palladium acetate were found to be necessary to get appreciable yields of the desired product **3.49**.¹⁸ Subsequent deprotection of the TBDPS ether went smoothly using TBAF, and the formed homoallylic alcohol **3.50** was oxidized with Dess-Martin Periodinane in the presence of a significant excess of K₂CO₃, providing

α,β -unsaturated aldehyde **3.39**. While this intermediate was isolable, it readily decomposed during subsequent attempted reactions necessary to furnish the methyl ester.

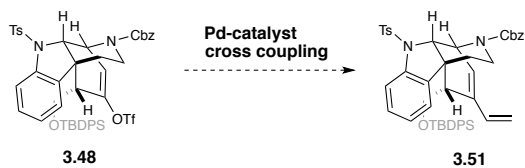
Scheme 3-24. Attempted synthesis of Michael acceptor for intramolecular conjugate addition.



3.4 Lactamization Revisited: Cross-Coupling/Hydrogenation Strategy for Synthesis of the E ring

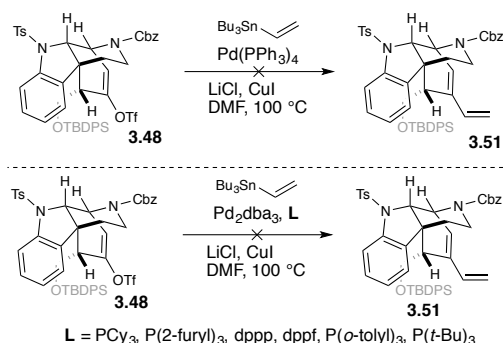
While examining the above approach, we also hypothesized that we could use the formed vinyl triflate as a reactive handle for C-C bond formation instead of removing it by reduction (**Scheme 3-25**). We envisioned we could couple in the required two carbon fragment necessary for building the E ring by reacting this vinyl triflate **3.48** with a simple vinyl organometallic. We chose to use vinyl(tributyl)stannane due to its commercial availability, as well as the neutral conditions and general reliability of Stille cross couplings in synthetic applications.

Scheme 3-25. Proposed coupling of necessary two carbon E ring fragment via cross-coupling methodology.



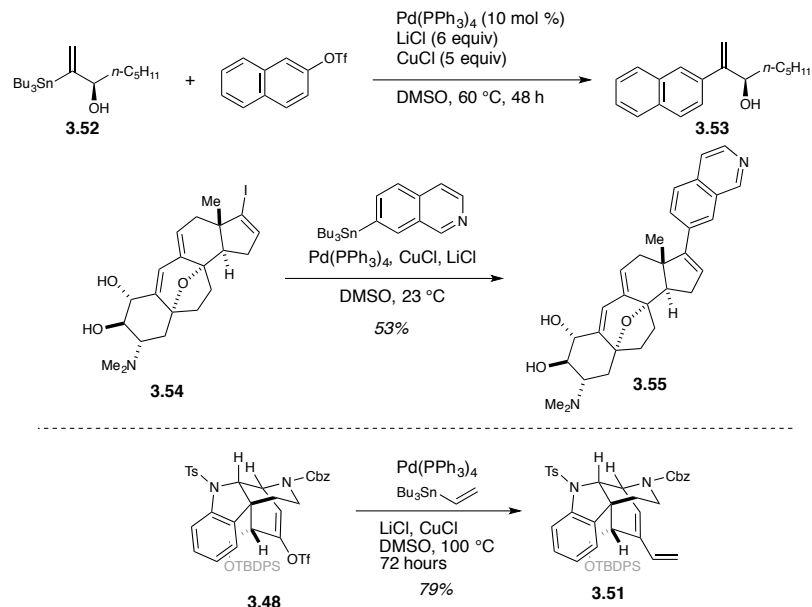
Initial attempts at the Stille cross coupling of the vinyl triflate **3.48** with vinyl(tributyl)stannane proved to be unsuccessful (**Scheme 3-26**). Standard conditions for Stille coupling with vinyl triflates, using lithium chloride¹⁹ and copper iodide²⁰ additives, were found to be unsuccessful when Pd(PPh₃)₄ was used as a catalyst. A selection of varying mono- and bisphosphine ligands were explored with Pd₂(dba)₃, but these cross couplings were also not successful. The lack of success for these reactions may have been due to the steric hindrance in reaction with the vinyl triflate **3.48**, a problem we had previously encountered when trying to perform reactions successfully on C15.

Scheme 3-26. Initial attempts at a Stille coupling of vinyl triflate 3.48 with vinyltributylstannane.



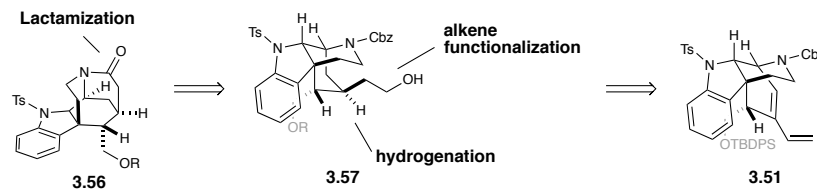
We examined the literature to see if there were conditions developed for Stille reactions of sterically congested systems (**Scheme 3-27**). We found work by E. J. Corey and coworkers where they were able to successfully couple 1-substituted vinylstannanes substrates (e.g. **3.52**), which traditionally don't successfully undergo successful Stille couplings, with triflates.²¹ These reactions conditions have later been successfully applied to reactions with vinyl halides and triflates that prove otherwise difficult to couple, as can be seen by its use for the coupling of an aryl stannane with hindered vinyl iodide **3.54** in Phil Baran's total synthesis of cortistatin A.²² Application of these reaction conditions to our system proved that for other substrates to produce significant yields of **3.51**.

Scheme 3-27. Successful Stille coupling protocol for the synthesis of diene 3.51.²¹⁻²²



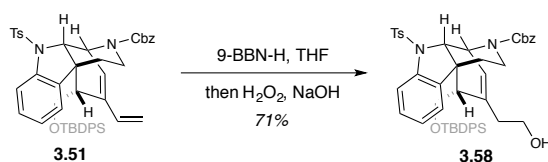
Successful formation of diene product **3.51**, with the correct carbon count in place for the E ring, led us to rework our synthetic strategy (**Scheme 3-28**). With the carbon framework in hand, we next needed to convert our diene intermediate into one with the correct oxidation state and desired functionality to successfully cyclize toward the methanoquinolizidine core. First, a functional handle would be needed at the terminal end of the diene in order to allow for proper coupling, presumably using an alkene functionalization selective for the external olefin of the diene substrate. Next, the internal olefin would need to undergo a diastereoselective reduction, effectively setting the C15 stereochemistry and positioning the substituent on this carbon in the required axial position for ring closure.

Scheme 3-28. Retrosynthetic analysis for conversion of diene 3.51 into a ring-closed lactam core 3.56.



We first set out to perform a selective anti-Markovnikov functionalization of the terminal olefin of the diene, introducing the functionality required for a later ring closing step (**Scheme 3-29**). Due to our desire to use an amide coupling protocol to close the E ring, we wished to selectively introduce an alcohol to the terminal position that could be later oxidized to the required carboxylic acid. We did not envision the selectivity of such a process being problematic due to the more internal trisubstituted olefin component of the diene being more sterically encumbered than the terminal olefin we wished to functionalize. Indeed, hydroboration of the terminal olefin portion of the diene with 9-BBN-H proceeded without incident, with subsequent oxidation providing homoallylic alcohol **3.58**. Use of commercial solutions of 9-BBN-H for this reaction, while sometimes successful, proved typically unreliable for this process, and it was found that using a THF solution freshly prepared from 9-BBN-H dimer weighted in a glovebox was necessary for consistent high yields.

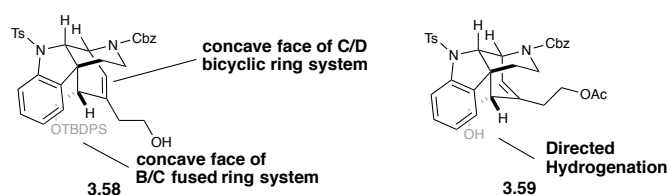
Scheme 3-29. Successful hydroboration of terminal olefin in diene 3.51 to homoallylic alcohol 3.58.



With successful selective functionalization of the terminal olefin of the diene, we next sought a method to diastereoselectively reduce the trisubstituted internal olefin of the

C ring to set the C15 stereocenter. However, potential challenges in the hydrogenation of this internal olefin were apparent, beyond just the inherent difficulty in reducing a trisubstituted olefin (**Scheme 3-30**). While the desired face of our olefin for reduction was present on the convex face of the C/D bicyclic system in intermediate **3.58**, it was also present on the concave face of the B/C 5,6-fused ring system. Additionally, the axially positioned TBDPS ether might block access to the desired face of the olefin, as it had done previously with reactions involving the exocyclic olefin **3.6**. Reductions of sterically hindered olefins can often successfully be accomplished using homogenous cationic rhodium or iridium catalysts.²³ These cationic complexes also may be directed to specific faces of olefins for hydrogenation by binding to neighboring Lewis basic functionality.²⁴ We hypothesized that the oxygen present on the C16 axial substituent could potentially bind to one of these catalysts, facilitating the desired selective hydrogenation. We therefore set out to synthesize a substrate **3.59** with a free alcohol on the C16 axial substituent.

Scheme 3-30. Analysis of faces of the internal olefin of the C ring of 3.58 in terms of potential for hydrogenation and proposed intermediate 3.59 for directed hydrogenation.



Synthesis of the desired directed hydrogenation substrate proceeded in a straightforward fashion (**Scheme 3-31**). We first protected the more exposed primary alcohol as the acetate in order to allow for more useful differentiation of the two alcohols in later synthetic steps. Unlike with prior intermediates, the TBDPS protecting group at this stage could not be removed with TBAF, but buffered HF·pyridine was found to be

sufficient to facilitate this cleavage, providing homoallylic alcohol **3.59** in 80% yield over two steps.

Scheme 3-31. Exposure of axially-position alcohol 3.59 for directed hydrogenation.

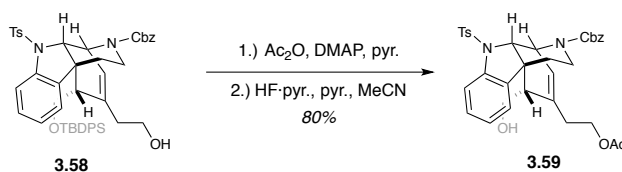
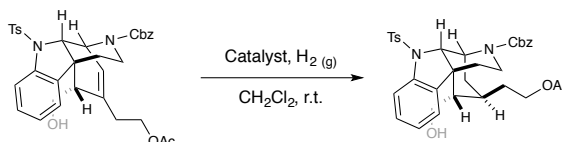


Table 3-1. Attempted directed hydrogenations of internal olefin 3.59 under various pressures.



Entry	Catalyst	Mol %	H ₂ (bar)	Time (h)	Yield ^a
1	[Ir(cod)(PCy ₃)(py)]PF ₆	2	1	24	-
2	[Ir(cod)(PCy ₃)(py)]PF ₆	2	10	24	-
3	[Ir(cod)(PCy ₃)(py)]PF ₆	2	30	24	-
4	[Ir(cod)(PCy ₃)(py)]PF ₆	2	60	24	-
5	[Ir(cod)(PCy ₃)(py)]PF ₆	20	60	48	-
6	[Ir(cod)(PCy ₃)(py)]BAR ^F ₄	2	1	24	-
7	[Ir(cod)(PCy ₃)(py)]BAR ^F ₄	2	30	24	-
8	[Ir(cod)(PCy ₃)(py)]BAR ^F ₄	2	60	72	26
9	[Ir(cod)(PCy ₃)(py)]BAR ^F ₄	5	90	48	-

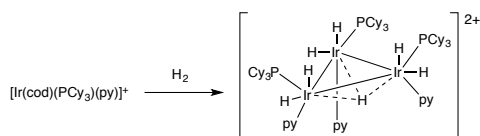
^aReaction conditions: substrate (10 mg unless otherwise stated), catalyst, dichloromethane (mL) were combined in a vial sealed with a teflon cap under nitrogen. The vial was either placed under a balloon of hydrogen gas (1 bar) or pierced with a needle and placed into a Parr reaction vessel under the stated hydrogen pressure.

With homoallylic alcohol **3.59** in hand, we next examined directed hydrogenations under a variety of conditions (**Table 3-1**). Initial examination with the commercially available PF₆⁻ salt of Crabtree's catalyst provided no product over a range of pressures (Entries 1-5). When instead using a more active variant of Crabtree's catalyst with the more weakly coordinating BAR^F₄⁻ anion (Entries 6-9),²⁵ hydrogenated product was obtained in 26% at 60 bar hydrogen pressure (Entry 8). We imagined better yields could be achieved

if the reaction was instead run at more forcing pressures. Instead, when increasing the pressure to 90 bar to attempt to force the reaction (Entry 9), reactivity appeared to shut down.

One diagnostic observation in all of these reactions was the propensity of the solutions to turn a pale yellow after a period of time, differing from the bright orange solutions that would initially persist upon fresh addition of the catalyst. It has been previously described that this yellow solution occurs when the iridium hydride intermediate produced by reaction of the catalyst with hydrogen forms an unreactive trimer that falls out of the catalytic cycle (**Scheme 3-22**).²⁶ Often this occurs before hydrogenation of the olefin can occur in especially hindered substrates, often leading to low yields of the desired product. This is a known problem with these hydrogenation catalysts, with many differing ligand sets having been explored that increase the lifetime of the active catalyst in the reaction solution.²⁷

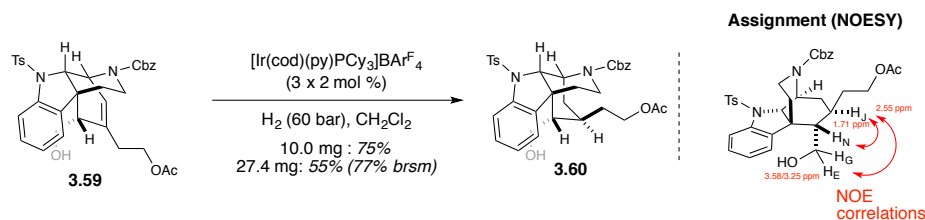
Scheme 3-32. Propensity of cationic iridium hydrogenation catalysts to undergo deactivating trimerization under typical hydrogenation conditions.²⁶



As an alternative approach, it was discovered that re-dosing the catalyst at select intervals could effectively lead to higher yields of product (**Scheme 3-33**). This result was surprising, since it means that the already present deactivated trimer does not interfere with subsequent hydrogenation attempts with fresh added catalyst. Initial attempts at this reaction on a test scale provided the desired reduction product **3.60** in 75% yield, with a slight decrease in yield observed on a somewhat larger scale due to incomplete reaction of

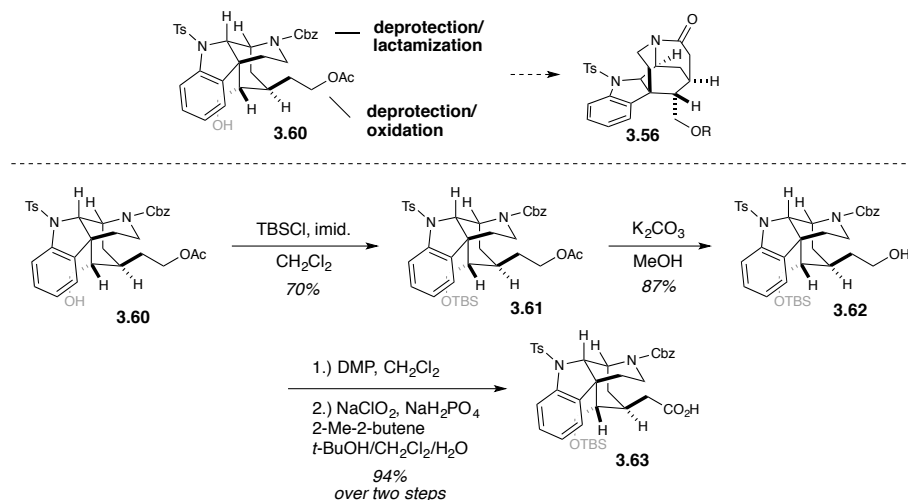
the olefin. The facial selectivity of the hydrogenation was confirmed by the observation of key correlations in the NOESY spectrum between the C15 hydrogen (2.55 ppm) and the hydrogens present on the C16 axial directing group (3.58/3.25 ppm); these observed NOEs would not be expected with the alternative diastereomer. Now having a preparatively useful route toward a reduced intermediate **3.60**, we next focused our efforts on developing a route to successfully close the E ring.

Scheme 3-33. Successful hydrogenation of internal olefin 3.59 with successive dosing of Crabtree's catalyst.



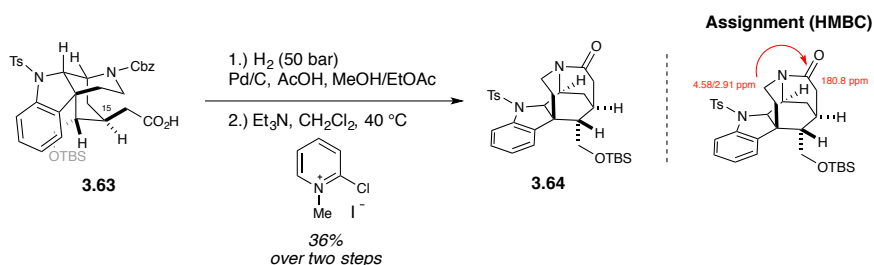
Synthesis of our lactamization precursor required several manipulations (**Scheme 3-34**). We had to deprotect the terminal pendant alcohol and oxidize it to a carboxylic acid, followed by subsequent deprotection of the D ring nitrogen and amide coupling to form the E ring. Toward this end, we protected the prior directing alcohol as the TBS ether **3.61** in 70% yield, followed by straightforward removal of the terminal acetate substituent to provide pendant alcohol **3.62**. Sequential oxidation with Dess-Martin Periodinane followed by Pinnick oxidation provided the terminal carboxylic acid **3.63** in 95% yield over two steps.

Scheme 3-34. Deprotection of terminal E ring alcohol and subsequent oxidation to carboxylic acid 3.63.



Our approach for the lactamization to form the final E ring is modeled off of that used in Yong Qin's synthesis of vincorine, so we used their conditions as initial guidelines to test the reaction (**Scheme 3-35**).¹ An initial roadblock to testing this reaction was the removal of the Cbz substituent on the D ring nitrogen, which was not successfully removed from this substrate under the milder conditions we had used previously with earlier intermediates. Indeed, 50 bar of hydrogen pressure as well as long reaction times (5 days) was necessary in order for complete removal of the Cbz protecting group to be observed by ¹H NMR. Presumably the presence of the now axial substituent on C15 made the environment around the Cbz substituent more sterically encumbered, requiring the use of more forcing conditions for its removal. This reaction mixture was filtered through celite, concentrated, and directly subjected to the coupling conditions used in the Qin synthesis of vincorine. When the residue from hydrogenation was reacted with Mukaiyama's reagent, lactam product **3.64** was obtained in 36% yield over two steps. Cyclization toward the lactam was confirmed by observation in the HMBC spectrum of a correlation between the hydrogens on C5 (4.58/2.91 ppm) and the lactam C=O carbon (180.8 ppm).

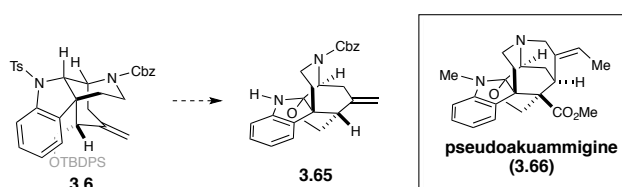
Scheme 3-35. Successful synthesis of pentacycle 3.64 via Cbz deprotection and lactamization with Mukaiyama's reagent.



Therefore, we had successfully completed a synthesis of a pentacyclic core of the natural product strictamine that contains the whole carbon framework of the methanoquinolizidine core of the natural product. From here, introduction of the E ring olefin and subsequent functional group manipulations would provide access to the natural product.

3.5 Synthesis of Pseudoakuammigine Furoindoline Core Model

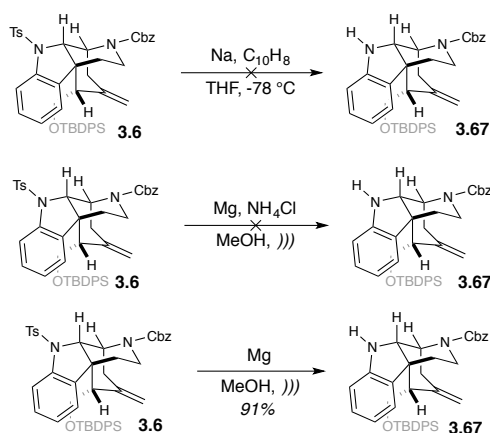
Scheme 3-36. Proposed conversion of tetracycle 3.6 into pseudoakuammigine core 3.65.



Upon examination of our tetracyclic core **3.6**, we noted that our C16 axial substituent was similar to the hydroxymethylene present off of the C16 quaternary center that formed the cyclized furoindoline motif present in such alkaloids as pseudoakuammigine (**3.66**). We were curious if we could use our tetracyclic core **3.6** as a model for a route to synthesize this motif (**3.65**), especially as it might be pertinent to the

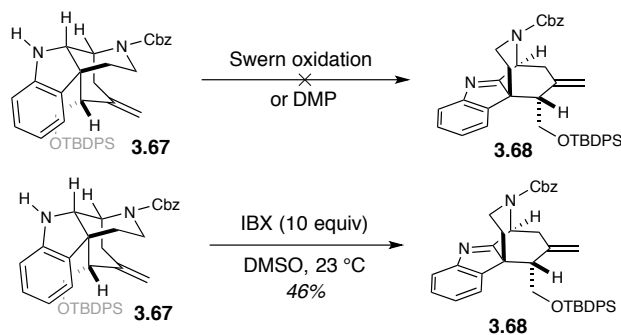
synthesis of some of these unsynthesized alkaloids (**Scheme 3-36**). We envisioned that tosyl deprotection of the indoline followed by oxidation would provide the indolenine, which we believed would readily cyclize into the furoindoline upon deprotection of the silyl ether.

Scheme 3-37. Conditions explored for removal of the indoline tosyl substituent (3.6).



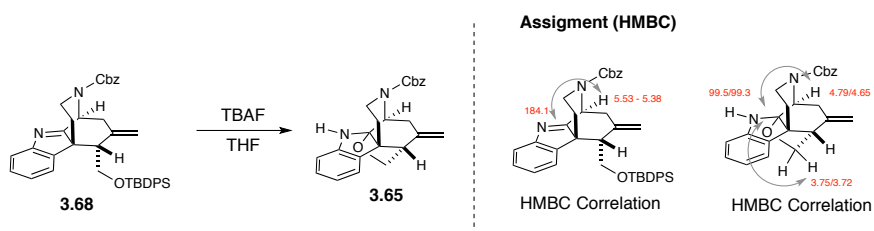
We first explored conditions to remove the tosyl protecting group on the indoline nitrogen (**Scheme 3-37**). Standard conditions (sodium naphthalenide) used to remove a tosyl protecting group in our related Malagasy core surprisingly proved ineffective.² We noted that Neil Garg and coworkers had used magnesium in methanol under sonication to mildly remove a tosyl substituent in their total synthesis of aspidophylline A.²⁸ When using their conditions, where ammonium chloride is added to buffer the system, we observed no reactivity. However, if the reaction was run in the absence of ammonium chloride, the tosyl group was removed cleanly, providing N-H indoline **3.67** in 91% yield.

Scheme 3-38. Oxidation of indoline 3.67 to indolenine 3.68.



We next sought conditions to successfully oxidize the N-H indoline **3.67** into the indolenine **3.68** (Scheme 3-38). Initial examination of the literature showed that Swern conditions could successfully perform this transformation in related systems, but no product was observed when they were attempted.²⁹ Attempts to use DMP also proved unsuccessful. When a reaction was trialed with 1.5 equiv of IBX, a small quantity of our desired indolenine was obtained. We found that we were able to access useful quantities of our desired indolenine **3.68** when a large excess of IBX was used.

Scheme 3-39. Silyl deprotection and cyclization to furoindoline pentacycle 3.65.



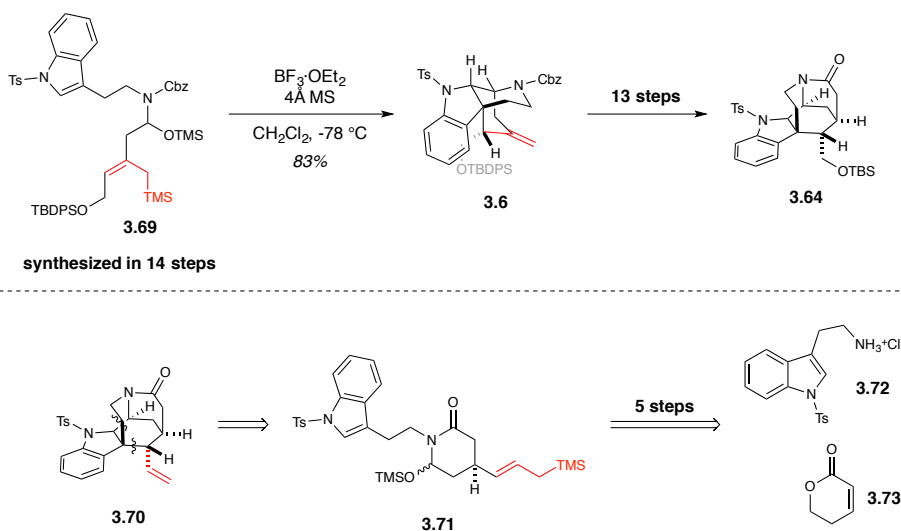
Indolenine **3.68** was next subjected to silyl deprotection conditions (Scheme 3-39). Upon reaction with TBAF, the silyl group was removed and the free alcohol chain readily cyclized on the indolenine to form furoindoline **3.65**. The structure of this intermediate was confirmed by comparison of the ¹H NMR data between the N-H indoline **3.67**, the indolenine **3.68**, and the furoindoline intermediate **3.65**, as well as the observation of key

HMBC correlations in the relevant indolenine **3.68** and furoindoline **3.65** spectra. Oxidation of the N-H indoline **3.67** to the indolenine **3.68** led to observable downfield shifts of the aromatic protons on the ring above 7.0 ppm. The indolenine C=N carbon is readily observable in the ^{13}C NMR (184.1 ppm) and a clear correlation between the C4 proton (5.53-5.38 ppm) and this carbon is seen in the HMBC spectrum. Upon deprotection and cyclization to the furoindoline **3.65**, the indoline aromatic protons shift slightly upfield. The C=N carbon shift disappears and a new carbon shifts appear (99.5/99.3 ppm, mixture of rotamers) in roughly the region expected for a hemiaminal carbon. There are now clearly correlations seen in the HMBC between the C4 proton (4.79/4.65 ppm, mixture of rotamers) and the oxygen-substituted CH_2 (3.75/3.72 ppm) and the new signal for the hemiaminal ether, confirming cyclization.

3.6 New Directions: Development of an Alternative Akuammiline Alkaloid Cascade

Annulation

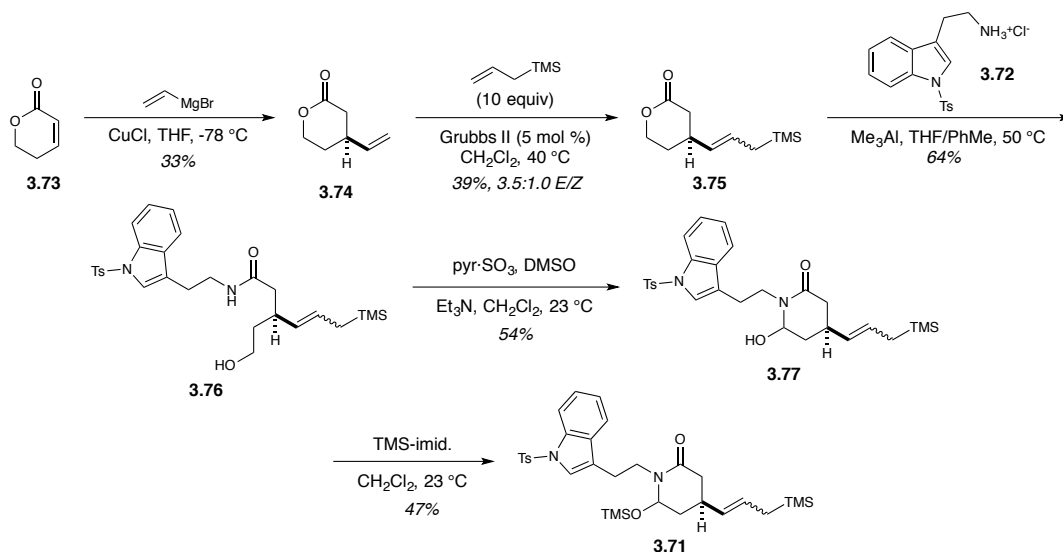
Scheme 3-40. Prior synthetic route to pentacycle **3.64** and proposed more succinct route to related pentacycle **3.70**.



Upon analysis of our route to lactam intermediate **3.64**, and in light of the successful syntheses of strictamine (**3.4**) published by several groups in 2016 and 2017, we felt it necessary to reexamine our approach to these natural products (Scheme 3-40). While we believed the disconnections used in our cascade were powerful due to their disassembly of the central C ring, actually moving forward from the core **3.6** we obtained from our cascade proved to be lengthy, presumably due to the steric hindrance present in this intermediate. Additionally, the step count to even get to this core intermediate required 15 total steps, leading to a total of 28 steps just to get pentacyclic lactam **3.64**. Due to the high step counts being the result of both synthesizing and manipulating tetracyclic core **3.6**, the result of our cascade reaction, we believed developing a cascade toward a more synthetically useful product polycycle would be necessary. The most problematic part of the synthesis of

pentacyclic lactam **3.64** was building the E ring, so we envisioned developing a cascade process that provides a core **3.70** with the E ring already in place. This would require a repositioning of the allylsilane where it would form instead a pendant arm on C16 instead of some of the central C ring structure. Using the same disconnections as in our previous cascade, we would need access to cyclic hemiaminal ether **3.71**. We believed this intermediate could be accessed in 5 steps from tryptamine hydrochloride **3.72** and unsaturated lactone **3.73**, meaning that we could potentially access our pentacyclic structure in 6 steps, a significant reduction in step count compared to our previous route. Additionally, the substrate would contain a preformed stereocenter, circumventing the need for the development of an asymmetric variant of these cascade reactions and instead inducing enantioselectivity in an earlier, more conventional step.

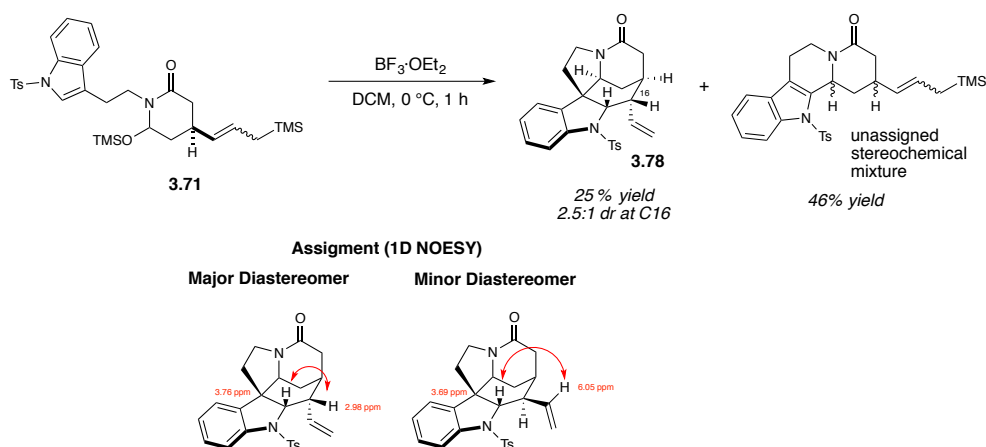
Scheme 3-41. Synthesis of cyclic hemiaminal ether substrate 3.71.



Examination of this possible cascade require the synthesis of cyclic hemiaminal ether **3.71**, which was synthesized from unsaturated lactone **3.73** in five steps (Scheme 3-41). Conjugate addition of the organocuprate formed from vinylmagnesium bromide

provided γ,δ -unsaturated lactone **3.74**.³⁰ Subsequent cross metathesis with allyltrimethylsilane provided the substituted allylsilane **3.75** as a 3.5:1.0 mixture of *E/Z* isomers which were unable to be separated at this point or in any later intermediate. Amide **3.76** was formed by a trimethylaluminum-mediated coupling of lactone **3.75** with tryptamine hydrochloride **3.72**.³¹ Subsequent oxidation of the free primary alcohol under Parikh-Doering conditions provided hemiaminal **3.77**, the result of condensation of the formed aldehyde on the amide.³² Subsequent reaction with trimethylsilylimidazole provided hemiaminal ether substrate.

Scheme 3-42. Cyclization of hemiaminal ether substrate 3.71 to strychnos-like core 3.78.

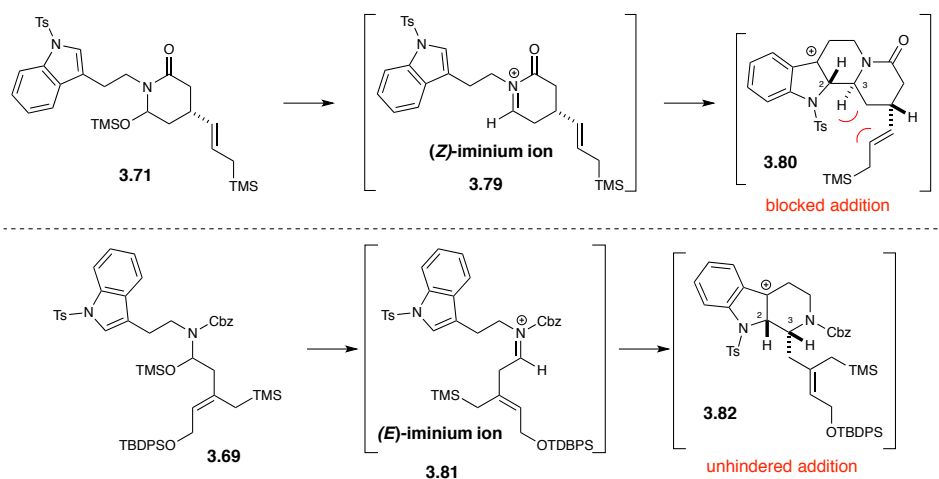


When hemiaminal ether **3.71** was reacted under Lewis acidic conditions, the major product was strychnos-like core **3.78** in 25% yield as a 2.5:1 mixture of C16 epimers (**Scheme 3-42**). A mixture of various Pictet-Spengler cyclization isomers was also obtained as a majority of the rest of the product distribution, with nothing resembling the desired pentacycle **3.70** found. The connectivity was established by analysis of ¹H NMR, COSY, and 1D TOCSY spectra. The C16 stereochemistry for both diastereomers was determined by observation of an NOE for the C2 proton (3.76 ppm) upon irradiation of the C16 proton

(2.98 ppm) with 1D NOESY, while an NOE is observed for a proton of the olefin (6.05 ppm) upon irradiation of the C2 proton (3.69 ppm) of the minor isomer. Based upon our prior cyclizations, this result is surprising; this particular nitrogen substitution pattern typically resulted in mainly the regiodivergent akuammiline alkaloid core, with no strychnos-like core being observed. The observation of mainly Pictet-Spengler products implies that this cyclization mode might have been preferred, but the allylsilane addition step was not able to successfully occur.

Scheme 3-43. Rationale for lack of observed akuammiline core with cyclic hemiaminal ether substrate

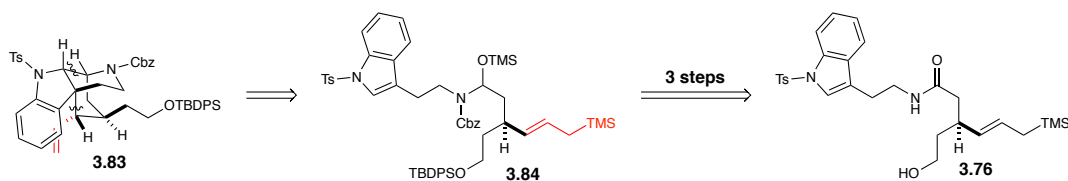
3.71.



The lack of a desired akuammiline core can be rationalized by examining both the geometry of the formed iminium ion as well as the relative stereochemistry of the benzylic cation intermediate the allylsilane must intercept to form an akuammiline alkaloid product in both our prior and currently explored cascade (**Scheme 3-43**). Due to the cyclic nature of hemiaminal ether **3.71**, only **(Z)-iminium ion 3.79** can be formed. When the **(Z)-iminium ion 3.79** cyclizes with the indole ring, it leads to a *trans* relationship between the C3 and C2 protons in intermediate **3.80**. This will effectively result in one proton blocking

allylsilane addition, leading to competing rearomatization, preventing a path forward for an akuammiline-type product. In comparison, our previous cascade with hemiaminal **3.69** which involves an acyclic iminium ion intermediate, appears to lead exclusively to formation of the (*E*)-iminium ion **3.81**. Cyclization of this iminium ion on the indole leads to a *cis* relationship between the C2 and C3 protons in intermediate **3.82**, effectively placing the allylsilane on the opposite face and positioned such that it can readily cyclize to form the desired tetracycle. Therefore, this results hints that the proper iminium ion geometry is very important for achieving the desired cyclization outcome from our cascade, with an (*E*)-iminium ion geometry as was obtained in our prior open-chain substrates being necessary for allylsilane addition to occur in the akuammiline alkaloid cascade pathway. This is not detrimental for the synthesis of strychnos-like cores, as can be seen in both the above result as well as with our labs exploration of developing an oxocarbenium ion variant of our cascade for the synthesis of mattogrossine.³³

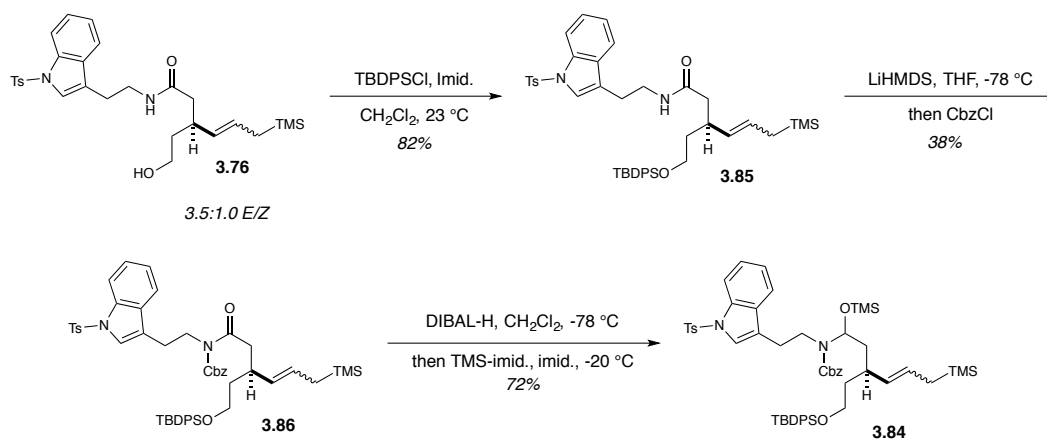
Scheme 3-44. Retrosynthetic analysis for proposed open-chain hemiaminal ether substrate 3.84.



As a result of this analysis, we decided to adopt a hybrid approach between our previous cascade and this newly developed one (**Scheme 3-44**). Instead of having the E ring already cyclized, we instead have a protected two carbon pendant chain that could be used to construct it already installed in cascade product **3.83**. This would allow for ready construction of this moiety, while still allowing for an open chain substrate that could provide us with the proper iminium ion geometry. Retrosynthetic disconnection would

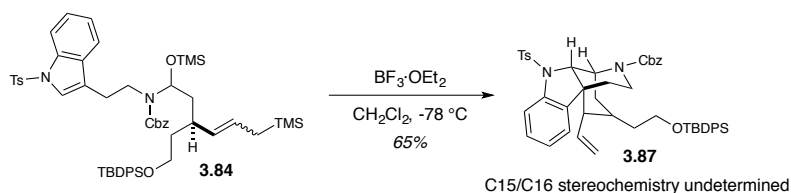
provide us with the acyclic hemiaminal ether **3.84**, which we could readily construct from intermediate **3.76** that we had previously synthesized. This would also allow us to use the same nitrogen protecting group pattern that we found necessary for our regioselectivity in our earlier cascade. In total, this tetracyclic product **3.83** would potentially be prepared in just seven steps from unsaturated lactone **3.73**.

Scheme 3-45. Synthesis of open-chain hemiaminal ether substrate 3.84.



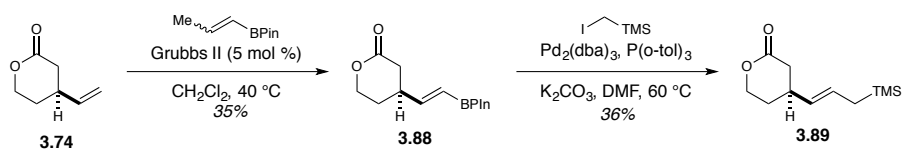
The desired hemiaminal ether was synthesized in short order from amide **3.76** (**Scheme 3-45**). Protection of the primary alcohol in amide **3.76** as the TBDPS ether **3.85** went in high yield. Installation of the Cbz group on the amide **3.85** by deprotonation with LiHMDS followed by reaction with benzylchloroformate provided the *N*-Cbz amide **3.86** in moderate yield. Reduction of the amide with DIBAL-H followed by trapping with trimethylsilylimidazole provided the hemiaminal ether **3.84**.

Scheme 3-46. Cyclization of open-chain hemiaminal ether substrate 3.84 to tentative tetracycle 3.87.



When hemiaminal ether **3.84** was subjected to Lewis acid, the tentatively assigned tetracycle **3.87** was obtained as the major product as an inseparable 2.0:1.0 mixture of diastereomers (**Scheme 3-46**). Initial assignment of this structure was difficult due to the presence of both rotamers from the Cbz substituent as well as a diastereomeric mixture. When heated to 80°C in d6-DMSO, the peaks partially resolved, allowing for a COSY spectrum to be obtained that helped in assigning the proper connectivity of the structure. However, a good quality NOESY spectrum was unable to be obtained under these conditions, so the relative stereochemistry at C15 and C16 was not able to be established.

Scheme 3-47. Preliminary data on the synthesis of (*E*)-allylsilane **3.89.**

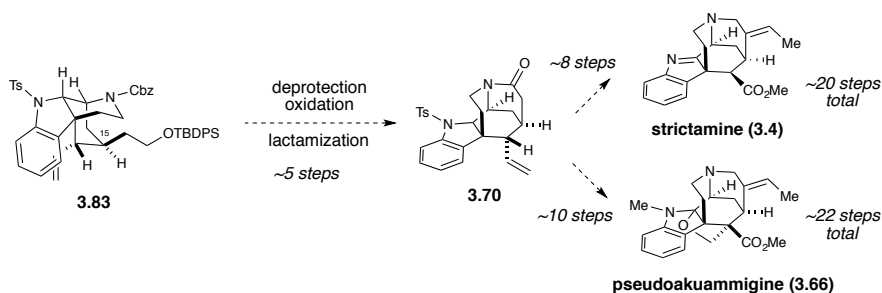


Due to the cyclized product present being an inseparable diastereomeric mixture, complicating spectroscopic assignment, and to the easier synthetic manipulation of synthetic intermediates when they are present as pure diastereomers, we needed to develop a method for accessing allylsilane **3.89** as a single olefin stereoisomer (**Scheme 3-47**). Robert Grubbs and coworkers have reported that cross metathesis reactions with vinyl boranes often go with high *E* selectivity, so we examined this reaction with our terminal olefin substrate **3.74**.³⁴ Indeed, reaction of propenyl pinacolborane with our terminal olefin provided the terminal pinacol borane **3.88** exclusively as the *E* isomer. The pinacolborane was found to successfully undergo a Suzuki coupling with iodotrimethylsilane to provide the (*E*)-allylsilane isomer of **3.89** exclusively.³⁵ While exciting, the yields for these steps were low, paralleling the low yields for similar steps in the previous route. We believe this

to be due to the volatility of these products, so our current efforts explore a similar sequence of reactions on a protected open chain variant of this material that should be less susceptible to material losses.

3.7 Conclusion and Future Directions

Scheme 3-48. Proposed Future Route of New Akuammiline Core Toward Strictamine (3.4) and Pseudoakuammigine (3.66).

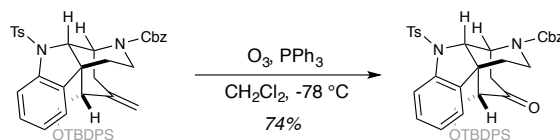


Herein, we have been able to demonstrate our ability to convert the tetracyclic akuammiline core **3.6** that we can obtain from our cascade annulation can be converted into a methanoquinolizidine-containing core **3.64** over 13 steps. However, the topology of our tetracyclic core **3.6** leads to the use of a circuitous route to achieve this result, leading to a total of 28 steps being necessary to synthesize pentacycle **3.64** from commercially available starting materials. The problematic last step for the synthesis of the methanoquinolizidine core is the installation of the final E ring of this structure. In light of published syntheses of the target alkaloid strictamine (**3.4**) that can access this natural product over fewer steps, a more succinct route toward a related pentacycle would be necessary. To this end, we are currently exploring the synthesis of a tetracyclic intermediate **3.83**, which we believe we can access in seven steps from simple starting materials, that

would already contain the necessary framework for quick synthesis of methanoquinolizidine structure **3.70** (Scheme 3-48). A requirement for this strategy to be successful would be correct establishment of the stereochemistry on C15 in **3.83**, positioning the substituent for proper E ring closure. Whether this would be the case with our cyclization has not yet been established. From pentacycle **3.70**, we can imagine accessing strictamine (**3.4**) over eight steps for a total of 20 steps from commercially available starting materials. Alternatively, we could potentially access pseudoakuammigine (**3.66**), an alkaloid in this family that has yet to have been synthesized, over ten steps from pentacycle **3.70** for a total of 22 steps. Finally, these routes could be made enantioselective if method for the enantioselective synthesis of terminal alkene **3.74** or a related intermediate could be developed, circumventing the need for the development of an asymmetric catalytic system for our iminium ion cascade. The feasibility of this route is currently being explored.

3.8 Experimental Procedures

Ketone 3.19:



Ozone (4% in O₂) was bubbled through a solution of tetracycle **3.6** (395.8 mg, 0.52 mmol, 1.0 equiv) in CH₂Cl₂ (20.0 mL) at -78 °C until a blue color persisted. After five minutes, ozone bubbling was ceased and the mixture was sparged with oxygen. After thirty minutes, oxygen bubbling was ceased, and a solution of PPh₃ (292.0 mg, 1.05 mmol, 2.0

equiv) in CH_2Cl_2 (8.0 mL) was added in one portion. The reaction mixture was warmed to room temperature, stirred for 12 hours, and subsequently concentrated under reduced pressure. Purification by flash column chromatography on silica gel (7:3 hexanes/EtOAc) provided ketone **3.19** (301.0 mg, 74%) as a crunchy foam.

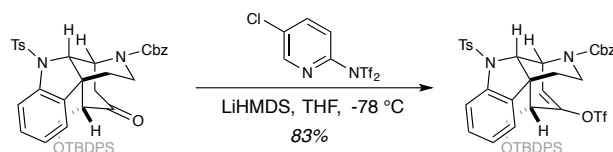
^1H NMR (500 MHz, CDCl_3) (1.0:0.8 mixture of rotamers) δ 7.79 - 7.74 (m, 3.6H), 7.56 - 7.31 (m, 27H), 7.25 - 7.17 (m, 3.6H), 7.00 - 6.92 (m, 3.6H), 6.81 (d, $J = 7.3$ Hz, 1.8H), 5.87 - 5.77 (m, 0.8H), 5.77 - 5.67 (m, 1H), 5.42 (d, $J = 12.3$ Hz, 1H), 5.26 - 5.11 (m, 2.6H), 4.22 (dd, $J = 15.1, 6.2$ Hz, 1H), 4.10 (dd, $J = 15.1, 6.1$ Hz, 0.8H), 3.82 (t, $J = 9.8$ Hz, 0.8H), 3.77 - 3.68 (m, 1H), 3.35 - 3.21 (m, 1.8H), 3.11 (td, $J = 16.3, 3.8$ Hz, 1.8H), 2.86 (d, $J = 9.0$ Hz, 1.8H), 2.79 (dd, $J = 10.6, 5.5$ Hz, 1.8H), 2.65 - 2.55 (m, 3.6H), 2.34 (d, $J = 25.6$ Hz, 5.4H), 2.14 - 2.03 (m, 1.8H), 1.79 (dd, $J = 12.9, 6.7$ Hz, 1.8H), 1.64 (s, 1H), 1.28 (s, 0.8H), 0.99 (s, 16.2H) ppm.

^{13}C NMR (126 MHz, CDCl_3) (1.0:0.8 mixture of rotamers) δ 214.9, 208.6, 155.1, 145.0, 143.0, 136.6, 135.8, 135.7, 133.9, 132.9, 130.9, 130.0, 129.9, 129.8, 129.7, 129.0, 128.9, 128.7, 128.5, 128.4, 128.3, 128.3, 128.0, 127.9, 127.8, 127.7, 124.8, 124.7, 122.6, 122.4, 115.3, 110.1, 68.7, 68.5, 67.9, 62.4, 59.9, 59.7, 52.8, 52.7, 47.5, 46.0, 39.4, 38.8, 37.7, 35.7, 35.4, 27.0, 21.7, 19.2, 10.7, 10.6 ppm.

IR (thin film, cm^{-1}) 3070, 2930, 2857, 1695, 1599, 1456, 1412, 1370, 1306, 1253, 1187, 1171, 1111, 1030, 998, 976, 908, 850, 814, 765, 729, 701, 659, 608, 580, 547.

HRMS (+NSI) calculated for $\text{C}_{46}\text{H}_{49}\text{O}_6\text{N}_2\text{SSi}$ $[\text{M}+\text{H}]^+$ 785.3075, found 785.3082.

Vinyl Triflate 3.48:



A solution of LiHMDS (142.2 mg, 0.85 mmol) in THF (1.85 mL) was cooled to -78 °C. A solution of ketone **3.19** (222.0 mg, 0.28 mmol) in THF (1.0 mL) was added dropwise over ten minutes, and the reaction mixture was stirred for 90 minutes at -78 °C. A solution of Comin's reagent (333.8 mg, 0.85 mmol) in THF (1.0 mL) was added in one portion, and the reaction mixture was stirred at -78 °C for four hours. The reaction mixture was quenched with saturated aqueous NH_4Cl (5.0 mL) and warmed to room temperature. The layers were separated, and the aqueous phase was extracted with Et_2O (3 x 10.0 mL). The combined organic layer was washed with brine (25.0 mL), dried over anhydrous MgSO_4 , filtered, and concentrated under reduced pressure. Purification by flash column chromatography on silica gel (4:1 hexanes/ EtOAc) provided vinyl triflate **3.48** (213.3 mg, 83%) as a crunchy foam.

$^1\text{H NMR}$ (500 MHz, CDCl_3) (1.0:1.0 mixture of rotamers) δ 7.82 (d, $J = 7.9$ Hz, 2H), 7.62 (dd, $J = 8.6, 4.2$ Hz, 2H), 7.55 (d, $J = 7.8$ Hz, 2H), 7.52 – 7.47 (m, 2H), 7.46 – 7.28 (m, 25H), 7.23 – 7.18 (m, 2H), 7.11 (ddd, $J = 8.6, 7.5, 1.6$ Hz, 2H), 6.90 – 6.78 (m, 6H), 6.13 (dd, $J = 7.5, 2.6$ Hz, 1H), 6.05 – 5.92 (m, 4H), 5.39 (d, $J = 12.5$ Hz, 1H), 5.24 – 5.09 (m, 3H), 4.23 (dd, $J = 14.5, 5.5$ Hz, 1H), 4.20 – 4.08 (m, 1H), 3.60 – 3.45 (m, 2H), 3.45 – 3.23 (m, 3H), 3.01 (dd, $J = 11.2, 5.1$ Hz, 2H), 2.92 (s, 3H), 2.69 (s, 4H), 2.43 – 2.23 (m, 6H), 2.20 – 2.06 (m, 2H), 1.77 (dtd, $J = 19.1, 13.1, 5.7$ Hz, 2H), 1.59 (s, 1H), 1.26 (s, 1H), 0.96 (s, 18H) ppm.

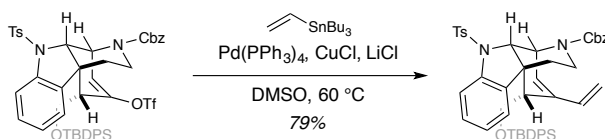
$^{19}\text{F NMR}$ (282 MHz, CDCl_3) (1.0:1.0 mixture of rotamers) δ -72.91, -78.99 ppm.

^{13}C NMR (151 MHz, CDCl_3) (1.0:1.0 mixture of rotamers) δ 173.6, 155.1, 154.5, 154.0, 144.8, 143.1, 141.4, 135.8, 135.7, 135.3, 135.1, 134.8, 132.9, 132.7, 131.0, 130.7, 129.9, 129.5, 128.8, 128.7, 128.6, 128.4, 127.8, 127.5, 127.4, 126.8, 124.7, 124.1, 124.0, 123.8, 123.7, 123.6, 123.1, 119.6, 119.3, 114.5, 113.6, 111.0, 68.9, 67.9, 67.8, 63.4, 63.1, 49.9, 49.7, 48.7, 48.5, 47.1, 45.3, 44.3, 36.2, 35.6, 27.4, 26.9, 24.3, 21.6, 18.9, -1.4 ppm.

IR (thin film, cm^{-1}) 2955, 2928, 2856, 1701, 1375, 1174, 1111, 846, 702, 604.

HRMS (+NSI) calculated for $\text{C}_{47}\text{H}_{48}\text{O}_8\text{N}_2\text{F}_3\text{S}_2\text{Si}$ $[\text{M}+\text{H}]^+$ 917.2568, found 917.2594.

Diene 3.51:



Vinyl triflate **3.48** (197.5 mg, 0.215 mmol, 1.0 equiv) was weighed into a Schlenk flask and brought into a N_2 -filled glove box. CuCl (106.6 mg, 1.077 mmol, 5.0 equiv) and LiCl (54.8 mg, 1.292 mmol, 6.0 equiv) were added to the Schlenk flask. The flask was subsequently sealed and removed from the glove box. $\text{Pd}(\text{Ph}_3)_4$ (24.9 mg, 0.022 mmol, 10 mol %) was then added, and the flask was subjected to three vacuum/ N_2 fill cycles. DMSO (2.2 mL) and vinyltributylstannane (100 μL , 0.323 mmol, 1.5 equiv) were added, and the reaction mixture was then degassed via four freeze/pump/thaw cycles (-78 $^\circ\text{C}$). The resultant slurry was heated to 60 $^\circ\text{C}$ and stirred for 48 hours. The reaction was cooled to room temperature and quenched with 1M aqueous NH_4OH (5.0 mL) and Et_2O (5.0 mL). The resultant biphasic mixture was stirred till both layers were homogenous. The layers were separated, and the aqueous phase was extracted with Et_2O (3 x 5.0 mL). The combined organic phase was washed with 1M potassium fluoride (3 x 10.0 mL) and brine (10.0 mL).

The organic phase was dried over anhydrous MgSO_4 , filtered, and concentrated under reduced pressure. Purification by flash column chromatography on silica gel (9:1 to 4:1 hexanes/EtOAc, 3% Et_3N) provided diene **3.51** (135.3 mg, 79%) as a sticky foam.

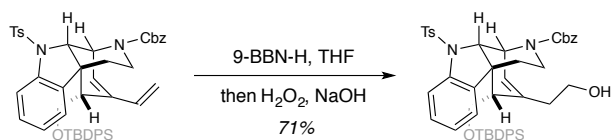
^1H NMR (500 MHz, CDCl_3) (1.0:1.0 mixture of rotamers) δ 7.89 (d, $J = 7.9$ Hz, 2H), 7.72 (d, $J = 8.3$ Hz, 2H), 7.62 (d, $J = 8.0$ Hz, 2H), 7.48 (d, $J = 6.8$ Hz, 6H), 7.44 – 7.20 (m, 30H), 6.97 – 6.85 (m, 4H), 6.01 – 5.74 (, 6H), 5.37 (d, $J = 12.3$ Hz, 1H), 5.14 (td, $J = 21.0, 12.4$ Hz, 3H), 4.92 (d, $J = 17.6$ Hz, 2H), 4.58 (d, $J = 11.0$ Hz, 2H), 4.08 (dd, $J = 15.1, 6.2$ Hz, 1H), 4.00 (dd, $J = 14.0, 4.9$ Hz, 1H), 3.41 (t, $J = 11.5$ Hz, 2H), 3.19 – 2.95 (m, 6H), 2.46 (s, 2H), 2.35 (s, 3H), 2.28 (s, 3H), 2.15 (d, $J = 10.9$ Hz, 1h), 2.09 (d, $J = 11.8$ Hz, 1H), 1.78 (dtd, $J = 18.1, 13.2, 5.7$ Hz, 2H), 0.92 (s, 18H) ppm.

^{13}C NMR (151 MHz, CDCl_3) (1.0:1.0 mixture of rotamers) δ 155.0, 154.9, 154.3, 153.9, 144.8, 144.3, 144.2, 143.8, 143.6, 143.5, 136.7, 136.6, 136.5, 136.4, 136.3, 136.0, 135.7, 135.3, 135.2, 135.0, 134.8, 133.4, 133.3, 131.4, 129.8, 129.7, 129.6, 129.4, 128.8, 128.5, 128.3, 128.1, 127.9, 127.8, 127.5, 127.3, 126.8, 124.7, 124.6, 124.5, 123.8, 123.5, 123.1, 119.9, 119.6, 119.5, 119.2, 114.5, 114.3, 114.0, 113.6, 70.1, 69.8, 68.5, 67.5, 67.4, 65.4, 65.3, 49.0, 48.8, 48.2, 44.1, 43.0, 37.0, 36.4, 36.1, 36.0, 29.7, 27.5, 27.0, 26.9, 26.6, 24.6, 21.6, 21.5, 20.9, 18.8 ppm.

IR (thin film, cm^{-1}) 3045, 2931, 2858, 1693, 1414, 1358, 1170, 1104, 1081, 910, 734, 702, 584.

HRMS (+NSI) calculated for $\text{C}_{48}\text{H}_{51}\text{O}_5\text{N}_2\text{SSi}$ $[\text{M}+\text{H}]^+$ 795.3283, found 795.3298.

Alcohol 3.58:



A solution of 9-BBN-H dimer (g, 0.518 mmol, 2.5 equiv) in THF (1.1 mL) was cooled to 0 °C. A solution of diene **3.51** (164.6 mg, 0.207 mmol, 1.0 equiv) in THF (1.1 mL) was added, and the reaction was warmed to room temperature and stirred for 24 hours. The reaction was cooled to 0 °C, and 2 N sodium hydroxide (2.1 mL) and 30 % hydrogen peroxide (2.1 mL) were slowly added. The mixture was stirred for one hour, and diethyl ether (10.0 mL) and water (10.0 mL) were added. The layers were separated, and the aqueous phase was extracted with diethyl ether (3 x 10.0 mL). The combined organic layer was washed with brine (25.0 mL), dried over anhydrous MgSO₄, filtered, and concentrated under reduced pressure. Purification by flash column chromatography on silica gel (3:2 to 1:1 hexanes/EtOAc) provided alcohol **3.58** (119.4 mg, 71%) as a sticky foam.

¹H NMR (600 MHz, CD₃OD) (1.0:0.8 mixture of rotamers) δ 7.80 (d, *J* = 8.1 Hz, 2H), 7.59 (dd, *J* = 13.5, 8.2 Hz, 3.6 Hz, 3.6H), 7.51 (d, *J* = 7.4 Hz, 1.8H) 7.45 – 7.27 (m, 24.6H), 7.19 (d, *J* = 8.0 Hz, 2H), 7.12 (t, *J* = 7.8 Hz, 1.8H), 6.97 (d, *J* = 8.0 Hz, 1.8H), 6.91 – 6.79 (m, 2.8H), 5.82 (d, *J* = 6.3 Hz, 1H), 5.74 (d, *J* = 8.0 Hz, 0.8H), 5.62 (t, *J* = 5.0 Hz, 1.8H), 5.36 (d, *J* = 12.4 Hz, 0.8 Hz), 5.22 – 5.09 (m, 2.8H), 4.03 – 3.93 (m, 1.8H), 4.04 – 3.94 (m, 3.6H), 3.44 – 3.36 (m, 1.8H), 3.31 – 3.25 (m, 1.8H), 2.89 – 2.81 (m, 3.6H), 2.51 – 2.45 (m, 1.8H), 2.40 – 2.23 (m, 9H), 2.09 (dd, *J* = 21.2, 13.9 Hz, 1.8H), 1.67 – 1.55 (m, 3.6H), 0.92 (s, 16.2H) ppm.

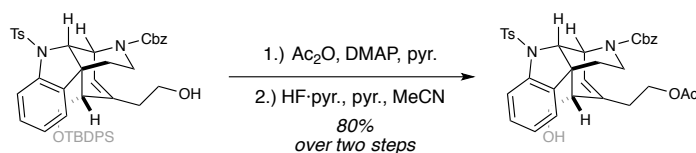
¹³C NMR (151 MHz, CD₃OD) (1.0:0.8 mixture of rotamers) δ 156.9, 156.4, 146.2, 145.9, 144.5, 144.4, 138.3, 138.2, 136.9, 134.5, 134.3, 132.5, 132.2, 130.9, 130.8, 130.7, 129.8,

129.6, 129.5, 129.4, 129.3, 129.1, 129.0, 128.7, 128.6, 125.3, 124.9, 119.0, 118.9, 115.6, 72.8, 71.3, 71.1, 68.7, 68.5, 66.9, 61.1, 50.3, 50.1, 44.8, 42.6, 39.9, 38.0, 37.3, 37.1, 37.0, 35.3, 34.2, 30.8, 28.6, 27.5, 26.3, 23.8, 21.5, 21.4, 19.7 ppm.

IR (thin film, cm^{-1}) 3408, 2923, 2853, 1684, 1456, 1418, 1357, 1285, 1254, 1169, 1112, 1072, 908, 730, 701, 613, 583.

HRMS (+NSI) calculated for $\text{C}_{48}\text{H}_{53}\text{O}_6\text{N}_2\text{SSi}$ $[\text{M}+\text{H}]^+$ 813.3388, found 813.3390.

Homoallylic Alcohol **3.59**:



To a solution of alcohol **3.58** (66.5 mg, 0.082 mmol, 1.0 equiv) in pyridine (0.9 mL) was added DMAP (99.8 mg, .817 mmol, 10 equiv) and acetic anhydride (80 μL , 0.817 mmol, 10 equiv). The reaction mixture was stirred for six hours at room temperature. The reaction was quenched with saturated sodium bicarbonate solution (5.0 mL) and ethyl ether (5.0 mL), and the layers were separated. The organic layer was washed with water (5.0 mL), saturated aqueous CuSO_4 (5.0 mL), and brine (5.0 mL). The organic layer was dried over anhydrous MgSO_4 , filtered, and concentrated under reduced pressure. The crude residue was brought up in CH_3CN (0.8 mL) and HF-pyridine (0.9 mL) and pyridine (0.9 mL) were added. The reaction was stirred for eight hours at room temperature. The reaction mixture was quenched with saturated sodium bicarbonate (5.0 mL) and ethyl acetate (5.0 mL), and the layers were separated. The organic layer was washed with water (5.0 mL), saturated

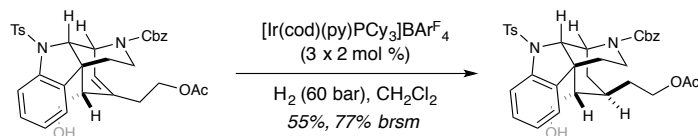
aqueous CuSO_4 (5.0 mL), and brine (5.0 mL). The organic layer was dried over anhydrous Na_2SO_4 , filtered, and concentrated under reduced pressure. Purification by flash column chromatography on silica gel (1:1 hexanes/EtOAc) provided homoallylic alcohol **3.59** (40.5 mg, 80% over two steps) as a sticky foam.

^1H NMR (500 MHz, CDCl_3) (1:0.5 mixture of rotamers) δ 7.90 (d, $J = 7.5$ Hz, 1.5H), 7.78 (d, $J = 7.4$ Hz, 1.5H), 7.61 (d, $J = 7.7$ Hz, 1.5H), 7.51 (d, $J = 7.0$ Hz, 1.5H), 7.45 – 7.31 (m, 4.5H), 7.31 – 7.27 (m, 3H), 7.22 (d, $J = 7.3$ Hz, 1.5 H), 7.07 (d, $J = 5.9$ Hz, 3H), 6.90 (d, $J = 7.6$ Hz, 1.5Hz), 6.00 – 5.73 (m, 3H), 5.39 (d, $J = 12.3$ Hz, 1H), 5.24 – 5.08 m, 2H), 4.31 – 4.31 (m, 3H), 4.16 – 3.99 (m, 1.5H), 3.39 – 3.27 (m, 1.5H), 3.20 (dt, $J = 27.4, 13.0$ Hz, 1.5H), 2.99 (s, 1.5H), 2.80 (d, $J = 10.2$ Hz, 1.5H), 2.64 (s, 3H), 2.43 – 2.23 (m, 6H), 2.10 – 1.96 (m, 6H), 1.85 – 1.68 (m, 1.5H), 1.50 (s, 1.5H) ppm.

^{13}C NMR (126 MHz, CDCl_3) (1:0.5 mixture of rotamers) δ 171.1, 155.2, 154.9, 144.9, 142.9, 141.7, 141.5, 137.0, 136.9, 130.9, 129.9, 129.8, 128.9, 128.8, 128.6, 128.5, 128.4, 128.2, 127.9, 124.6, 124.4, 123.2, 123.1, 120.4, 120.1, 115.6, 69.5, 69.3, 67.7, 67.5, 62.6, 62.4, 62.0, 48.7, 48.6, 48.4, 44.0, 36.6, 36.0, 35.8, 34.6, 29.8, 21.7, 21.6, 21.1 ppm.

IR (thin film, cm^{-1}) 3534, 2923, 1734, 1687, 1455, 1414, 1357, 1284, 1237, 1169, 1122, 1092, 762, 731, 582.

HRMS (+NSI) calculated for $\text{C}_{34}\text{H}_{37}\text{O}_7\text{N}_2\text{S}$ $[\text{M}+\text{H}]^+$ 617.2316, found 617.2319.

Alcohol 3.60:

To a solution of homoallylic alcohol **X** (27.4 mg, 0.044 mmol) in CH_2Cl_2 (0.5 mL) was added $[\text{Ir}(\text{cod})(\text{py})(\text{PCy}_3)]\text{BARF}_4$ (1.4 mg, 0.0009 mmol, 2 mol %). The solution was subjected to hydrogen gas (60 bar) for 36 hours. The reaction mixture was depressurized, and additional $[\text{Ir}(\text{cod})(\text{py})(\text{PCy}_3)]\text{BARF}_4$ (1.4 mg, 0.0009 mmol, 2 mol %) was added. The solution was resubjected to hydrogen gas (60 bar) for 36 hours. The reaction mixture was depressurized, and additional $[\text{Ir}(\text{cod})(\text{py})(\text{PCy}_3)]\text{BARF}_4$ (1.4 mg, 0.0009 mmol, 2.4 mol %) was added. The reaction mixture was resubjected to hydrogen gas (60 bar) for 36 hours. The reaction mixture was depressurized and concentrated under reduced pressure. Purification by column chromatography on silica gel (1:1 hexanes/EtOAc) provided reduced alcohol **3.60** (15.0 mg, 55%) as a sticky foam. Additionally, starting material was recovered from the reaction mixture (6.3 mg, 23%).

Assignment of relative stereochemistry was accomplished by examination of COSY and NOESY spectra (vide infra).

$^1\text{H NMR}$ (500 MHz, CDCl_3) (1.0:0.7 mixture of rotamers) δ 7.80 (t, $J = 9.0$ Hz, 3.4H), 7.57 (d, $J = 8.0$ Hz, 1.7H), 7.50 (d, $J = 7.4$ Hz, 1.7H), 7.44 (t, $J = 7.4$ Hz, 1.7H), 7.38 (s, 3.4H), 7.32 – 7.21 (m, 6.8H), 7.10 – 6.98 (m, 3.4H), 5.66 (d, $J = 9.0$ Hz, 0.7H), 5.58 (d, $J = 7.7$ Hz, 1H), 5.38 (d, $J = 12.4$ Hz, 1H), 5.26 – 5.10 (m, 2.4H), 4.23 – 4.02 (m, 5.1H), 3.58 (d, $J = 11.9$ Hz, 1.7H), 3.47 – 3.32 (m, 1.7H), 3.30 – 3.21 (m, 1.7H), 2.94 – 2.83 (m, 1.7H),

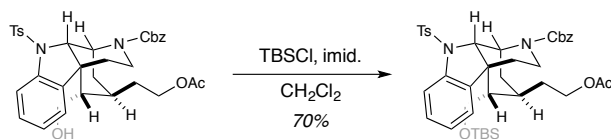
2.85 – 2.71 (m, 1.7H), 2.55 (s, 1.7H), 2.37 (s, 2.1H), 2.32 (s, 3H), 2.16 – 2.00 (m, 6.8H), 1.99 – 1.90 (m, 1.7H), 1.90 – 1.57 (m, 5.1H), 1.44 – 1.28 (m, 3.4H) ppm.

^{13}C NMR (126 MHz, CDCl_3) (1.0:0.7 mixture of rotamers) δ 171.3, 155.7, 155.0, 144.7, 144.6, 143.5, 136.8, 136.7, 135.0, 134.9, 131.4, 129.9, 128.7, 128.2, 127.8, 124.3, 124.0, 123.8, 114.7, 71.1, 70.8, 67.6, 62.3, 61.1, 61.0, 60.5, 48.5, 48.4, 47.2, 47.1, 43.5, 36.9, 35.2, 34.7, 33.2, 32.6, 32.1, 29.8, 26.5, 26.3, 21.6, 21.2, 14.3 ppm.

IR (thin film, cm^{-1}) 3533, 2922, 1733, 1686, 1454, 1413, 1356, 1284, 1236, 1168, 1121, 1091, 761, 730, 582.

HRMS (-NSI) calculated for $\text{C}_{34}\text{H}_{37}\text{O}_7\text{N}_2\text{S}$ $[\text{M}-\text{H}]^-$ 617.2316, found 617.2319.

TBS Ether **3.61**:



A solution of alcohol **3.60** (34.9 mg, 0.0564 mmol, 1.0 equiv) in CH_2Cl_2 (0.56 mL) was cooled to 0 °C. TBSCl (9.3 mg, 0.0620 mmol, 1.1 equiv) and imidazole (8.4 mg, 0.1241, 2.2 equiv) were added, and the reaction mixture was warmed to room temperature and stirred 16 hours. The mixture was quenched with saturated aqueous NH_4Cl (2.0 mL) and CH_2Cl_2 (2.0 mL), and the layers were separated. The aqueous phase was extracted with CH_2Cl_2 (3 x 2.0 mL). The combined organic layer was dried over anhydrous Na_2SO_4 , filtered, and concentrated under reduced pressure. Purification by column chromatography

on silica gel (7:3 hexanes/EtOAc) provided TBS ether **3.61** (29.1 mg, 70%) as a colorless oil.

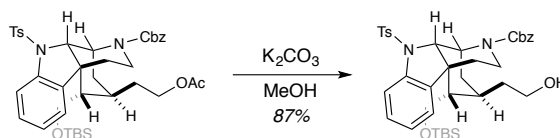
¹H NMR (500 MHz, CDCl₃) (1.0:1.0 mixture of rotamers) δ 7.77 (d, J = 13.9, 8.1 Hz, 3H), 7.58 (d, J = 7.8 Hz, 2H), 7.50 (d, J = 7.6 Hz, 2H), 7.44 (t, J = 7.3 Hz, 2H), 7.41 – 7.34 (m, 5H), 7.32 – 7.26 (m, 3H), 7.23 (t, J = 7.6 Hz, 5H), 7.03 (d, J = 7.9 Hz, 2H), 6.97 (q, J = 7.3 Hz, 2H), 5.63 (d, J = 9.2 Hz, 1H), 5.53 (d, J = 6.8 Hz, 1H), 5.37 (d, J = 12.4 Hz, 1H), 5.26 – 5.11 (m, 3H), 4.19 – 3.99 (m, 6H), 3.51 – 3.34 (m, 4H), 2.92 – 2.83 (m, 4H), 2.76 (tt, J = 15.7, 8.2 Hz, 2H), 2.35 (d, J = 20.7 Hz, 6H), 2.31 – 2.17 (m, 4H), 2.07 (s, 6H), 1.91 – 1.72 (m, 4H), 1.71 – 1.57 (m, 2H), 1.44 – 1.29 (m, 4H), 0.86 (s, 18H), -0.06 (d, J = 19.6 Hz, 12H) ppm.

¹³C NMR (126 MHz, CDCl₃) (1.0:1.0 mixture of rotamers) δ 171.3, 155.8, 155.7, 144.5, 144.4, 143.4, 136.9, 134.9, 134.8, 129.9, 128.8, 128.3, 128.1, 127.8, 125.7, 123.2, 123.1, 114.3, 71.3, 71.0, 67.5, 62.3, 62.2, 48.8, 48.7, 47.7, 47.5, 43.8, 37.4, 37.1, 35.7, 35.2, 33.3, 33.2, 32.7, 27.0, 26.8, 26.1, 21.1, 18.3, -5.3, -5.4 ppm.

IR (thin film, cm⁻¹) 2952, 1736, 1693, 1238, 1184, 1170, 1071, 1005, 754, 732, 606, 546.

HRMS (+NSI) calculated for C₄₀H₅₃O₇N₂SSi [M+H]⁺ 733.3337, found 733.3348.

Alcohol 3.62:



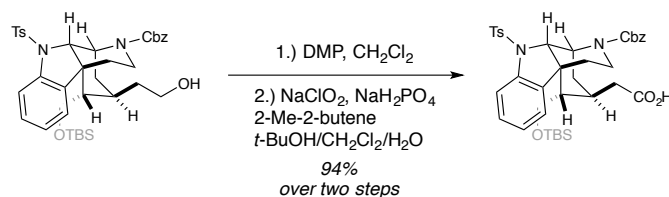
To a solution of TBS ether **3.61** (13.3 mg, 0.0181 mmol, 1.0 equiv) in MeOH (1.8 mL) was added K_2CO_3 (25.1 mg, 0.1814 mmol, 10 equiv), and the resultant mixture was stirred for 18 hours. The reaction was quenched with water (5.0 mL) and CH_2Cl_2 (5.0 mL), and the layers were separated. The aqueous phase was extracted with CH_2Cl_2 (3 x 5.0 mL). The combined organic layer was dried over anhydrous Na_2SO_4 and filtered. The solution was concentrated under reduced pressure to provide alcohol **3.62** (10.9 mg, 87%) as a colorless oil, which was used without further purification.

1H NMR (500 MHz, $CDCl_3$) (1.0:1.0 mixture of rotamers) δ 7.75 (t, $J = 9.6$ Hz, 3H), 7.56 (d, $J = 7.9$ Hz, 2H), 7.48 (d, $J = 7.1$ Hz, 2H), 7.45 – 7.32 (m, 7H), 7.29 (d, $J = 6.7$ Hz, 2H), 7.21 (t, $J = 7.2$ Hz, 5H), 7.06 – 6.92 (m, 4H), 5.59 (d, $J = 7.1$ Hz, 1H), 5.51 (d, $J = 8.1$ Hz, 1H), 5.34 (d, $J = 12.4$ Hz, 1H), 5.25 – 5.08 (m, 3H), 4.11 – 3.96 (m, 2H), 3.79 – 3.57 (m, 4H), 3.53 – 3.38 (m, 4H), 2.87 (s, 2H), 2.84 – 2.77 (m, 2H), 2.77 – 2.64 (m, 2H), 2.38 – 2.17 (m, 10H), 1.87 – 1.73 (m, 5H), 1.67 – 1.54 (m, 3H), 1.42 – 1.28 (m, 2H), 0.85 (s, 18H), -0.07 (d, $J = 14.1$ Hz, 12H) ppm.

^{13}C NMR (126 MHz, $CDCl_3$) δ 158.2, 158.0, 155.9, 155.7, 144.6, 144.4, 143.4, 137.0, 136.8, 134.9, 131.5, 131.4, 129.9, 128.8, 128.7, 128.3, 128.1, 127.9, 125.8, 123.3, 123.1, 114.3, 71.3, 71.0, 67.5, 62.7, 62.6, 60.5, 48.9, 48.8, 47.8, 47.5, 43.8, 37.7, 37.5, 35.7, 35.3, 33.4, 32.8, 29.8, 27.1, 27.0, 26.1, 21.7, 18.3, -5.3, -5.4 ppm.

IR (thin film, cm^{-1}) 3428, 2951, 2927, 1692, 1494, 1456, 1360, 1255, 1170, 1112, 1088, 1067, 837, 814, 737, 658, 605, 547.

HRMS (+NSI) calculated for $C_{38}H_{50}O_6N_2KSSi$ $[M+K]^+$ 729.2790, found 729.2804.

Carboxylic Acid 3.63:

To a solution of alcohol **3.62** (7.4 mg, 0.011 mmol, 1.0 equiv) in CH₂Cl₂ (0.5 mL) was added K₂CO₃ (15.2 mg, 0.11 mmol) and DMP (6.7 mg, 0.016 mmol, 1.5 equiv), and the reaction was stirred for 12 hours. The reaction mixture was quenched with saturated aqueous Na₂SO₃ (5.0 mL) and CH₂Cl₂ (5.0 mL), and the biphasic mixture was stirred for 30 minutes until both layers were clear. The layers were separated, and the aqueous phase was extracted with CH₂Cl₂ (3 x 5.0 mL). The combined organic layer was dried over Na₂SO₄, filtered, and concentrated in vacuo. The crude residue was brought up in *t*-BuOH (0.25 mL) and CH₂Cl₂ (0.5 mL), and 2-methyl-2-butene (0.5 mL) was added. A solution of NaClO₂ (19.0 mg, 0.210 mmol, 20.0 equiv) and NaH₂PO₄ (30.2 mg, 0.252 mmol, 24.0 equiv) in water was added, and the reaction mixture was stirred for three hours. The reaction was quenched with water (10.0 mL) and EtOAc (10.0 mL), and the layers were separated. The aqueous phase was extracted with EtOAc (3 x 10.0 mL). The combined organic was washed with brine, dried over anhydrous Na₂SO₄, filtered, and concentrated under reduced pressure. Purification by preparatory thin layer chromatography on silica gel (1:1 hexanes/EtOAc) provided carboxylic acid **3.63** (7.1 mg, 94% over two steps) as a sticky foam.

¹H NMR (500 MHz, CDCl₃) (1.0:1.0 mixture of rotamers) δ 7.78 (d, *J* = 8.1 Hz, 2H), 7.74 (d, *J* = 8.2 Hz, 2H), 7.55 (d, *J* = 8.1 Hz, 2H), 7.47 (d, *J* = 7.3 Hz, 2H), 7.41 (t, *J* = 7.4 Hz, 3H), 7.38 – 7.30 (m, 5H), 7.23 – 7.15 (m, 6H), 7.03 – 6.91 (m, 4H), 5.66 (d, *J* = 8.5 Hz,

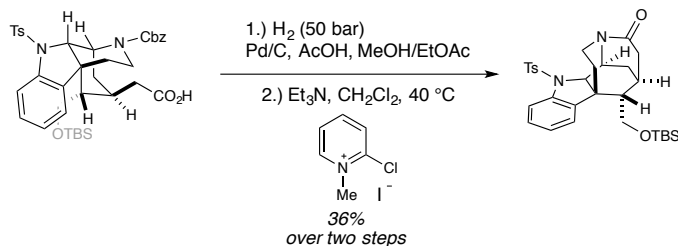
1H), 5.56 (d, $J = 7.9$ Hz, 1H), 5.37 (d, $J = 12.4$ Hz, 1H), 5.25 – 5.07 (m, 3H), 4.18 – 4.01 (m, 2H), 3.54 – 3.39 (m, 2H), 3.18 (dd, $J = 10.5, 4.7$ Hz, 2H), 3.08 (dd, $J = 10.4, 7.0$ Hz, 2H), 2.86 (s, 2H), 2.80 – 2.63 (m, 4H), 2.42 (td, $J = 17.6, 4.8$ Hz, 3H), 2.32 (d, $J = 24.7$ Hz, 9H), 2.21 – 1.99 (m, 5H), 1.72 – 1.55 (m, 3H), 0.81 (s, 18H), -0.06 (s, 6H), -0.11 (s, 6H) ppm.

^{13}C NMR (151 MHz, CDCl_3) (1.0:1.0 mixture of rotamers) δ 176.2, 155.6, 155.4, 144.5, 144.3, 143.3, 136.8, 136.7, 134.7, 134.5, 131.4, 131.3, 129.8, 128.7, 128.5, 128.3, 128.2, 128.0, 127.9, 127.8, 125.1, 125.0, 123.2, 122.9, 114.4, 114.3, 71.4, 71.1, 67.4, 63.6, 63.4, 60.4, 56.0, 48.6, 48.5, 45.6, 45.5, 43.5, 38.5, 38.3, 37.0, 36.8, 35.7, 35.1, 32.8, 32.1, 31.9, 29.7, 27.9, 27.8, 25.9, 22.7, 21.5, 21.1, 18.2, 14.2, 14.1, -5.5, -5.7 ppm.

IR (thin film, cm^{-1}) 2952, 2927, 2855, 1698, 1469, 1257, 1171, 1122, 1083, 837, 754, 585.

HRMS (+NSI) calculated for $\text{C}_{38}\text{H}_{49}\text{O}_7\text{N}_2\text{SSi}$ $[\text{M}+\text{H}]^+$ 705.3024, found 705.3033.

Pentacycle 3.64:



To a solution of carboxylic acid **3.63** (7.1 mg, 0.0105 mmol, 1.0 equiv) in EtOAc (0.25 mL) and MeOH (0.25 mL) was added Pd/C (10 % w/w, 1.1 mg, 10 mol %) and AcOH (0.25 mL). The reaction mixture was placed under hydrogen pressure (50 bar) and was stirred for five days. The reaction was depressurized and was diluted with MeOH (2.0 mL).

The reaction mixture was filtered, and the filter cake was rinsed with MeOH (5 x 2.0 mL). The reaction mixture was concentrated under reduced pressure. The crude residue was brought up in CH₂Cl₂ (1.0 mL) and transferred to a pressure vessel. Et₃N (30 μL, 0.21 mmol, 20.0 equiv) and Mukaiyama's reagent (13.4 mg, 0.0525 mmol, 5.0 equiv) were added, and the reaction was sealed and heated to 40 °C. The reaction mixture was stirred for three days. The reaction mixture was cooled to room temperature and concentrated under reduced pressure. Purification by preparatory thin layer chromatography on silica gel (1:1 hexanes/EtOAc) provided pentacycle **3.64** (2.1 mg, 36% over two steps) as a colorless oil.

Structural assignment was confirmed by examination of COSY, HMQC, and HMBC spectra (vide infra).

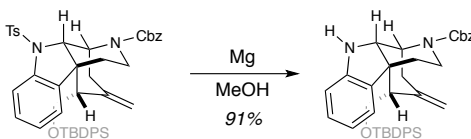
¹H NMR (600 MHz, CDCl₃) δ 7.72 (d, *J* = 8.2 Hz, 1H), 7.69 (d, *J* = 8.3 Hz, 2H), 7.28 (d, *J* = 8.1 Hz, 2H), 7.22 (t, *J* = 8.5 Hz, 1H), 7.01 (t, *J* = 7.7 Hz, 1H), 6.96 (d, *J* = 7.3 Hz, 1H), 4.55 (dd, *J* = 13.9, 7.8 Hz, 1H), 4.52 (t, *J* = 5.6 Hz, 1H), 3.52 (d, *J* = 5.5 Hz, 1H), 2.99 (dt, *J* = 14.1, 4.4 Hz, 1H), 2.90 (ddd, *J* = 13.8, 10.7, 6.0 Hz, 1H), 2.79 (t, *J* = 10.3 Hz, 1H), 2.64 (s, 1H), 2.59 (dd, *J* = 9.9, 4.1 Hz, 1H), 2.56 (d, *J* = 3.6 Hz, 1H), 2.51 (t, *J* = 3.0 Hz, 1H), 2.49 – 2.41 (m, 1H), p2.38 (s, 3H), 1.89 (dd, *J* = 13.2, 6.0 Hz, 1H), 1.81 (dd, *J* = 14.2, 5.7 Hz, 1H), 1.53 (dd, *J* = 10.5, 4.1 Hz, 1H), 0.75 (s, 9H), -0.19 (s, 6H) ppm.

¹³C NMR (151 MHz, CDCl₃) δ 181.0, 145.2, 143.4, 136.3, 131.2, 130.0, 128.4, 124.4, 124.2, 115.3, 67.1, 64.3, 56.1, 53.7, 51.6, 45.6, 44.8, 42.7, 41.4, 32.1, 29.9, 28.7, 26.0, 24.0, 22.9, 21.8, 18.2, 14.3, -5.4 ppm.

IR (thin film, cm⁻¹) 2953, 2925, 2854, 1662, 1459, 1340, 1170, 1090, 938, 778, 665, 582.

HRMS (+NSI) calculated for $C_{30}H_{41}O_4N_2SSi$ $[M+H]^+$ 553.2551, found 553.2570.

N-H Indoline 3.67:



To a solution of indoline **3.6** (37.9 mg, 0.060 mmol, 1.0 equiv) in DMSO (0.6 mL) is added IBX (168.0 mg, 0.6 mmol, 10 equiv), and the reaction mixture is stirred for 14 hours. The mixture is quenched with saturated aqueous Na_2SO_3 (5.0 mL) and EtOAc (5.0 mL), and the layers are separated. The aqueous layer is extracted with EtOAc (3 x 5.0 mL). The combined organic layer is washed with brine (10.0 mL), dried over anhydrous Na_2SO_4 , filtered, and concentrated under reduced pressure. Purification by flash column chromatography on silica gel (4:1 hexanes/EtOAc) provided N-H indoline **3.67** (17.4 mg, 46%) as colorless oil.

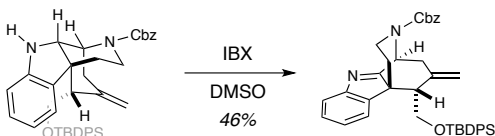
1H NMR (500 MHz, $CDCl_3$) (1.0:1.0 mixture of rotamers) δ 7.74 (d, $J = 7.3$ Hz, 2H), 7.56 – 7.18 (m, 32H), 7.02 (dd, $J = 18.8, 6.9$ Hz, 4H), 5.44 (d, $J = 32.5$ Hz, 2H), 5.31 – 5.06 (m, 8H), 4.03 (td, $J = 13.8, 4.3$ Hz, 2H), 3.73 (d, $J = 10.7$ Hz, 1H), 3.60 (d, $J = 13.2$ Hz, 2H), 3.33 – 3.24 (m, 2H), 3.22 – 2.97 (m, 8H), 2.52 – 2.39 (m, 2H), 1.57 – 1.45 (m, 2H), 0.85 (d, $J = 8.5$ Hz, 18H) ppm.

^{13}C NMR (126 MHz, $CDCl_3$) (1.0:1.0 mixture of rotamers) δ 184.1, 155.8, 155.2, 145.6, 142.8, 136.5, 135.4, 135.3, 132.7, 132.3, 129.5, 129.4, 128.6, 128.1, 128.0, 127.5, 125.5, 125.4, 122.7, 122.6, 122.0, 115.4, 67.5, 66.4, 55.4, 55.2, 52.8, 52.7, 41.3, 40.3, 39.4, 39.3, 38.8, 38.6, 29.7, 26.5, 18.9 ppm.

IR (thin film, cm^{-1}) 3069, 2929, 2856, 1697, 1414, 1105, 736, 702.

HRMS (+NSI) calculated for $\text{C}_{40}\text{H}_{43}\text{O}_3\text{N}_2\text{Si}$ $[\text{M}+\text{H}]^+$ 627.3038, found 627.3040.

Indolenine 3.68:



To a solution of indoline **3.67** (37.9 mg, 0.060 mmol, 1.0 equiv) in DMSO (0.6 mL) is added IBX (168.0 mg, 0.6 mmol, 10 equiv), and the reaction mixture is stirred for 14 hours. The mixture is quenched with saturated aqueous Na_2SO_3 (5.0 mL) and EtOAc (5.0 mL), and the layers are separated. The aqueous layer is extracted with EtOAc (3 x 5.0 mL). The combined organic layer is washed with brine (10.0 mL), dried over anhydrous Na_2SO_4 , filtered, and concentrated under reduced pressure. Purification by flash column chromatography on silica gel (4:1 hexanes/EtOAc) provided indolenine **3.68** (17.4 mg, 46%) as colorless oil.

Structural assignment was confirmed by examination of COSY, HMQC, and HMBC spectra (vide infra).

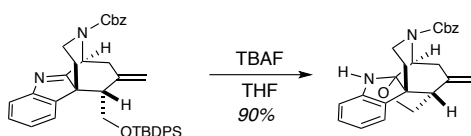
^1H NMR (500 MHz, CDCl_3) (1.0:1.0 mixture of rotamers) δ 7.74 (d, $J = 7.3$ Hz, 2H), 7.56 – 7.18 (m, 32H), 7.02 (dd, $J = 18.8, 6.9$ Hz, 4H), 5.44 (d, $J = 32.5$ Hz, 2H), 5.31 – 5.06 (m, 8H), 4.03 (td, $J = 13.8, 4.3$ Hz, 2H), 3.73 (d, $J = 10.7$ Hz, 1H), 3.60 (d, $J = 13.2$ Hz, 2H), 3.33 – 3.24 (m, 2H), 3.22 – 2.97 (m, 8H), 2.52 – 2.39 (m, 2H), 1.57 – 1.45 (m, 2H), 0.85 (d, $J = 8.5$ Hz, 18H) ppm.

^{13}C NMR (126 MHz, CDCl_3) (1.0:1.0 mixture of rotamers) δ 184.1, 155.8, 155.2, 145.6, 142.8, 136.5, 135.4, 135.3, 132.7, 132.3, 129.5, 129.4, 128.6, 128.1, 128.0, 127.5, 125.5, 125.4, 122.7, 122.6, 122.0, 115.4, 67.5, 66.4, 55.4, 55.2, 52.8, 52.7, 41.3, 40.3, 39.4, 39.3, 38.8, 38.6, 29.7, 26.5, 18.9 ppm.

IR (thin film, cm^{-1}) 3069, 2929, 2856, 1697, 1414, 1105, 736, 702.

HRMS (+NSI) calculated for $\text{C}_{40}\text{H}_{43}\text{O}_3\text{N}_2\text{Si}$ $[\text{M}+\text{H}]^+$ 627.3038, found 627.3040.

Furoindoline **3.65**:



To a solution of indolenine **3.68** (5.1 mg, 0.008 mmol, 1.0 equiv) in THF (0.04 mL) was added TBAF solution (1.0 M in THF, 0.04 mL, 0.040 mmol, 5.0 equiv), and the mixture was stirred for 24 hours. The reaction was quenched with saturated aqueous NH_4Cl (1.0 mL) and EtOAc (1.0 mL), and the layers were separated. The aqueous phase was extracted with EtOAc (3 x 2.0 mL). The combined organic was washed with brine (5.0 mL), dried over Na_2SO_4 , filtered, and concentrated under reduced pressure. Purification by preparatory thin layer chromatography on silica gel (4:1 hexanes/EtOAc) provided furoindoline **3.65** (2.8 mg, 90%) as a sticky foam.

Structural assignment was confirmed by examination of COSY, HMQC, and HMBC spectra (vide infra).

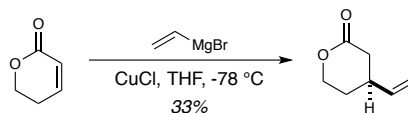
^1H NMR (500 MHz, CDCl_3) (1.0:1.0 mixture of rotamers) δ 7.44 – 7.30 (m, 10H), 7.18 – 7.08 (m, 4H), 6.89 – 6.78 (m, 3H), 6.72 (d, $J = 7.7$ Hz, 1H), 5.27 (d, $J = 12.3$ Hz, 1H), 5.22 – 5.07 (m, 3H), 4.98 (s, 2H), 4.93 (s, 2H), 4.79 (d, $J = 6.0$ Hz, 1H), 4.75 (bs, 1H), 4.66 (d, $J = 6.0$ Hz, 1H), 4.45 (bs, 1H), 3.73 (d, $J = 15.1$ Hz, 4H), 3.69 – 3.60 (m, 2H), 3.58 – 3.44 (m, 2H), 3.34 (s, 2H), 3.04 – 2.86 (m, 2H), 2.56 – 2.44 (m, 2H), 2.24 – 2.13 (m, 2H), 1.64 – 1.53 (m, 2H) ppm.

^{13}C NMR (126 MHz, CDCl_3) (1.0:1.0 mixture of rotamers) δ 155.8, 155.5, 148.7, 148.4, 147.5, 147.3, 136.8, 136.7, 134.6, 128.6, 128.4, 128.2, 128.1, 127.9, 127.7, 122.0, 121.9, 120.3, 120.2, 112.0, 111.9, 111.0, 110.9, 99.5, 99.3, 74.7, 67.2, 67.0, 56.0, 52.9, 52.8, 52.7, 52.5, 52.3, 52.2, 37.4, 37.2, 35.5, 35.3, 32.0, 31.5, 29.7 ppm.

IR (thin film, cm^{-1}) 3311, 2927, 1693, 1246, 1099, 1016, 744.

HRMS (+NSI) calculated for $\text{C}_{24}\text{H}_{25}\text{O}_3\text{N}_2$ $[\text{M}+\text{H}]^+$ 389.1860, found 389.1859.

Alkene 3.74:

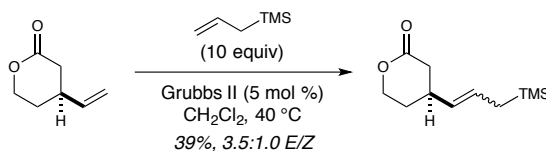


A solution of vinylmagnesium bromide (1.0 M in THF, 17.3 mL, 17.3 mmol, 1.5 equiv) was added to CuCl (1.71 g, 17.3 mmol, 1.5 equiv) at -78 $^\circ\text{C}$, and the resultant slurry was stirred for one hour. A solution of unsaturated lactone **3.73** (1.13 g, 11.5 mmol, 1.0 equiv) in THF (60.0 mL) was then added drop-wise over ten minutes, and the reaction mixture was then stirred at -78 $^\circ\text{C}$ for two hours. The reaction was quenched with 1:1 saturated aqueous NH_4OH /saturated aqueous NH_4Cl (100.0 mL), and was warmed to room

temperature. The layers were separated, and the aqueous phase was extracted with ether (3 x 50.0 mL). The combined organic layer was washed with saturated aqueous NH_4Cl (3 x 50.0 mL) and brine (50.0 mL), dried over anhydrous MgSO_4 , filtered, and concentrated under reduced pressure. Purification by Kugelrohr distillation provided alkene **3.74** (473.3 mg, 33%) as a colorless oil. Spectral data matched that previously reported.³⁰

^1H NMR (500 MHz, CDCl_3) δ 5.79 (ddd, $J = 16.8, 10.8, 6.1$ Hz, 1H), 5.17-4.98 (m, 2H), 4.45 (dt, $J = 11.3, 4.7$ Hz, 1H), 4.31 (ddd, $J = 11.3, 10.1, 3.9$ Hz, 1H), 2.78-2.62 (m, 2H), 2.49-2.27 (m, 1H), 2.08-1.95 (m, 1H), 1.76-1.67 (m, 1H) ppm.

Allylsilane **3.75**:



To a solution of of alkene **3.74** (357.7 mg, 2.84 mmol, 1.0 equiv) in CH_2Cl_2 (14.2 mL) was added second generation Grubbs catalyst (120.6 mg, 0.142 mmol, 5 mol %) and allyltrimethylsilane (4.5 mL, 28.4 mmol, 10.0 equiv). The reaction mixture was heated to reflux for 18 hours. The reaction mixture was cooled to room temperature and then concentrated under reduced pressure. Purification by flash column chromatography on silica gel (95:5 pentane/ Et_2O) provided allylsilane **3.75** (237.5 mg, 39%) as a pale brown oil.

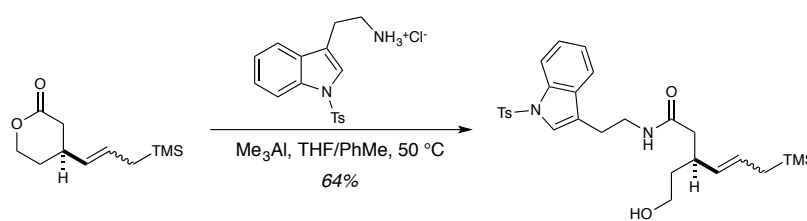
^1H NMR (400 MHz, CDCl_3) δ 5.55-5.38 (m, 1H), 5.17 (dd, $J = 15.2, 6.7$ Hz, 1H), 4.40 (dt, $J = 11.4, 4.7$, 1H), 4.28 (dd, $J = 10.0, 3.9$ Hz, 1H), 2.72-2.50 (m, 2H), 2.38-2.21 (m, 1H),

2.01-1.85 (m, 1H), 1.65 (ddt, $J = 14.7, 9.8, 4.9$ Hz, 1H), 1.42 (d, $J = 9.0$ Hz, 2H), -0.03 (s, 9H) ppm.

^{13}C NMR (126 MHz, CDCl_3) δ 170.4, 136.4, 123.3, 70.2, 44.6, 38.2, 31.2, 30.2, 1.7 ppm.

HRMS (+NSI) calculated for $\text{C}_{11}\text{H}_{21}\text{O}_2\text{Si}$ $[\text{M}+\text{H}]^+$ 213.1311, found 213.1312.

Amide 3.76:



To a slurry of N-tosyltryptamine hydrochloride **3.72** (1.69 g, 4.83 mmol, 3.0 equiv) in THF was added trimethylaluminum solution (2.0 M in toluene, 2.50 mL, 4.83 mmol, 3.0 equiv) at $0\text{ }^\circ\text{C}$, and the reaction mixture was stirred for one hour. A solution of allylsilane **3.75** (342.4 mg, 1.61 mmol, 1.0 equiv) in THF (8.0 mL) was then added, and the reaction mixture was heated up to $50\text{ }^\circ\text{C}$ for 16 hours. The reaction mixture was cooled to room temperature and quenched with saturated Rochelle's salt solution (10.0 mL). The biphasic mixture was stirred until both layers were clear. The layers were separated, and the aqueous phase was extracted with EtOAc (3 x 10.0 mL). The combined organic layer was washed with brine, dried over anhydrous Na_2SO_4 , filtered, and concentrated under reduced pressure. Purification by flash column chromatography on silica gel (EtOAc) provided amide **3.76** (543.6 mg, 64%) as a sticky foam.

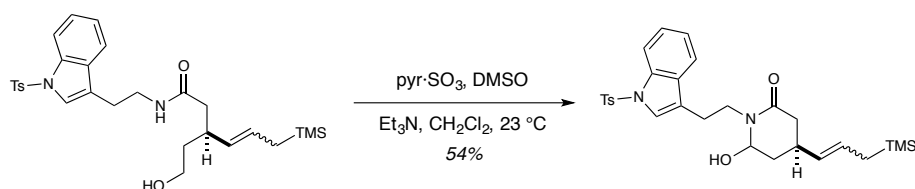
^1H NMR (500 MHz, CDCl_3) δ 7.99 (d, $J = 8.4$ Hz, 1H), 7.75 (d, $J = 8.4$ Hz, 2H), 7.51 (d, $J = 7.8$ Hz, 1H), 7.38 (s, 1H), 7.33 (t, $J = 7.8$ Hz, 1H), 7.25-7.20 (m, 3H), 5.61 (t, $J = 5.5$

Hz, 1H), 5.46 (dt, $J = 16.2, 8.3$ Hz, 1H), 5.05 (dd, $J = 15.1, 8.7$ Hz, 1H), 3.70-3.58 (m, 2H), 3.54 (q, $J = 6.5$ Hz, 2H), 2.93-2.79 (m, 2H), 2.72-2.55 (m, 1H), 2.24-2.09 (m, 2H), 1.66-1.48 (m, 2H), 1.36 (ddd, $J = 7.8, 5.4, 1.2$ Hz, 2H) ppm.

^{13}C NMR (126 MHz, CDCl_3) δ 172.6, 139.4, 136.4, 134.8, 131.0, 130.0, 129.0, 128.2, 124.9, 124.6, 123.3, 123.0, 119.8, 119.4, 113.7, 60.0, 45.0, 41.7, 37.5, 34.2, 31.2, 25.5, 21.3, 1.7 ppm.

HRMS (+NSI) calculated for $\text{C}_{28}\text{H}_{39}\text{O}_4\text{N}_2\text{SSi}$ $[\text{M}+\text{H}]^+$ 537.2400, found 537.2398.

Hemiaminal **3.77**:



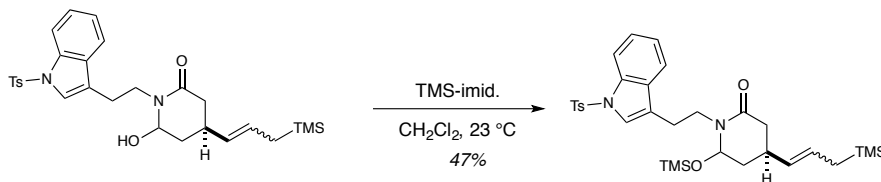
DMSO (1.6 mL) and pyr·SO₃ (297.7 mg, 1.87 mmol, 3.3 equiv) were combined in a round-bottom flask, and the resultant mixture was stirred for 30 minutes. A solution of amide **3.76** (297.8 mg, 0.57 mmol, 1.0 equiv) in CH₂Cl₂ (2.9 mL) and triethylamine (1.33 mL, 9.61 mmol, 17.0 equiv) was then added, and the reaction was stirred for three hours. The reaction was quenched with saturated NH₄Cl (10.0 mL), and the layers were separated. The aqueous phase was extracted with CH₂Cl₂ (3 x 10.0 mL). The combined organic layer was washed with water (2 x 10.0 mL), dried over anhydrous Na₂SO₄, filtered, and concentrated under reduced pressure. Purification by flash column chromatography on silica gel (3:2 hexanes/EtOAc) provided hemiaminal **3.77** (160.5 g, 54%) as a sticky foam.

¹H NMR (600 MHz, CDCl₃) δ 7.98 (d, *J* = 8.3 Hz, 1H), 7.75 (d, *J* = 8.3 Hz, 2H), 7.38 (d, *J* = 5.8 Hz, 1H), 7.33-7.29 (m, 2H), 7.26-7.22 (m, 1H), 7.21 (d, *J* = 8.1 Hz, 2H), 5.56 – 5.38 (m, 1H), 5.25 (dd, *J* = 15.4, 6.1 Hz, 1H), 4.65 (dt, *J* = 11.2, 5.4 Hz, 1H) 3.78-3.61 (m, 2H), 3.49-3.40 (m, 2H), 3.10-2.99 (m, 1H), 2.99-2.86 (m, 1H), 2.49 (ddd, *J* = 16.7, 4.8, 1.8 Hz, 1H), 2.15-2.03 (m, 2H), 1.44 (d, *J* = 8.0 Hz, 2H), -0.02 (s, 9H) ppm.

¹³C NMR (126 MHz, CDCl₃) δ 168.9, 139.4, 136.4, 134.8, 131.0, 130.0, 129.0, 128.2, 124.9, 124.6, 123.3, 123.0, 119.8, 119.4, 113.7, 83.2, 45.5, 44.0, 42.1, 39.3, 31.2, 24.3, 21.4, 1.6 ppm.

HRMS (+NSI) calculated for C₂₈H₃₆O₄N₂NaSi [M+Na]⁺ 547.2063, found 547.2059.

Hemiaminal Ether **3.71**:

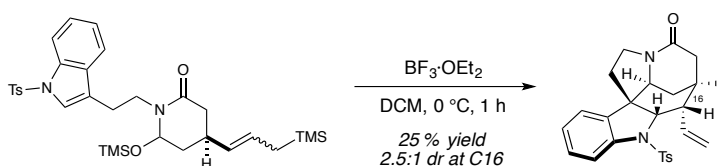


To a solution of hemiaminal **3.77** (160.5 g, mmol, equiv) in CH₂Cl₂ (1.0 mL) was added trimethylsilylimidazole (0.23 mL, 1.53 mmol, 5.0 equiv), and the solution was stirred at room temperature for two hours. The reaction was quenched with saturated aqueous NH₄Cl (2.0 mL), and the layers were separated. The aqueous phase was extracted with CH₂Cl₂ (3 x 2.0 mL). The combined organic layer was dried over anhydrous Na₂SO₄, filtered, and concentrated under reduced pressure. Purification by flash column chromatography on silica gel (9:1 hexanes/EtOAc) provided hemiaminal ether **3.71** (75.3 mg, 47%) as a stick foam.

$^1\text{H NMR}$ (500 MHz, CDCl_3) δ 7.97 (d, $J = 8.1$ Hz, 1H), 7.74 (d, $J = 8.4$ Hz, 2H), 7.34-7.27 (m, 3H), 7.25-7.17 (m, 3H), 5.48-5.39 (m, 1H), 5.15 (dd, $J = 15.2, 7.0$ Hz, 1H), 4.82 (dd, $J = 8.2, 5.7$ Hz, 1H), 3.64 (ddd, $J = 13.3, 9.9, 6.3$ Hz, 2H), 3.58-3.49 (m, 2H), 3.08-2.96 (m, 1H), 2.88 (dtd, 10.5, 9.9, 5.3, 1H), 2.47 (dd, $J = 16.5, 4.1$ Hz, 1H), 2.02 (dd, $J = 16.1, 5.7$ Hz, 1H), 1.54-1.43 (m, 1H), 1.42 (d, $J = 7.7$ Hz, 2H), 0.07 (s, 9H), -0.01 (s, 9H) ppm.

HRMS (+NSI) calculated for $\text{C}_{31}\text{H}_{45}\text{O}_4\text{N}_2\text{SSi}_2$ $[\text{M}+\text{H}]^+$ 597.2369, found 597.2364.

Tetracycle **3.78**:



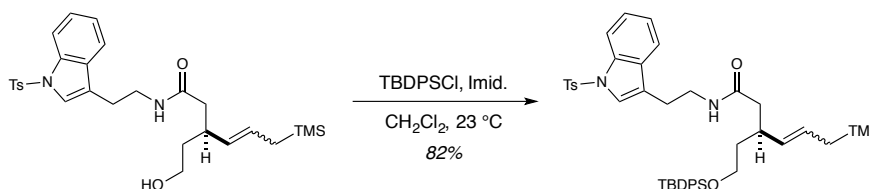
To a solution of hemiaminal ether **3.71** (75.3 mg, 0.123 mmol, 1.0 equiv) in CH_2Cl_2 (1.3 mL) at 0 °C was added $\text{BF}_3 \cdot \text{OEt}_2$ (0.05 mL, 0.370 mmol, 3.0 equiv). The resultant mixture was stirred for one hour and was then quenched with saturated aqueous NaHCO_3 (2.0 mL). The layers were separated, and the aqueous phase was extracted with CH_2Cl_2 (3 x 2.0 mL). The combined organic layer was dried over anhydrous Na_2SO_4 , filtered, and concentrated under reduced pressure. Purification by preparatory thin layer chromatography on silica gel (4:1 hexanes/EtOAc, rinsed with EtOAc) provided tetracycle **3.78** (13.3 mg, 25%, 2.5:1 mixture of C16 epimers) as a colorless oil.

$^1\text{H NMR}$ (600 MHz, CDCl_3) (2.5:1.0 mixture of epimers) δ 7.67 (t, $J = 8.0$ Hz, 5H), 7.61 (d, $J = 8.1$ Hz, 2H), 7.58 (d, $J = 8.2$ Hz, 2H), 7.34-7.27 (m, 6H), 7.22 (d, $J = 8.2$ Hz, 5H), 7.17 (d, $J = 8.1$ Hz, 2H), 7.13 (t, $J = 7.5$ Hz, 1H), 7.05 (t, $J = 7.5$ Hz, 2.5H), 6.97 (t, $J = 9.5$

Hz, 2.5H), 6.12-6.00 (m, 1H), 5.37-5.25 (m, 2.5H), 5.22 (d, $J = 10.3$ Hz, 1H), 5.13 (d, $J = 13.9$ Hz, 2.5H), 5.07 (d, $J = 17.0$ Hz, 1H), 4.93 (d, $J = 10.1$ Hz, 2.5H), 4.11-4.02 (m, 3.5H), 3.78 (d, $J = 7.5$ Hz, 2.5H), 3.69 (d, $J = 3.0$ Hz, 1H), 3.63 (d, $J = 10.1$ Hz, 1H), 2.98 (t, $J = 8.9$ Hz, 2.5H), 2.87 (qd, $J = 11.0, 4.0$ Hz, 3.5H), 2.75-2.69 (m, 3.5H), 2.67 (d, $J = 18.4$ Hz, 2H), 2.57 (d, $J = 17.8$ Hz, 2.5H), 2.47 (dd, $J = 17.7, 5.3$ Hz, 1H), 2.42-2.30 (m, 12.5H), 2.17-2.11 (m, 4.5H), 2.04-1.99 (m, 4.5H), 1.85 (dt, $J = 12.8, 2.3$ Hz, 1H), 1.25-1.17 (m, 3.5H), 0.97-0.82 (m, 3.5H) ppm.

HRMS (+NSI) calculated for $C_{25}H_{27}O_3N_2S$ $[M+H]^+$ 435.1737, found 435.1741.

TBDPS Ether **3.85**:

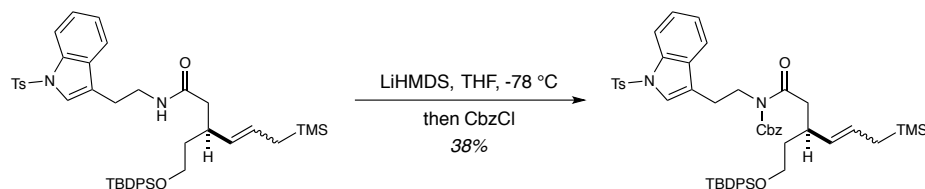


To a solution of amide **3.76** (543.6 mg, 1.01 mmol, 1.0 equiv) in CH_2Cl_2 (10.1 mL) was added imidazole (151.8 mg, 2.23 mmol, 2.2 equiv) and TBDPSCI (0.29 mL, 1.11 mmol, 1.1 equiv). The reaction mixture was stirred for 6 hours and was then quenched with saturated aqueous NH_4Cl (20.0 mL). The layers were separated, and the aqueous phase was extracted with CH_2Cl_2 (3 x 20.0 mL). The combined organic layer was dried over anhydrous Na_2SO_4 , filtered, and concentrated under reduced pressure. Purification by column chromatography on silica gel (4:1 to 7:3 hexanes/EtOAc) provided TBDPS ether **3.85** (632.7 mg, 82%) as a colorless oil.

¹H NMR (500 MHz, CDCl₃) δ 7.99 (d, *J* = 8.3 Hz, 1H), 7.74 (d, *J* = 8.4 Hz, 2H), 7.64 (d, *J* = 8.0 Hz, 4H), 7.48 (d, *J* = 7.1 Hz, 1H), 7.43-7.29 (m, 7H), 7.24-7.18 (m, 3H), 7.14 (s, 1H), 5.57 (t, *J* = 5.1 Hz, 1H), 5.42-5.32 (m, 1H), 4.94 (dd, *J* = 15.2, 8.7 Hz, 1H), 3.72-3.61 (m, 2H), 3.48 (q, *J* = 7.0 Hz, 2H), 2.87-2.75 (m, 2H), 2.67-2.55 (m, 1H), 2.20 (dd, *J* = 14.3, 5.9 Hz, 1H), 2.04 (dd, *J* = 14.3, 8.6 Hz, 1H), 1.70-1.63 (m, 1H), 1.55-1.42 (m, 1H), 1.29 (d, *J* = 4.7 Hz, 2H), 1.04 (s, 9H), -0.09 (s, 9H) ppm.

HRMS (+NSI) calculated for C₄₄H₅₆O₄N₂NaSSi₂ [M+Na]⁺ 787.3397, found 787.3393.

Cbz Amide **3.86**:



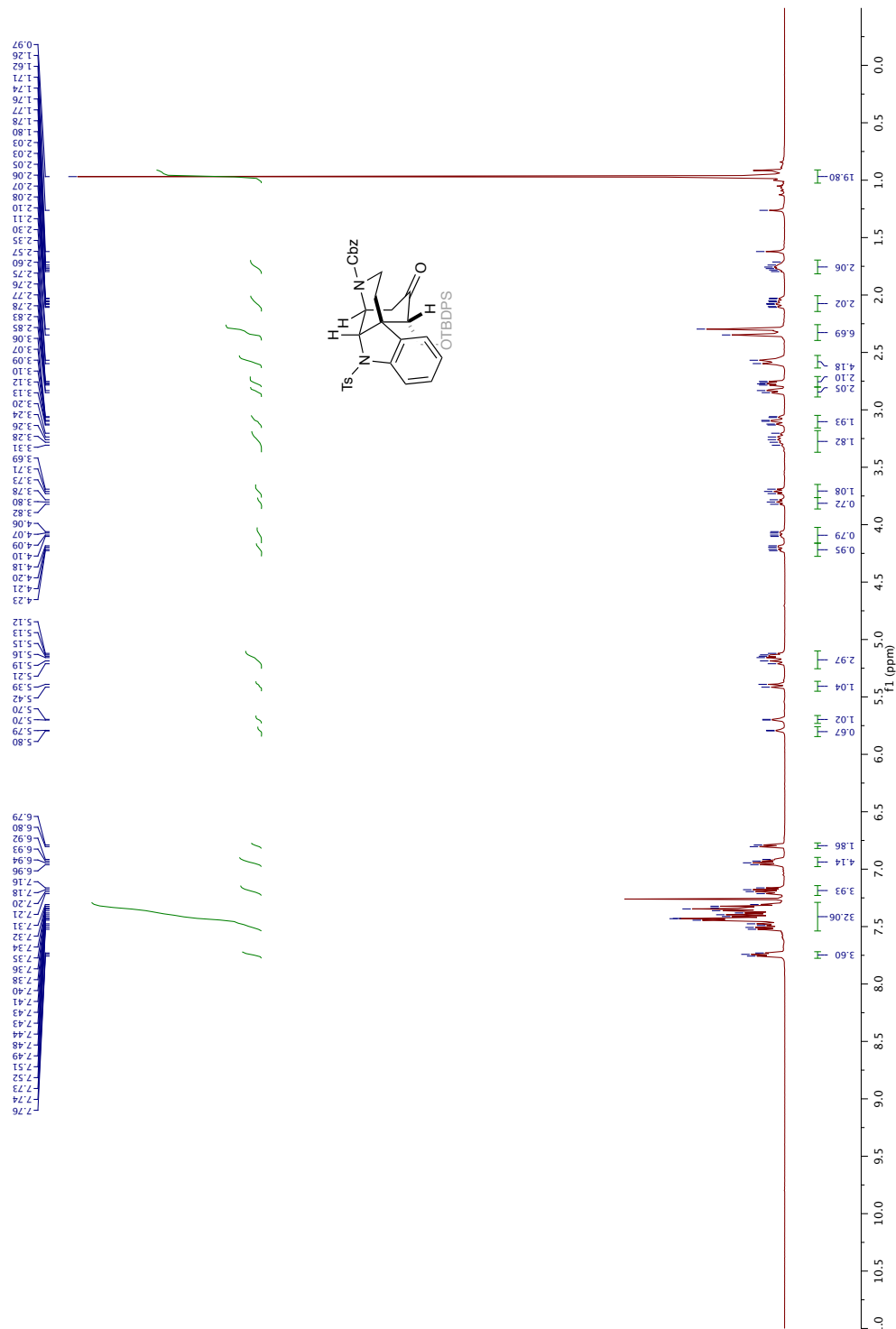
To a solution of TBDPS ether **3.85** (632.7 mg, 0.83 mmol, 1.0 equiv) in THF (4.1 mL) at -78 °C was added a solution of LiHMDS (152.3 mg, 0.91 mmol, 1.1 equiv) in THF (4.1 mL). The reaction mixture was stirred at -78 °C for one hour, then CbzCl (0.16 mL, 1.08 mmol, 1.3 equiv) was added. The resultant mixture was warmed to room temperature and stirred for one hour. The reaction mixture was quenched with saturated aqueous NH₄Cl (10.0 mL). The layers were separated, and the aqueous layer was extracted with Et₂O (3 x 10.0 mL). The combined organic layer was washed with brine (20.0 mL), dried over anhydrous Na₂SO₄, filtered, and concentrated under reduced pressure. Purification by flash column chromatography on silica gel (9:1 hexanes/EtOAc) provided Cbz Amide **3.86** (281.3 mg, 38%) as a colorless oil.

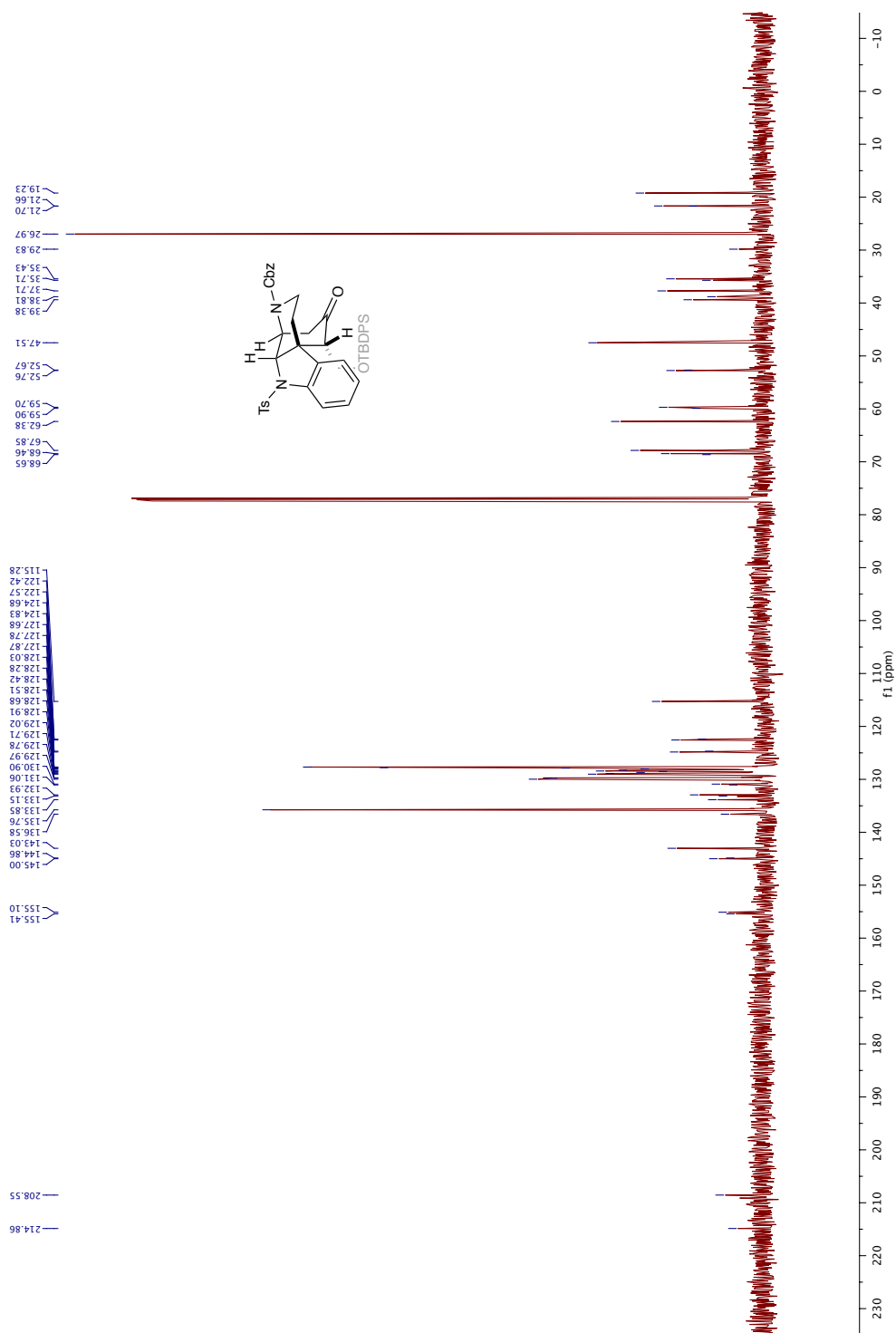
¹H NMR (500 MHz, CDCl₃) δ 7.96 (d, *J* = 8.3, 1H), 7.74 (d, *J* = 8.3 Hz, 2H), 7.67 (d, *J* = 6.4 Hz, 4H), 7.43-7.26 (m, 14H), 7.20 (d, *J* = 8.0 Hz, 2H), 7.12 (t, *J* = 7.6 Hz, 1H), 5.38 (dt, *J* = 15.6, 8.1 Hz, 1H), 5.07 (s, 2H), 5.00 (dd, *J* = 15.1, 8.7 Hz, 1H), 3.96-3.84 (m, 2H), 3.70-3.61 (m, 2H), 3.05-2.90 (m, 2H), 2.90-2.69 (m, 3H), 2.62 (s, 3H), 1.75-1.66 (m, 1H), 1.56-1.45 (m, 1H), 1.34 (d, *J* = 7.9 Hz, 2H), 1.05 (s, 9H), -0.08 (s, 9H) ppm.

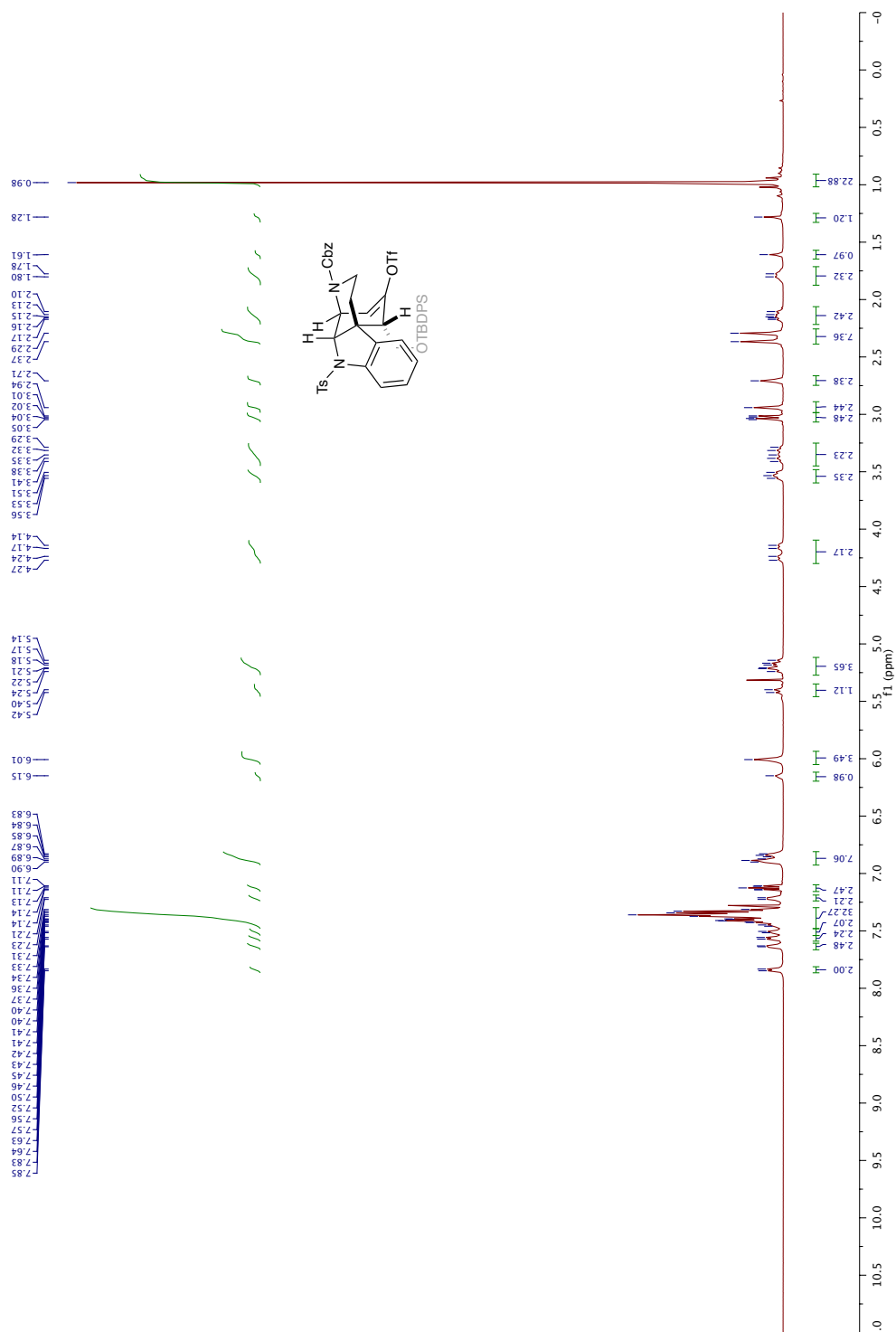
HRMS (+NSI) calculated for C₅₂H₆₂O₆N₂NaSSi₂ [M+Na]⁺ 921.3765, found 921.3765.

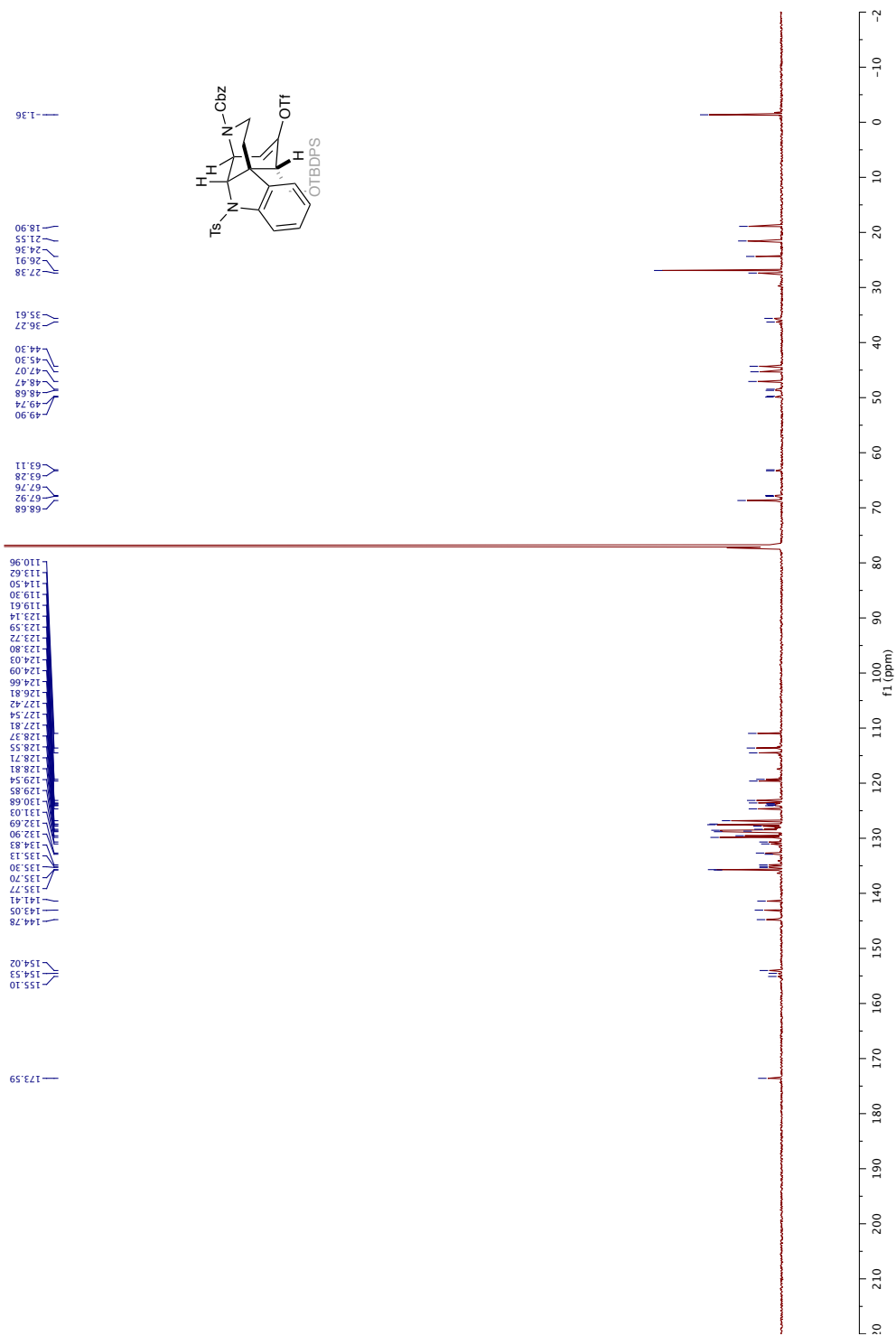
3.9 Spectra Data for Key Intermediates

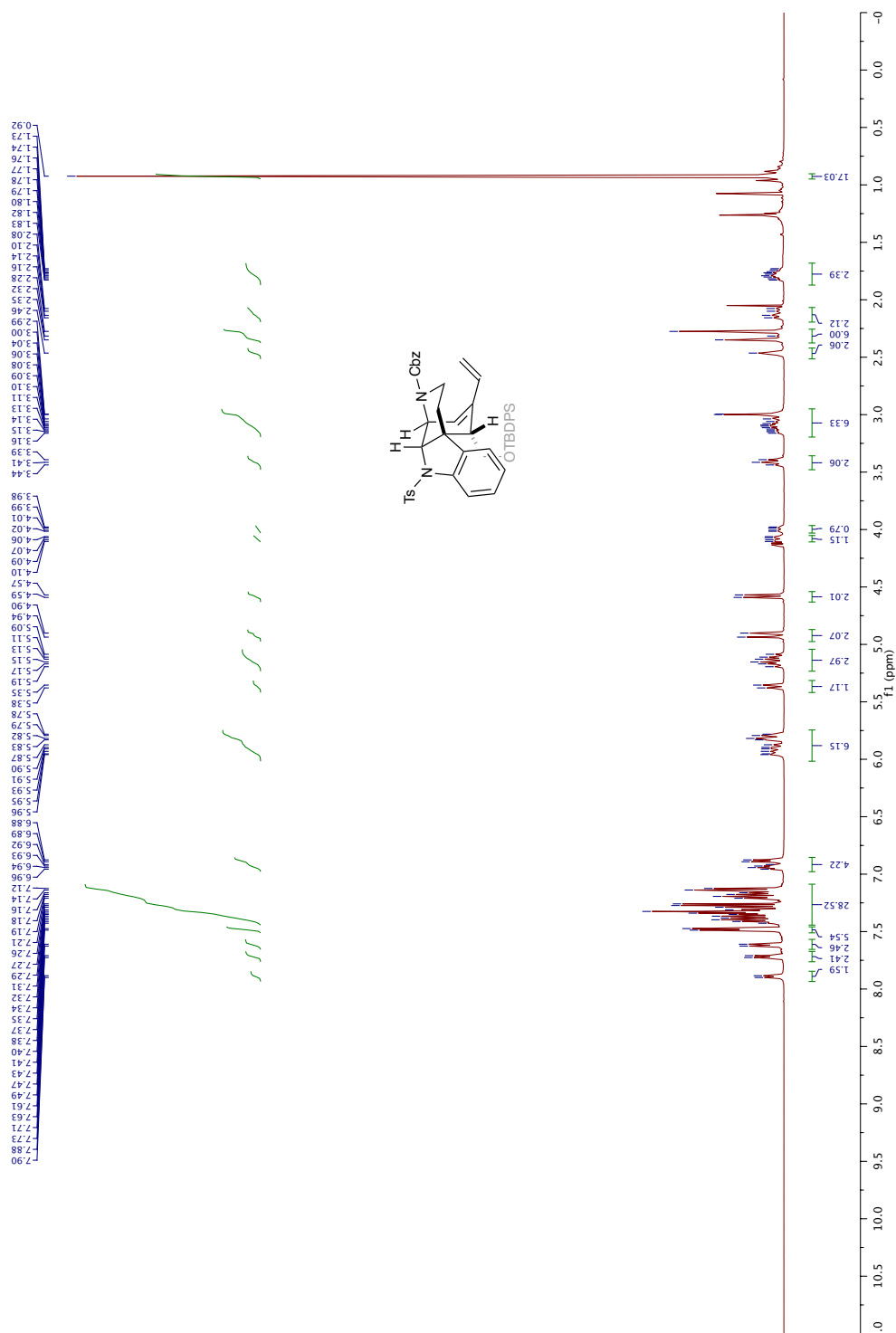
Ketone 3.19: ^1H NMR (500 MHz, CDCl_3)

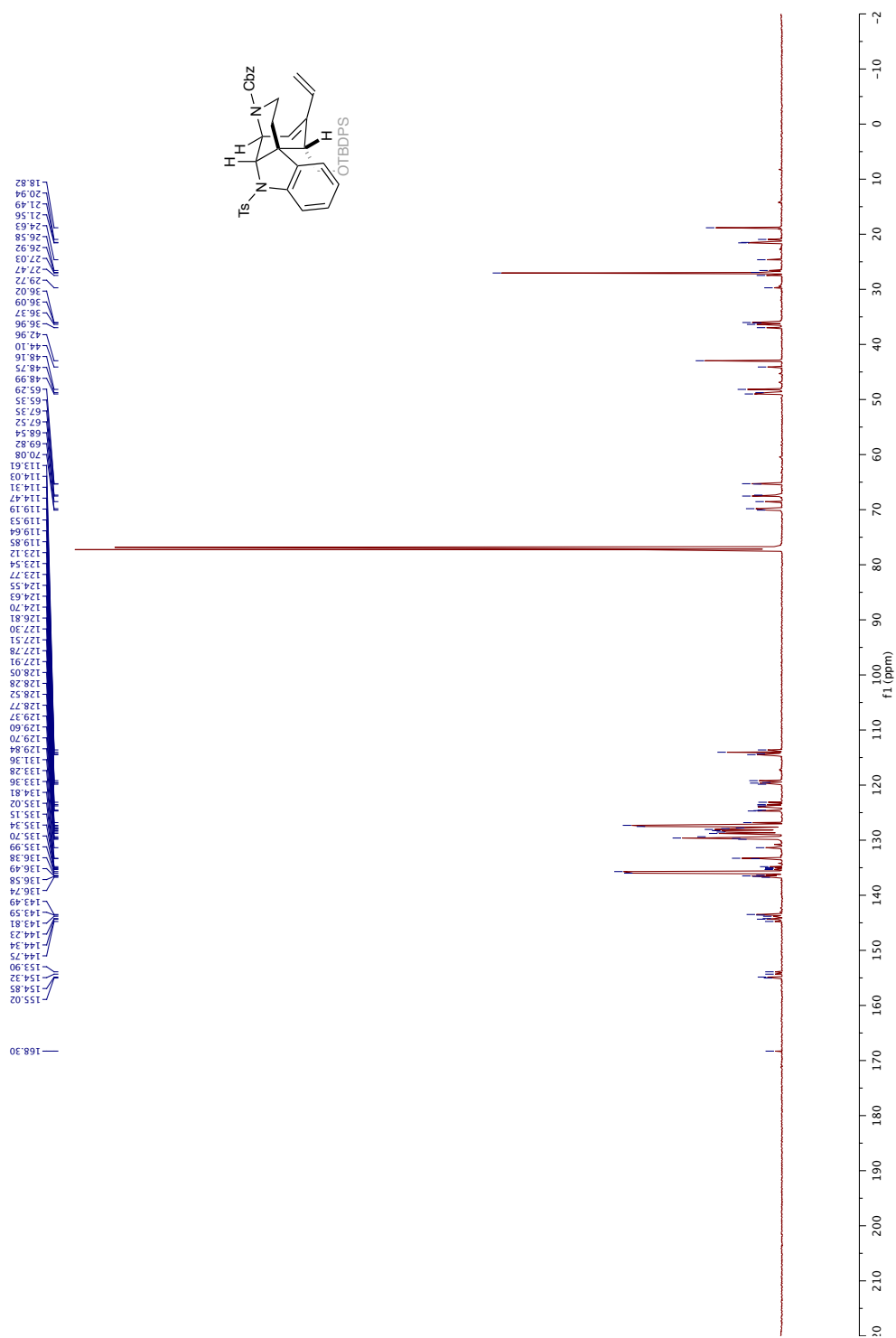


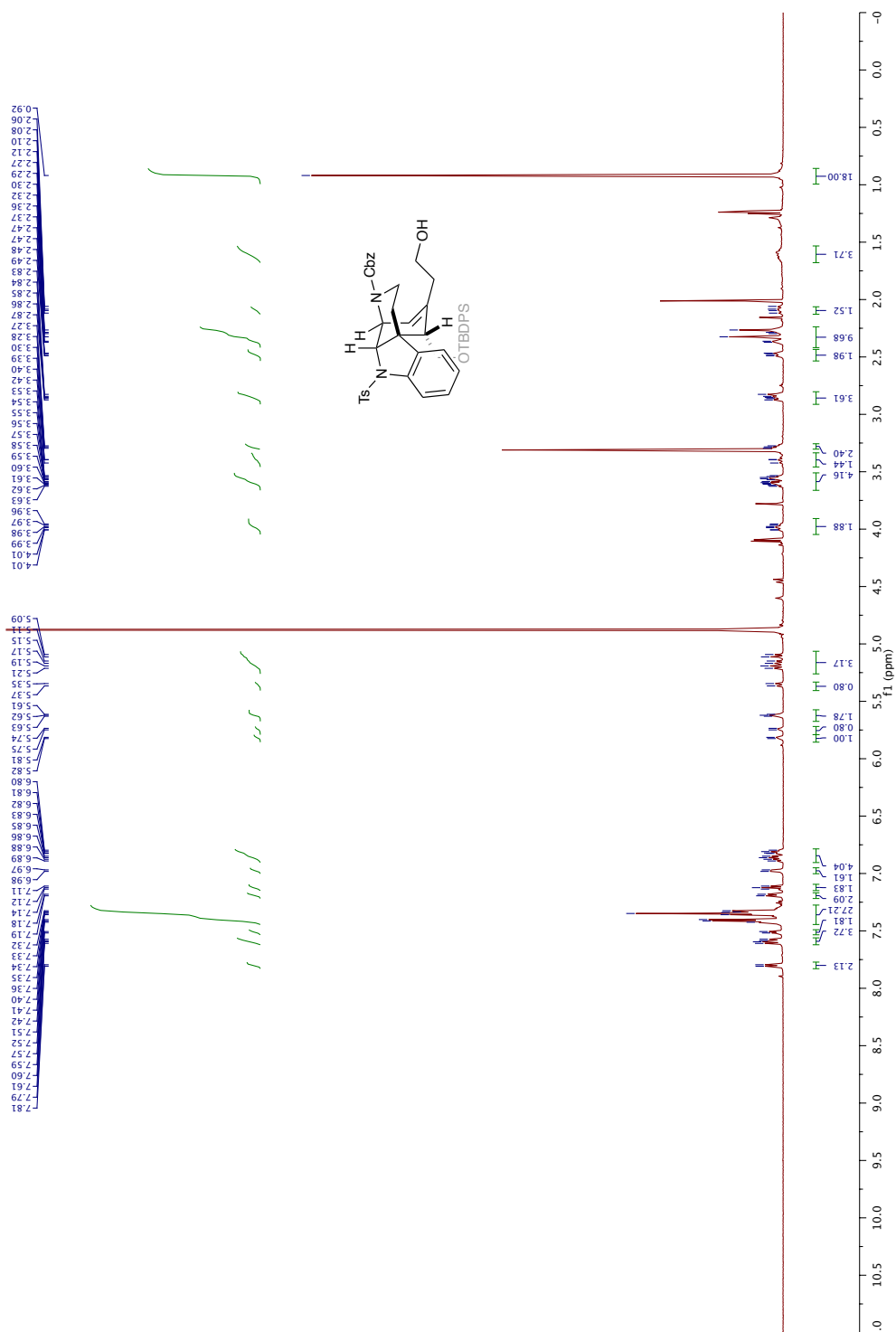
Ketone 3.19: ^{13}C NMR (126 MHz, CDCl_3)

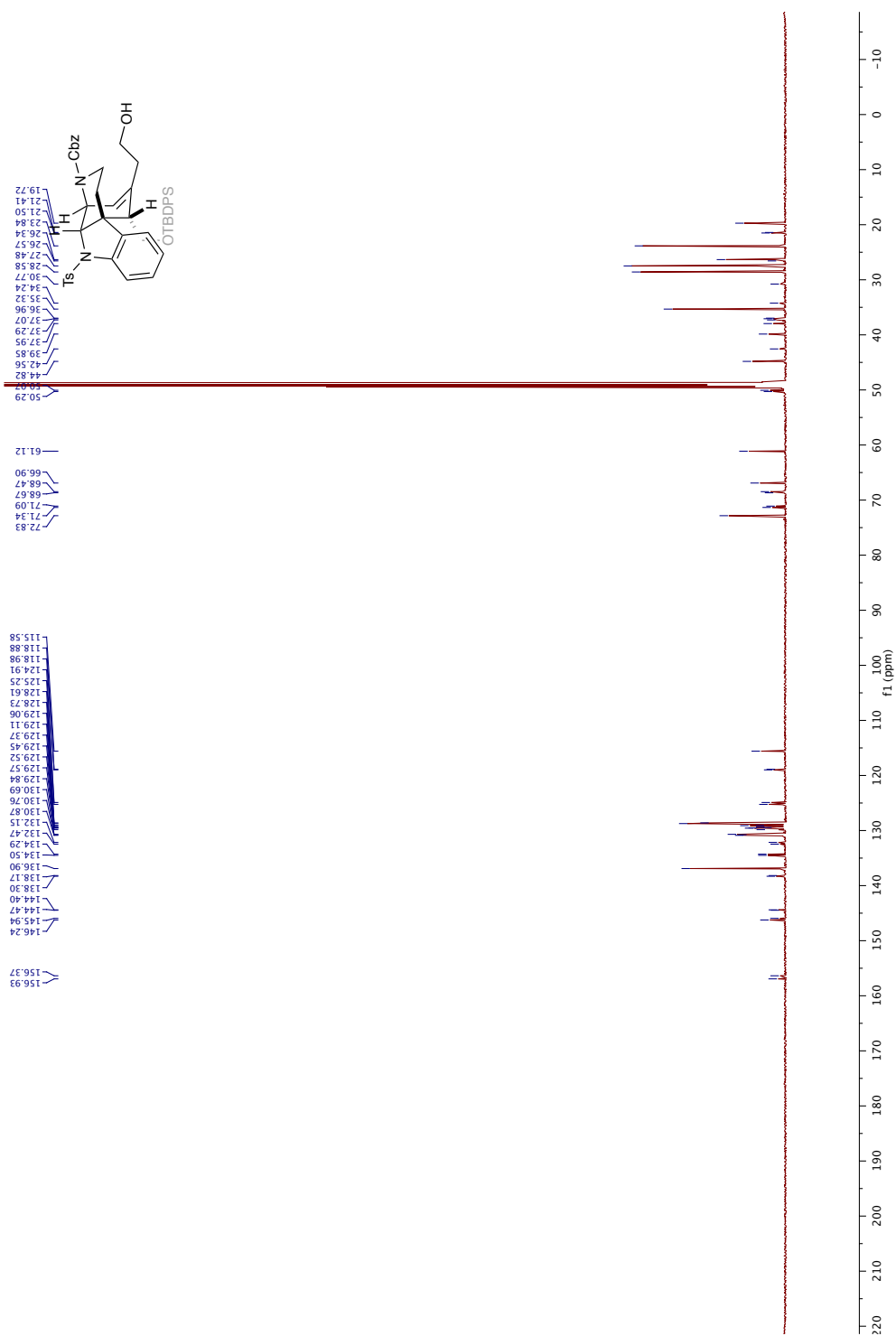
Vinyl Triflate 3.48: ^1H NMR (500 MHz, CDCl_3)

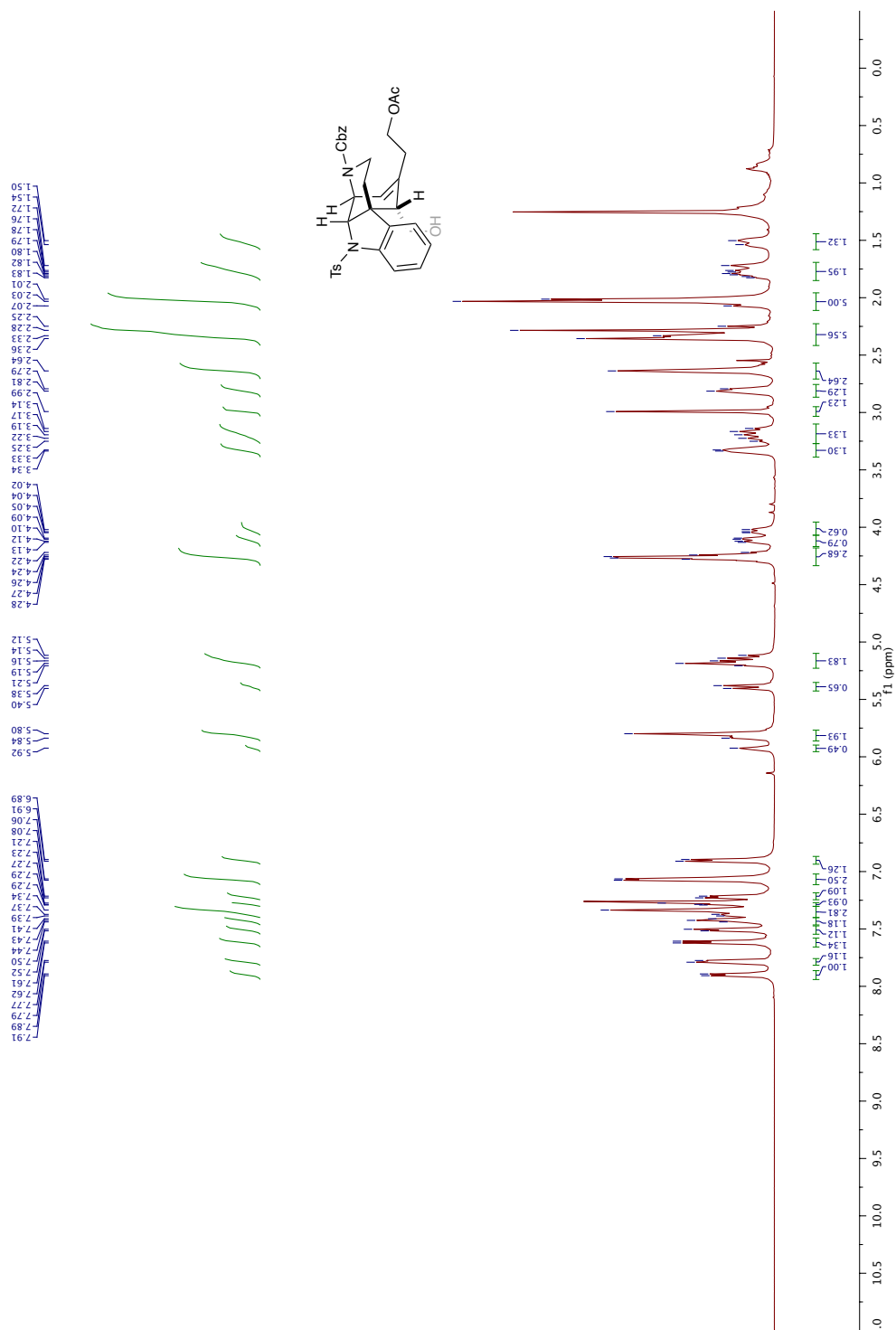
Vinyl Triflate 3.48: ^{13}C NMR (151 MHz, CDCl_3)

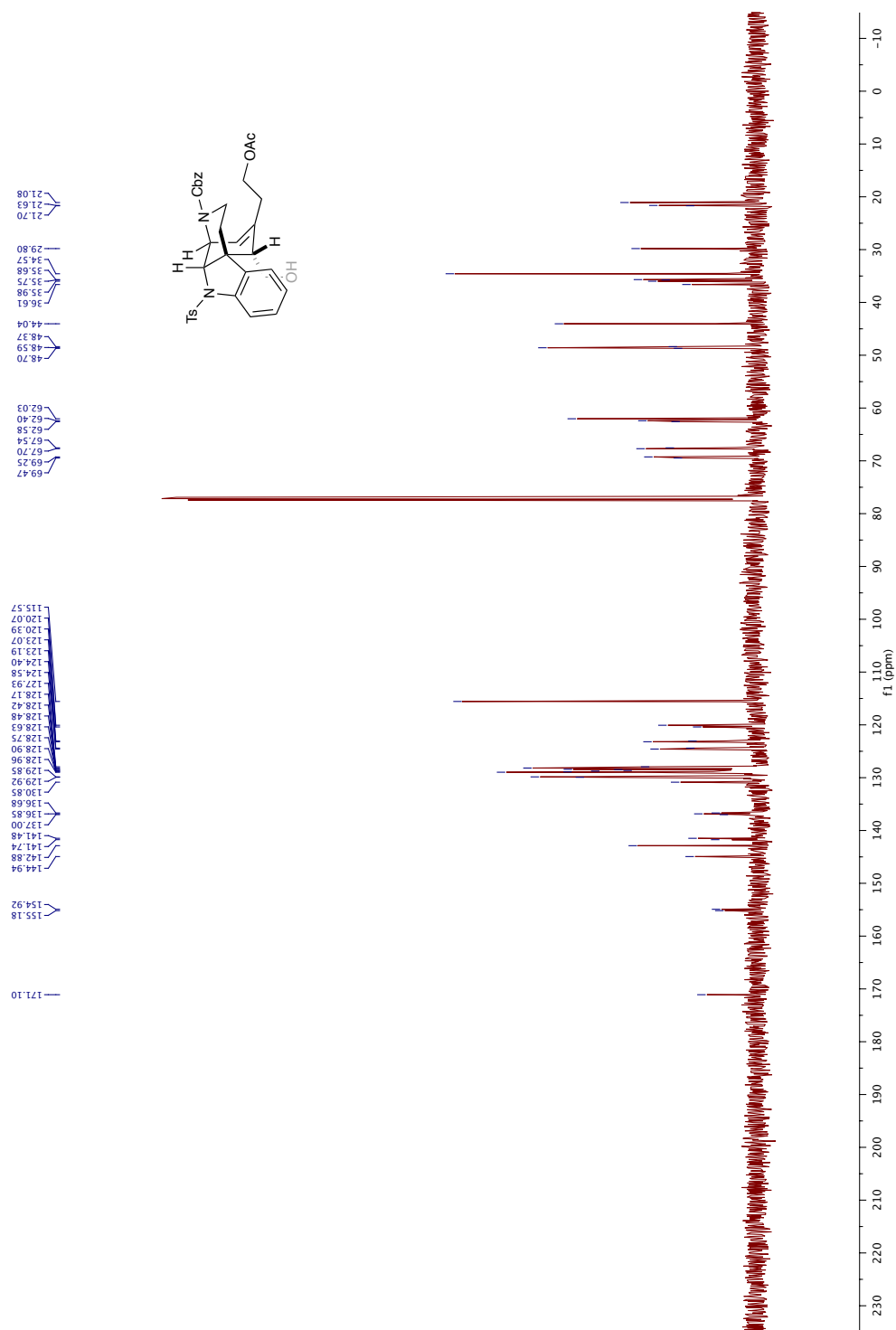
Diene 3.51: ^1H NMR (500 MHz, CDCl_3)

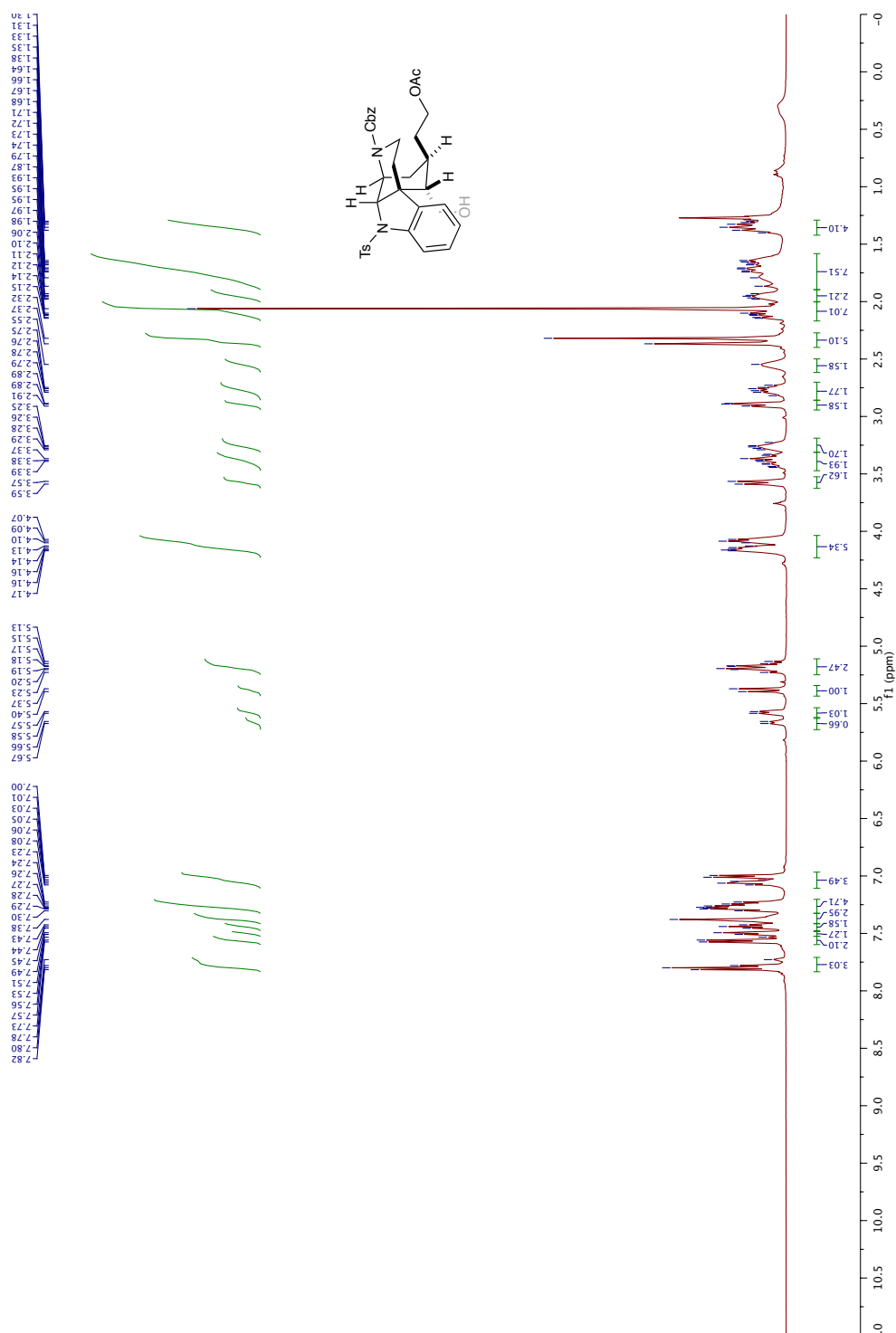
Diene 3.51: ^{13}C NMR (151 MHz, CDCl_3)

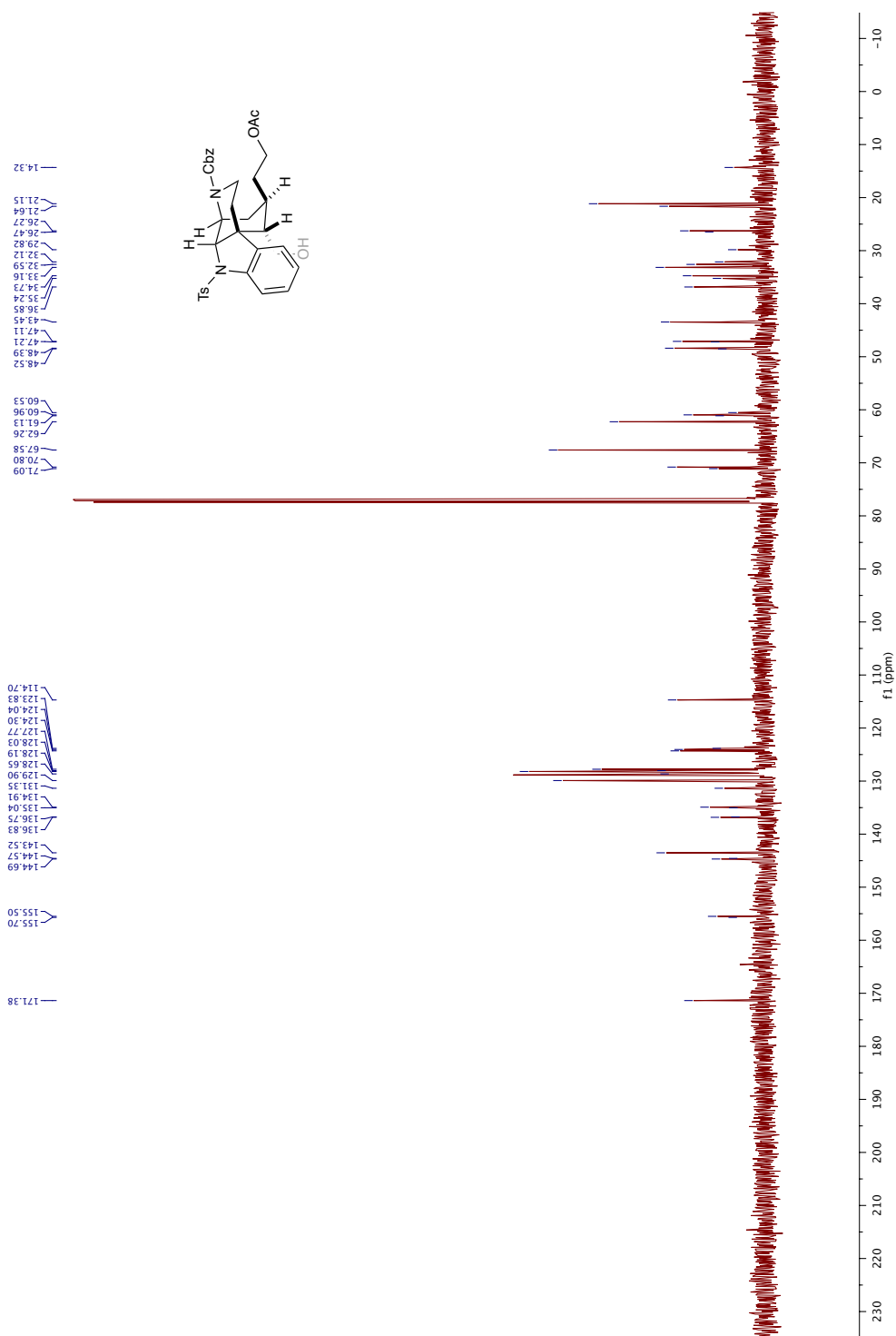
Alcohol 3.58: ^1H NMR (600 MHz, CD_3OD)

Alcohol 3.58: ^{13}C NMR (151 MHz, CD_3OD)

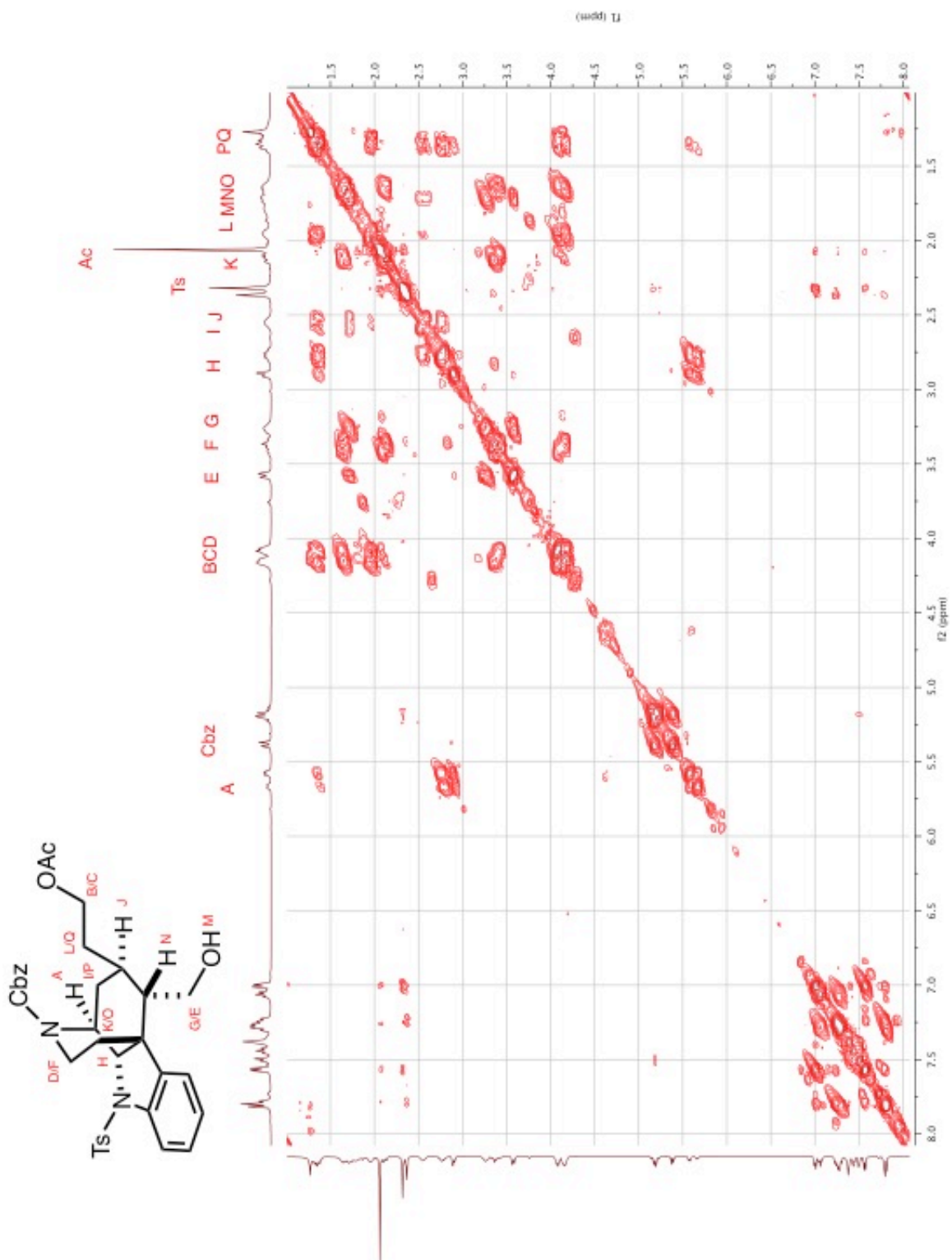
Homoallylic Alcohol 3.59: ^1H NMR (500 MHz, CDCl_3)

Homoallylic Alcohol 3.59: ^{13}C NMR (126 MHz, CDCl_3)

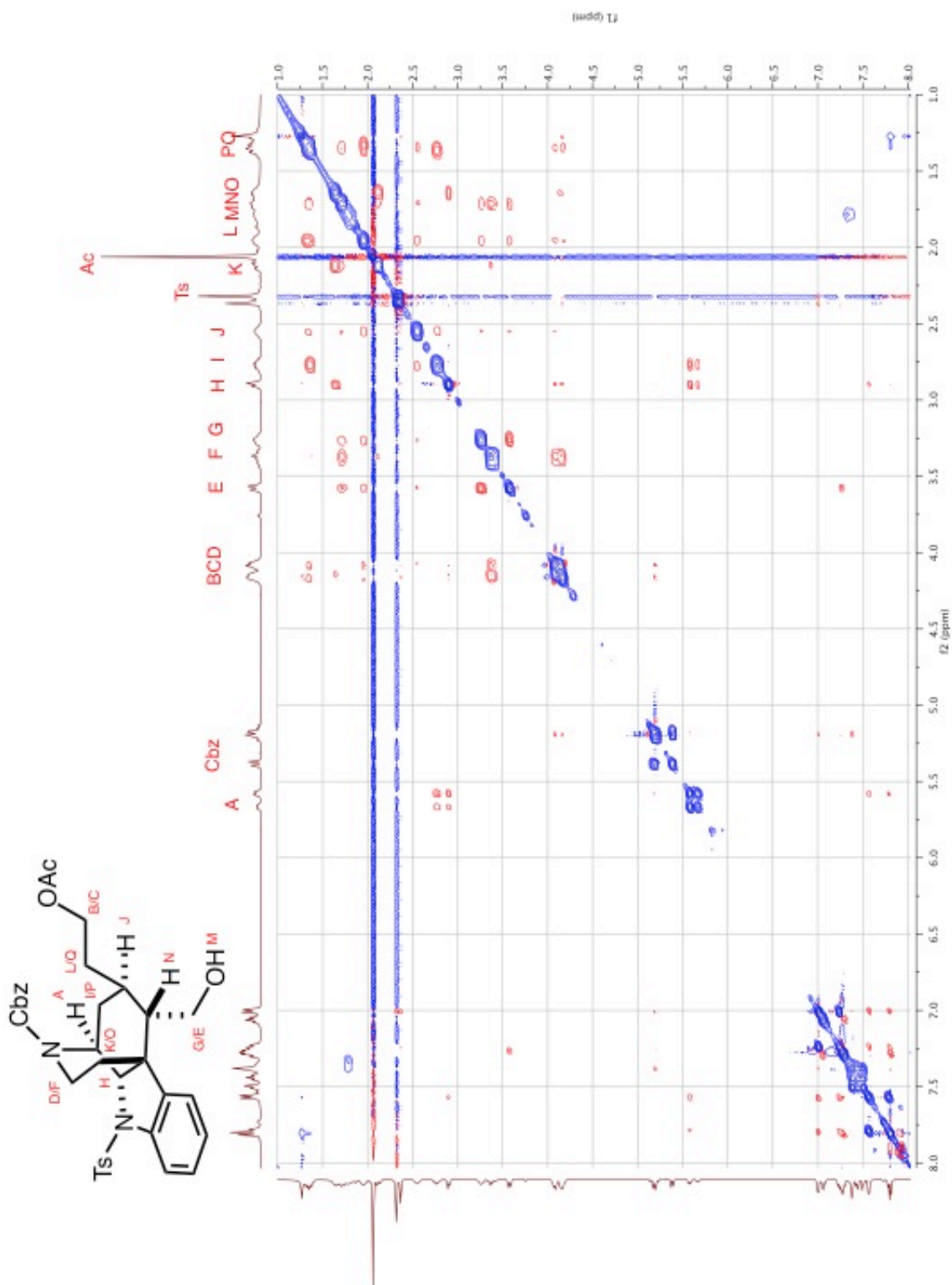
Alcohol 3.60: ^1H NMR (500 MHz, CDCl_3)

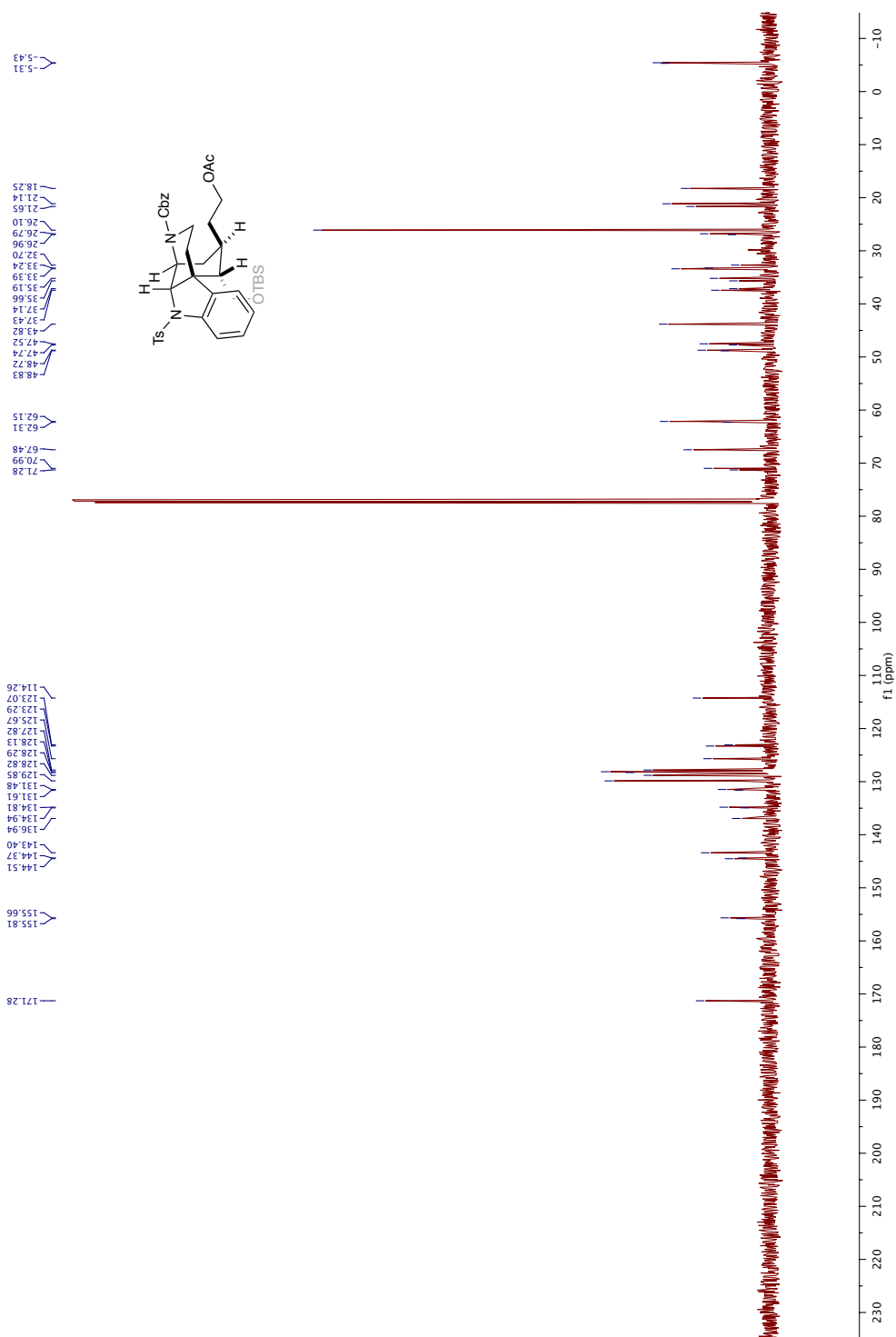
Alcohol 3.60: ^{13}C NMR (126 MHz, CDCl_3)

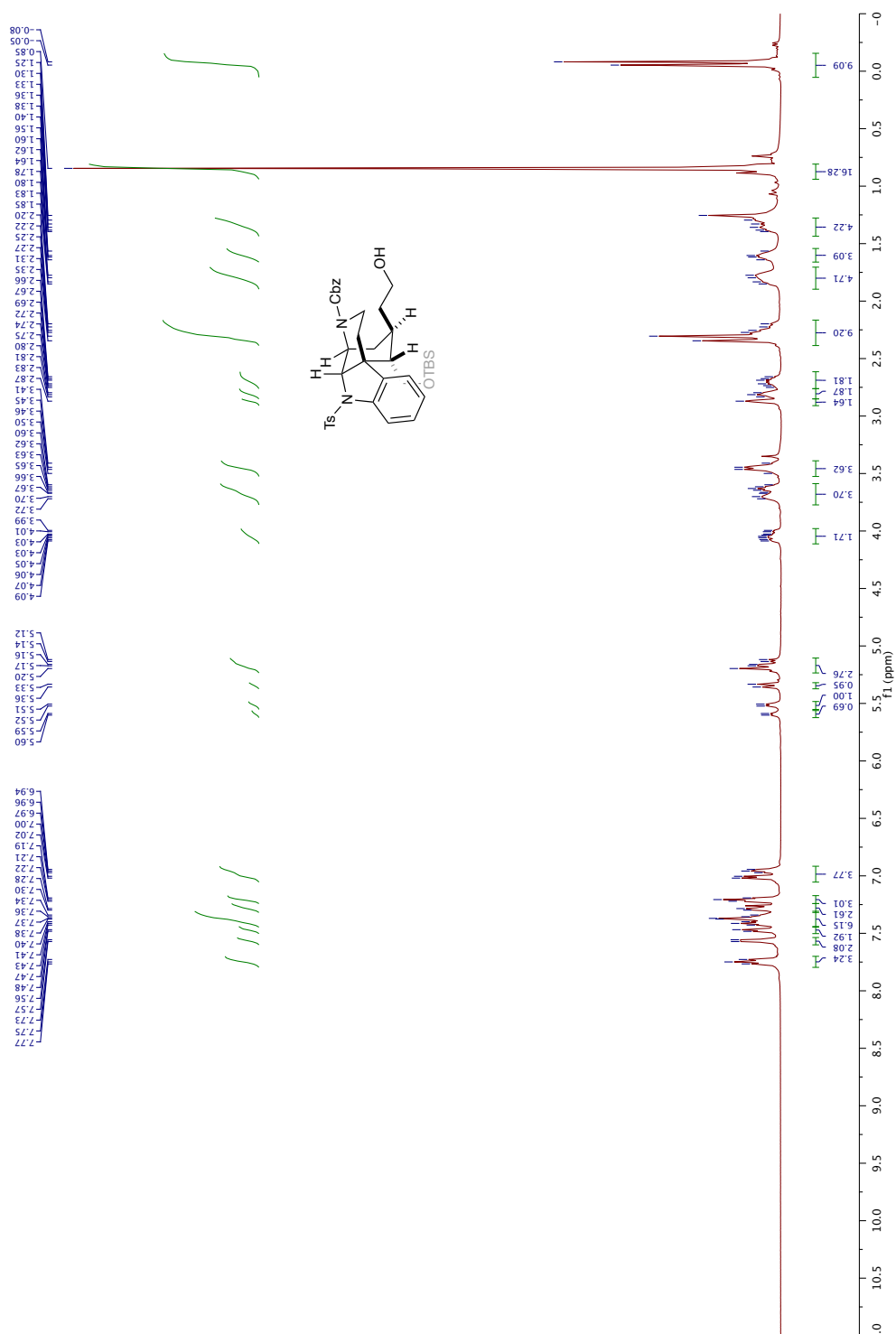
Alcohol 3.60: COSY

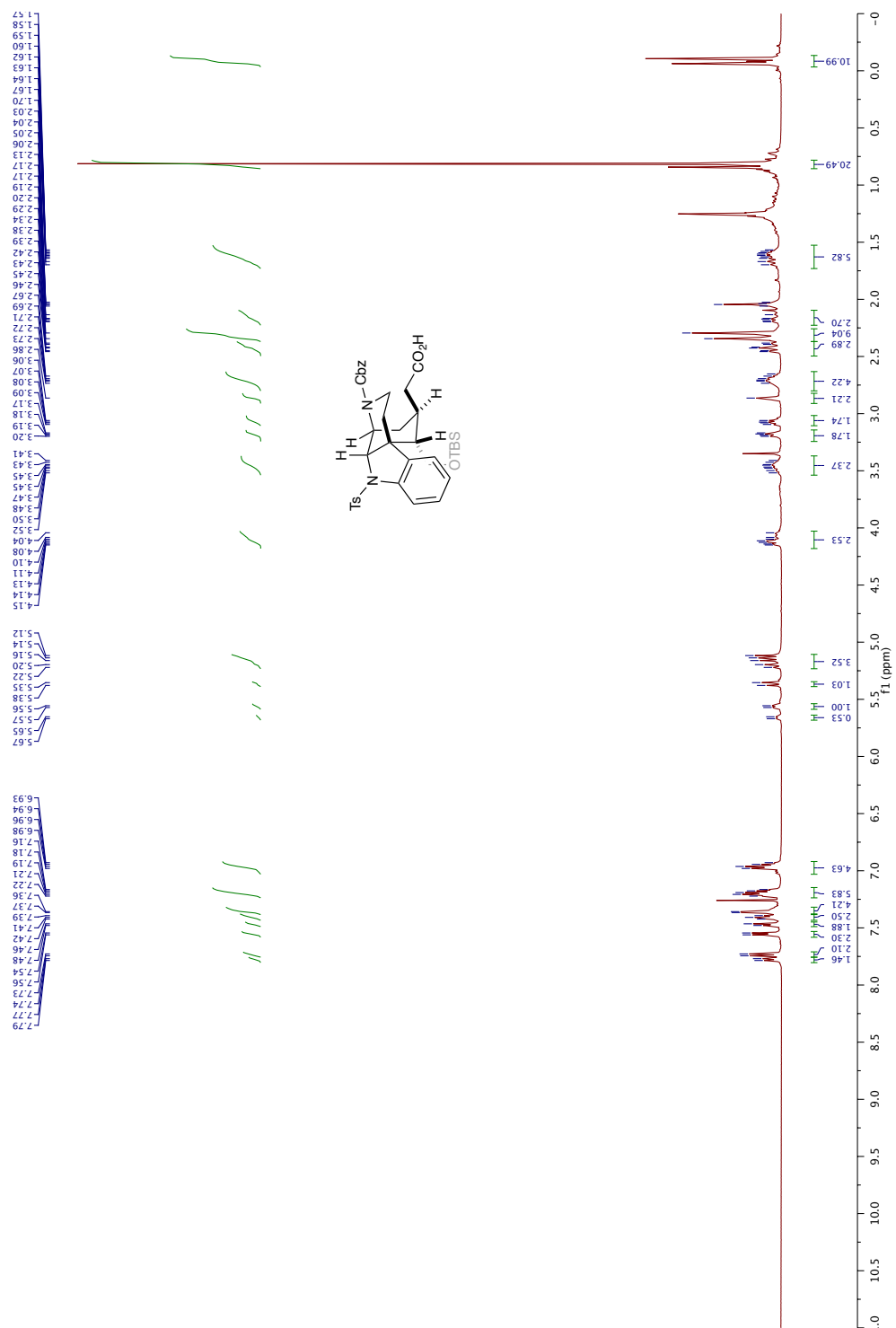


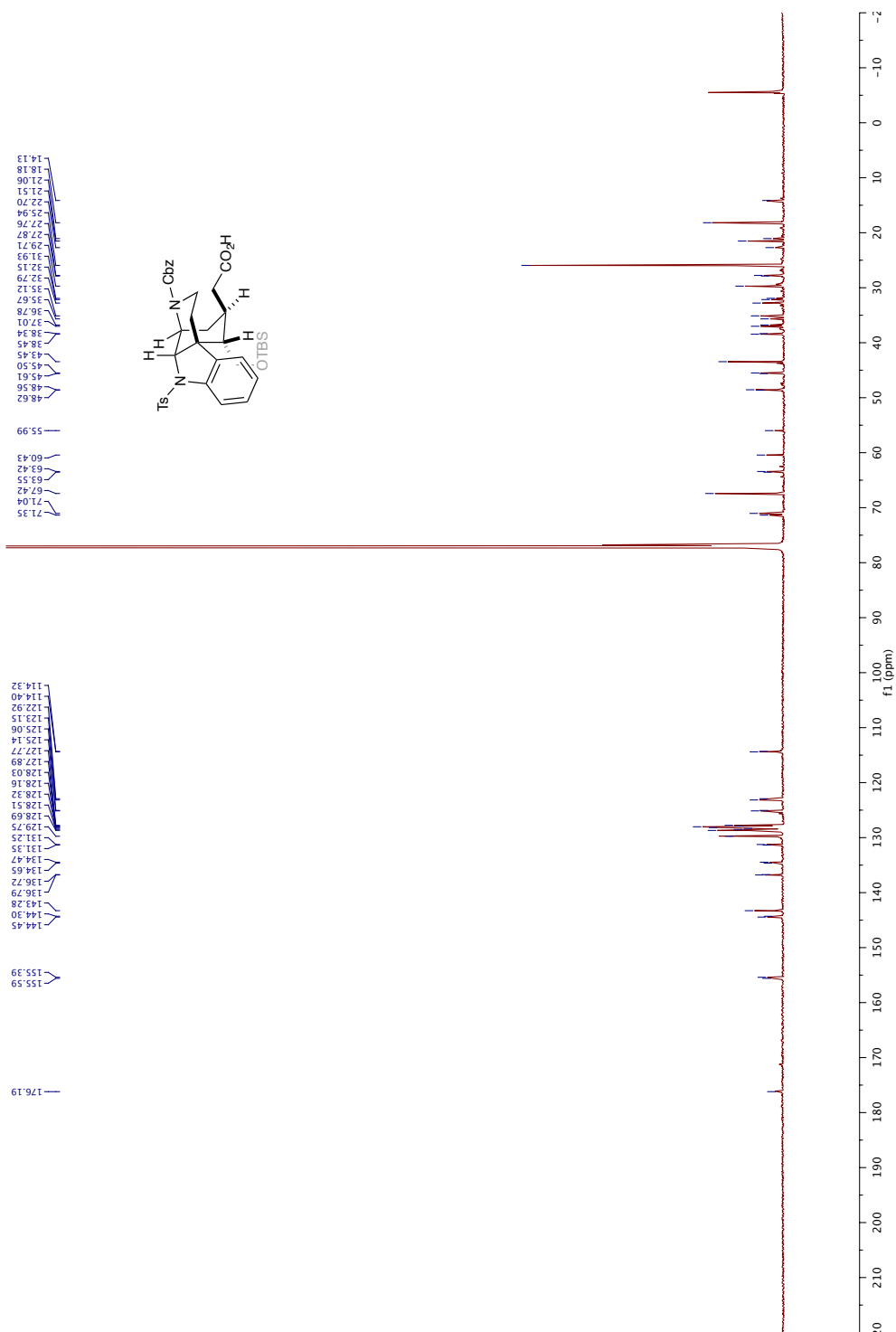
Alcohol 3.60: NOESY



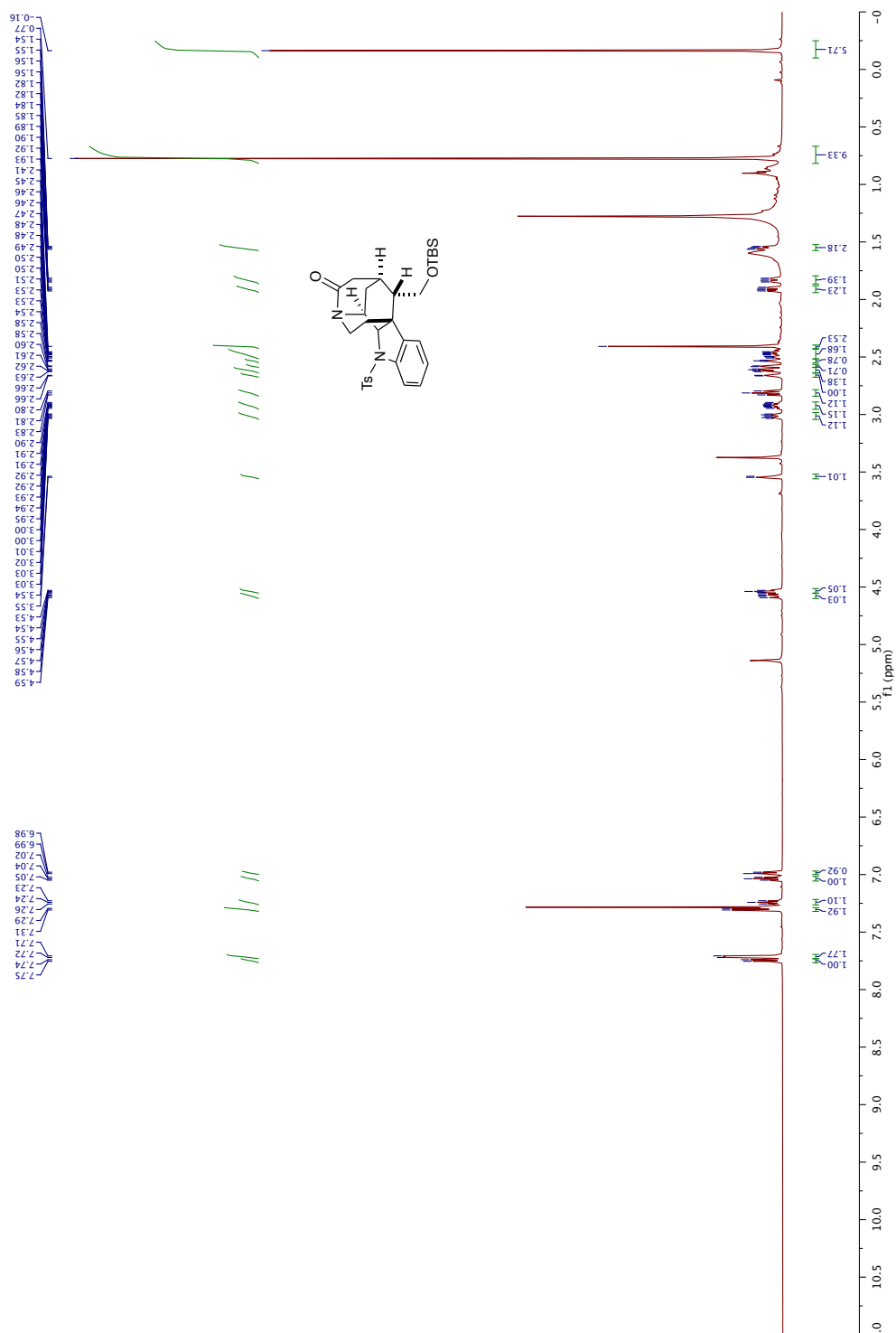
TBS Ether 3.61: ^{13}C NMR (126 MHz, CDCl_3)

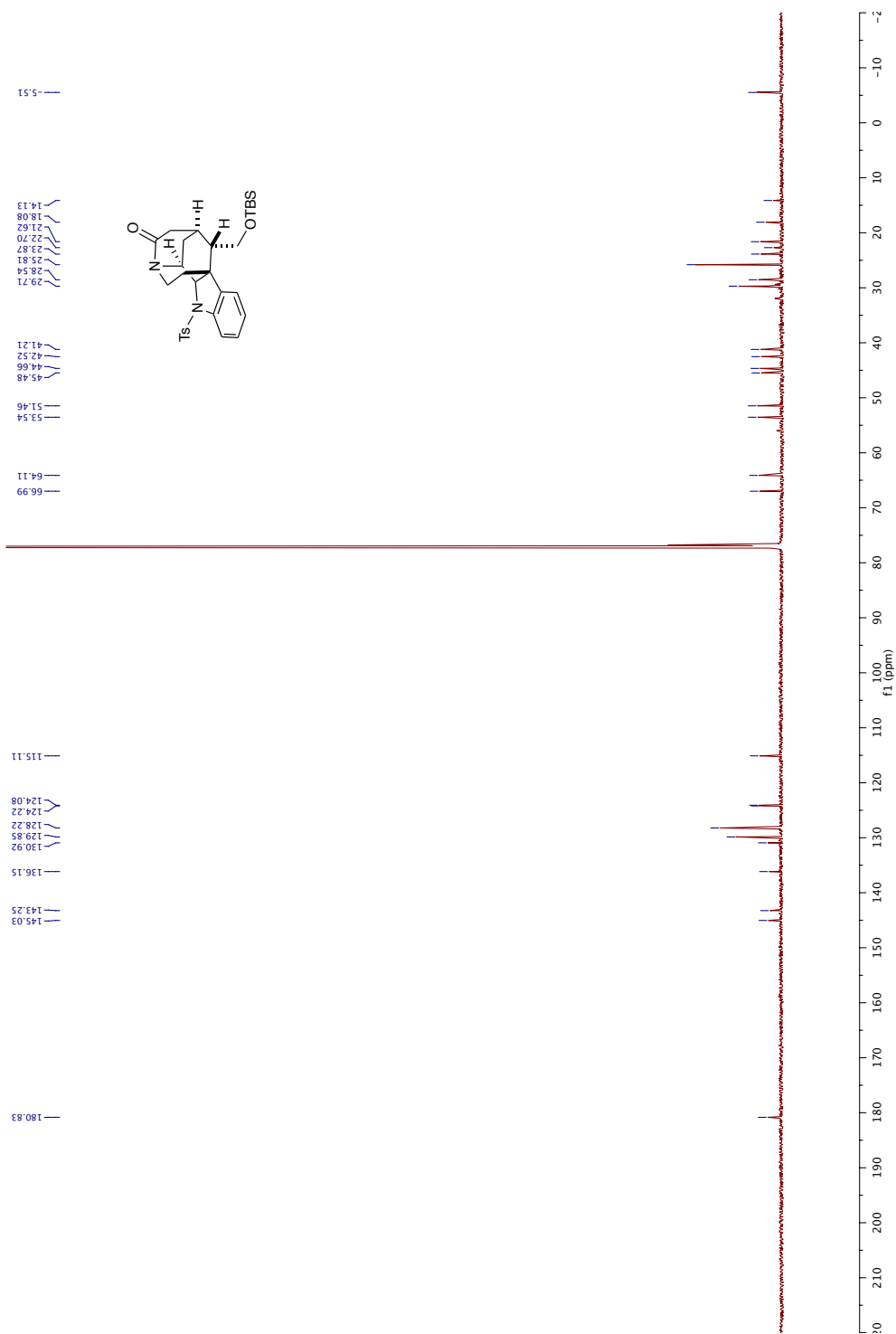
Alcohol 3.62: ^1H NMR (500 MHz, CDCl_3)

Carboxylic Acid 3.63: ^1H NMR (500 MHz, CDCl_3)

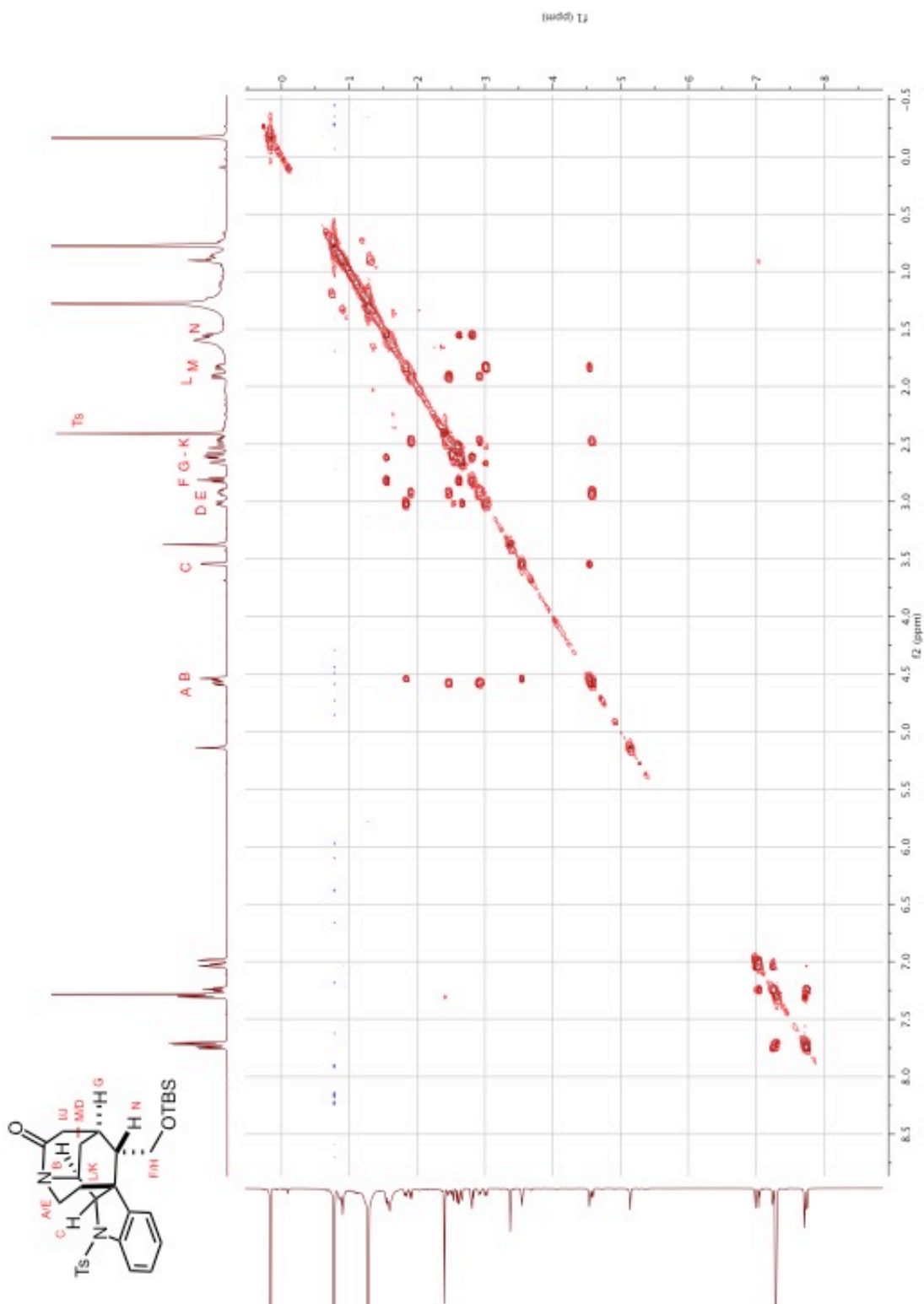
Carboxylic Acid 3.63: ^{13}C NMR (151 MHz, CDCl_3)

Pentacycle 3.64: ^1H NMR (600 MHz, CDCl_3)

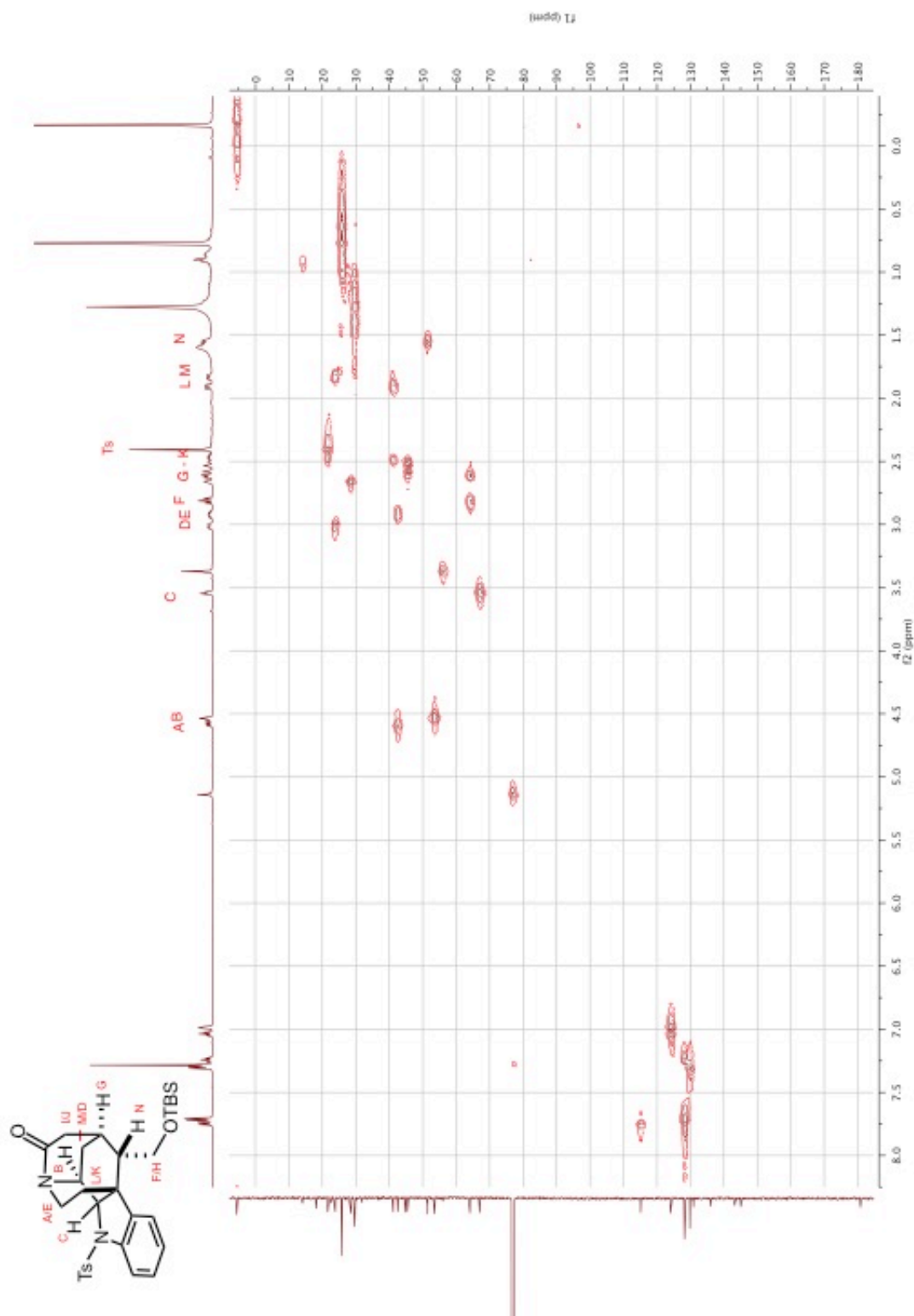


Pentacycle 3.64: ^{13}C NMR (151 MHz, CDCl_3)

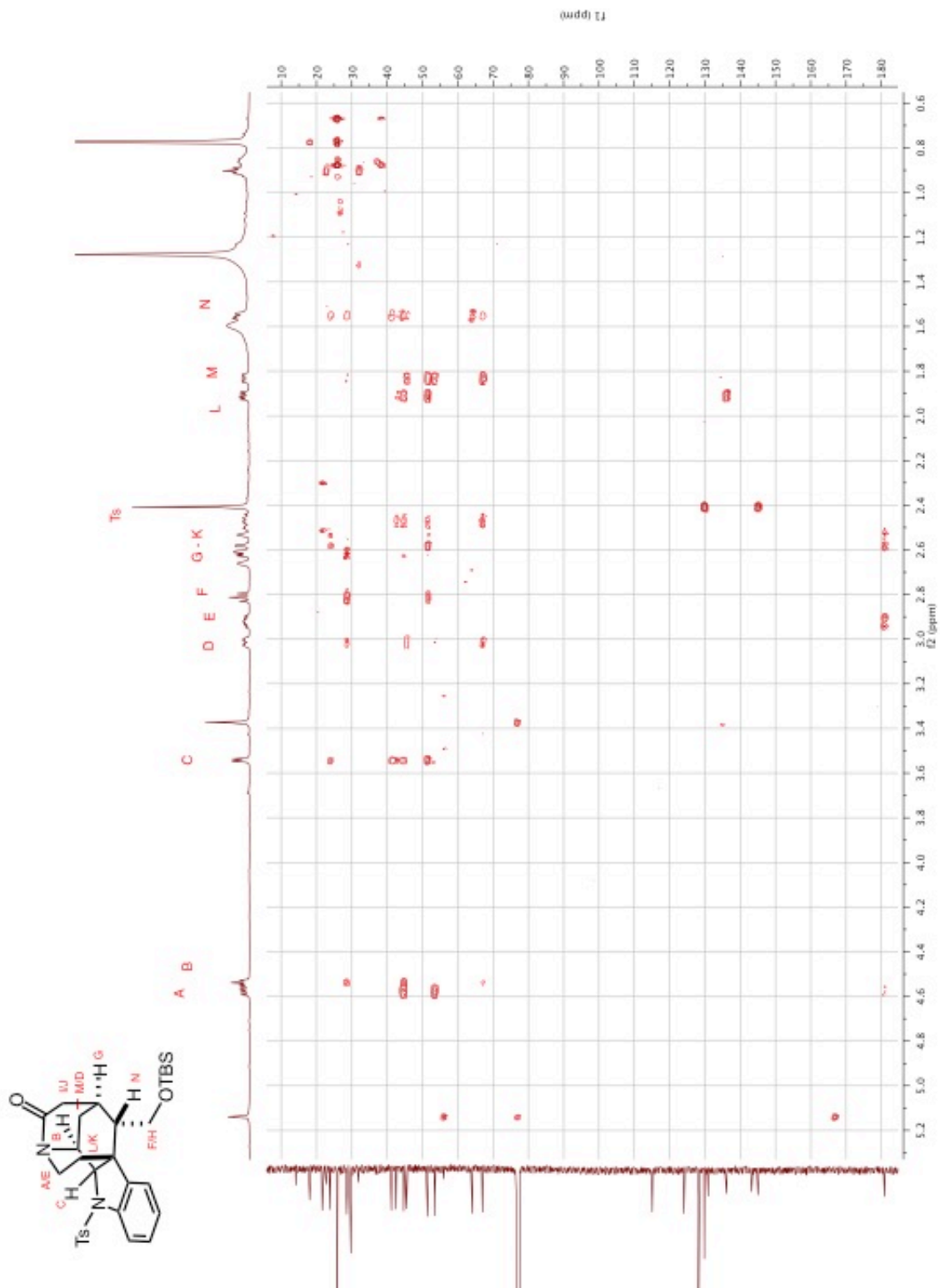
Pentacycle 3.64: COSY

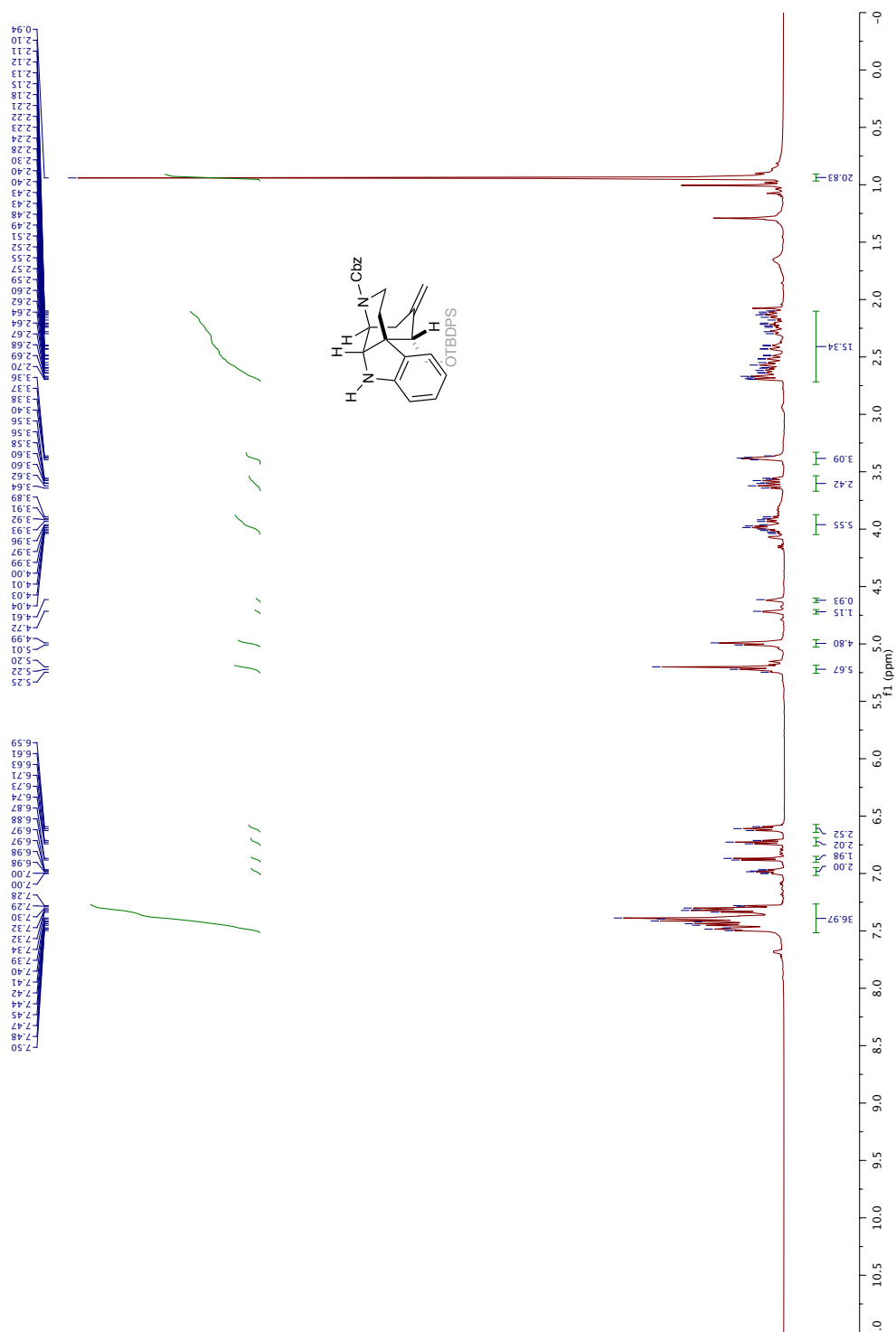


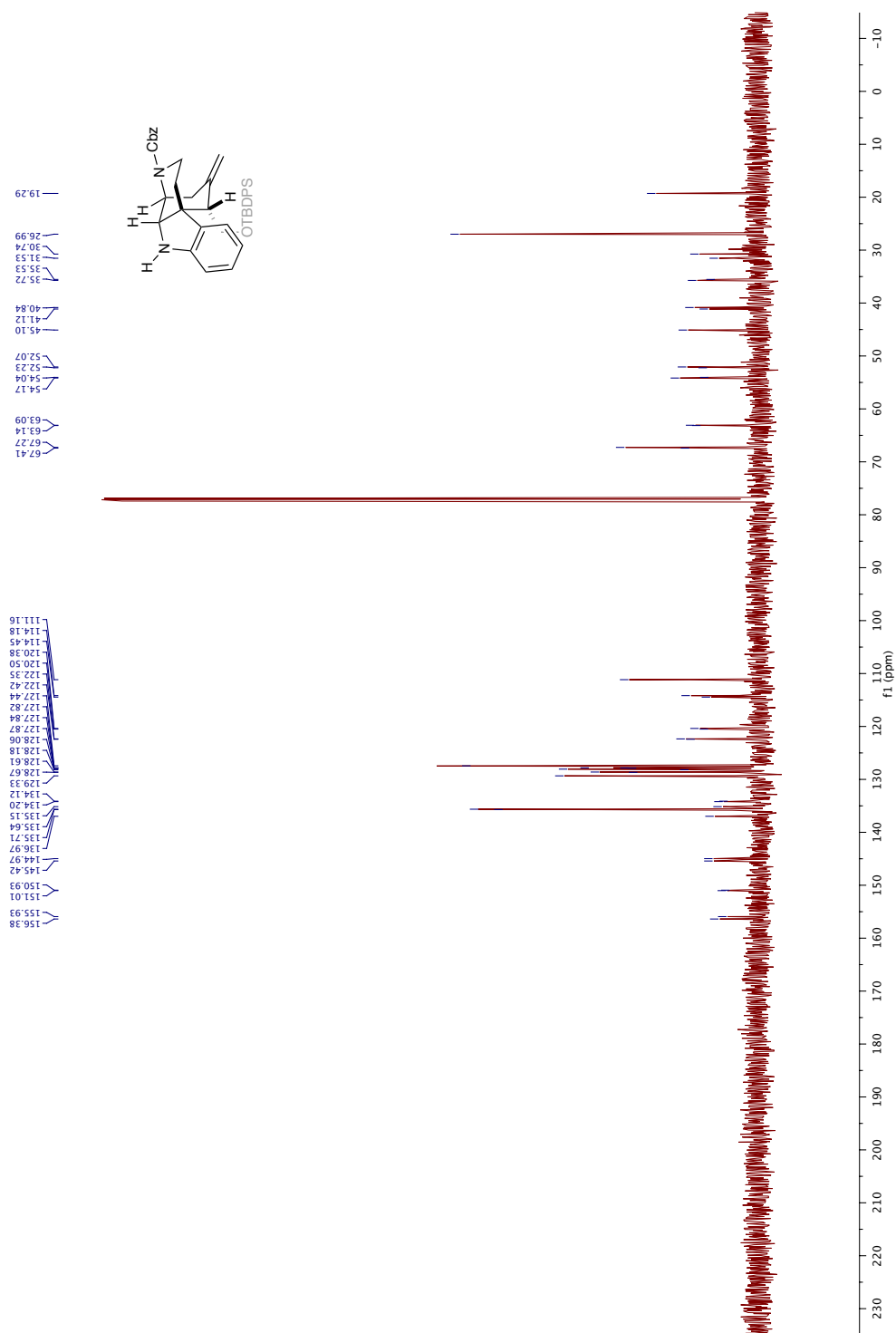
Pentacycle 3.64: HMQC

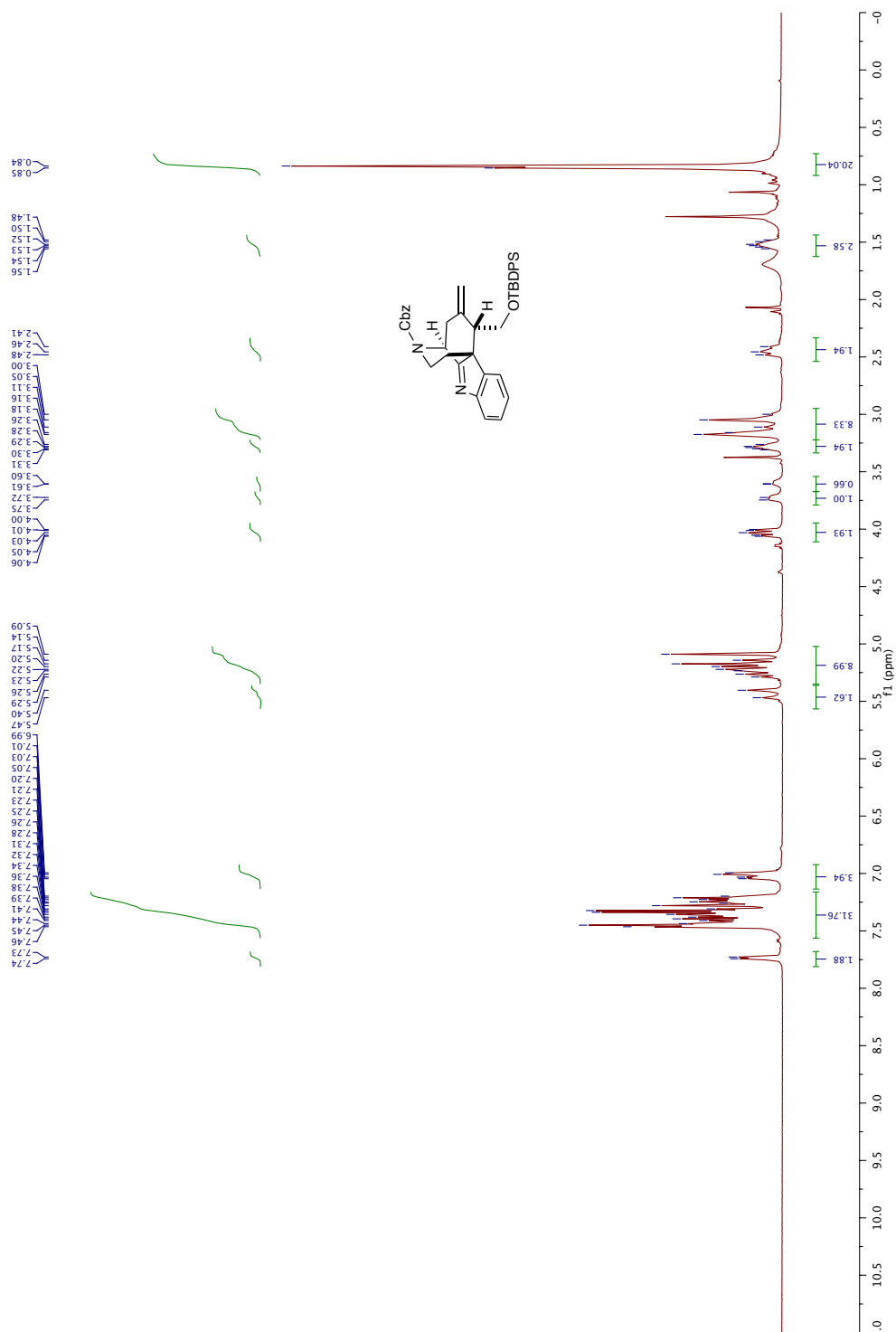


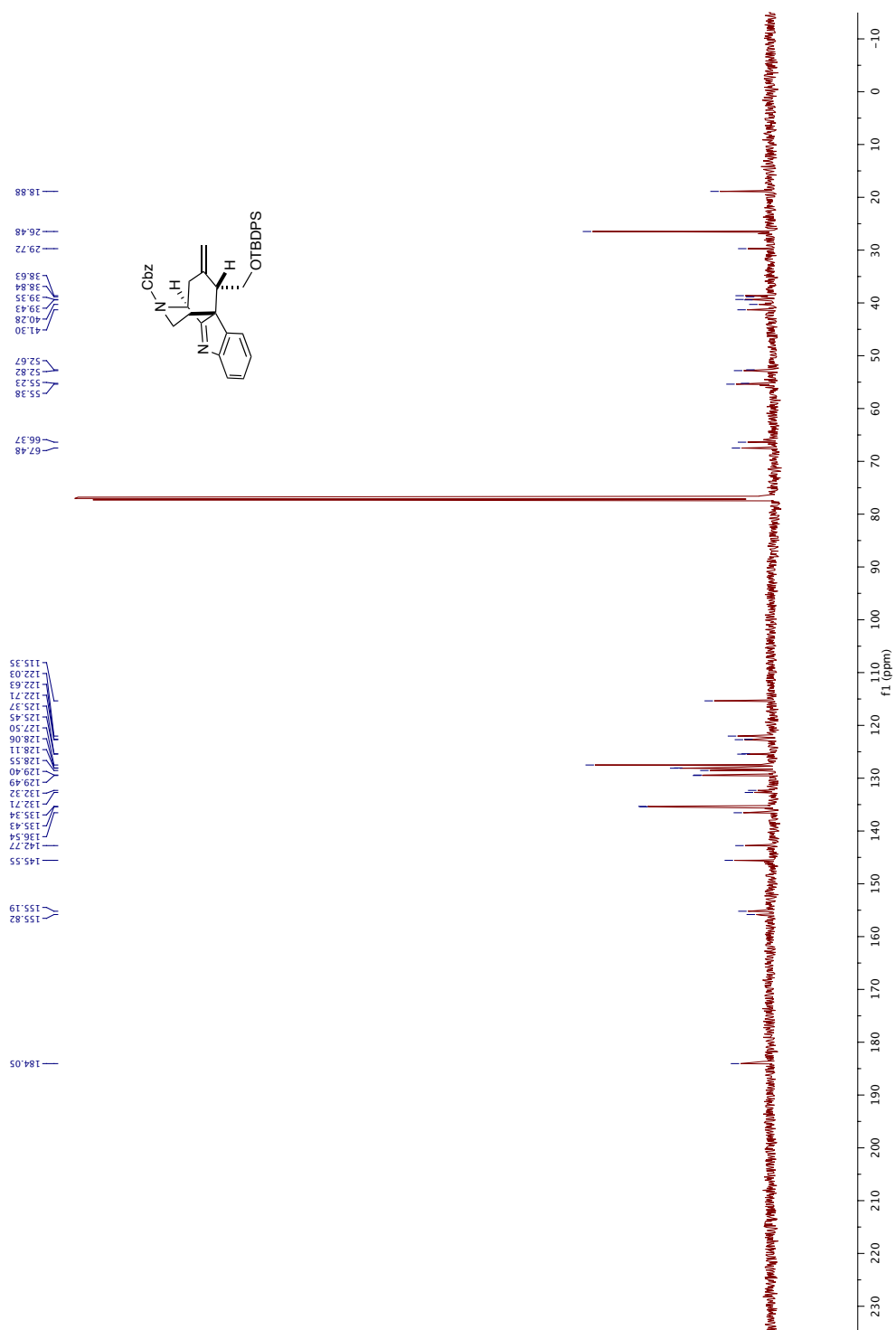
Pentacycle 3.64: HMBC



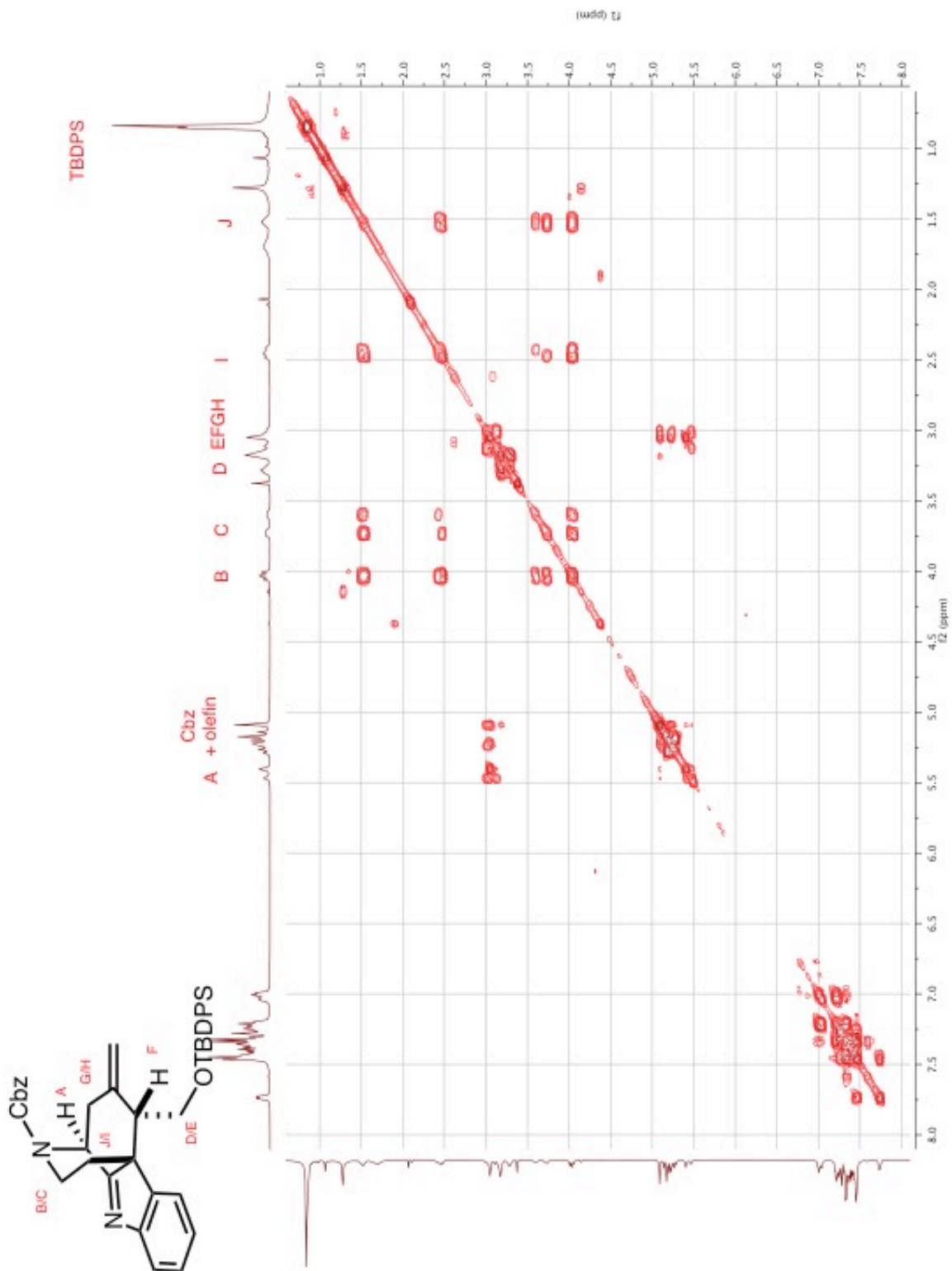
Indoline 3.67: ^1H NMR (500 MHz, CDCl_3)

Indoline 3.67: ^{13}C NMR (126 Mhz, CDCl_3)

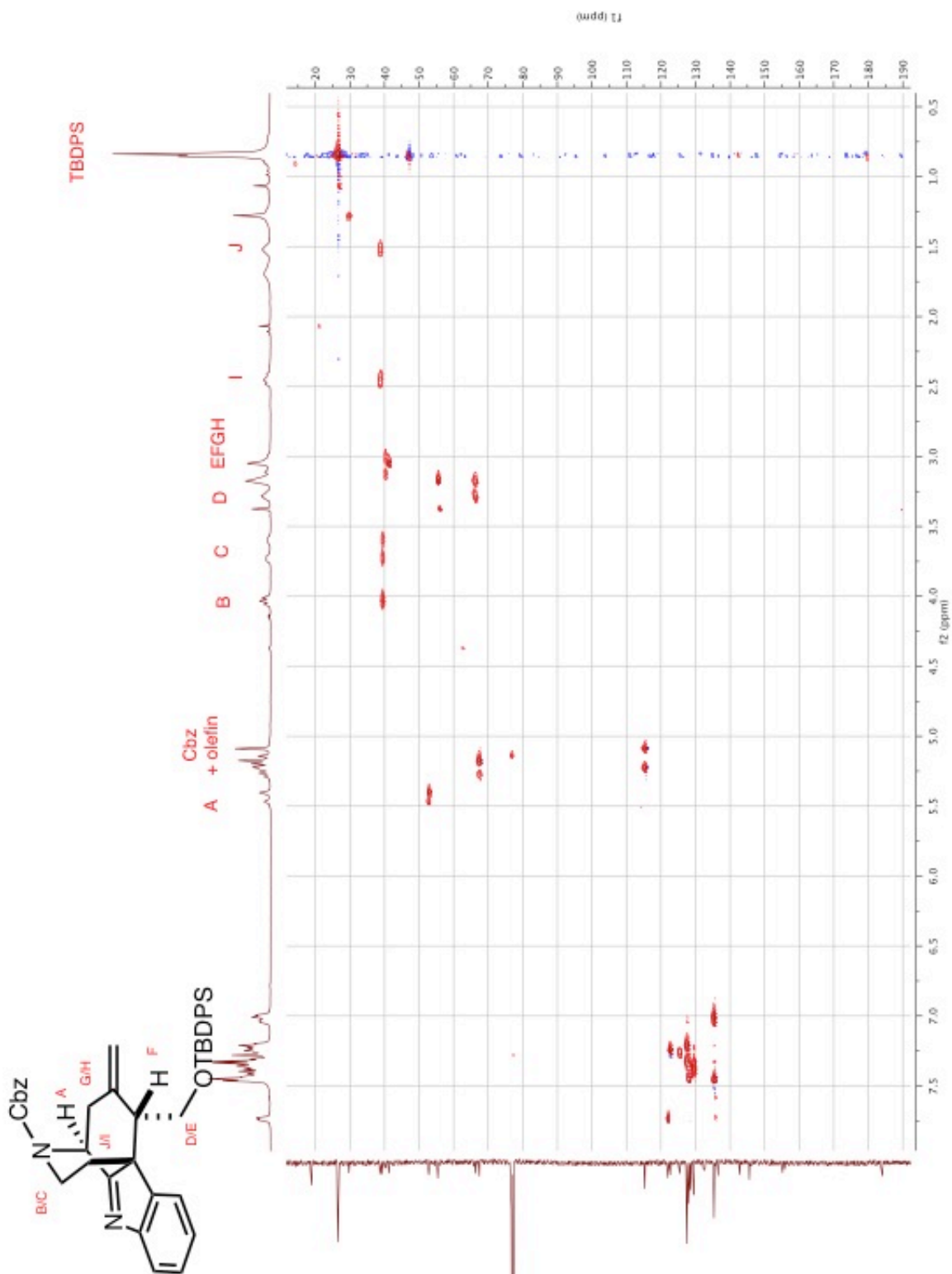
Indolenine 3.68: ^1H NMR (500 MHz, CDCl_3)

Indolenine 3.68: ^1H NMR (126 MHz, CDCl_3)

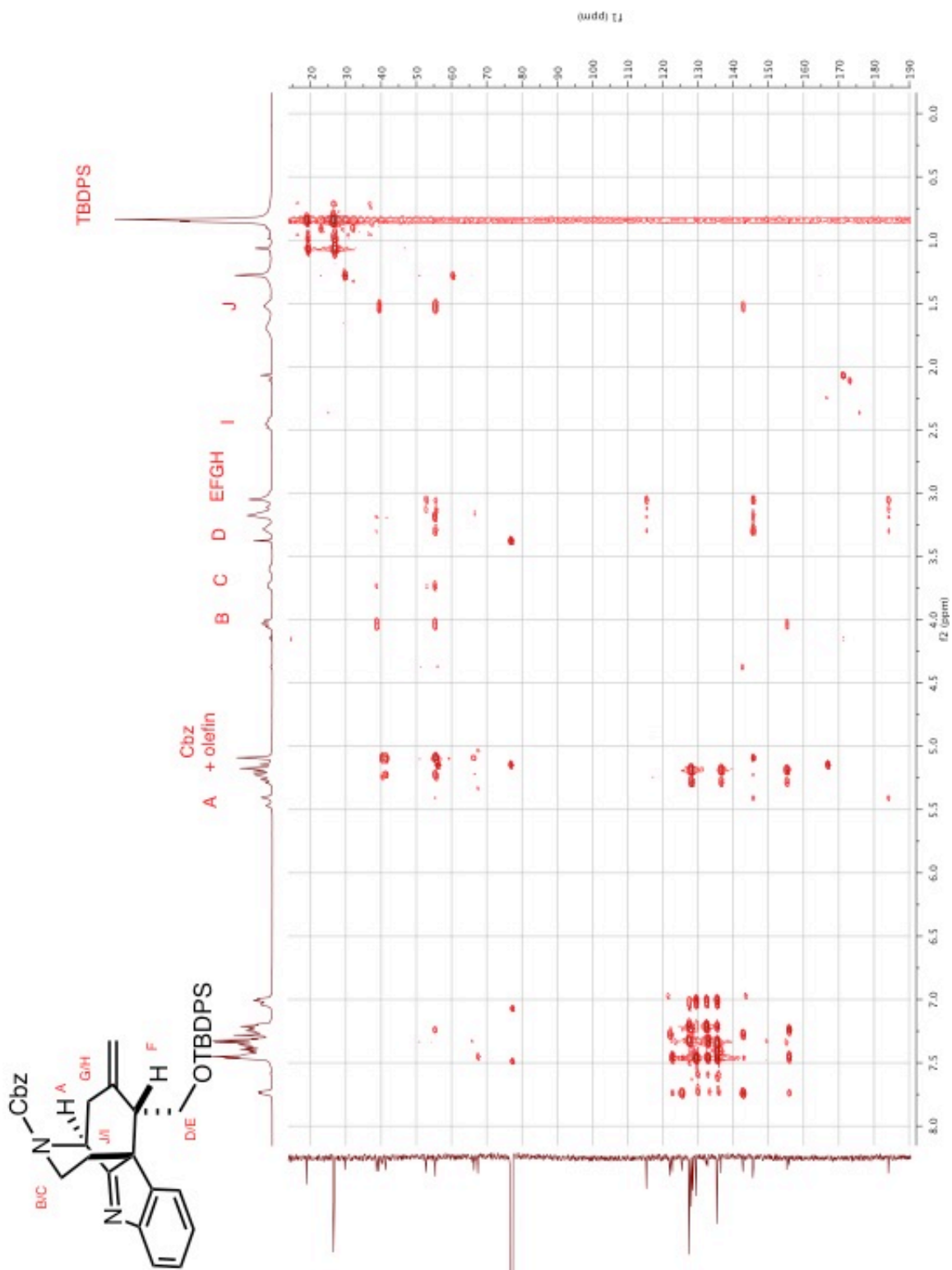
Indolenine 3.68: COSY

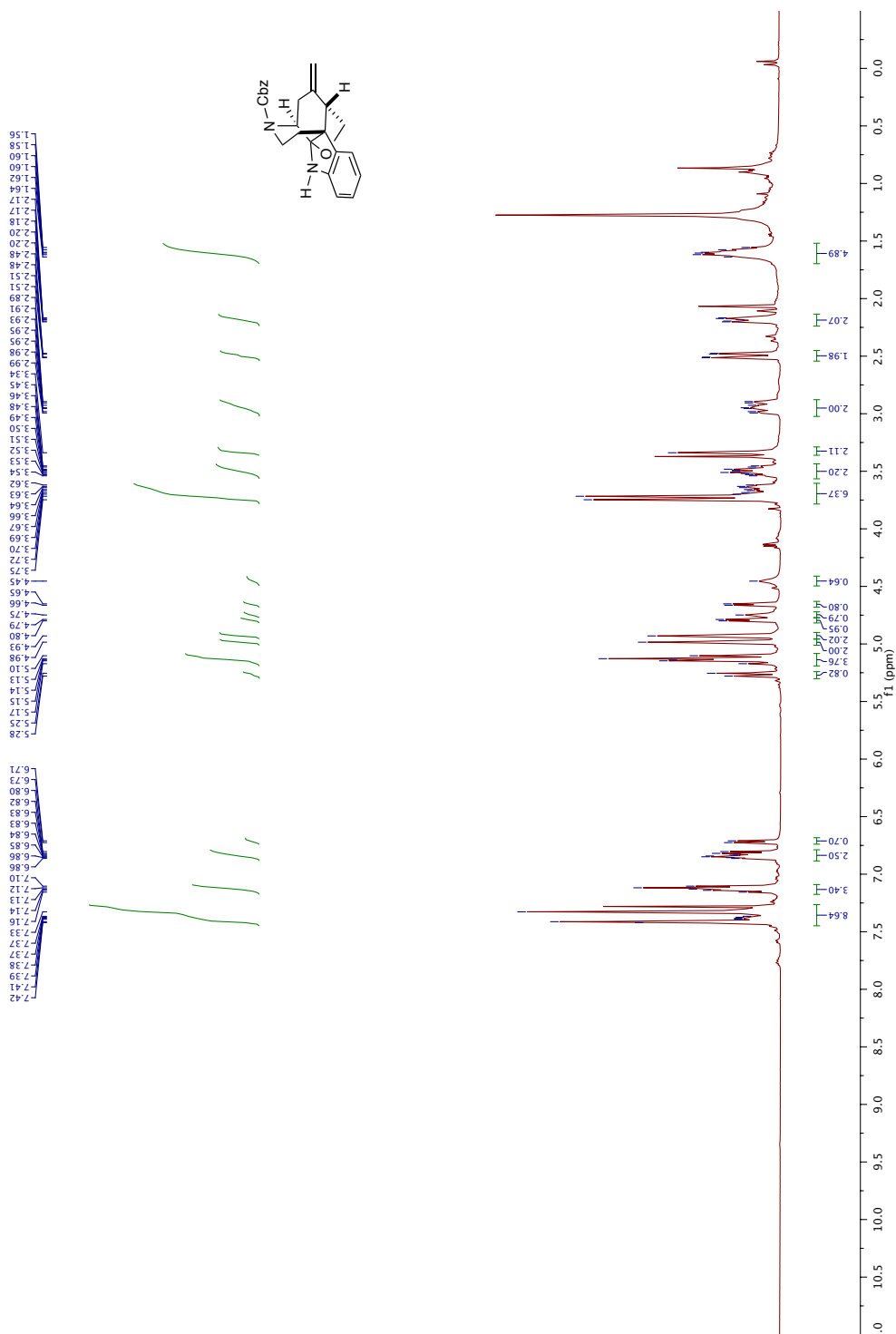


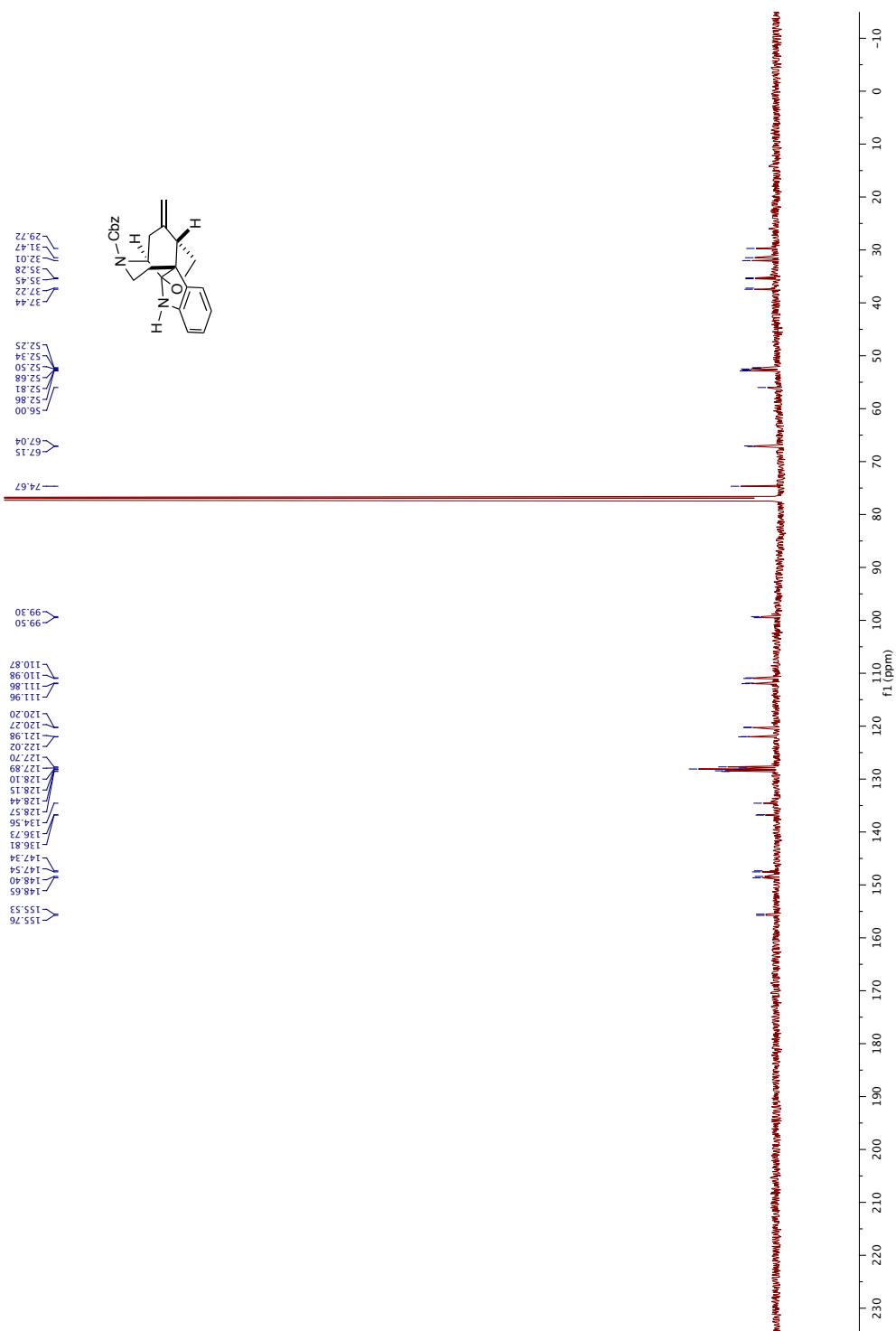
Indolenine 3.68: HMQC



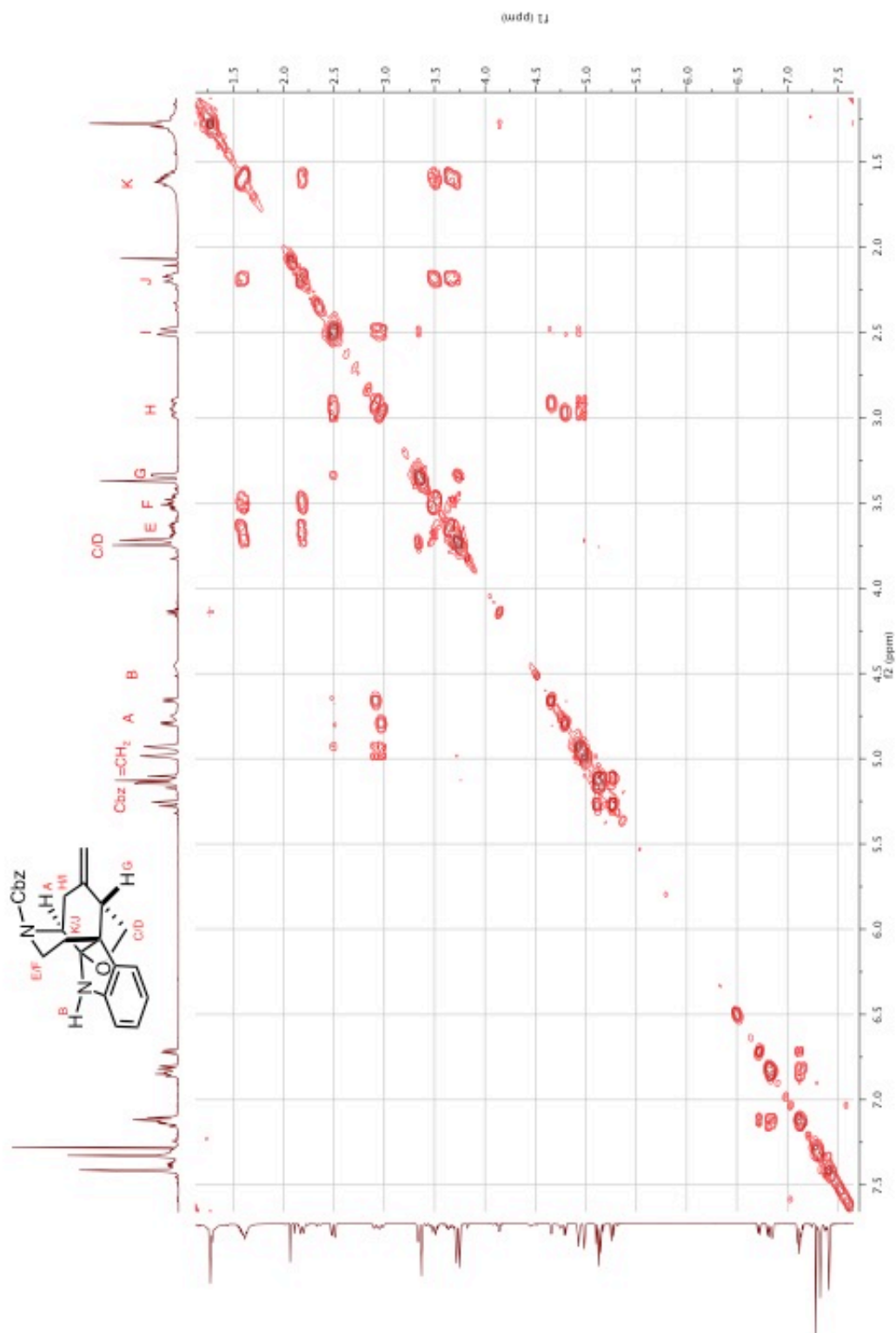
Indolenine 3.68: HMBC



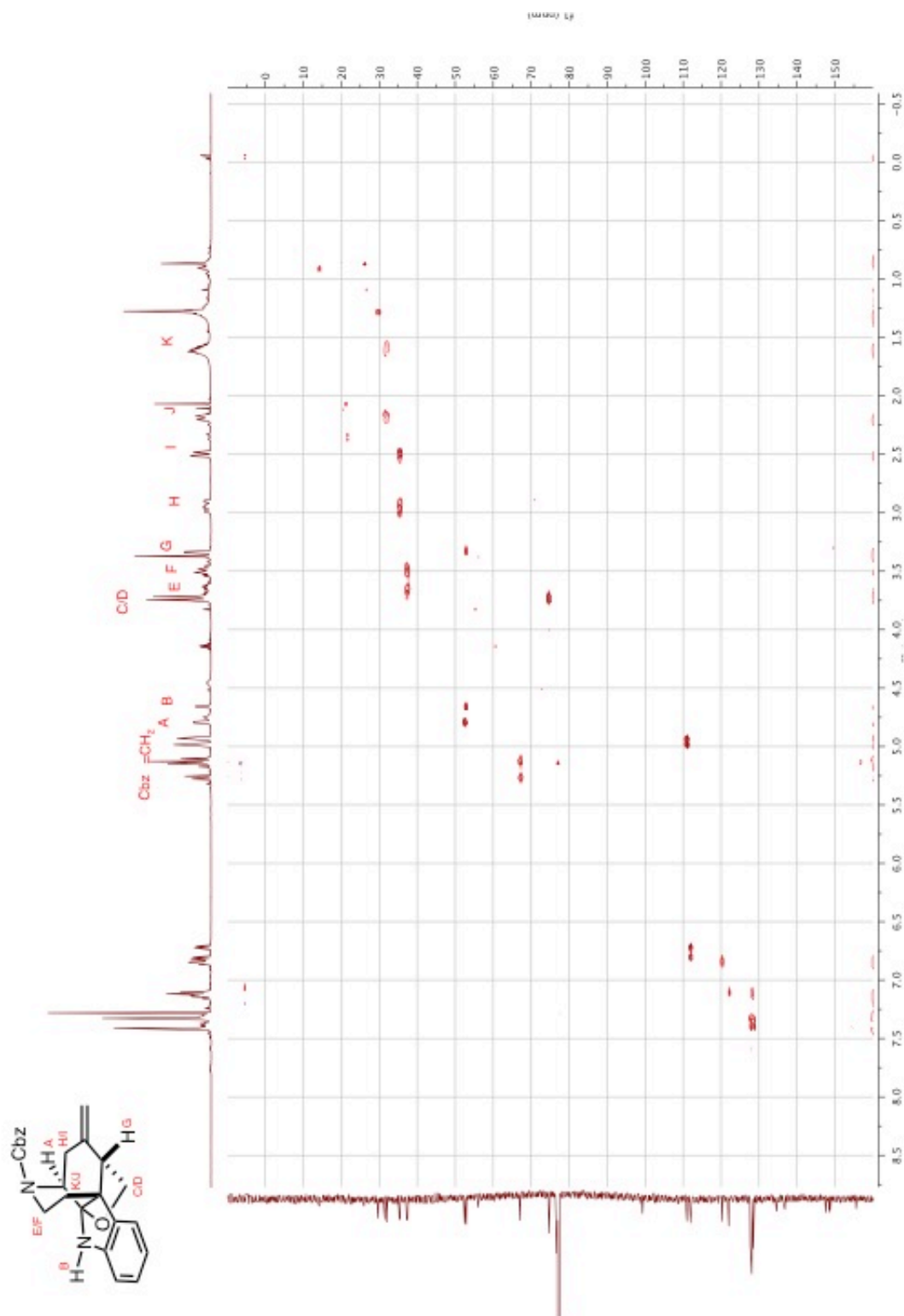
Furoindoline 3.65: ^1H NMR (500 MHz, CDCl_3)

Furoindoline 3.65: ^{13}C NMR (126 MHz, CDCl_3)

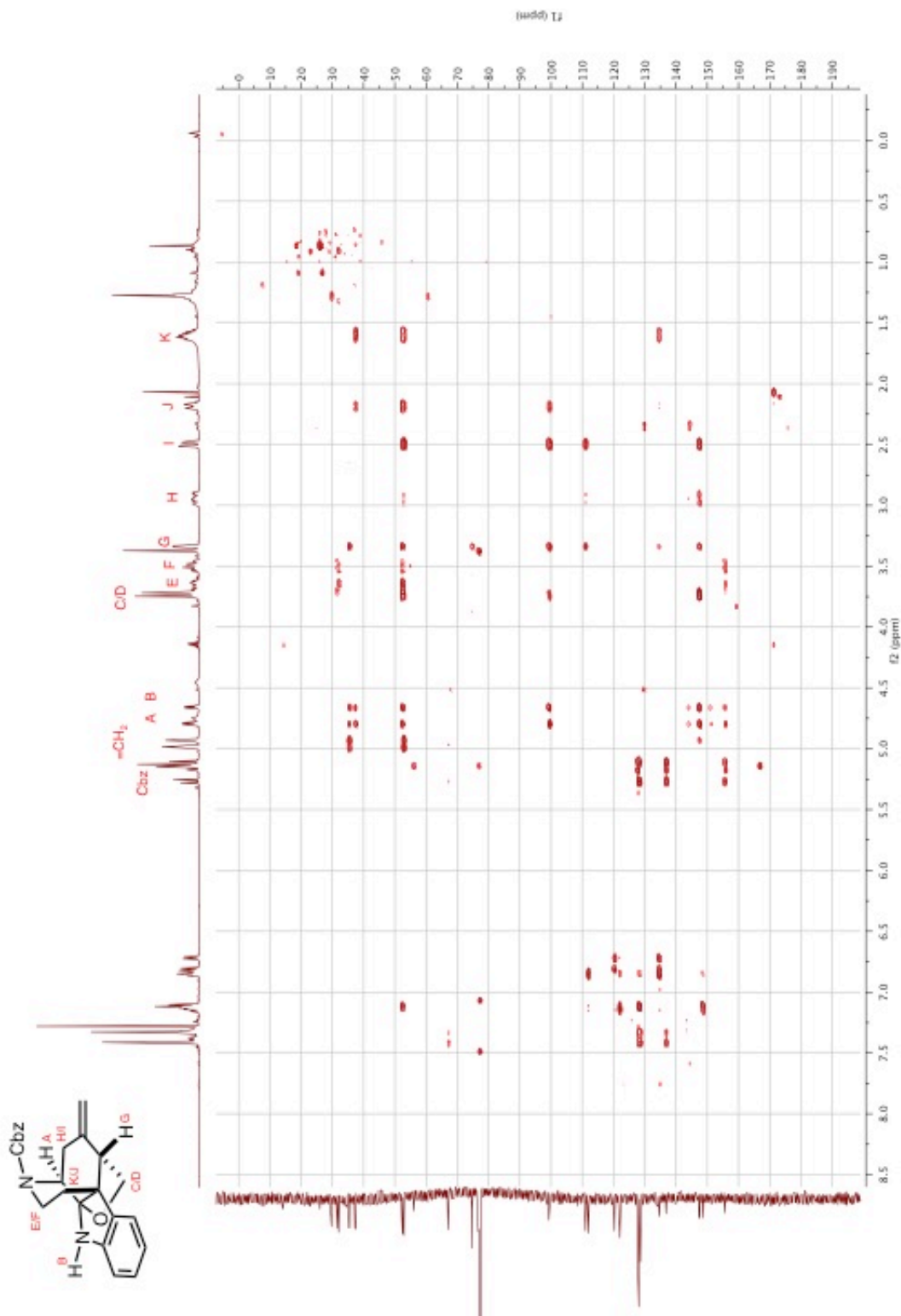
Furoindoline 3.65: COSY



Furoindoline 3.65: HMQC



Furoindoline 3.65: HMBC



3.10 References

1. Zhang, M.; Huang, X.; Shen, L.; Qin, Y., Total Synthesis of the Akuammiline Alkaloid (\pm)-Vincorine. *Journal of the American Chemical Society* **2009**, *131*, 6013-6020.
2. Kong, A.; Mancheno, D. E.; Boudet, N.; Delgado, R.; Andreansky, E. S.; Blakey, S. B., Total Synthesis of Malagashanine: A Chloroquine Potentiating Indole Alkaloid with Unusual Stereochemistry. *Chemical Science* **2017**, *8*, 697-700.
3. Hupe, E.; Calaza, M. I.; Knochel, P., Diastereoselective Synthesis and Reactions of Diorganozinc Reagents Obtained After Hydroborations with 9-BBN-H, Thexylborane, and Catecholborane. *Tetrahedron Letters* **2001**, *42*, 8829-8831.
4. Mancheno, D. E. Development of a Copper Catalyzed Aminoacetoxylation Reaction of Olefins, Development of an Intermolecular and Diastereoselective Iminium Cascade Reaction and Studies Towards the Synthesis of a Malagasy Alkaloid. Emory University, 2013.
5. Brown, H. C.; Rogic, M. M.; Rathke, M. W.; Kabalka, G. W., Stereochemistry of the Carbonylation, Carbethoxymethylation, and Gamma-Propanalation Reactions of Organoboranes. Substitution Reactions at Carbon That Proceed with Retention of Configuration. *Journal of the American Chemical Society* **1969**, *91*, 2150-2152.
6. Ohishi, T.; Zhang, L.; Nishiura, M.; Hou, Z., Carboxylation of Alkyboranes by N-Heterocyclic Carbene Copper Catalysts: Synthesis of Carboxylic Acids from Terminal Alkenes and Carbon Dioxide. *Angewandte Chemie International Edition* **2011**, *50*, 8114-8117.
7. Bertelo, C. A.; Schwartz, J., Hydrozirconation. II. Oxidative Homologation of Olefins via Carbon Monoxide Insertion into the Carbon-Zirconium Bond. *Journal of the American Chemical Society* **1975**, *97*, 228-230.
8. Delgado, R. Development of a Novel Cascade Cyclization Reaction and Its Application Towards the Total Synthesis of Malagashanine: A Chloroquine Efflux Inhibitor. Emory University, 2010.
9. He, F.; Altom, J. D.; Corey, E. J., Enantioselective Total Synthesis of Aspidophytine. *Journal of the American Chemical Society* **1999**, *121*, 6771-6772.
10. Takai, K., Addition of Organochromium Reagents to Carbonyl Compounds. In *Organic Reactions*, 2004; Vol. 64, pp 253-612.
11. Liu, P.; Wang, J.; Zhang, J.; Qui, F. G., A Concise Total Synthesis of (\pm)-Minfiensine. *Organic Letters* **2011**, *13*, 6426-6428.
12. Teng, M.; Zi, W.; Ma, D., Total Synthesis of the Monoterpenoid Indole Alkaloid (\pm)-Aspidophylline A. *Angewandte Chemie International Edition* **2014**, *53*, 1814-1817.
13. Jones, S. B.; Simmons, B.; Mastracchio, A.; MacMillan, D. W. C., Collective Synthesis of Natural Products by Means of Organocascade Catalysis. *Nature* **2011**, *475*, 183-188.
14. Mico, A. D.; Margarita, R.; Parlanti, L.; Vescovi, A.; Piancatelli, G., A Versative and Highly Selective Hypervalent Iodine (III)/2,2,6,6-Tetramethyl-1-piperidinyloxy-Mediated Oxidation of Alcohols to Carbonyl Compounds. *The Journal of Organic Chemistry* **1997**, *62*, 6974-6977.
15. Hoover, J. M.; Stahl, S. S., Highly Practical Copper(I)/TEMPO Catalyst System for Chemoselective Aerobic Oxidation of Primary Alcohols. *Journal of the American Chemical Society* **2011**, *133*, 16901-16910.

16. Krafft, M. E.; Holton, R. A., Regiospecific Preparation of Thermodynamically Silyl Enol Ethers Using Bromomagnesium Dialkylamides. *Tetrahedron Letters* **1983**, *24*, 1345-1348.
17. Comins, D. L.; Deghani, A., Pyridine-Derived Triflating Reagents: An Improved Preparation of Vinyl Triflates from Metallo Enolates. *Tetrahedron Letters* **1992**, *33*, 6299-6302.
18. Cacchi, S.; Morera, E.; Ortar, G., Palladium-Catalyzed Reduction of Vinyl Trifluoromethanesulfonates to Alkenes: Cholesta-3,5-diene. *Organic Syntheses* **1990**, *68*, 138.
19. Scott, W. J.; Stille, J. K., Palladium-Catalyzed Coupling of Vinyl Triflates with Organostannanes. Synthetic and Mechanistic Studies. *Journal of the American Chemical Society* **1986**, *108*, 3033-3040.
20. Farina, V.; Kapadia, S.; Krishnan, B.; Wang, C.; Liebeskin, L. S., On the Nature of the "Copper Effect" in the Stille Cross-Coupling. *The Journal of Organic Chemistry* **1994**, *59*, 5905-5911.
21. Han, X.; Stoltz, B. M.; Corey, E. J., Cuprous Chloride Accelerated Stille Reactions. A General and Effective Coupling System for Sterically Congested Substrates and for Enantioselective Synthesis. *Journal of the American Chemical Society* **1999**, *121*, 7600-7605.
22. Shenvi, R. A.; Guerrero, C. A.; Shi, J.; Li, C.-C.; Baran, P. S., Synthesis of (+)-Cortistatin A. *Journal of the American Chemical Society* **2008**, *130*, 7241-7243.
23. Birch, A. J.; Williamson, D. H., Homogenous Hydrogenation Catalysts in Organic Synthesis. *Organic Reactions* **2011**, *24*, 1-186.
24. Brown, J. M., Directed Homogenous Hydrogenation [New Synthetic Methods (65)]. *Angewandte Chemie International Edition* **1985**, *26*, 190-203.
25. Smidt, S. P.; Zimmermann, N.; Studer, M.; Pfaltz, A., Enantioselective Hydrogenation of Alkenes with Iridium-PHOX Catalysts: A Kinetic Study of Anion Effects. *Chemistry: A European Journal* **2004**, *10*, 4685-4693.
26. Crabtree, R., Iridium Compounds in Catalysis. *Accounts of Chemical Research* **1979**, *12*, 331-337.
27. Xu, Y.; Mingos, D. M. P.; Brown, J. M., Crabtree's Catalyst Revisited; Ligand Effects on Stability and Durability. *Chemical Communications* **2008**, 199-201.
28. Zu, L.; Boal, B. W.; Garg, N. K., Total Synthesis of (\pm)-Aspidophylline A. *Journal of the American Chemical Society* **2011**, *133*, 8877-8879.
29. Keirs, D.; Overton, K., Conversion of Amines to Imines by Swern Oxidation. *Journal of the Chemical Society, Chemical Communications* **1987**, 1660-1661.
30. Molander, G. A.; Harris, C. R., Sequenced Reactions with Samarium(II) Iodide. Tandem Intramolecular Nucleophilic Acyl Substitution/Intramolecular Barbier Cyclizations. *Journal of the American Chemical Society* **1995**, *117*, 3705-3716.
31. Levin, J. I.; Tuross, E.; Weinreb, S. M., An Alternative Procedure for the Aluminum-Mediated Conversion of Esters to Amides. *Synthetic Communications* **1982**, *12*, 989-993.
32. Kawanaka, Y.; Kobayashi, K.; Kusuda, S.; Tatsumi, T.; Moruta, M.; Nishiyama, T.; Hisaichi, K.; Fujii, A.; Hirai, K.; Naka, M.; Komeno, M.; Odagaki, Y.; Nakai, H.; Toda, M., Design and Synthesis of Orally Bioavailable Inhibitors of Inducible Nitric Oxide Synthase. Identification of 2-Azabicyclo[4.1.0]heptan-3-imines. *Bioorganic & Medicinal Chemistry* **2003**, *11*, 1723-1743.

33. Kong, A.; Andreansky, E. S.; Blakey, S. B., Stereochemical Complexity in Oxocarbenium-Ion-Initiated Cascade Annulations for the Synthesis of the ABCD Core of Mattogrossine. *The Journal of Organic Chemistry* **2017**, DOI: 10.1021/acs.joc.7b00503.
34. Morrill, C.; Grubbs, R. H., Synthesis of Functionalized Vinyl Boronates via Ruthenium-Catalyzed Olefin Cross-Metathesis and Subsequent Conversion to Vinyl Halides. *The Journal of Organic Chemistry* **2003**, *68*, 6031-6034.
35. Doi, H.; Ban, I.; Nonoyama, A.; Sumi, K.; Kuang, C.; Hosoya, T.; Tsukada, H.; Suzuki, M., Palladium(0)-Mediated Rapid Methylation and Fluoromethylation on Carbon Frameworks by Reacting Methyl and Fluoromethyl Iodide with Aryl and Alkenyl Boronic Acid Esters: Useful for the Synthesis of [¹¹C]CH₃-C- and [¹⁸F]FCH₂-C-Containing PET Tracers. *Chemistry: A European Journal* **2009**, *15*, 4165-4171.